THE EFFECT OF GRAIN SIZE ON MORPHOLOGICAL PATTERNS AND LAND COVER WITHIN BOREAL WILDFIRE RESIDUAL PATCHES

BUDHENDRA (ALEX) SINGH

A THESIS SUBMITTED TO THE FACULTY OF GRADUATE STUDIES IN PARTIAL FULFILMENT OF THE REQUIREMENTS FOR THE DEGREE OF MASTER OF SCIENCE

GRADUATE PROGRAM IN GEOGRAPHY
YORK UNIVERSITY
TORONTO, ONTARIO

June 2015

Abstract

Ontario experiences an annual mean of over 1000 fires, affecting over 1.3 million hectares. The post-fire conditions comprise a matrix of burned, partially burned, and unburned patches that are ecologically important in providing habitat, food, and seed resources, suppressing infestations, facilitating succession, enabling nutrient cycling and exposing mineral soils for regeneration. Studying the unburned post-fire residuals helps planners assess the effectiveness of emulating natural disturbance patterns with selective harvesting techniques in the boreal forest. The MSPA tool quantifies spatial patterns in terms of the geometry and connectivity of the landscape features. The core, islet, perforation, edge, loop, bridge, branch, and background features are identified for residual patches extracted from the 55,000 ha RED-084 fire event. Grain size coarsening (4 m to 64 m) and parameterizations were measured to find if they altered the frequency of 7 morphological elements within 10 land cover classes. Sparse conifer, dense conifer, bedrock and non-vegetation, and water were the land cover classes that were in most abundance and significantly different from other classes across most morphological elements. The connectivity change had a significant effect on islets, while transitioning only had a significant effect on edge elements. Edge width had a significant effect on core, perforation, edge, loop, and branch elements across all grain sizes. These findings can assist in developing a set of rules on the composition and configuration of land cover and morphological patterns left behind after harvesting.

Dedication

I dedicate this thesis to my wonderful and loving partner Rose and my supporting family. Without their efforts and love, my education at York University would not have been possible.

Acknowledgements

I would like to thank the following people for their support in my research project. Firstly, I thank Dr. Tarmo K. Remmel for allowing me the opportunity to pursue my master's degree and continuing my educational endeavors. I am grateful for his encouragement, time, energy, instructions, and wealth of knowledge that he continues to bestow unto me during my studies. I am truly humbled and yet privileged to have worked under a hardworking and motivating supervisor like Dr. Remmel. I also thank my committee member Dr. André Robert for his advice and helpful feedback on my research.

I thank the Ontario Ministry of Natural Resources, Dr. Tarmo Remmel (through York University), and the Forest Ecology Landscape Program under the directorship of Dr. Ajith Perera for their data and technical support, with specific contributions in their reports of the RED-084 fire event. I am also indebted and grateful to Dr. Tarmo Remmel, Yikalo Araya, Ajith Perera, and Marc Ouellette for their dedicated work in the field and tireless hours in gathering data at the RED-084 site. I thank York University's Department of Geography, the Faculty of Graduate Studies and CUPE 3903 for their financial support and academic advice prior to and during my studies at York University. I thank the National Forestry Database for their extensive catalogue of wildfire statistics. Without the permitted use of their data, I would not have been able to produce several graphs in my report.

I thank Dr. Tarmo Remmel for the usage of his lab (Geoinformatics Lab) at York University. This lab allowed me to use computing services, printing, field equipment, and reading material. I would also like to thank my lab partners and colleagues Yikalo Araya, Yuestas David, Doris Siu, Connie Ko, Patrick Mojdehi, and Emma Gunn, for their support and assistance in my research.

I am especially grateful for my family (Rosalind, Robin, Ash, and Adrian) for their sacrifices and support throughout my time at York University. Their guidance and advice was crucial in helping me attain my goals and ambitions. I am absolutely thankful for my partner Rose for her never-ending love, care, and emotional boost. I am also thankful for my friends for their support and social relief during my studies.

Table of Contents

List of Tables

List of Figures

List of Acronyms

AOU	Area of Undertaking
AVHRR	Advanced Very High Resolution Radiometer
BAI	Burned Area Index
CFSA	Crown Forest Sustainability Act
DEM	Digital Elevation Model
ED	Edge density
ETM+	Enhanced Thematic Mapper plus
GEMI	Global Environmental Monitoring Index
HANDS	Hotspot and NDVI Differencing Synergy
LPI	Largest patch index
LSI	Landscape shape index
MODIS	Moderate Resolution Imaging Spectroradiometer
MPS	Mean patch size
MSPA	Morphological Spatial Pattern Analysis
NDVI	Normalized Difference Vegetation Index
NP	Number of patches
NTDB	National Topographic Data Base
OMNR	Ontario Ministry of Natural Resources
PD	Patch density
SAVI	Soil Adjusted Vegetation Index
SPAN	Spatial Analysis Program
SPOT	Systeme Pour l'Observation de la Terre
TE	Total edge
UTM	Universal Transverse Mercator
WGS84	World Geodetic System of 1984

Land Cover Acronyms

AS	Aldershrub Woodland
BV	Bedrock and Non-vegetation

DE	Deciduous
DC	Dense Conifer
LS	Low Shrub
MA	Marsh
OP	Open Wetland
SC	Sparse Conifer
TW	Treed Wetland
WA	Water

MSPA Acronyms

Conn	Neighbourhood Connectivity
EW	Edge Width
TR	Transition

1. Introduction

1.1 Global Boreal Forest

The boreal biome occupies a large areal extent of the northern hemisphere. The boreal zone is a vast, circumpolar vegetation zone in the high northern latitudes, which is primarily populated with cold-tolerant forests and wooded land (Brandt 2009). In North America the boreal zone occupies Newfoundland in the east, and extends through the northern portions of other Canadian provinces and the southern portions of the territories into Alaska in the west (Weber and Stocks 1998). In Eurasia, this zone extends from Scandinavia and Russia, to some parts of China, Mongolia and Kazakhstan (Figure 1). Boreal forests account for 32% of the global forest cover making it the largest terrestrial biome on earth (Burton et al. 2008), occupying approximately 1.66 billion hectares (Runesson 2011).

The northern boundary borders the tundra zone, while the southern boundary interfaces with the temperate forests and grasslands (Brandt 2009). The vegetation mainly comprises cold-tolerant tree species in the genera *Abies* (firs)*, Larix* (larches or tamaracks)*, Picea* (spruces)*, Pinus* (pines)*, Populus* (poplars) and *Betula* (birches). It is important to note that the humid continental and taiga subarctic climates dominate the boreal regions with long, harsh winters, and relatively short, cool summers (de Blij et al. 2009). These tree species can withstand periodic droughts as a result of the podzolic soils freezing during the winter amid the overall cold 1.4°C mean annual temperature (de Blij et al. 2009).

The boreal region can directly provide timber, pulp extract, and fuelwood from the softwood tree species. Boreal forest ecosystems can store fresh water in lakes and rivers, and in the winter a copious amount is stored in snow, ice, permafrost, and the active layer. The boreal region can also be deemed as an ecosystem regulator, balancing and controlling climatic conditions, flooding, diseases, and water purification (Brandt et al. 2013). Brandt (2009) suggested that boreal forests are also culturally and spiritually important to the aboriginal and indigenous peoples of North America and Eurasia. Cultural, spiritual, and educational values are often associated with the boreal region especially among the First Nations communities and scientific researchers. Bogdanski (2008) also noted the importance of the boreal region to non-renewable

mineral and energy resources. Waterways and rivers within the boreal region also provide hydroelectric power and offer the potential of future hydroelectric projects.

Humans benefit from the boreal region by way of renewable raw materials for construction purposes and recreational activities. The management of boreal forests is often decided by the timber harvesting in the forms of saw logs and pulp wood, within a timely fashion (Kellomäki et al. 1997). Specifically coniferous forests are used extensively in the pulp and paper mill industry due to the structurally rigid cellulose fibre in the wood (Waye et al. 2014). The woodlands, wetlands, water courses, and lakes that co-exist with the coniferous and deciduous forests also provide habitat for wildlife, drive nutrient cycles, control soil erosion, maintain air and water quality, and regulate regional and global climates (Brandt 2009). The nutrient cycle in particular is sustained by the decomposition of litter and humus, which accumulate on the soil surface as a result of root, branch, and foliage loss (Kellomäki et al. 1997).

In addition, boreal forests store more carbon in their trees, soils, and peat than all other terrestrial ecosystems (Chu and Guo 2014), accounting for almost 30% of the global terrestrial carbon (Burke et al. 1997). Of the 714 Pg of carbon stored in the boreal forest region, 419 Pg are stored in the peatland soils, 231 Pg are stored in the soil layer or dead matter of the forested areas, and 58 Pg are stored within the living biomass (Kasischke et al. 1995). Carbon released into the atmosphere via oxidation from fire disturbances (Kurz et al 2013) is a major factor in influencing climate change. Amiro et al. (2001) estimated that about 27 Tg of carbon have been released every year between 1959 and 1999 as a result of forest fires in Canada. The managed boreal forest in Canada represents a 28 Tg per year carbon sink for the past 25 years, which potentially supplants the 17 Tg of carbon that is lost through harvesting operations (Kurz et al. 2013).

Figure 1. Global distribution of the boreal zone. Source: Natural Resources Defense Council (NRDC) 2011 (http://www.nrdc.org/land/forests/boreal/images/map.gif)

1.2 Canadian Boreal Forest

The Canadian boreal zone can be separated into 3 major components. The tree limit to the north represents the forest-tundra or the subarctic region of the northern boreal boundary (Rowe and Scotter 1973; Brandt 2009). The middle portion represents the continuous boreal forest which contains open and closed forests or woodlands (Brandt 2009). Open forests are indicative of areas where the forests occupy between 10 and 40% of the total land area, while closed forests occupy at least 40% of the total area (United Nations Environment Programme 2009). The southern boundary is delineated by the hemiboreal or sub-boreal forest region, containing closed-crown forest (Rowe and Scotter 1973). These 3 zones can then be further subdivided into 7

ecozones which represent the boreal forest in relation to their location on the Canadian Shield, plains and cordillera surfaces (Figure 2). Common species in Canada include the softwood coniferous trees: white spruce (*Picea glauca* (Moench) Voss), black spruce (*Picea mariana* (Mill.) B.S.P.), tamarack (*Larix laricina* (Du Roi) K. Koch.), balsam fir (*Abies balsamia* (L.) Mill.), and jack pine (*Pinus banksiana* Lamb.). Hardwood deciduous trees, which often occur in pure stands or mixed in with coniferous species include trembling aspen (*Populus tremuloides* Michx.), balsam poplar (*Populus balsamifera* L.), and white birch (*Betula papyrifera* Marsh.).

Canada's northern boreal forests occupy about 81% of the total forested area in Canada (Amiro et al. 2008) and the boreal region accounts for almost 35% of Canada's landmass (Volney and Hirsch 2005; Akhter and Hassan 2011). The forest sector in Canada provides a major source of income, especially to habitants of about 200 rural communities (State of Canada's Forests Annual Report 2013). It is in these communities that the forest sector accounts for at least 50% of the economic foundations. The boreal forest is an important provider to Canada's economy. The forest sector within the boreal region (overseeing lumber, pulp, logging, and forestry services) employed about 58,000 workers in 2001, contributing to 15.5% of the total workers employed in the Canadian forestry sector (Patriquin et al. 2007). In addition, the agricultural, mining, fishing, trapping, and energy resources sectors are found within the boreal region, owing to the employment of 189,000 workers in 2001 (Patriquin et al. 2007). Furthermore, commercial and recreational activities such as hunting, fishing, and camping are prevalent within boreal forest and generate revenue in the tourism sector. Fishing, hunting, and trapping in the boreal forest has employed 24,700 people in 2001, which comprises 28% of the fishing and trapping workers in Canada (Patriquin et al. 2007). When factoring all possible sources of employment, the boreal forest sector in Canada employed over 1.6 million workers in 2001 (Patriquin et al. 2007).

The forest sector in Canada is valued at around $82 billion (Volney and Hirsch 2005), which includes timber, pulp, paper, and recreational sectors. The Canadian Gross Domestic Product (GDP) receives $33 billion annually from the forest industry (Volney and Hirsch 2005). However, the forest sector has suffered financially within the past decade, contributing only $18.7 billion to Canada's GDP in 2012 (State of Canada's Forests Annual Report 2013). This valuation represented about 1.1% of Canada's total

GDP in 2012. The revenue generated from timber sales alone within Canada has been consistently over $1 billion each year from the mid-1990s to the mid-2000s (Figure 3). The economic recession in 2007-2008 affected the timber industry due to the lowered demand for timber-based products (Figure 3). Figure 3 shows that Ontario accounts for almost 10% of the total revenue generated from the sale of timber in Canada.

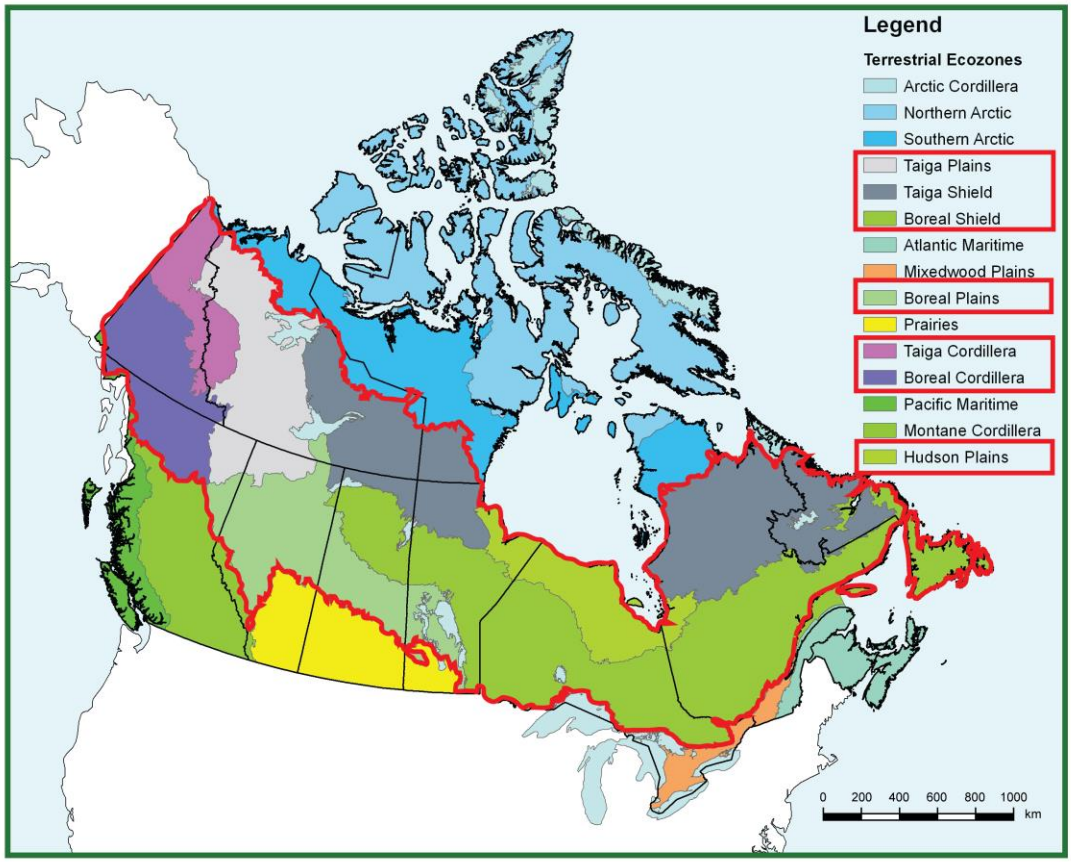

Figure 2. The terrestrial ecozones found within the boreal region (demarcation in red) of Canada. Source: National Resources Canada 2014 (www.nrcan.gc.ca/forests/canada/classification/13179).

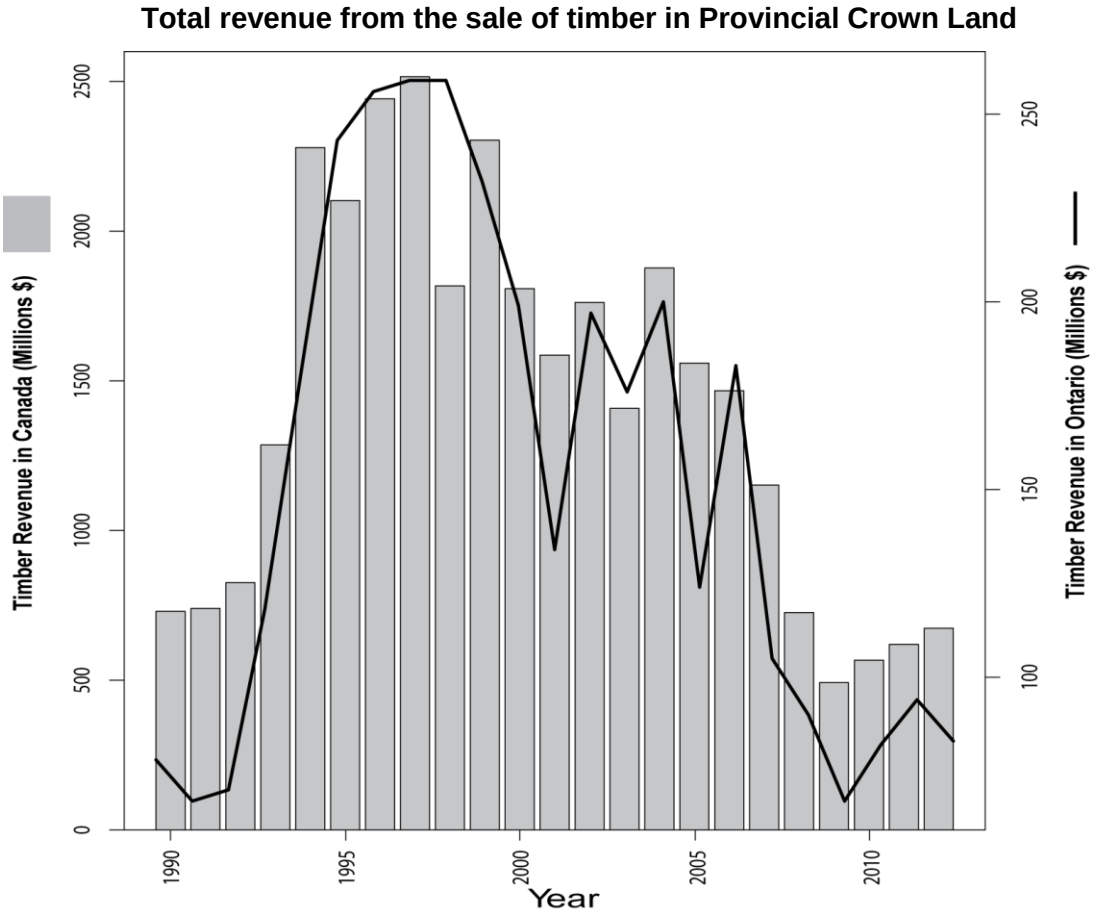

Figure 3. Sales from timber have been consistently on the rise within the last 2 decades, except for the recent economic downturn in 2007. Data Source: National Forestry Database 2014 (http://nfdp.ccfm.org/dynamic_report/dynamic_report_ui_e.php)

Ontario accounts for 71 million ha of Canada's forest cover, of which 56 million ha are deemed productive by the Ministry of Natural Resources (Watkins 2011). More specifically, 50 million ha of these forests are boreal, which is mainly dominated by coniferous tree species (Ontario Forest Research Institute 2008). The Area of Undertaking (AOU) represents the forested areas where forest management and commercial forestry are practiced (Watkins 2011) (Figure 4). The AOU contains large patches of connected forests perforated by water and wetlands, and originally delineated

in the Class Environmental Assessment report for forest managers in 1994 (Watkins 2011). Additionally, the Ontario Ministry of Natural Resources (OMNR) designates these areas as potential harvesting sites, totaling to about 44 million ha of Ontario forests. Estimates show that the viably productive boreal forests within the AOU represent about 34.8 million ha. Approximately over 20,000 ha of forest are harvested each year from 1990 to 2005 in Ontario, with a decline in the last 7 years due to the aforementioned economic downturn (Figure 5). Within the Canadian context, an immense 1 million ha of forest have been harvested annually in the late-1990s and early-2000s, contributing to revenue by the forest sector.

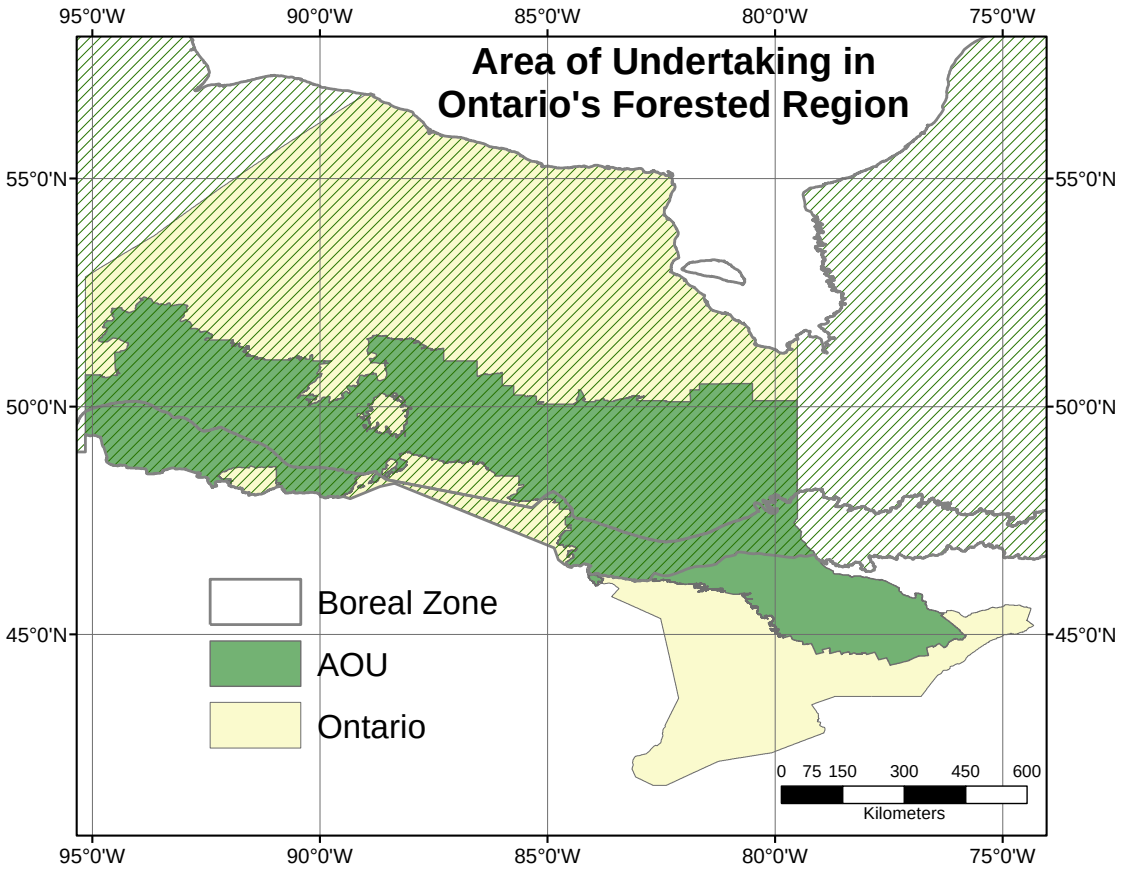

Figure 4. Most of the AOU in Ontario is found within the boreal region; this forested zone is economically important for harvesting, recreational, hunting, and trapping activities.

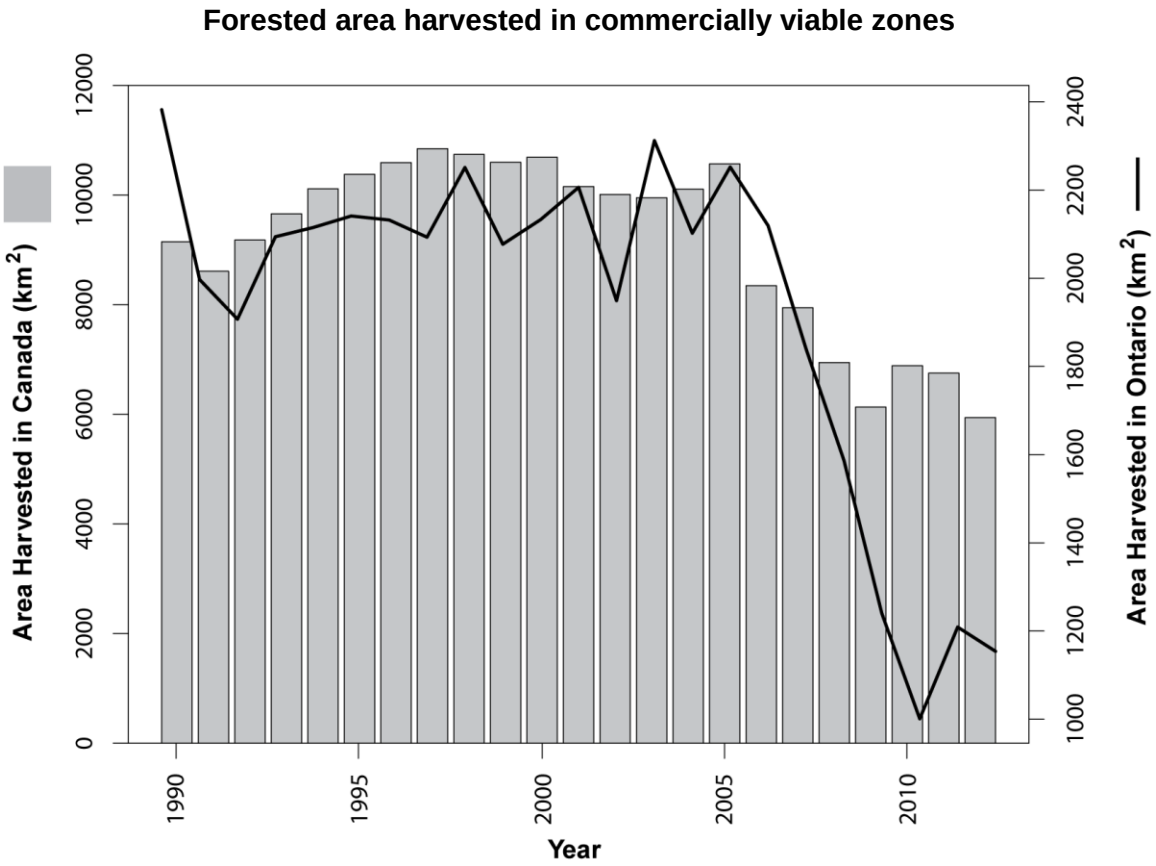

Figure 5. Harvested areas of forest in Ontario and Canada for the past 22 years reflect the demand for timber and pulp based products. Data Source: National Forestry Database 2014 (http://nfdp.ccfm.org/dynamic_report/dynamic_report_ui_e.php)

1.3 Disturbances

An ecological disturbance has been defined as an event that is highly destructive and rare (Rykiel Jr. 1985), but landscape ecologists struggle with the ambiguity of this statement. Forman and Godron (1986) define disturbances as disruptive forces acting on ecosystems that cause considerable change to the normal structure and function. A revision conducted by Rykiel Jr. (1985) reflected on the magnitude of the effect of the term disturbance: a physical force, agent, abiotic or biotic process which causes a change in the motion, course or stability in an ecological system. It may often lead to a stress effect on the landscape. Disturbances reduce the landscape's existing biomass, reduce, eliminate or increase specific populations, inhibit the matter and energy exchange processes, and allow for the prevention of further natural disturbances (Rykiel

Jr. 1985). The vulnerability to disturbances within Canada's boreal forests is noted by the 5 to 6 million ha, which are disturbed each year by fire, insects, and disease (National Resources Canada 2012).

The main disturbances which affect Canada's boreal forests are fire, insect infestation, disease, harvesting and extreme weather-related events. These disturbances can also be classified as natural drivers of the boreal ecosystem. Disturbances in the boreal forest contribute to biogeochemical cycling, structural food web alterations, and productivity with respect to ecosystem and community interactions (Brandt et al. 2013). In terms of landscape variability, disturbances can regulate and promote species composition and diversity, maintain the size of the ecosystem, and provide various stages of succession in vegetation (Brandt et al. 2013).

The mountain pine beetle (*Dendroctonus ponderosae*), which is prevalent in western Canada, is the most devastating insect in recent years, killing about 18.3 million ha of pine forests in British Columbia from 1998 to 2012 (Natural Resources Canada and BC Forestry 2013). This is equivalent to more than 720 million m^3 of pine timber and represents about 55% of British Columbia's commercially available pine timber (Natural Resources Canada 2013). The spruce budworm (*Choristoneura fumiferana* Clemens), a native insect of North America, presents the most damage to Ontario's boreal forests (Gray 2013), defoliating about 850,000 ha of forest between 2006 and 2007 (Natural Resources Canada 2014). Spruce budworm stunts the growth of trees and increases the probability of fire occurrence on the severely affected trees (Gray 2013). Diseases can also change the forest configuration, biodiversity, and composition as they can destroy particular species and even increase the population of other species as a result. The most prevalent disease in Canada is the *Armillaria* root disease, which has affected the roots and tree bases of almost 203 million ha of forest in Canada in 2012 (Natural Resources Canada 2013). Forest managers observe the natural disturbances in order to harvest forests with the intent of creating similar patterns in the landscape.

Harvesting is an anthropogenic disturbance that also shapes the forest configuration and composition albeit in a controlled manner. An average of 1 million ha of forest was harvested each year between 1995 and 2005 (Natural Resources Canada 2013). However, there has been a slight decrease in the area of forest land harvested

since 2005, as this period corresponded with the global economic recession (Natural Resources Canada 2013).

1.4 Wildfires

Wildfires are widely studied disturbances that have the ability to cause destruction (a loss in biomass quantity) and stress on populations (specific populations are reduced, increased or destroyed). They can be generally regarded as unplanned (and unwanted), whereby lightning strikes and human-caused factors (negligence and carelessness) initiate the ignition (Canadian Interagency Forest Fire Centre 2003). Lightning induced fires are often larger in area than human-caused fires as a result of the remoteness of the ignition and the feasibility of taking suppressive actions to extinguish these wildfires (Rowe and Scotter 1973). Wildfires can also cause interference in the cycling of nutrients and energy, as the flow of nutrients can become impeded or enhanced (Rykiel Jr. 1985). A forest fire according to the Canadian Interagency Forest Fire Centre (2003) is a wildfire or prescribed fire that has burnt forested areas, grass, alpine or tundra vegetation.

During the past decade in Canada, there have been on average >7200 wildfires reported annually (Figure 6). This translates to almost 2 million ha of forested area burned each year, totaling almost 23 million ha of forested area burned from 2001 to 2012 (Figure 6). In the past 3 decades, fire in Canadian forests has accounted for an average annual loss of 2.8 million ha (Stocks et al. 1998), owing to the increased fire activity in the 1980s which observed an average of 10000 wildfires every year (Weber and Stocks 1998). The ignition of 35% of these wildfires are due to lightning strikes, however, they account for 85% of the total burned area in Canada (Weber and Stocks 1998). There have been about 1100 wildfires reported annually from 2001 to 2012 in Ontario (Figure 7). Although the area burned has fluctuated over this period, the total area burned is approximately 1.6 billion ha of forested land cover (Figure 7). Larger wildfires impact large extents of landscapes, whereby only 3% of wildfires are greater than 200 ha but account for 97% of the total burned area (Natural Resources Canada 2009). Each year in Ontario about 1% of the boreal forest burns as a result of wildfires (Remmel and Perera 2009). The larger fires tend to display more convoluted landscape patterns as the longer the fire burns the greater the effects from meteorological and

physiographic conditions (Foster 1983). These larger wildfire occurrences closely overlap the extent of the Canadian boreal zone (Figure 8).

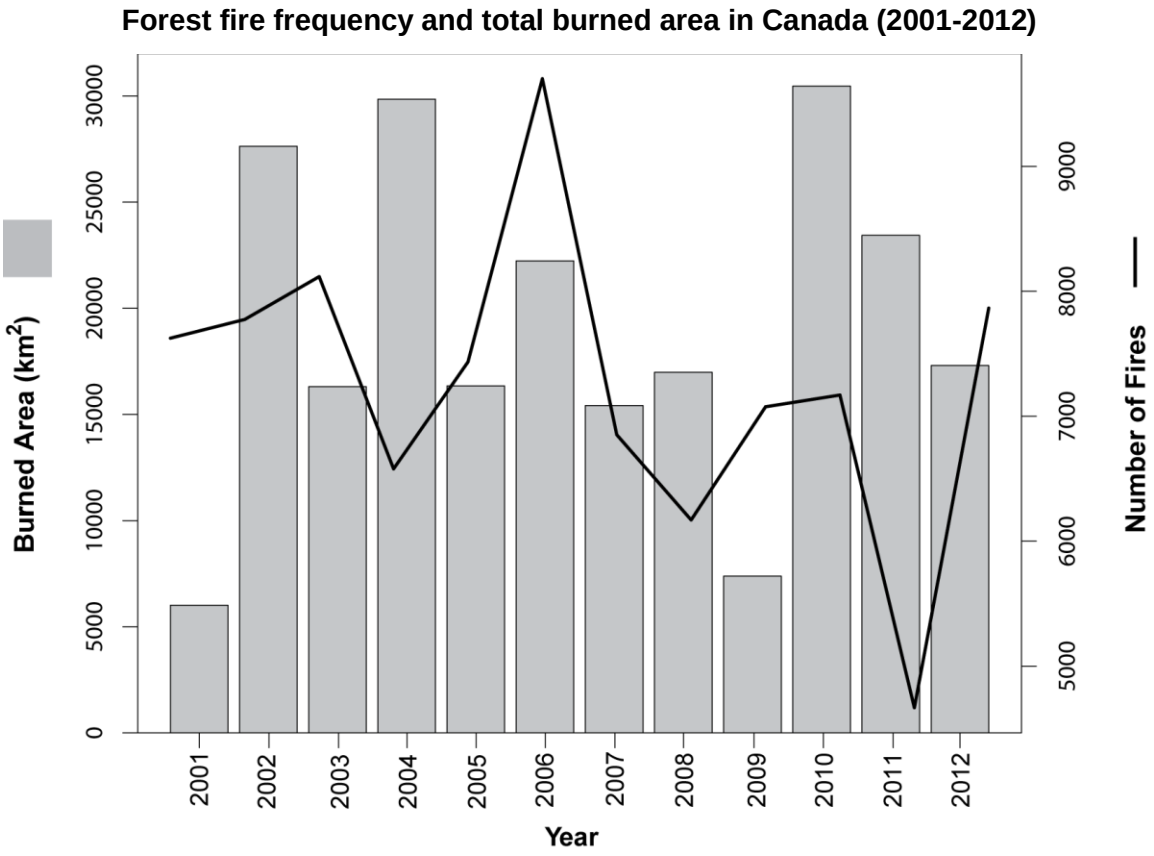

Figure 6. The total area and number of fires burned in Canada. Data Source: National Forestry Database 2014 (http://nfdp.ccfm.org/dynamic_report/dynamic_report_ui_e.php)

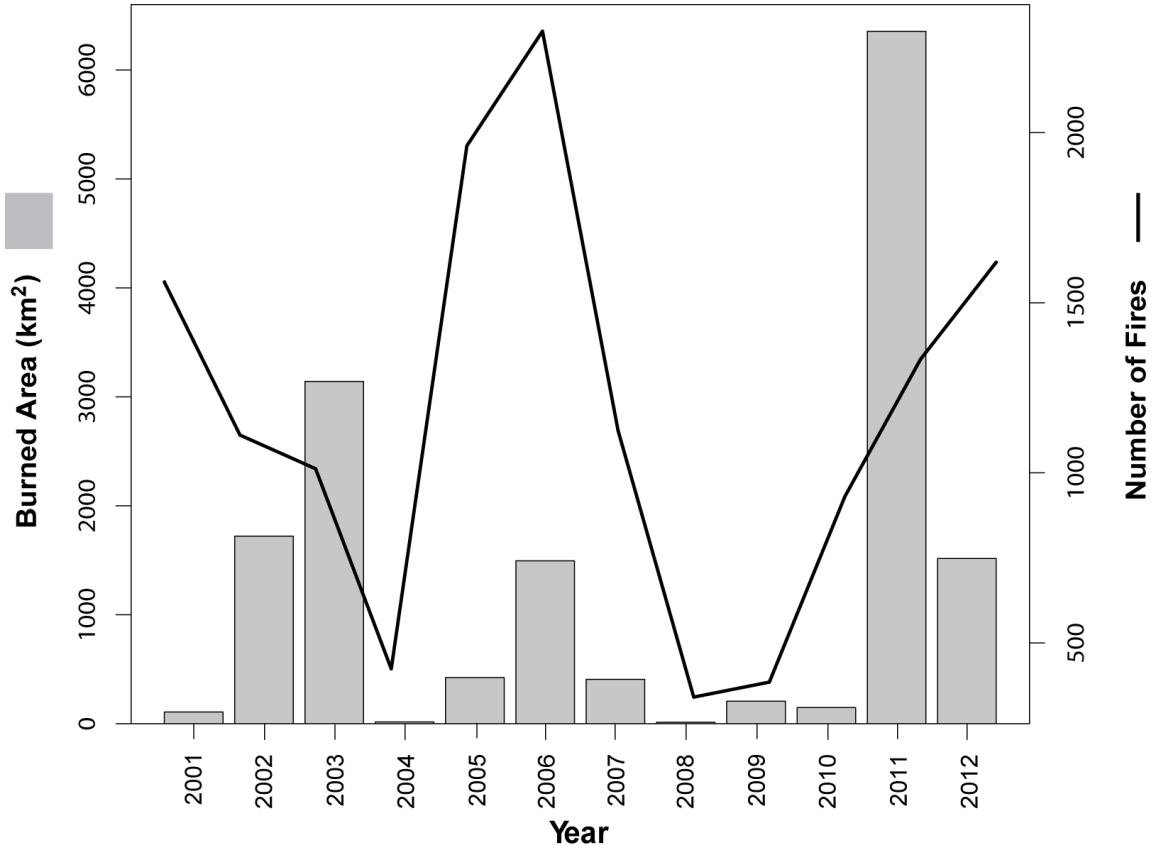

Figure 7. The number of fires has fluctuated in Ontario over the past decade, however a large fire event in 2011 has resulted in a relatively large burned area. Data Source: National Forestry Database 2014 (http://nfdp.ccfm.org/dynamic_report/dynamic_report_ui_e.php)

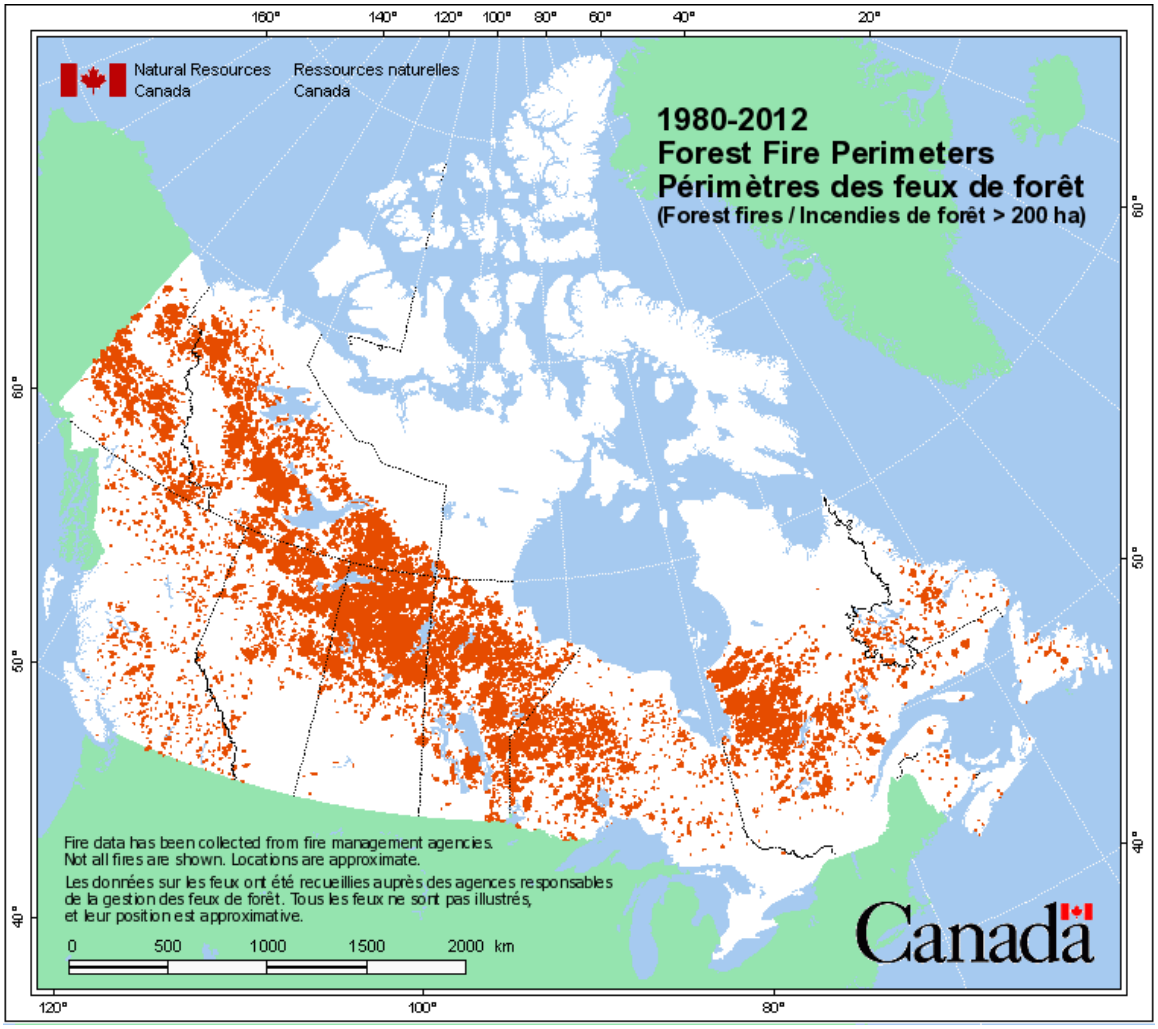

Figure 8. The extent and distribution of forest fires in Canada over the past 32 years. Source: Natural Resources Canada (2014).

1.4.1 Importance of Wildfires

Wildfires are important stand-renewal mechanisms in the boreal region (Brandt et al. 2013) as they facilitate the replacement of old growth forests and downed trees with a new generation of trees. This mechanism allows for biodiversity, forest stand age structure, and species composition within the boreal forest (Morissette et al. 2002; Brandt et al. 2013). Stocks et al. (2003) noted that wildfires are necessary to ensure the continuity in the boreal dominant species; spruce, pine, and aspen. Eberhart and Woodard (1987) discussed the role of fires in providing a natural way of forest

restoration especially through the seed sources provided by the residual forest that are interspersed in a post-wildfire landscape. Forest fires can contribute to secondary succession and plant growth. The landscape heterogeneity and structure are often shaped by the location, frequency, and intensity of wildfires (Morissette et al. 2002). The successional stages of forest after a fire disturbance can accommodate larger and non-overlapping ranges for animals as distinct habitats are created (Morissette et al. 2002). In addition, wildfires control the pest population and eradicate diseases which affect healthy boreal forest.

Energy and biogeochemical cycles are kept in constant motion and renewal in landscapes affected by wildfire disturbances. Fires tend to renew the vegetation, reducing the old growth and mature forests, and releasing nutrients. This process becomes important in the boreal forest where decomposition of organic matter occurs at a slow rate; wildfires increase the rate of nutrient cycling and maintaining biological productivity (Brais et al. 2000; Berkes and Davidson-Hunt 2006). They are able to release nutrients that were locked up in leaves, needles, cones, and branches, which can all help in the regeneration of vegetation following wildfires. As stated previously, the boreal forest can contribute in regulating the global climate by storing carbon in soils, peat deposits, trees, and litter. One particular nutrient salt that benefits from wildfires is the ammonium ion (NH_4^+), which increases in post-fire boreal landscapes. Grogan et al. (2000) explained that the below-canopy vegetation burned during fires coupled with the scorching of the forest floor and mineralisation of organic matter can lead to the insurgence of NH_4^+. The plant community during regrowth benefits from this disturbance as it facilitates the conversion to nitrogen (Grogan et al. 2000). The ash remaining after a wildfire event is also nitrogen rich, enabling regeneration.

1.4.2 Negative Impacts of Wildfires

Forest fires have impacted the boreal region by heavily reducing commercial and private property value due to the loss of timber, cabins, and biomass burning. Wildfires can also pose severe health risks as a result of smoke hazards and possible dangers of combating fires (Akther and Hassan 2011). Wildfires become problematic for ecosystems as they increase greenhouse gas emissions, reduce biomass and biodiversity, decrease nutrient rich top soil, and facilitate soil erosion (Chu and Guo 2014). Forest fires are substantial disturbances as they contribute to the increased

carbon dioxide (CO_2) composition in the atmosphere, potentially affecting global climate. These problems center on the steady rise in atmospheric temperature which increases the probability of wildfires. A positive feedback mechanism can result as the increased fires release more carbon dioxide, which in turn increases atmospheric temperature via the greenhouse effect (Randerson et al. 2006). Wildfires can unlock the carbon stores through combustion of the biomass (Kasischke et al. 1995) and release them via CO_2 and methane; both of which are greenhouse gases. Hurteau et al. (2009) investigated that the carbon emissions from wildfires have led to a contribution of 4 to 6% in the annual anthropogenic emission of carbon.

Connections have already been drawn between increased fire activity and global climate change. By using the Seasonal Severity Rating (SSR), researchers have incorporated this measure of fire danger conditions in a fire season into Global Generation Circulation Models (Natural Resources Canada 2009) and predicted more frequent and severe forest fires. The SSR is a measure of the mean seasonal fire danger based on a daily estimate of the probability and intensity of fire occurrences (Flannigan et al. 2000) of a given site. The daily estimate is referred to as the Daily Severity Rating (DSR), which is calculated by averaging daily weather conditions (atmospheric temperature, relative humidity, wind speed, and accumulated precipitation) and the contribution of these conditions to fires (Durão and Soares 2010). The SSR also represents a key component in the design of the Canadian Forest Fire Weather Index (FWI), which is an approximation of the potential danger of fire for a particular fuel class (Flannigan et al. 2000).

The frequency and size of fire disturbance events are known to increase with warmer, drier weather conditions in the boreal region (Gerard et al. 2003). A doubling of the carbon dioxide concentrations in the atmosphere can lead to a potentially harmful positive feedback; resulting in a 50% fire danger increase, and a lengthening of the annual fire season by as much as 30 days in the Canadian boreal zone (Kasischke et al. 1995, Gerard et al. 2003). This is greatly adding to a fire season, which is relatively short in the boreal region and usually lasts from May to August (Fauria and Johnson 2008). Volney and Hirsch (2005) reiterated that the change in climatic conditions can increase the severity of droughts in many parts of Canada, hence increasing the fire activity, fire season, and fire danger conditions.

1.4.3 Progression of Wildfires

A wildfire event can completely or partially burn landscape elements, while some land cover features escape burning altogether. The disturbed landscape can be burned at varying intensities, and the resultant fire footprint with varying degrees of burn and scar severity would exhibit a complex heterogeneous landscape. The fire severity is explained as the degree to which the forest canopy is burned and depleted after a fire event (Román-Cuesta et al. 2009). Within the heterogeneous landscape there can be localized areas where the vegetation type and physiography can influence the fire severity and scars (Foster 1983). Some landscape features are naturally non-burnable firebreaks (e.g., lakes, streams, bedrock outcrops, and for the most part, wetlands), which impede the passage of fire (Foster 1983). Eberhart and Woodard (1987) suggested that these firebreaks tend to hinder the effectiveness and stability of fuel beds.

A reduced wind speed and/or a change in wind direction will prevent some areas from being subjected to burning. On a larger scale (for larger fires), Foster (1983) suggested that meteorological conditions, including wind speed and direction, are likely to influence the outcomes of burning especially over a longer time frame. The topography, weather, and fuel types all influence the fire's behavior and/or response to the wind. The fire spreads as embers are blown ahead of the fire front where combustible and unburned fuel types exist (Moon et al. 2013), and moderate slope angles facilitate the movement of flames. Other meteorological conditions, for example precipitation, and anthropogenic influences such as fire suppression can also limit fire spread.

The fire regime constitutes factors such as fire frequency, size, pattern, seasonality, intensity, and severity. Scale is important in explaining different levels of focus within the extent and the perimeter, as it takes into account the phenomenon under scrutiny, the sampling design, and the statistical analysis involved. The fire perimeter is the entire outer interface between burned and unburned areas (EUFOFINET 2012). The inside of this perimeter is considered the footprint and is the resultant impression created by a fire that burned within an area of fuel combustion (EUFOFINET 2012) (Figure 9). The fire perimeter can also be defined by, for example, a measurement based on Remmel and Perera (2009) that utilizes a focal sum moving

window across burned and unburned pixels in a raster image to obtain a footprint of the burned area that is then shrunk inward by 1 pixel to obtain the true position of the fire perimeter.

Mapping fire perimeters in Canada was first operationalized by the Canadian Forest Service and the Canada Centre for Remote Sensing. These divisions of Natural Resources Canada incorporate not just mapping fire occurrences but also fire monitoring and modelling in a system called Fire M3 (Lee et al. 2002). With the Fire M3 initiative, researchers are able to locate active wildfires, map the burned areas (within the footprint), and to model wildfire behaviour. The data were based on a coarse spatial resolution AVHRR imagery (1 km^2), which offered extensive coverage of Canada. This method was adopted in subsequent research in digitizing and mapping fire perimeters for Alaska (Kasischke et al. 1993). In Ontario, Remmel and Perera (2002) utilized the coarse resolution AVHRR data to assess the accuracy of fire occurrences (through polygons) when compared to digitized aerial photographs and hard copy maps.

The other fire management information system overseen by NRC is the Canadian Wildland Fire Information System (CWFIS). Since the 1970s both systems (Fire M3 and CWFIS) have utilized computer-based technology and in 1992 incorporated GIS technology, leading to the development of a spatial fire management system engine (sFMS) (Lee et al. 2002). This engine facilitates data management, analysis, modelling, and mapping.

Upon focusing on a smaller ecological scale an observation can be made that fire footprints contain a mosaic of land cover features that have escaped burning as a series of patches and corridors. These patches are relatively homogenous and non-linear, and can be distinguished from the surrounding landscape (Leitão et al. 2006). These patches within fire footprints can provide various ecological functions, including wildlife habitat, water storage, and nutrient sources. Corridors are similar to patches but possess a linear structure which contains a land cover type that is different from its surrounding landscape matrix (Forman 1995). They are considered as pathways for the movement of plants, animals, and nutrients (Leitão et al. 2006), and are important for the survival of species in post-fire conditions.

1.3 Residual Patches

Patches refer to any contiguous area that differs in appearance, form, and function from its surroundings (Forman and Godron 1986). These patches are known to have structures and compositions that differ from their surroundings (Forman and Godron 1986; Vogt et al. 2007). Patches can therefore be found within a forest matrix, which is a contiguous and relatively homogeneous forest layer (DeLong and Kessler 2000). The forest matrix would have a different structure, composition, and function from the remnants of a fire event. Perera et al. (2007) defined these remnants as post-fire residual structures (Figure 9), which are patches of a forest stand that did not burn completely to ash or gas in a fire event. This structure is an indication of the remnants of the forest community which existed before the fire event. Escapees are post-fire residuals that are completely unburned, owing to the fact that the fire was unable to reach those areas (Perera et al. 2007). Some areas may also be subjected to the fire but may only be partially burned; these are known as tolerant residuals (Perera et al. 2007). Some residual vegetation may have been impacted by fire but survived, and are referred to as resilient patches.

The vegetation pattern and structure, and the community of organisms are often affected by the passage of the wildfire. Foster (1983) further explained that the same vegetation, community, and topographic patterns and features have an influence on the passage of the wildfire. The effects of these factors were reiterated by Román-Cuesta et al. (2009); the topography and fuel types control fire behavior creating a mosaicked landscape with patches of burned and unburned vegetation.

Residual patches can be defined further in terms of their relationship with the fire perimeter. Insular residual patches are noted for being isolated from the fire perimeter boundary by at least 20 m (OMNR 2009). In addition, they are at least 0.25 ha in area, and are composed of mainly treed land cover (e.g. dense conifer, deciduous, and alder shrub) and consist of other vegetation types (e.g. marsh, low shrub, and open wetland) (OMNR 2009). Conversely, peninsular patches are unburned clusters that are found outside of the fire footprint but continue into the footprint (across the perimeter), as fingers into the burned matrix. They are found within 20 m of the fire perimeter (OMNR 2009).

In northern Ontario, the residual patches can be quite large and numerous, usually ranging from 250 ha to over 16500 ha (Watkins 2011). Foster (1983) suggested that larger fires exhibited more detail and unevenness in the landscape within the fire footprint as the wind speed, wind direction, topography and vegetation influence the progression of the fire. Within a specific residual patch there can be one or multiple land cover types, which are dependent on the classification criteria (Figure 9). The residual patches contribute to the heterogeneity of the landscape. The spatial heterogeneity is representative of natural interactions between communities and maintains a high level of biodiversity (Duning and Xiezhen 1999). The shape and type of patches can provide us with information on the natural progression of a disturbance event and how the landscape features can be left behind after the event. The composition and configuration of the heterogeneous nature of the patches facilitate regeneration, specifically in the forest-edge properties between mature stands and young successional forests (Roman-Cuesta et al. 2009).

Residual patches provide important ecological functions within a landscape disturbed by fires. Residual patches become remnant habitats and provide a source of seed stocks for maintaining the diversity of tree species. Wildfires allow for regeneration of vegetation through seed germination and seed dispersal. These processes control and maintain the age structure of forest, species composition, energy flows, and biogeochemical cycles (Chu and Guo 2014). The regeneration of plant and tree species is dependent on these surviving patches. The Ontario Forest Research Institute (2007) suggested that the ecological value of these trees is important, as they can represent habitat, den, and seed trees.

Fires can bring about the germination of seed stores in the soil, and facilitate the germination within the first year of the post-fire event (Keeley 1987). Fire tolerant tree species, such as jack pine and black spruce, have the properties to resist the direct effects of wildfires. Jack pine produces serotinous, resin-covered cones, while black spruce produces semi-serotinous cones, which open up and release their seeds during and after a fire event once the resins melt and allow the cone to open, thereby releasing their seeds (de Groot et al. 2002; Jayen et al. 2006). This mechanism of seed dispersal helps with the regeneration of these pine and spruce trees. Residual patches can act as

an ecological haven for other tree species which do not possess this serotinous feature, and these patches can facilitate the continuation and survival of certain tree species.

Forest fires are regarded as disease suppressors as they control the spread of pests and diseases in the boreal regime. These patches also provide required habitat for animals displaced by fires, and can provide important food resources during post-fire succession (Roman-Cuesta et al. 2009; Pasch and Koprowski 2011). Minerals can become exposed and made available to the soils after fire events. According to Akther and Hassan (2011), smaller fires tend to control the occurrences and spread of larger fires by minimizing the amount of dead vegetation. In addition, patches can prevent erosion and preserve the watershed dynamics in the fire footprint (Lathrop Jr. 1994).

Forest management and guideline in Ontario are practiced and implemented based on the composition and configuration of residual patches. The legal requirements when clear-cutting boreal forest is that 80% of the planned area should be less than 260 ha and insular patches should account for 2 to 8% of the proposed harvesting or managed area (depending on the forest cover type). When observing at patch level, the minimum patch size should be 0.25 ha, which matches the defined natural occurring patches. This patch area is large enough for detection on current satellite platforms used by the MNR.

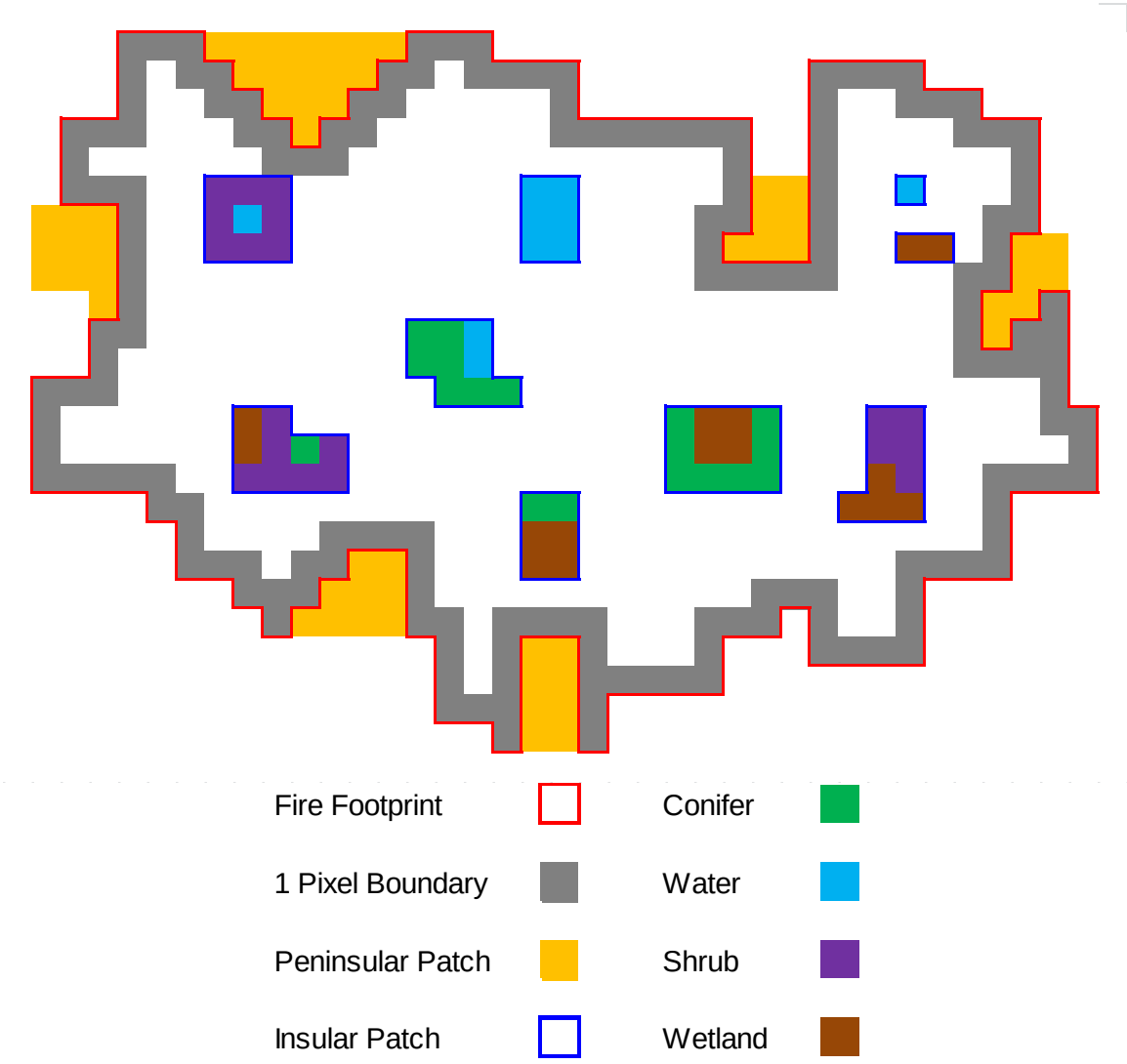

Figure 9. The fire footprint can contain residual patches that are unburned following a fire event.

1.4 Wildfire Mapping

Wildfire disturbances, insect infestations, and timber harvesting all impose varying levels of damage or change, often ranging from leaf level to landscape level (Attiwill 1994). The extent or size of the disturbance event can often influence the spatial resolution or mapping scale in which to accurately observe the event. A series of spatial resolutions can also be used to determine the most effective way of displaying the

elements of a disturbance and to compare how the disturbance patterns change with each spatial resolution. The severity and succession rate of the disturbed landscape have to be taken into consideration when choosing the scale and method in which to observe the disturbance; accurate detection and observation are a function of the spatial and temporal properties of the sensor used (Rogan and Chen 2004). Challenges can arise when observing heterogeneous landscapes as the variety of land cover classes and post-disturbance classes can limit how accurately we can observe and characterize post-disturbance patterns from remotely sensed images. Rogan and Miller (2006) suggested that using both GIS coverage and remotely sensed data prior to and after a disturbance is applicable in measuring and detecting the change in the landscape.

Numerous researchers have used satellite images in forest fire occurrence, wildfire spread and progression, and in post-fire pattern analysis (Chuvieco and Congalton 1989; Lasaponara and Lanorte 2007; Remmel and Perera 2009; Gairola et al. 2013). Kasischke et al. (2007) explained that there are generally 4 different classes in which remote sensing scientists can observe when studying fire: pre-fire environment (site characteristics prior to fire), fire environment (processes, behavior, and characteristics during the fire), post-fire environment (site characteristics immediately after the fire), and response (the biological, physical, and chemical responses from the environment as the ecosystem is impacted by the effects of the fire). These classes can be applied to the temporal scale of a fire event. Chuvieco and Cocero (1996) suggested that the applications of remote sensing techniques can be used for: short-term fire danger estimation, long-term fire risk valuation (both of these are closely related to pre-fire management), fire detection at the onset and during a fire event, and assessment of fire effects in a post-fire environment. In order to study residual patches, researchers use remotely sensed images to map the large extent of the fires, and then focus on a larger cartographic scale to observe residual patches. It is important to distinguish between the burned area and the unburned area, including residual patches. This discrimination between burned and unburned patches can lead to more accurate classification and characterization of the inherent patterns in the landscape.

Studying fires with large extents and long and complex perimeters can be very difficult using field-surveying methods to identify the land cover types in the study area. Large fire perimeters, isolated fires, and remote study areas which include some parts of

the boreal region are difficult to access and collect data via field methods, and hence present valid reasons for the use of satellite-based detection (French et al. 1994; Remmel and Perera 2001). Remmel and Perera (2001) described the inaccessibility, and remoteness of northern Ontario's boreal forest, which have researchers depending less on relatively expensive field surveying techniques for mapping fire perimeters. Frolking et al. (2009) reiterated that accessibility issues and the vast expanse of the large geographic scales of forests require appropriate large-scale satellite coverage. Remote sensing offers a timely, cost-efficient method of detecting fire occurrences and their inherent patterns, while providing different spatial scales, including local, regional, and global scales (Chu and Guo 2014). Limited accessibility to boreal forests coupled with the immense vastness of the wildfire perimeter encourages researchers to implement remote sensing technology rather than traditional methods (Gitas et al. 2012).

To accurately map the ignition and spread of wildfires factors such as fuel types can be categorized to predict the wildfire progression (Van Wagner 1977). In addition, topographic maps and digital elevation models (DEM) can be utilized to measure fire hazard variables such as slope angle, aspect, and elevation (Chuvieco and Congalton 1989). Ancillary data are actively being used in fire mapping studies, and are mainly in the form of meteorological data to assess pre-fire conditions, predicting which areas were more prone to fire ignition (Sunar and Ozkan 2001). These supporting data allow for early detection of wildfires in fire-prone regions and can be used to post early warnings and enact fire suppression.

The first use of remote sensing in the Canadian Forest Service was in aerial photography in the 1920s and 1930s (Leckie 1990). The detection of fires and mapping their progression improved in the 1960s with infrared scanners attached to aircrafts, becoming one of the main applications of GIS and remote sensing (Chuvieco and Congalton 1988; French et al. 1994). The implementation of GIS and remote sensing in forest fire mapping is timely and cost effective (Chuvieco and Congalton 1989; Remmel and Perera 2001; Sunar and Ozkan 2001). The launching of the Earth Resources Technology Satellite (ERTS 1) (renamed as Landsat 1) in 1972 allowed forest researchers to make use of the digital remote sensing technology in change detection (Leckie 1990). Even with the launch of the Landsat program, researchers were skeptical in using space-borne sensors for fuel mapping, as there was a likely difficulty in

detecting the understory component of vegetation (Chuvieco and Congalton 1989). An integrated approach was therefore required to link remotely sensed imagery with in-situ data so that fuel types and land cover types could be mapped more accurately. As a result, modelling the potential for fire ignition and fire hazard would be improved with validation data.

The mapping of the boreal zone is challenging as it comprises not only boreal tree cover but a wide array of terrestrial, aquatic, and riparian land cover types. Kasischke (1994) described the boreal zone in Alaska as being a region with rivers, lakes, peatlands, sub-alpine tundra, alpine tundra, and non-vegetated surfaces. Digitizing of hard copy maps that were obtained by rigorous aerial and ground surveys allows users to manage the boreal mapping in a GIS environment. The pioneering of specific GIS applications in the 1980s and 1990s was integral in the level of detail in the spatial information that can be achieved in Ontario's forests. Kasischke (1994) combined U.S. Geological Survey topographic maps and AVHRR (Advanced Very High Resolution Radiometer) satellite images to estimate both the boreal forest and the non-forested areas. The mapping of total burned areas in the boreal region is now more accurately completed with integrated GIS and ground validation information.

Burn detection during an event is one of the major applications of remote sensing in wildfire studies. Simple methods of visual interpretation with selected bands and more complex classification algorithm methods are often used in mapping burned areas (Chu and Guo 2014). The latter method is used for mapping both burned and unburned land cover within a fire perimeter. These techniques include unsupervised and supervised classifications, decision tree classifiers, image differencing, and thresholding of spectral indices. Michalek et al. (2000) performed a supervised classification on Landsat TM imagery, producing 3 classes of burn severity. They incorporated aerial photographs and field data to establish light, moderate, and severe classes. The Hotspot and NDVI (Normalized Difference Vegetation Index) Differencing Synergy (HANDS) algorithm for example, allowed users to detect hotspots in both pre-fire and post-fire AVHRR images based on the NDVI threshold values of brightness temperatures in the thermal infrared band (3.53 – 3.93 μm) (Fraser et al. 2000). Additional indices such as the Global Environmental Monitoring Index (GEMI) were tested to accurately map hotspots in a time series. Hotspots are image pixels which display intensities in the infrared band

indicating burning vegetation and they are used in active fire detection studies. Chuvieco et al. (2008) implemented the Burned Area Index (BAI) and near-infrared brightness values of a 10-day AVHRR composite image to detect hotspots. The BAI is a spectral index which identifies the burned areas in post-fire conditions by highlighting the brightest pixel values in the NIR region (Chuvieco et al. 2008).

1.5 Post-fire Analysis with Remote Sensing

Mapping the burned area in post-fire analysis is another major application in forest fire management. The flexibility of using satellite imagery is that images can be acquired on (or near) or before the date of ignition and at multiple time-steps for years after the end of the fire event. Bourgeau-Chavez et al. (1994) were able to map the fire scars in Alaskan boreal forests using radar imagery (ERS-1 SAR). They found that fire signatures can be detected in recent fire events between 1 and 5 years old, mainly due to higher backscatter values received for fire scars as compared to the unburned portion of the forests. French et al. (1994) similarly used the differences in spectral reflectance and greenness as calculated by the NDVI to observe fire scars over a 9 year span. The NDVI is effective in change detection of fire mapping, especially when compared with validation data (Remmel and Perera 2001).

An objective way in conducting post-fire observations would be to conduct field-based surveys on the burned and unburned areas of the site, primarily with the use of GPS units (Corona et al. 2008). Extensive vegetation cover and orographic features can affect the signals between GPS receivers and satellites (Corona et al. 2008). The errors resulting from the poor signals can reduce the accuracy of the location of features being collected. Access to the residual patches in rugged terrain and seasonally flooded environments is often difficult and large wildfire extents can make field-based surveys onerous and costly. Remote sensing-based surveys in the form of aerial photography and Earth observation satellite imaging are advantageous over field-based observations, as they mitigate and/or minimize these problems by providing users with greater control over the selecting of potential sample sites. The use of aerial photography is beneficial in understanding past trends in burned areas, especially when an individual burn can be observed up to 100 years on an aerial photo (Foster 1983). Foster (1983) suggested

that air photos are the most accurate source of recorded fire events, and in the 1980s provided researchers with a very complete account of fire occurrences.

The spatial resolution in wildfire mapping is important in detecting each land cover found within post-fire conditions. Remmel and Perera (2009) explained that the nature of a wildfire requires more stringent selection of spatial resolutions with which to observe them as the edges of wildfires are never discrete. The data representation used, along with the scaling, can result in varying depictions of the mapped area and perimeter (Remmel and Perera 2009). The level of detail required and size of the footprint and perimeter can determine the spatial resolution. High spatial resolution (20-30 m) sensors such as Landsat Enhanced Thematic Mapper (ETM+) and SPOT (Systeme Pour l'Observation de la Terre) are equipped for detailed mapping purposes (Fraser et al. 2005). However, the costs and processing requirements can be expensive and the time spent in processing can be highly variable. Low spatial resolution sensors (approximately 1 km) can be utilized for regional and global scales while providing daily coverage of the study area (Fraser et al. 2005). However, the coarse spatial resolution would not be appropriate for detection and inventory of the ecosystem level. There can be difficulty in accurately mapping land cover features with coarser spatial resolution satellite imagery and specifically in classifying land cover features in partially burned fire footprints. Chuvieco and Congalton (1988) explained that there is a tendency for discrepancies in differentiating between slightly or partially burned and non-burned vegetation; and within transition areas. The selection of the satellite sensor is indicative and reflective of the scale and size of the wildfire being observed. Medium to high spatial resolution sensors are often used to map local scales in boreal environments; satellite sensors such as Landsat TM (Thematic Mapper) and ETM+ (Enhanced Thematic Mapper Plus). Regional and global scales of boreal regions can be mapped for the burned areas by medium to low spatial resolution sensors; for example AVHRR, MODIS (Moderate Resolution Imaging Spectroradiometer), and SPOT (Chu and Guo 2014).

In addition to studying burned areas in post-fire environments, researchers also study how the forests have responded to the disturbance. Forest succession, regeneration, structure, and recovery after a wildfire disturbance can be observed and monitored in terms of their patterns and spatial variability (Gitas et al. 2012). Post-fire

regeneration is most effectively mapped when vegetation indices are used in image analysis. The difference in above-ground vegetation and canopy, and the substrate can be detected using the NDVI or Soil Adjusted Vegetation Index (SAVI) (Qi et al. 1994). The recovery and structural detection will depend on the amount of vegetation cover and spatial heterogeneity, which can be a result of the species composition, richness, and community diversity (Kazanis and Arianoutsou 2004). The improvements in airborne and spaceborne sensors have allowed researchers to observe these patterns with greater spatial, temporal, and spectral resolution.

Large wildfires have important effects on the ecology of boreal landscapes, and residual patches are indicative of the potential recovery of both plants and animals after a wildfire event. Eberhart and Woodard (1987) argued that given the importance of these residual patches in landscape ecology, there has not been sufficient research on the properties and characteristics of residual patches. They further discussed that the effects of wildfire events have been documented in studies involving the disturbed or burned areas. Mapping and characterizing post-fire residual patches, especially vegetation, provide forest managers with vital information as to strategize and reestablish vegetation after large disturbances (Eberhart and Woodard 1987). These post-fire residual maps can help us to understand how ecological communities recover and how these communities are impacted by disturbances.

In order to study residual patches, some researchers obtain, process, and analyze high spatial resolution remotely sensed imagery. Researchers are able to capture the spatial heterogeneity of the patches by measuring and characterizing their composition and structure. Satellite imagery and aerial photos are used to extract the residual patches and then GIS software is used to analyze the spatial patterns within those residuals. Typically spatial data layers of these images can be stored and manipulated in a GIS environment (Wang et al. 2012); the landscape composition and structure can be measured via spatial analyst tools, spatial statistics, landscape pattern metric calculation tools, and land cover classification results.

A higher spatial resolution dataset can provide substantial spatial detail of residual patches. Using 25 m spatial resolution Landsat data, Burton et al. (2008) were able to comprehensively classify land cover types and delineate unburned islands within wildfire extents greater than 200 ha in the Canadian boreal region from 1959 to 1999.

Furthermore, they consistently found that the unburned patches contained a higher composition of wetland-herb, broadleaf vegetation and dense mixedwood forest cover types than the burned patches. Burton et al. (2008) concluded that coniferous forest, grasslands, and sedge cover burned more than other vegetation cover types in wildfires. The deductions were made at a 25 m spatial resolution, and the composition within residuals may change when observing the boreal forest at higher and lower spatial resolutions. Burton et al. (2008) suggested that the patterns created and shaped from wildfires can generate varying degrees of landscape heterogeneity hence multiple scales of observation have to be considered. The grain sizes can help to explain how these patterns change across larger ecozones and within smaller isolated fires.

Kachmar and Sánchez-Azofeifa (2006) mapped out the residual patches of the Chisholm fire event in the northern boreal forests of Alberta using 28.5 m spatial resolution Landsat ETM+ data and a higher spatial resolution (4 m) IKONOS imagery. They explained that previous studies concentrated on qualitative descriptions of the fire perimeter, which only observed unburned and burned areas. A more expansive comparison can be made with different spatial resolutions of the same study site. Kachmar and Sánchez-Azofeifa (2006) observed how the 2 satellite sensors differed in the level of spatial detail that can be represented. The residual forest patches were observed as individual patches when 4 m IKONOS imagery was used, while those same patches were only detected as a collective, contiguous patch with 28.5 m Landsat ETM+ imagery (Kachmar and Sánchez-Azofeifa 2006). This representation influenced the residual size, shape, and number that can be quantified by patch metrics such as patch number, mean patch size, and patch shape. Observations of the same landscape with different spatial resolutions can more comprehensively illustrate the patterns in a post-fire disturbance.

Our project deals with a single remote sensing platform's coverage of a wildfire disturbance and aggregating the spatial resolution to obtain 5 grain sizes and then asses how the morphology of land cover within residual patches changes. The measurements of composition and configuration at different grain sizes within wildfire residual patches can lead to an understanding of how we can emulate those spatial patterns when harvesting forest stands. These measurements can be used to provide rules and guidelines to base the harvesting practices on as the effects of harvesting are similar to

the effects of wildfire disturbances. Quantifying spatial patterns in naturally disturbed settings can lead to the emulation of such patterns when managing anthropogenic disturbances, like selective cutting and conservation planning.

1.6 Emulating Natural Disturbances (END)

1.6.1 Definition

The term emulation in landscape management is defined as the ability to mimic the layout and characteristics of the natural landscape (Kimmins 2004). Landscape planners in an attempt to emulate natural disturbances can manage and modify the landscape components in a way that would reflect the layout of the landscape in a post-disturbance setting. The OMNR (2001) described END as the need to simulate the natural disturbance patterns when managing forested landscapes, and to simulate the wildlife settings and structural appearance of the natural landscape. Fuhrer (2000) further described the term emulation as the process of managing a landscape section and equaling the effects of a natural disturbance within that studied landscape. Emulation can be used interchangeably with the term mimic; hence the goal for forest managers would be to equal the disturbed landscape with a managed landscape.

Kimmins (2004) described the emulation of natural disturbance as spatially and temporally managing an ecosystem to mimic the biotic and abiotic effects of a disturbance event on a similar ecosystem. The management of the ecosystem is also based on the frequency and intensity of the effects of the disturbance event. Perera and Buse (2014) expanded on END, elaborating that with the appropriate spatial and temporal scales, forest managers can develop and implement tactics and approaches to produce a managed forest landscape that can be similar in structure and function to a naturally disturbed landscape. The ultimate goal is to produce forested landscapes that can mirror (or as close as possible) the ecosystems resulting from natural disturbances (Perera and Buse 2014). Andison (2012) explained that emulation can help to propose forest management guidelines with the intention of connecting spatial patterns (from natural and anthropogenic disturbances) with biological and ecological benefits. The proposed goals of END are to achieve the patterns, functions, successional progression, and conditions of the managed ecosystem with the disturbed ecosystem (Kimmins

2004). The spatial and temporal resolutions can be determined to complete the prescribed END.

1.6.2 Background

Hunter (1993) explored the concept of understanding how fires and insects can shape landscape patterns and processes, and how we can use this information to manage forests. In the early 1990s, the Ontario Forest Policy Panel facilitated the feedback of forest managers and the general public in how forest management can be improved (Hunter 1993). This gave rise to the CFSA which suggested how forest practices and management can be used to emulate the natural disturbances in Ontario's Crown land.

The planners and policy makers were required to make a decision on which natural disturbance was best suited to emulate in the boreal forest. It was therefore important to gather available data and information on the types and frequencies of disturbances affecting boreal forests (McNicol and Baker 2004). The data were based on a 30 year period of recorded fires from 1920 to 1950, and were at least 200 ha in size. This timeline was chosen as more recent fires (from 1950 to present) were often affected by humans, especially by ignition and suppression. Data from insect infestations were unavailable during this time period and hence were not used to develop the guidelines. In addition, wildfires unlike insect or disease infestations are able to destroy most of the standing structure of trees and are minor in comparison to the effects of clearcutting (McNicol and Baker 2004).

1.6.3 Rationale for END

Perera et al. (2004) described emulating natural disturbance as an approach in which forest managers and planners can develop and implement certain policies and strategies that allow forest ecosystems to operate structurally and functionally analogous to the ecosystems' response to natural disturbances. These practices should be conducted on the appropriate spatial and temporal scales to achieve the most suitable simulation of the various levels of the forest ecosystem. The spatial patterns within residual patches provide explicit representations of the landscape patterns manifested

by natural disturbances (Baldwin et al. 2004). Emulation of these spatial patterns and structures by forest harvesting practices is deemed feasible to allow more natural and faster recovery of landscapes, while maintaining ecosystem integrity. Emulating natural disturbances helps to maintain the long term health and state of Crown forests; and hence reducing the adverse effects on plants, animals, hydrology, lithosphere, atmosphere, and social and economic values (OMNR 2014). The implementation of END can be conducted when the residual forest (post-fire disturbance landscapes) are quantified in terms of their size, shape, composition, and configuration (OMNR 2010). In order to achieve this, remote sensing techniques and landscape metrics can be used to measure the spatial pattern elements in the footprint.

There is a need to understand natural landscape disturbances, as emulation strategies can be implemented in resource management applications to minimize the risks involved with ecosystem degradation and subsequent regeneration (Baldwin et al. 2004). Managed or human influenced disturbances (including harvesting) can be planned in different ways to mimic natural disturbances. The principle behind this design is that the forest biota have always adapted to and are adapting to natural disturbances. Therefore, the ecological changes that are associated with timber harvesting are not as destructive if harvesting patterns resemble the patterns produced by natural disturbances (DeLong and Tanner 1996).

This research is centered on the spatial patterns that exist within the residual patches. The sensitivity and response of the spatial patterns based on morphological indices are dependent on the properties of the input data (Baldwin et al. 2004). A wildfire residual when observed at various scales (manipulated by altering the spatial resolution) can characterize the landscape, and will allow forest managers to emulate a natural process through harvesting blocks of various sizes, shapes, configurations, and compositions. Therefore, a spatial pattern analysis can be applied in assessing the type and abundance of land cover, specifically tree species that should be preserved when selectively harvesting forest blocks.

In order to complete the emulation process, researchers in Ontario must adhere to legal requirements of the Crown Forest Sustainability Act (CFSA) (OMNR 2014). The CFSA is a policy (legislative) document that serves the purpose of ensuring the long-term health of forest ecosystems, and providing for material and social needs. This

forest management guide in Ontario is based on 2 principles; one which maintains the healthy, productive Crown forests, and conserves their ecological mechanisms and biodiversity (OMNR 2014). The other principle focuses on emulating natural disturbances and landscape patterns through silvicultural practices and guidelines, while maintaining the forest, environmental, social and economic values (OMNR 2014).

1.6.4 Coarse and Fine Filter Approaches

The coarse and fine filter management approach is implemented in the CFSA framework. The landscape patterns created by silvicultural practices are the coarse filters, which aim to achieve healthy, productive forests (OMNR 2014). The coarse filter is based on the emulation of natural disturbances and the resultant landscape patterns, which are deemed as the overall goal in forest management in Ontario (OMNR 2014). The pattern, composition, and structure are the overlying forest management factors by which the coarse filter approach focuses on. Some examples of coarse filter considerations that should be made when applying emulation of natural disturbance patterns are forest composition, age class structure, forest patches, residual patches, and residual trees (OMNR 2001).

The fine filters target the potential effects of these practices and emulation strategies on the flora and fauna community, abiotic factors, physiography, economic, heritage, and recreational factors (OMNR 2014). Fine filters are the specific components that are designed for different habitats; a site specific approach. These components can include the vulnerable, threatened, and endangered species (e.g., patch size considerations for caribou and site-specific habitat protection for bald eagle and ginseng), and featured species (e.g., marten and moose habitat at the landscape level) (OMNR 2001). Woodland caribou have variable ecological ranges, in the summer they can be found in a range of 25 km^2, and in the winter it can extend to 390 km^2 (Racey et al. 1999). Therefore, a range between 6000 ha and 30000 ha for caribou refuge and winter habitat should be maintained to protect and induce species' survival (OMNR 2014). Bald eagles require habitat patches of 255 ha, consisting of contiguous deciduous and mixed vegetation near large lakes or rivers (James 1984). In addition, bald eagles prefer island patches within lakes so as to avoid potential fire and logging disturbances on their nesting sites (James 1984). Ginseng patches of ≥ 20 ginseng

plants and ≤ 120 m habitat radius should be preserved, with potential harvesting of trees occurring no less than 20 m from the patch (OMNR 2010). Moose habitats generally thrive best in a predominantly young forest interspersed with older forest with patch sizes ranging from 10 to 500 ha (OMNR 2010). One goal of the fine filter is to encourage the increase in rare plant species and breeding sites for rare animal species. Forest management through fine filters maximizes the regeneration of forest stands by allowing sufficient time between harvesting cycles.

Table 1. A few examples of coarse and fine filter applications in emulating natural disturbance patterns in the boreal forest.

Coarse Filters	**Fine Filters**
Forest Composition	Vulnerable, Threatened and Endangered Species
Maintaining habitats	*Habitat protection e.g. bald eagle, ginseng*
	Patch size e.g. caribou herds
Age Class Structure	
Maintenance of old growth forest	Featured Species
	Site-specific habitat protection e.g. moose feeding sites, osprey nests
Forest Patches	*Landscape-level habitat management e.g. moose, marten*
Configuration	
Size	
Placement	
Prescribed burns	
Residual Patches	
Peninsular	
Insular	

Source: Forest Management Guide for Natural Disturbance Pattern Emulation (OMNR 2001).

1.6.5 Implementing END

Guidelines of the END need to be explicit to control and determine the area and distribution of the forest clearcuts (McNicol and Baker 2004). According to the NDPE

(Natural Disturbance Pattern Emulation) Guide, insular residual patches should be retained when the minimum patch size is 0.25 ha, and the total number of patches should account for about 2 to 8% of the planned disturbance area (as determined by the forest type, the scale, and spatial resolution of the site) (OMNR 2001; OMNR 2009). However, there is ambiguity in the guidelines which suggest that residual patches should be well distributed within the harvested areas; there are no discrete values or arrangement of how these patches are distributed.

The practical guidelines of implementing an END plan are based on the frequency and size class of the disturbance patterns; comparing the measurements from the naturally disturbed landscape with the anthropogenic disturbed landscape. Initially, the first draft of these guidelines proposed that the frequency and size class were to be used in the managed forest site. A finalized draft suggested a limitation on the size of clearcuts in Ontario: about 80% of clearcuts in the boreal region should be no greater than 260 ha. Table 2 below shows the specifications of the practical guidelines of END in Ontario.

Table 2. The OMNR uses information gathered from forest disturbances to implement the following guidelines when harvesting forest stands.

Factors	**Forest Disturbance**	**Individual Clearcuts**
Maximum size (ha)	10,000	1,000
Time frame for creation	≤ 20 years	≤ 3 years
Distance between	200 – 5,000 m (depending on size of disturbance)	200 – 500 m
Time between adjacent harvest areas	20 years	20 years (or at 3 m tall regeneration of trees)
Acceptable break between cuts	10 – 10,000 ha: at least 200 – 300 m of young forest, 3 m in height1,001 – 10,000 ha: at least 70% break in immature forest (≥ 6 m in height)	500 m, with ≤ 300 m would be young forest (3 m in height)

Source: McNicol & Baker (2004). Emulating Natural Forest Disturbance: From Policy to Practical Guidance in Ontario.

1.7 Landscape Pattern Measurement

Forman and Godron (1986) defined landscape ecology as the spatial relationships that exist among the components of a given landscape; these elements can include ecosystems, species, and energy or nutrient flows operating at different scales and time. Moreover, landscape ecology explores the change in structure and function when impacted by natural and anthropogenic disturbances (Forman and Godron 1986). McGarigal and Marks (1995) focused on the pattern-process dynamics and defined landscape ecology as the study of landscape patterns and the interactions among processes within and among patches contained by a landscape mosaic. Turner (1990) elaborated that these patterns represent the ecological functions of the landscape components, which include ecosystems, habitats, and communities. Landscape ecology often requires statistical tools to identify patterns that depict community behaviour, diversity, community structure, and landscape structure (Fortin et al. 2003). It is by identifying and comparing the configuration and composition of these patterns that researchers can make inferences about the ecological processes.

Composition and configuration are important spatial pattern descriptors in landscape ecology and more specifically forest management (Wang et al. 2012). Remmel and Csillag (2003) define the term composition as a way to characterize the different categorical groups (colours) in a landscape as portrayed on a classified satellite image. Generally, composition states how different or variable landscape elements are (Remmel and Csillag 2003). In terms of mapping, composition refers to the number of classes in a given landscape and the proportion of each class with respect to the entire map (Gustafson 1998). The way these classes or elements are distributed or arranged in space is defined as configuration (Remmel and Csillag 2003). More specifically, configuration refers to the shape, size and arrangement of patches and land cover features within a landscape (Wang et al. 2012). Spatial patterns in disturbed landscapes can be quantified and mapped, providing information on the changes in composition and configuration and hence reflecting on the behavior of ecological processes on ecosystems.

Gustafson (1998) suggested that there is an increasing demand in measuring and monitoring landscape patterns and processes, as it is often hypothesized that landscape patterns are linked to ecological processes. These interactions and patterns

change over time and space. Turner (1989) stated that spatial and temporal scales have to be considered in studying landscapes due to the spatial heterogeneity that exists in nature. While the relationship between the spatial structure and process is important in landscape ecological research, there is still a need to understand the advantages and limitations of spatial data representation on the structure-process (and function) relationship.

1.7.1 Scaling and Pattern Measurement

Scale is an important factor to consider when studying spatial patterns in landscapes. O'Neill et al. (1986) observed this importance in observing landscapes and the components within them, and suggested that researchers need to observe the spatial scale at which the environment responds to, and not the space in which humans operate. The difficulty in choosing an appropriate scale or scales for describing landscape patterns is as a result of scale being multi-dimensional; it incorporates extent, grain size and thematic resolution (Šímová and Gdulová 2012). Multi-scale approaches to landscape pattern and metric measurements have to be considered. Many researchers have investigated how the landscape patterns and composition change when altering the scale and extent of the observation (Turner et al. 1989, Cullinan and Thomas 1992, Qi and Wu 1996). However, there is some uncertainty in how landscape patterns respond to a change in scale and extent. Cullinan and Thomas (1992) defined scale as the area of coverage and corresponding minimum mapping unit set by the limits of the observer. In an ecological context, the scale can be represented by the extent of an ecological phenomenon which incorporates the ecological interactions being studied (Cullinan and Thomas 1992).

The terms grain size and spatial resolution are often used interchangeably with scale. Grain size will be referred to as the spatial resolution of the data and more specifically, the minimum mapping unit or pixel size (Gustafson 1998). The problem with studying landscape patterns with one scale or grain size may result in inconclusive findings. Landscape elements are scale dependent, and pattern measures such as total number of patches, total patch area, average patch size, and landscape or patch perimeter can change when mapping at different grain sizes (Hengl 2006). Hengl (2006) further noted that landscape pattern analysis can benefit from spatial aggregation as to

reduce small scale irregularities and also to generate a more thorough understanding of general patterns. Landscape heterogeneity is scale dependent, and one scale may only be appropriate for one level of studying landscape patterns (Cullinan and Thomas 1992). A lack of multi-scale design or using an improper scale may lead to misleading results of landscape patterns. These unsound conclusions have resulted in detrimental planning practices in forest management, conservation authorities, land use management, and urban planning (Šímová and Gdulová 2012).

Landscape patterns and their inherent proportions of land cover classes are dependent on map scale or the scale at which those patterns are observed. Landscape structure, composition, and function can be partly explained in terms of their scaling relationships through grain size and extent (Wu et al. 2000; Dale et al. 2002; Wu 2004). A collection of landscape metrics were analyzed by Wu et al. (2002) and Wu (2004) to test their response to scaling operations. In both studies, the spatial aggregation was conducted based on an independent aggregation scheme which increases the grain size of each dataset (4 raster images used) based on the finest grain size of the original image. The increase in pixel size was conducted by systematically increasing each pixel side by 1 on a 30 m Landsat image until a 100 × 100 grain size was achieved (Wu et al. 2002; Wu et al. 2004). The areal extent of each raster image was also kept constant to match the original (starting) image (Wu et al. 2002; Wu et al. 2004). The metrics were mainly affected by changing the grain size in a response that was predictable. Changing the areal extent of the landscape was unpredictable in the responses of the landscape metrics (Wu and Hobbs 2007). We can better understand landscape patterns and the way they change and transform when encountered with different datasets (with different spatial resolutions).

Features and processes that may be considered as important at one scale are sometimes not important or predictive when observed at a different scale. Wickham and Riitters (1995) found that certain land cover types, such as transportation lines, decreased gradually as the pixel size increased from 12 to 28 m, and then disappearing altogether at 80 m spatial resolution. However, when observing landscape metrics and their behavior towards increasing grain size, Wickham and Riitters (1995) found that most of the metrics they used were not dependent on grain size. This suggests that multi-scale approaches to landscape pattern measurement may not yield results that

reflect the diversity in common metrics. Conversely, studies conducted by Wu et al. (2002) resulted in some landscape metrics (12 out of a possible 19 reviewed metrics) being affected by the change in grain size. These metrics included NP, PD, TE, ED, LSI, MPS, and LPI; they were found to have predictable reactions to basic scaling operations (Wu et al. 2002). A more unpredictable result could be generated by identifying different map scales in which to change; these include grain size, map extent, and number of attribute classes (Riitters et al. 1995). Key landscape metrics need to be assessed initially, and the elimination of additional metrics, which can be strongly correlated, may be necessary (Riitters et al. 1995).

Turner (1990) found that as spatial resolution is lowered, information on the less dominant land cover components were lost. Qi and Wu (1996) observed a decrease in spatial autocorrelation among 3 pattern indices as the spatial resolution was decreased; this scaling process can improve our understanding of ecological processes as spatial relationships are observed from micro to macro scales. Micro scales can range from 0.0001 ha to 100 ha (Delcourt and Delcourt 1988) and can allow us to examine differences in soil, vegetation, and weather (micro-climatic) conditions (Du-ning and Xiu-zhen 1999). The macro scales correspond to a range of 10^6 ha to 10^8 ha of landscape surface (Delcourt and Delcourt 1988) and generally reflect a regional or global climatic zone (Du-ning and Xiu-zhen 1999). Therefore we can characterize and map landscape patterns spanning from individual trees to large swaths of forest cover. Clustered land cover components tend to have their information preserved when the grain size is increased, while dispersed land cover components' information may be lost (Turner 1990). O'Neill et al. (1996) added that complications can arise when observing a heterogeneous landscape consisting of patches of various sizes with only one grain size. Generally, patches that may be smaller than the grain size used can be lost or misclassified as another land cover type (O'Neill et al. 1996). The lowering of the spatial resolution also affects the smaller patches by combining them with larger ones or by losing them altogether (Saura 2004). The values of the landscape metrics calculated for smaller patches may not be constructive when operating at larger grain sizes (Saura 2004).

1.7.2 Landscape Metrics

Landscape ecology explores the relationship and interactions between pattern and process (Li and Wu 2004). This principle explains the idea that processes occurring in a given landscape generate, alter and maintain patterns, while in return those patterns limit, stimulate, and neutralize ecological processes (Li and Wu 2004). In terms of wildfire process and post-fire landscape patterns, wildfires are the disturbance process that shapes the vegetation pattern and distribution. In turn, the existing (pre-fire) or resultant (post-fire) vegetation and land cover affects the wildfire process and its ability to disturb the landscape.

In order to study landscape patterns, researchers have computed landscape metrics that quantify the composition and configuration of the landscape (McGarigal and Marks 1995; Haines-Young and Chopping 1996; Uuemaa et al. 2009). The information that landscape metrics provide can be used to make interpretations of ecological processes and patterns within a given landscape mosaic (Haines-Young and Chopping 1996). The computation of these metrics can be based on the entire landscape, the attribute classes of the patches or refined to each attribute class within a patch (McGarigal and Marks 1995; Riitters et al. 2005; McGarigal 2013). This gave rise to the term patch metrics, which summarize the shape or size of patches. Furthermore, neighbour metrics were developed to quantify the spatial relationships existing among patches and the objects found in patches (Turner et al. 2001).

There are 4 different hierarchal levels of landscape metrics: cell-level, patch-level, class-level, and landscape-level. Occurring in raster images at the smallest or most accurate grid size, cell-level metrics characterize the spatial patterns for each given cell (McGarigal 2013). Cell-level metrics are often computed by identifying a group of nearby cells or focal cells, which would provide information on the inherent spatial pattern of the location. Each cell would therefore have a specific metric value, which is the same as the surrounding cells (depending on the focal window size). Patch-level metrics are designed to characterize the spatial pattern for individual patches (McGarigal 2013), therefore each patch can display a single metric value. Class-level metrics provide spatial information on landscape patches at a specific land cover type (or associated class) (Wu 2004; Remmel and Fortin 2013). Each land cover type or class will then have a specific metric value (Remmel and Fortin 2013). Landscape-level

metrics take the entire landscape into consideration, quantifying the spatial composition and configuration for all patches within the landscape (Wu 2004). Sometimes in a given landscape analysis study we are unable to identify which metrics or metric levels should be used to characterize the landscape and its patches. A highly selective and smaller number of metrics may be generally required to extensively quantify the landscape patterns (Cushman et al. 2008).

There are several factors that we consider when computing a specific metric; these include the boundary, components, and extent of the landscape, and the spatial grain at which the landscape is being observed (McGarigal 2013). The landscape and its inherent patterns are connected to ecological processes, for example fire disturbances, and to flora and fauna habitats and communities. The connection between the metrics selected and these processes is important in understanding the research goals and methods of the landscape pattern analysis. The choice of choosing between structural and functional landscape metrics (or both) can signify whether there is emphasis on the organism, process or physical composition in the landscape or patch. A structural metric quantifies the physical composition or configuration of a patch and/or landscape element (or class) while the functional metric measures the landscape pattern with specific relevance to the ecological processes or organism(s) inhabiting that landscape (McGarigal 2013). McGarigal (2013) stated that the type of data being collected and the method of data collection will highlight these research objectives, and hence the correct metrics can be implemented.

Various spatial pattern analyses have been designed to monitor and analyze the landscape structure. Landscape metrics have been incorporated into GIS software to quantify landscape composition and configuration (Uuemaa et al. 2009). These linkages are common in r.le (Baker and Cui 1992) and FRAGSTATS (McGarigal and Marks 1995). Westervelt (2004) utilized the software GRASS GIS to analyze land use changes and vegetative cover disturbances, such as forest fires. The metrics computed by r.le are able to observe the spatial and temporal relationships within landscapes, and provided the user with an integrated environment to model spatial processes (Mitasova et al. 1995).

FRAGSTATS computes landscape metrics within the structure, composition, and configurations of a landscape (McGarigal and Marks 1995). This tool quantifies the

spatial heterogeneity in the landscape under study. It also gives consideration to the spatial resolution of the input categorical map. The limitation to using FRAGSTATS is that many landscape metrics are highly correlated, leading to a less intuitive observation of the landscape patterns. Riitters et al. (1995) observed the redundancy of several metrics when assessing the accuracy of landscape pattern indices, such as patch density and mean patch size, which explain the same landscape pattern. Riitters et al.'s (1995) factor analysis study was unable to determine which landscape metrics were the most relevant, which is dependent on the goal of the study and the level at which the landscape is being observed (cell, patch, class or landscape).

SPAN (Spatial Analysis Program) was developed by Turner (1990) to measure the types of landscape patterns and their changes. Similar to other tools, SPAN requires categorical data input and has the allowance for the user to change the spatial resolution of the dataset. This program is flexible in that it measures the proportion of each land cover type while calculating the nearest neighbour probabilities among those classes (Turner 1990). In addition, SPAN measures patch metrics, such as patch size and mean patch size, and ecological indices, such as dominance, diversity, and contagion (Turner 1990).

The r.le (for GRASS GIS) characterizes the spatial patterns found within landscapes. r.le measures patch, core, perimeter, and shape metrics. The sampling area used in r.le can be modified in terms of its shape, size, number, and distribution to suit the purpose of the study (Baker 2001), which allows for increased flexibility in landscape pattern analysis. The sampling area can be altered by the user to encompass the entire extent of the map, geographical regions, a fixed pixel size (scale) and shape, or a moving window (Baker 2001). Moreover, the moving window sampling can account for variations in the distribution in land cover types across the study area and this window can be altered in grid size to provide a more dynamic and detailed landscape pattern analysis.

1.7.3 Effectiveness of Landscape Metrics

One landscape index cannot explain the joint complexity of composition and configuration for a given landscape, hence a set of metrics is often used to conduct landscape pattern analyses. Turner et al. (2001) argued that we have to be aware of the

number of useful metrics being used and that their combination should be able to explain the landscape pattern. The comprehensive factor analysis of landscape metrics of Riitters et al. (1995) presented a way by which a limited (but useful) number of individual metrics can be identified due to high correlation in metrics. The key goal is to minimize the redundancy in these metrics and select the major ones that can describe pattern variability at different scales and location (Turner et al. 2001).

Cushman et al. (2008) investigated the effectiveness of landscape metrics using FRAGSTATS, concluding that the entire landscape structure can be described and quantified using only 8 combinations of metrics. The current list of landscape metrics does not entirely explain the diverse range of landscape patterns (Uuemaa et al. 2009). Many of these metrics are strongly correlated, quantifying similar variables. Remmel and Csillag (2003) simulated 27000 binary landscapes with varying proportions of foreground to background pixels (increments of 10% from 10-90%), and calculated various landscape pattern indices, including number of patches, contagion, and edge density. They found that even when the landscapes were simulated varying spatial autocorrelation, differentiating landscape by pattern indices was often difficult (Remmel and Csillag 2003). Therefore, the different configurations have not been effectively measured within the landscapes. There is also difficulty in comparing and choosing metrics when moving from one scale to another, owing to the large variability and high correlation of metrics and indices. Metrics can then be more meaningful in their quantification of spatial patterns if they are calculated across multiple scales. The issue of scale should be considered in describing and quantifying landscape patterns.

A reoccurring issue in applying a specific landscape metric to a spatial pattern analysis is that the spatial scale at which patterns and processes occur may differ (Wu 1999). The process-pattern principle cannot function with interactions at different spatial and temporal scales. The type of phenomenon being studied and the purpose of the study need to be clearly stated in order to determine the spatial scale to use and the time period in which to record or observe the inherent patterns. The complex spatial heterogeneity of a disturbed landscape requires that the characteristics be quantified at multiple scales (Li and Wu 2004). Landscape indices would not be able to detect these patterns adequately with just one scale or level of observation.

Spatial heterogeneity can be observed in landscapes impacted by disturbances. Kashian et al. (2004) found that fires result in a heterogeneous structure imprinted on the landscape. Disturbances such as fires can fragment and disconnect the landscape, altering the structure and configuration of the landscape (Uuemaa et al. 2009). Habitat fragmentation is an ecological process involving the transformation of a larger habitat into smaller habitat patches that are often isolated from each other (Fahrig 2003). The habitat pattern is affected by fragmentation in 4 main ways: 1) habitat reduction, 2) increase in habitat patch number, 3) decrease in area of habitat patches, and 4) increase in habitat patch isolation (Fahrig 2003). Fragmentation is generally viewed at the landscape-scale due to the size of the disturbances (e.g. wildfires and harvesting), and the patch-scale observation becomes limited due to smaller sample sizes (Fahrig 2003). Moreover, the structure, composition, and configuration of post-fire landscapes can be quantified using landscape metrics. This provides information on the factors which determine fire spread, as patch measurement can reveal the size and shape of unburned land cover types. Wang et al. (2012) focused on the most explicit and descriptive metrics, which quantify fire footprint fragments, and divided the metrics into groups of shape, core area, spatial, and matrix indices. Wang et al. (2012) suggested that the distribution of the patches is reflective of the propagation of the disturbance agent, such as a wildfire. Similarly, Turner (1990) was keen on the spread of the disturbance, which can be indicated by the landscape pattern in a post-disturbance environment. This makes use of landscape pattern analysis that takes into account the effect of spatial scale on the landscape composition and the distribution of those elements within the landscape. It becomes critical to understand and to set the scale(s) in which a spatial pattern is measured (Turner 1989).

Li and Wu (2004) stated that landscape ecology is in great need to have more effective landscape indices. These indices should be able to quantify the different aspects of that spatial pattern while maintaining the simplicity in which to interpret the values of those indices. Interpretation becomes even more difficult as most indices describe more than one characteristic of spatial patterns (Riitters et al. 1995). In addition, one specific landscape index cannot describe the entire list of spatial patterns of a selected landscape (Riitters et al. 1995). A balance in the number of indices used and the number of observable spatial patterns must be established.

1.7.4 Limitations and Challenges in Landscape Pattern Analysis

Earlier studies in landscape pattern measurement focused on 5 ways of measuring and characterizing spatial patterns, hence leading to correlation in subsequent indices derived from those 5 measurements (number of patch types, proportion, perimeter-area scaling, distance, and contrast) (Li and Reynolds 1994; Riitters et al. 1995). A high correlation among these types of measurements would mean that the results of landscape pattern analyses can become repetitive (Wu and Hobbs 2007). This has made it challenging to select the most appropriate indices for landscape pattern studies. Riitters et al. (1995) conducted a factor analysis on 55 landscape metrics used to quantify a series of landscape maps of the United States. In that study they found at least 50% of the indices were highly correlated with at least one other index; these correlations had a coefficient of at least 0.9. These highly correlated indices were grouped into the 5 aforementioned measurement types (patch compaction, texture, patch shape, perimeter-area, and number of patch types).

An objective of landscape pattern analysis studies and in landscape ecology is to determine and understand the relationship between pattern and process (Wu and Hobbs 2007). Several researchers have established 4 reoccurring challenges in landscape pattern analysis studies: 1) issues in interpretation of results and how they relate to the research problem or goals, 2) forming clear relationships between landscape pattern and process, 3) ability to predict to landscape change and scaling relation based on spatial heterogeneity, and 4) the difficulty in comparing and observing changes in 2 landscapes (Turner et al. 2001; Wu and Hobbs 2002; Remmel and Csillag 2003; Fortin et al. 2003; Li and Wu 2004). Specifically, there are also challenges in understanding the meaning of landscape pattern metrics; what does the metric actually measure and how can it measure an ecological process (O'Neill et al. 1999; Ludwig et al. 2000).

1.7.5 Common Metrics and Inherent Limitations

Patch Richness (PR) is regarded as the number of different land cover classes within a given study area (Turner et al. 2001); it is a direct measure of landscape

composition. PR does not take into account the spatial location or arrangement of these land cover classes but represents a composition or variety within the landscape. Scaling functions can affect the PR; a larger map extent or landscape level will tend to include more land cover types. One major issue with this metric is that it does not provide information about the area occupied by each land cover class. The area would be important in understanding the actual proportions of each land cover, and indicating the general functions within that given landscape.

The Class Area Proportion (CAP) is a landscape metric that actually solves part of the areal extent problem in Patch Richness. It simply measures the area of each land cover type within the landscape and is therefore dependent on the thematic resolution. The composition of the landscape is important, however, it fails to provide information on how these land cover types are arranged in space. Most landscape pattern analyses that incorporate remote sensing and/or GIS mapping techniques generally create land cover classification maps. These maps of the study area display each land cover class by their representation through the number of pixels and the area with which the pixels occupy. Therefore, conducting a CAP metric would be redundant for these particular studies.

The number of patches within a landscape or land cover class level is referred to as the Patch Number (PN) or the number of patches (NP) (Leitao et al. 2006). At the class level, the NP refers to all patches occurring within that particular land cover type. At the landscape level, the patch number refers to all patches occurring in all land cover types. If comparisons of 2 landscapes or 2 class levels are being conducted then a Patch Density (PD) metric can be used to support these comparisons. PD is calculated by dividing the NP by the landscape area (Leitao et al. 2006). Both metrics describe the same information if one landscape is being studied.

The NP and PD are useful in showing proportions of patches across the landscape and class levels, however they lack information on the configuration and arrangement of the patches, and the concentration (or dispersion) of patches occupying greater areas (McGarigal and Marks 1995). If we were comparing similar landscapes with the same number of patches, the NP would not indicate if there are clusters of certain patches. The PD would indicate if one landscape contains a higher

concentration of patches than the other but cannot illustrate where the clustering of those patches occur.

The Mean Patch Size (AREA_MN) is another commonly used landscape metric, and it measures the average patch size within a landscape or land cover type (Leitao et al. 2006). The spatial distribution of the patches however is not expressed by the Mean Patch Size. Another limitation of using this metric is the lack of information that it provides on the distribution of patches across different land cover types. We cannot infer that larger patches (or smaller ones) are found in one land cover type as compared to another.

SHAPE is the ratio of the patch perimeter to the simplest shaped patch within a given landscape (Leitao et al. 2006); it is a metric representing the geometry of a patch. The SHAPE index, a measure of compactness, has values closer to 1.0 when the patch shapes are compact and relatively simple, such as a circle or square shaped patch (Leitao et al. 2006). A more complex shaped patch would have values far greater than 1.0. The main limitation to using this index is that the geometric complexity occurring among patches is not highlighted; we are only given the value but not the actual shape that it represents. Morphological analysis can account for the discrepancies and complexities in the shapes of patches with varying geometries. Morphology is the mathematical theory and application that interprets the shape and structure of objects (Vogt 2007). The morphology of the patches are not specified, hence there is a need to utilize a landscape pattern analysis that adapts to the patch composition and configuration.

1.8 Morphological Spatial Pattern Analysis

The computation of morphological metrics in MSPA is based on a customized sequence of mathematical operators which describe the geometry and connectivity of the landscape features on two-dimensional (2D) binary images. The European Commission funded Joint Research Centre (JRC) developed tools and methodologies to analyze spatial patterns in various environments (Vogt 2009). The morphological spatial pattern analysis (MSPA) application is one of these key morphological landscape pattern analyzers. MSPA is part of the *GuidosToolbox* application which describes and analyzes objects within images and the shapes of these objects. *Guidos* conducts

quantitative analysis on spatial pattern, connectivity, and fragmentation on images of varying scales. *Guidos* also features several GIS software, including SAGA, GRASS, and QGIS.

Landscape metrics are commonly implemented to perform direct measurements on the input image; however, MSPA segments the input image and classifies each pixel as one of 7 morphological classes (and 1 background class), which provide information on the size, shape, and connectivity of the objects in the image (Soille and Vogt 2008). The methodology developed by the JRC concentrates on characterizing the foreground pixels, which represent the focus of the landscape pattern. The 7 mutually exclusive morphological pattern elements computed from the MSPA are: core, islet, bridge, loop, edge, perforation, and branch (Figure 10). Morphological metrics differ from the aforementioned landscape metrics in that they provide a geometric approach in defining the landscape as compared to landscape and patch metrics. The morphological indicators used are dependent on classification and spatial patterns of connectivity from an observed or simulated event (Vogt 2009).

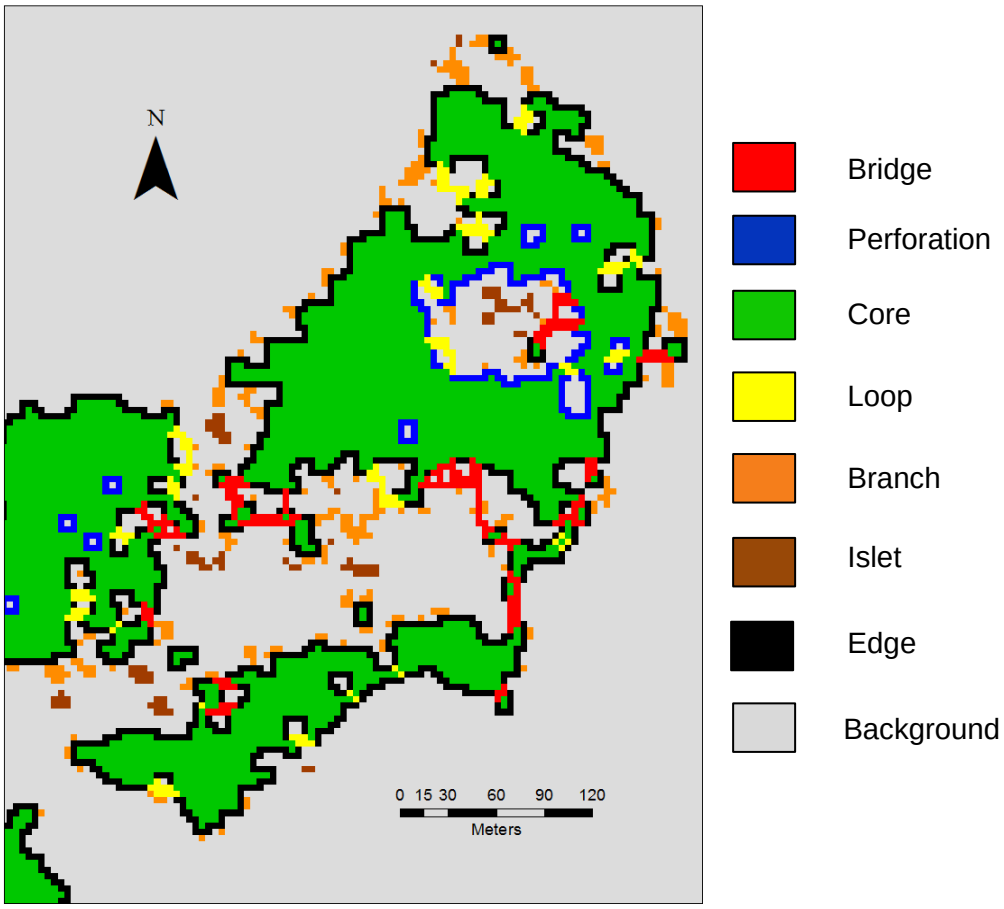

Figure 10. The morphological spatial element output of an MSPA analysis in *Guidos* results in the several landscape pattern elements, each with a unique structure and contribution to the landscape.

Emulating the natural resulting patterns of wildfires on a boreal forest landscape requires us to identify the spatial patterns of residuals. This identification is necessary to better equip us with the composition and configuration of residuals that we aim to leave behind after harvesting. The post-fire residual patterns can potentially be identified using the MSPA technique. The morphological elements produced can be classified as the actual land cover types of the residuals, with each element occupying a certain space within the fire footprint. We can then identify which land cover types in a specific geometry, structure (morphology), and size can remain after harvesting forest stands within the matrix of the AOU. The configuration and composition of the morphological pattern elements can be replicated to maximize forest regeneration and succession.

Forest fires and forest management have become integral factors in understanding ecosystem recovery and vulnerability in high stress environments (Saura et al. 2011). The MSPA is reliable in identifying interconnecting (and non-connecting) landscape structures in forest ecosystems (Saura et al. 2011).

Vogt et al. (2007) indicated that the morphological patterns found in a landscape were important in understanding habitat patterns and biodiversity. Ecological disturbances can alter the processes occurring within ecosystems, and simultaneously degrade the actual structure and components within them. The MSPA technique will be implemented to observe the structure, components, and configuration within a large disturbance. This proposed research will utilise the MSPA approach to observe the morphological pattern components that characterize individual land cover classes within residual patches within a northern boreal fire event with the goal of developing emulation rules for forest harvesting and management planning.

1.8 Research Goals and Objectives

This research is designed to analyze and characterize the inherent morphological spatial patterns within residual patches collectively at a large wildfire in north-western Ontario, using the morphological metrics from MSPA. By using the MSPA analysis I will be able to quantify the proportion of land cover types with regards to their contribution to each morphological spatial pattern element. The more frequent morphological elements and their presence in more frequent land cover classes at different grain sizes can help forest planners and managers with a set of rules and guidelines as to which morphological elements within specific residual vegetation (and other land cover classes) can remain after harvesting.

The main goal of this study is to analyze how landscape pattern elements change with increasing grain size in residual patches. In addition I will analyze the scaling relationships of pattern measurement and residual patch characterization across multiple grain sizes and assess spatial trends of morphological metrics across the extent of this fire event. The scaling relationships can provide forest managers with a set of grain sizes that are comparable to the satellite image data that they use to observe potential harvesting (and planning) sites in the AOU. Moreover, a specific grain size or grain sizes can be chosen in this study to reflect the range with which morphological

elements are preserved. In setting these goals, I will illustrate how changing certain parameters (neighbourhood connectivity, edge width, and transitioning) in the MSPA can affect the outcomes of the pattern elements across grain sizes and land cover classes. I will attempt to address the following research questions:

1) Are the morphological pattern elements of each land cover class stable across grain sizes?
2) Are the land cover classes within residual patches of vegetation consistent in terms of their morphological patterns?
3) Are the morphological pattern elements of each land cover class within all residuals affected by the changing the neighbourhood connectivity, edge width, and transitioning at each grain size?

The objectives listed will detail the steps in attempting to answer the above research questions:

1) Measure the land cover class frequencies and morphological pattern element frequencies for individual land cover classes within residual patches over multiple scales.
    a) A supervised classification scheme of 14 land cover classes will be created for each residual patch for the RED-084 fire event.
    b) Binary maps for a refined 10 land cover type map will be resampled 5 times from 4 m pixel size to 64 m.
    c) MSPA will be used to quantify the overall morphological pattern element frequencies, and the pattern element frequencies characterized by each land cover class.
2) Understand how changing the grain size can affect the proportions of morphological pattern elements.
    a) Binary maps for each land cover class for residual patches will be processed in MSPA to measure the proportions of the 7 spatial morphological components and the background matrix value.
3) Test for significant differences in land cover class frequencies and morphological pattern element frequencies as the grain size changes.

a) An ANOVA analysis will test whether the pattern area means of certain land cover classes are significantly different from other land cover classes at varying grain sizes.
b) If the ANOVA revealed significant results then a Tukey post-hoc test will determine which land cover classes are significantly different from other land cover classes at each morphological element for all grain sizes.

4) Understand how changing the parameters within MSPA can affect the frequency and area of morphological pattern element.
   a) An ANOVA analysis will test whether the area means of morphological pattern elements are significantly different at 4 and 8 neighbourhood connectivity across all grain sizes.
   b) An ANOVA analysis will test whether the area means of morphological pattern elements are significantly different at 1 and 2 edge width pixels across all grain sizes.
   c) An ANOVA analysis will test whether the area means of morphological pattern elements are significantly different when transition was turned on (1) and when transition was turned off (0) across all grain sizes.

2. Methods

2.1 Study Area: Red Lake Fire Event

During the summer of 2011 the RED-084 wildfire burned in the Red Lake, Sioux Lookout, and Nipigon districts in northwestern Ontario for 23 days. The area of the fire was approximately 55,000 ha, leading to evacuations of northern communities (OMNR 2011). This fire was ignited by a lightning strike and was reported to have started spreading on 10 July northeast of Ear Falls (Figure 11). In the month leading up to ignition, the drought code (DC) and build up index (BUI) were increasing gradually mainly as a result of a lack of rainfall. The DC represents a deep layer of compacted organic matter which is sensitive to rainfall and temperature, and the BUI refers to the total fuel that is available to combust, and is dependent on the DC (Alexander and Cole 2001). The BUI at the time of ignition was 80 (OMNR 2011), which is within the threshold range (60 to 80) for extreme fire behaviour (Alexander and Cole 2001). The rate of spread (ROS) and progression of RED-084 was highly variable, ranging from a slow spreading fire to a high severity crown fire (OMNR 2011). Normal fire suppression techniques were unsuccessful and eventually the fire was left to extinguish naturally (OMNR 2011). The fire perimeter was mapped at about 169 km when the fire stopped spreading on 2 August, and was deemed extinguished by the OMNR on 3 September (OMNR 2011). The dominant land cover types found along the perimeter were black spruce (45%), water bodies (37%), and jack pine (10%) (OMNR 2011).

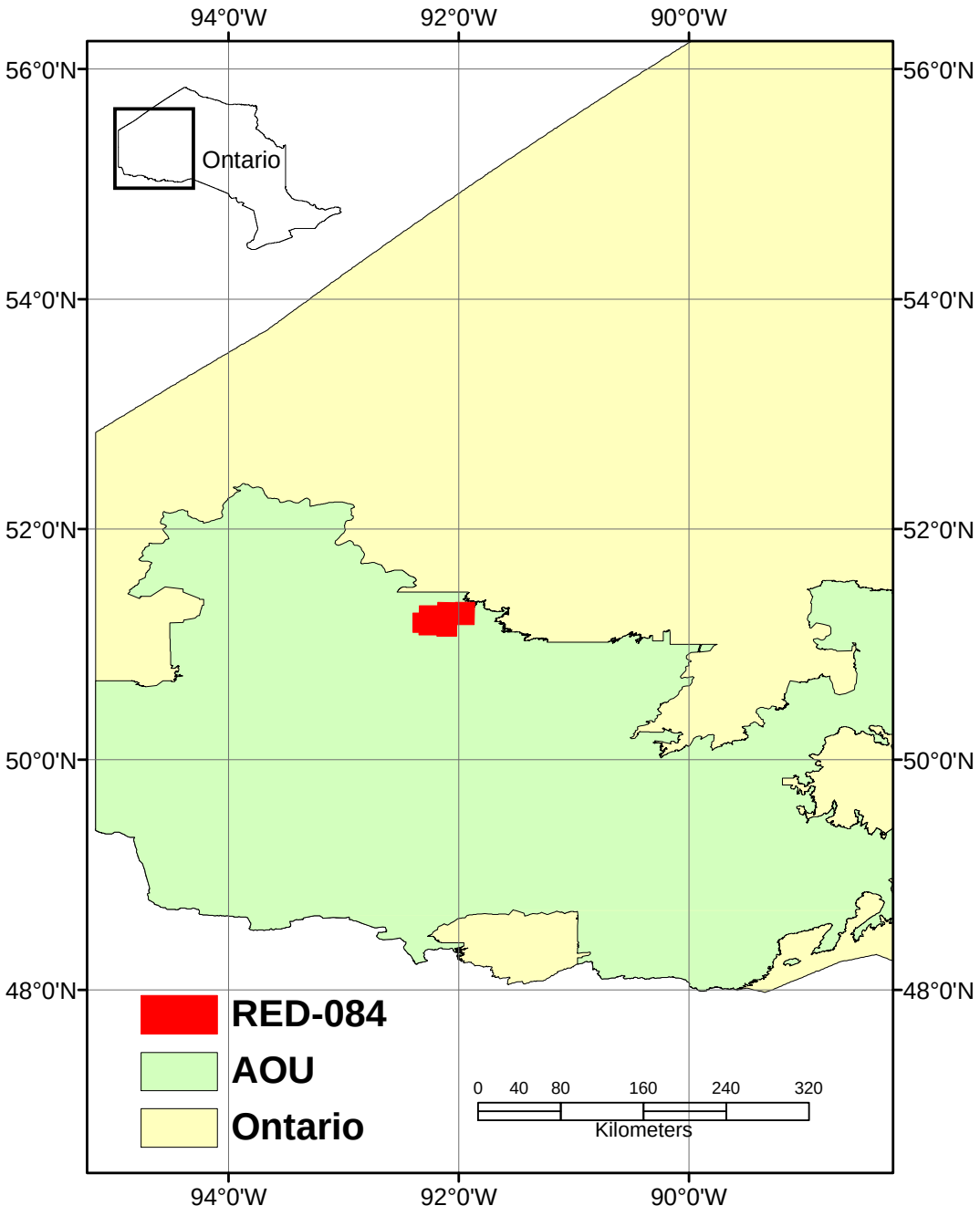

Figure 11. Location of the RED-084 fire event in northwestern Ontario in 2011; note that the fire perimeter interacts with both the AOU and the non-AOU areas.

2.2 Pre-burn Conditions

The pre-burn forest was dominated by black spruce and jack pine, with a smaller contribution (with respect to area) from other species, such as balsam fir (OMNR 2011). This area was also affected by a fire event (RED-058) in August 1999, but was substantially less destructive to the landscape; burning about 5,300 ha. This wildfire event accounted for a small section of old burn land cover within the RED-084 perimeter. The regeneration and succession of vegetation from the RED-058 disturbance, specifically in the form of immature jack pine, were observed in the northwestern area of the fire footprint. Most of the RED-084 event occurred within the AOU (Figure 11), and some sections of the mature stands were scheduled for timber harvesting but were burned during the disturbance. In addition, piles of harvested timber burned near the northwest corner of the fire footprint.

2.3 Image Data

Six IKONOS images of the fire event were acquired with a spatial resolution of 3.2 m (Figure 12). The IKONOS satellite is capable of observing surfaces at 4 multispectral bands; blue (0.445 – 0.516 µm), green (0.506 – 0.595 µm), red (0.632 – 0.698 µm), and near infrared (0.757 – 0.853 µm). A panchromatic band (0.526 – 0.929 µm) at 0.82 m spatial resolution was also purchased in this imagery but not used for classification purposes in this study. The images were acquired after the fire was completely extinguished and on different dates (Table 3) due to the presence of cloud cover and haze in the imagery acquired of RED-084 in October 2011 (22-30 October). The 2 images acquired in 2012 were cloud free and hence were important in presenting an unobstructed view (and permitted a land cover classification) of the fire footprint area. All images were projected with the Universal Transverse Mercator map projection (Zone 15 N) and spatially referenced using the WGS84 (World Geodetic System) datum. Figure 13 illustrates the flow sequence of image processing operations, preparation, land cover classification, and patch extraction processes, which were implemented on the original IKONOS dataset.

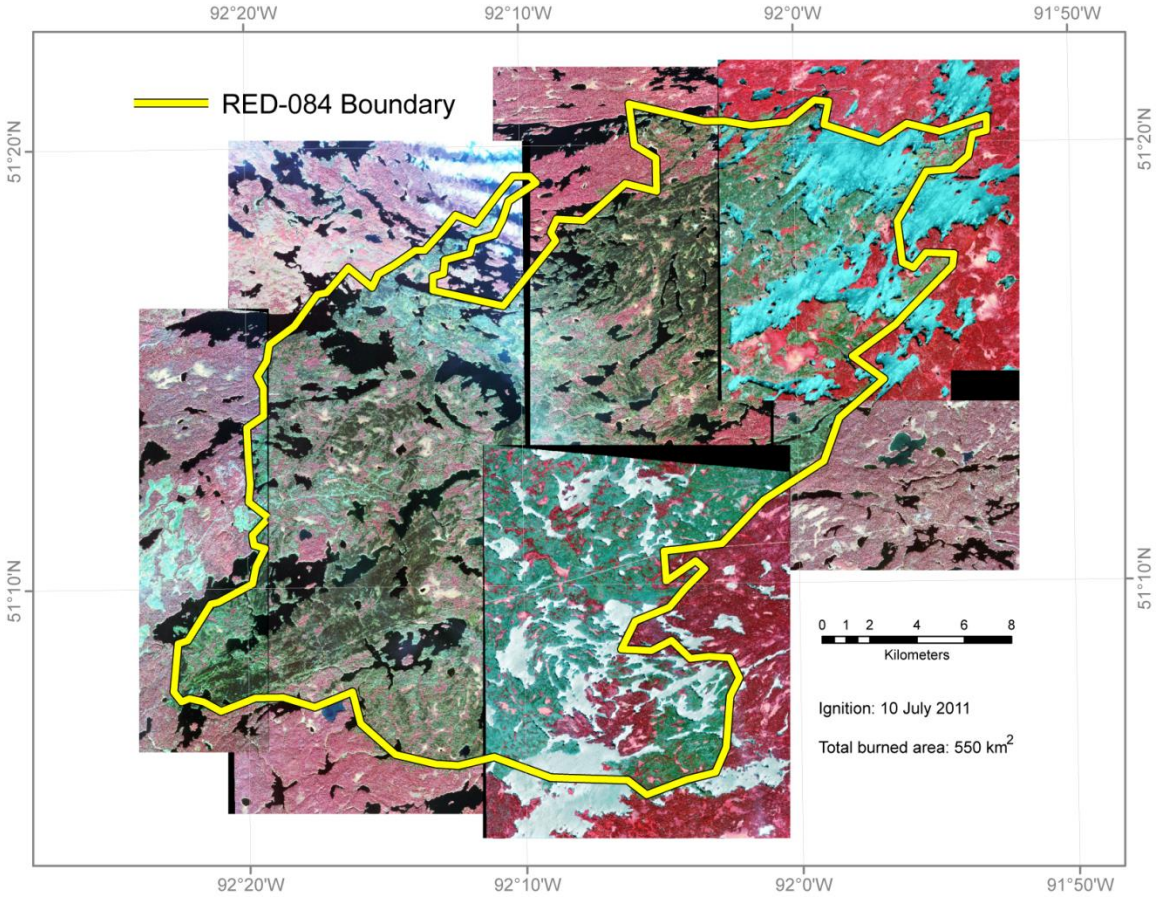

Figure 12. Unmosaicked 3.2 m spatial resolution IKONOS images of RED-084, acquired in October 2011 and July 2012, and observed under a false colour composite (NIR, red, and green bands). The boundary in this map is the original footprint created by the OMNR but was subsequently modified for this study.

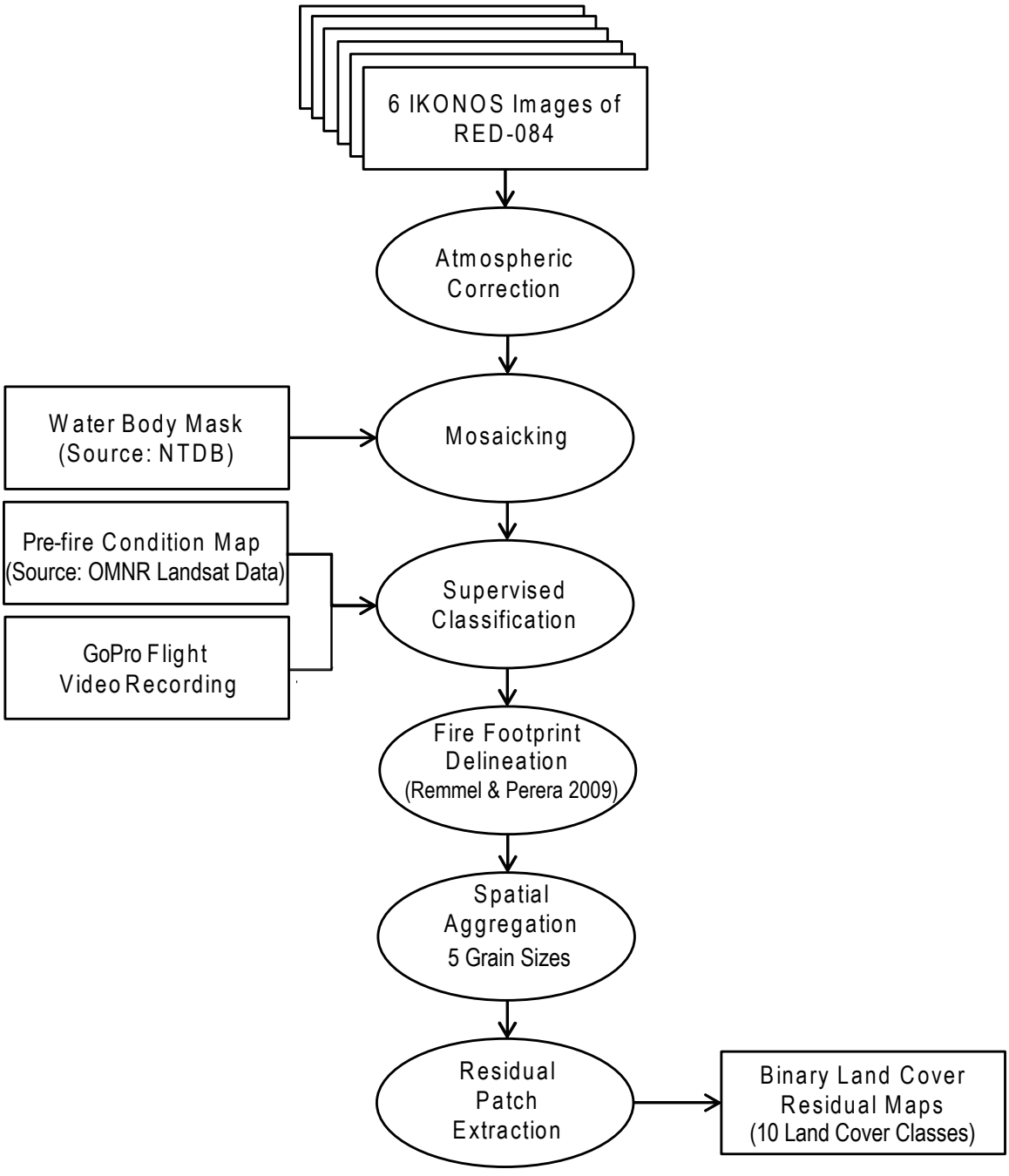

Figure 13. Stepwise processes used to prepare the IKONOS images of RED-084 for MSPA analyses.

2.4 Image Processing

2.4.1 Atmospheric Correction (ATCOR-2)

In order to prepare the images for quantitative analysis an atmospheric correction was performed to minimize the effects of atmospheric haze, solar illumination, and particulate matter on the reflectance values of the image (Martin et al. 2008). The scattering and absorption of electromagnetic radiation signals passing through the atmosphere occur via gases, aerosols, and particulates (Song et al. 2001). The signals are disrupted between the satellite sensor and the receiver on the earth's surface. When atmospheric correction is performed on a satellite image, it can also help improve the mosaicking process, change detection results, and selection of training sites for image classification (Richter 1996).

The ATCOR-2 algorithm was used to atmospherically correct the images. The radiative transfer model in ATCOR-2 is designed to include the physical properties of the atmosphere, the features and conditions present on the ground surface, and the sensor properties and positioning. This model accounts for the absorption and scattering properties by using knowledge of the satellite sensor properties, meteorological conditions, and atmospheric properties at the specific time that the remote sensing data were collected (Neubert and Meinel 2005). ATCOR-2 is also dependent on a 2-dimensional earth surface; it responds to a relatively uniform topography and does not require DEMs for correction (Neubert and Meinel 2005). ATCOR-2 also performs correction in a specific optical spectral ranging from 0.4 µm to 2.5 µm.

Each image possesses its own unique set of physical properties such as the tilt of the IKONOS sensor and the atmospheric condition (Tables 3 and 4). The solar zenith angles in Table 3 were derived by subtracting the solar elevation angle from 90°. The radiometric calibration file "ikonos_2001_std.cal" was sourced and implemented from the ATCOR database. In addition to the parameters in Tables 3 and 4, all of the 6 images had a consistent mean ground elevation of 403 m, and their atmospheric site definition was classified as being rural. A DEM was not required as the land surface was relatively uniform throughout all of the image scenes.

A haze removal was performed on the scenes, and depending on the amount of observable haze within each scene, the percentage of haze cover was adjusted accordingly. Scenes 2, 3, and 6 contained the most haze and the percentage of cover

ranged from 5% to 15% (Figure 14). Haze correction was applied for multispectral bands under 0.853 μm, in order to accommodate the wavelength range in the blue, green, red, and near infrared bands. The cloud masking option was not included in the atmospheric correction as most of the clouds were removed by overlapping the scenes 5 and 6 unto the remaining image scenes.

The atmospheric visibility information of the images varied among scenes due to the season during which the respective images were acquired. The atmospheric condition was entered as fall/spring for scenes 1 to 4 as they were acquired in October, and was entered as mid-latitude summer for scenes 5 and 6 as they were acquired in July (Tables 3 and 4). Due to the remoteness of RED-084, the aerosol type was listed as rural, which is described in the ATCOR manual as a model that accounts for the continental areas that are unaffected by urban and industrial aerosol emissions. The satellite sensor geometry was also included in the atmospheric correction with the sensor tilt angle (Table 4) calculated by subtracting the satellite elevation from 90°.

Table 3. Input parameters for the atmospheric correction process based on the acquisition date, centroid location and time.

Image No.	Location (Centre of Scene)		Acquisition			
	Latitude (North)	Longitude (West)	Year	Month	Day	Time (CDT)
1	51°11’23”	92°21’33”	2011	10	30	12:09
2	51°12’35”	92°15’19”	2011	10	30	12:09
3	51°13’05”	92°06’05”	2011	10	22	12:17
4	51°16’08”	91°56’51"	2011	10	22	12:17
5	51°18’03”	91°57’22”	2012	7	12	12:34
6	51°08’45”	92°06’00”	2012	7	12	12:34

1. CDT refers to Central Daylight Time as observed in northwestern Ontario.

Table 4. Solar radiation angles, sensor tilt configuration and general atmospheric conditions at the time of image acquisition.

Image No.	Solar Configuration			Sensor Tilt		Atmospheric
	Elevation	Azimuth	Zenith	Degree	Direction	Condition
1	24.40989	168.1939	65.5901	30	East	Fall(Spring)
2	24.39165	168.3014	65.6084	20	East	Fall(Spring)
3	27.32064	170.0904	62.6794	10	East	Fall(Spring)
4	27.27952	170.1959	62.7205	Nadir	East	Fall(Spring)
5	59.65499	161.3230	30.3450	20	North	Summer
6	59.77386	160.8431	30.2261	30	West	Summer

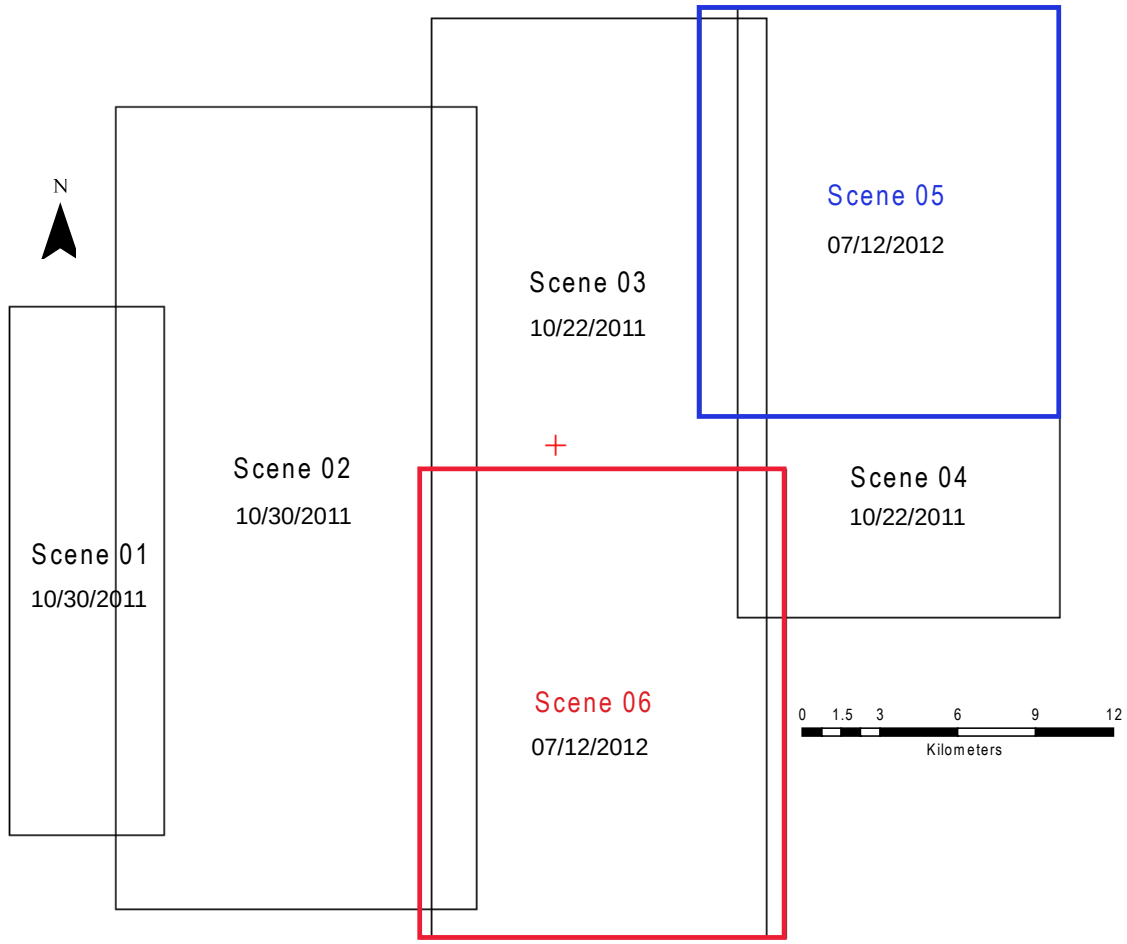

Figure 14. Outlines of the IKONOS image scenes used to capture the entire RED-084 event; with scenes 5 (blue) and 6 (red) overlapped to reduce the effects of cloud cover (+ denotes the center of the images).

2.4.2 Water Mask

3 shapefiles were acquired from the NTDB comprising all of the water bodies within the RED-084 study area, and appended them to create one shapefile. This vector polygon file when overlaid on the IKONOS images did not align properly to the IKONOS boundaries of the water bodies resulting in overlapping between the 2 datasets. We used a vector editing tool in the ArcGIS environment to manually reshape the polygon layer to match the lakes and rivers of the study site. This edited vector polygon file was then converted to a bitmap layer. 2 classes were created in the bitmap layer; a value of

1 represented the inside areas of the water bodies, and a value of 0 represented all other areas (absence of water bodies). A pixel size of 3.2 m was used in creating the bitmap to match the spatial resolution of the image scenes. The resultant water mask was created for use in the mosaicking process by eliminating haze, cloud cover, and particulate matter that existed over the water bodies of the scenes. The water mask also ignores all water bodies from the mosaicking process in order to attain the correct colour balancing among the image scenes. By creating the water mask, cutlines generated in the mosaicking process would not be affected by the differences in the colour of the terrestrial and aquatic environments.

2.4.3 Mosaicking

Clipping was conducted before mosaicking to focus on the RED-084 boundary and lessen the processing time for mosaicking. Using a vector editing tool, the boundaries of the scenes were altered to line up with linear and riparian features, which would allow for an easier cutline generation in the mosaicking process. In order to create a seamless image map of the study area, colour balancing parameters were considered to piece together the 6 image scenes. The IKONOS images contain radiometric and tonal differences, hence colour balancing is applied to create a more uniform mosaic, which has minimal colour contrasts (PCI Geomatics 2003). Applying a colour balance also minimizes the colour difference between the seams of the images. The colour balancing method used to smooth the colour differences among each image was the neighbourhood method and the cutline method implemented was the edge feature technique.

Mosaicking was conducted by setting automatic cutlines in the OrthoEngine environment. Cutlines are outlines or seams between adjacent (overlapping) images that are the least conspicuous due to their radiometric values (PCI Geomatics 2003). The edge feature function within the mosaicking process was chosen to delineate cutlines, giving greater consideration to rivers, riparian boundaries, treed patch edges, and other distinctive linear landscape features when attempting to produce a seamless colour transition between the overlapping areas. The edge feature technique gives the most control on the placement of cutlines and the cutlines generated are the least conspicuous in the final mosaic map as compared to open areas or homogenous

features on the images. The cutline width or blend width was set at a 5 pixel distance on either side of the cutline and this area is used to blend the seam between any 2 adjacent images. 5 pixels were large enough to create a gradual transition between images, rather than a lower pixel count which would have created abrupt seams.

Using OrthoEngine, all image scenes were mosaicked based on the starting or reference image of Scene 01 as it produced a well-distributed and uniform colour balance throughout all of the scenes. Each IKONOS scene from 02 to 06 was then mosaicked successively after the preceding scene was mosaicked unto to the starting Scene 01. The water mask was input and overlaid unto the mosaicked scene in order to exclude water pixels from the statistics used to balance the colour scheme. Large water bodies in particular have to be excluded as they tend to interfere with the colour balancing of the terrestrial features. Large lakes can also have colour differences depending on sediment content, algae content, and varying depths, which can influence the colour balance of the entire image.

2.4.4 Supervised Classification

A supervised classification was conducted on the final mosaicked scene and the training sites for each land cover type (Table 5) were determined using visual interpretation and spectral evidence. A maximum likelihood classifier was used as the statistical decision criterion in classifying each pixel by using a probability function that a pixel belongs to particular class. The maximum likelihood classifier algorithm was selected so as to classify every pixel and avoid ambiguity, even those that may have occurred within potential overlapping areas in other classifiers, such as with a parallelepiped classifier. A null class was not selected so as to account for all of the pixels within the scene and to match the classification scheme provided by the OMNR (Figure 16).

On 04 October 2011 an aerial survey was conducted over the fire footprint using a Go-Pro HD camera attached to a fixed-wing aircraft flying at an altitude of about 600 m. This 2 hour flight followed a planned route to survey the general fire perimeter and the enclosed footprint (Figure 15). The video recordings were used to supplement the ground survey data collected in October 2011 and 2012. The data collected were in the form of observations of fire behavior, residuals, blowdown, harvest, animal activities,

regeneration, and changes in the landscape relative to pre-burn conditions, which were all recorded and tracked with GPS. These observations aided in the training of the classifier.

The training sites collected in the supervised classification process were selected based on the video recordings of selected points within the fire footprint, training data via ground surveying, and a pre-fire condition map. This pre-fire land classification map was produced by the OMNR in conjunction with SPECTRANALYSIS Inc. (Spectranalysis 2004), and based on Landsat 7 ETM+ 30 m spatial resolution (later resampled to 25 m spatial resolution) data acquired from 1999 to 2002 (Figure 16). An initial 27 land cover classification scheme was developed for all areas north of the southern boundary of the Canadian Shield. Only 15 of those classes exist within the fire boundary (Figure 16).

An updated classification approach by SPECTRANALYSIS Inc. and the Forest Landscape Ecology Program (subdivision of the OMNR) in 2005 further refined the initial 27 classes into 14 land cover classes (Table 5) (Spectranalysis 2004). This 2005 classification scheme was used to create the land cover classes of the RED-084 mosaicked scene as the scheme is based on IKONOS imagery rather than the coarser spatial resolution Landsat ETM+ data. The IKONOS data were classified via training sites and based on 21 fire sites within 14 different areas. The training data through visual observation and spectral signatures of fires in the region within a supervised classification environment was also another reason why this classification scheme was used for the RED-084 event.

Problems arose when attempting to collect training sites as some of these sampling sites cannot be identified using visual interpretation and field data due to their locations being far from the flightpath and ground survey path. The classification of these remote areas under supervised classification is not extensive to cover the entire fire footprint. In addition, for example, marshes and open wetlands may have similar spectral properties that can result in displaying similar reflectance values, resulting in confusion in classifying these land cover types. Rogan and Miller (2006) noted similar issues with forest cover classification schemes whereby some land cover classes are not always mutually exclusive, leading to class confusion.

Interactive editing and comparative classification were utilized to improve the accuracy of the classification process. Firstly, the boundaries of adjacent clusters were

dissolved of the same class. Filtering was then conducted on the classified image to smooth the edges of the land cover classes, and remove any isolated pixels or noise in the final scene. During the filtering process, a resampling of the original 3.2 m spatial resolution to 4 m was conducted using a nearest neighbourhood method; a task that was done to ensure that the footprint extraction could be matched with the requirements of the OMNR.

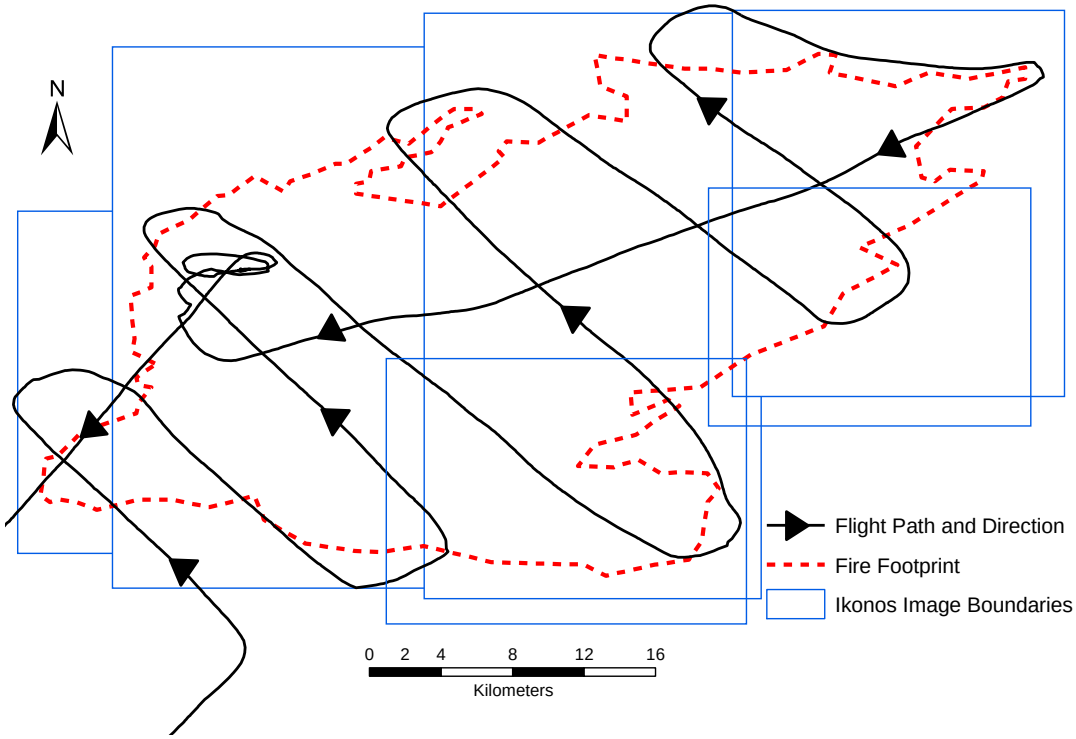

Figure 15. Aerial survey reconnaissance over the RED-084 fire event in 2011 was conducted with video recordings, visual observations and noted positions via GPS units.

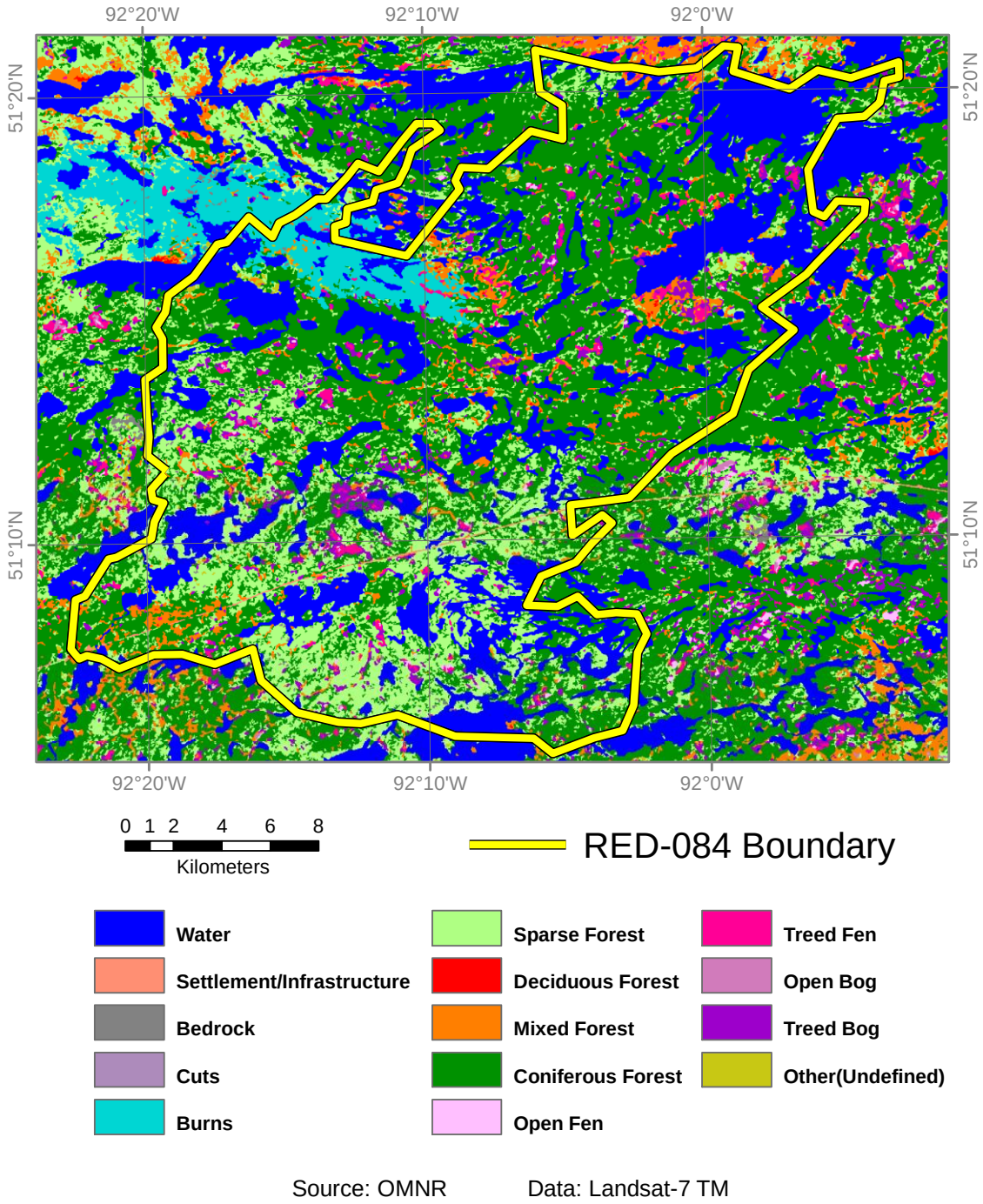

Figure 16. Pre-fire land cover classification map based on Landsat imagery acquired from the OMNR and data used for the original fire boundary. (Data: Landsat-7 ETM+)

Table 5. Land cover class description for IKONOS image classification of RED-084 (Spectranalysis 2004).

Land Cover Class	Class Description
Complete burn	Any vegetated area that has been burned over its full extent, leaving little or no evidence of vegetation
Partial burn	Vegetated areas that been burned over part of their extent, some scattered vegetation
Old burn	Regenerated vegetation plots found within the charred areas of previous fires
Dense conifer	Vegetation cover with predominantly coniferous trees, and minor deciduous cover
Sparse conifer	Vegetative cover distinctive of conifer trees, but contains a minor deciduous component
Deciduous	Dense cover of predominantly deciduous species, but may contain a minor coniferous component
Alder shrub woodland	Large trees that are found exclusively along watercourses
Low shrub	Low shrub growth and grasses near lakes and deltas, and old burns. Does not include trees
Treed wetland	Bogs and fens including trees
Open wetland	Bogs and fens with little or no tree cover
Water	Water bodies, both clear and sediment-laden. May contain large string bogs
Marsh	Areas inundated continuously, seasonally or intermittently with emergent vegetation; adjacent to lakes and watercourses
Bedrock and non-vegetation	Areas with no vegetation (or very sparse), often bedrock outcrops
Cloud and shadow	Areas obscured by cloud and shadow effects

2.4.5 Fire Footprint Extraction

There were discrepancies between the fire footprint boundary obtained by the OMNR via Landsat-7 data and the observable fire boundary obtained from the supervised classification map. There were a lot of areas that appeared burnt in the aerial survey and video recordings that were located outside of the original fire perimeter boundary. It was therefore necessary to delineate the fire footprint from the contiguous

landscape surrounding the fire event. Transition zones exist between the burned, partially burned, and unburned landscape, and these zones are not discrete boundaries but rather fire scars of varying burn severity. The fire footprint is required to focus on the insular residual patches and hence it has to be extracted and separated from the rest of surrounding landscape (the forest matrix and peninsular patches).

A stepwise decision scheme designed by the OMNR and implemented in the Remmel and Perera (2009) study, was used to delineate the fire footprint of RED-084 (Figure 17). Firstly, all of the pixels in the landscape were classified as burned (1) or unburned (0). This binary map generation uses a focal sum technique to distinguish which pixels are found within the footprint (Remmel and Perera 2009). A moving 3×3 focal window within which a focal sum was computed was then passed over the binary map. The focal sum was calculated and the resulting sum value is expressed within a range from 0 (all pixels are unburned) to 9 (all pixels are burned). Any value ≥ 1 represents some probability of the centre pixel belonging to the fire footprint. If the value is 0 then the pixel is found outside of the fire footprint. The centre pixel contains the resulting value and will cause the footprint area to be inflated; not representing the actual footprint size. The focal sum layer was shrunk inward by 1 pixel to adjust for this deviation and preserved the fire footprint.

The insular residual patches are isolated based on the criteria implemented by the OMNR (Figure 17), with the distance from the fire perimeter (1 pixel) being a major determinant in separating insular residual patches from peninsular patches. The focus of this study is on insular residual patches; the peninsular patches are not considered. In order to define and extract patches, the OMNR (2009) proposed that all unburned pixels within a fire footprint should be highlighted and observed to test whether those unburned pixels were burnable. Residual patches have to be burnable, hence old burn, partial burn, and complete burn land cover classes have to be ignored (Figure 17). Burnable pixels were classified as all vegetation cover and wetland types, and these pixels occurring in clusters of at least 0.25 ha were defined as patches (OMNR 2001; OMNR 2009). For this study, we explored all burnable cover, as well as land cover types that were not burned in RED-084, including bedrock, non-vegetation surfaces (e.g., logging roads), and water bodies. The patches also had to occur at least 1 pixel

from the fire perimeter and within the footprint to be classified as insular patches. Peninsular patches were not included in this study as they exist outside of the footprint.

The extracted insular residuals were then spatially aggregated to 4 m, 8 m, 16 m, 32 m, and 64 m grain sizes; with each aggregation based on the original 4 m grain size. A non-overlapping block function was used in the neighbourhood statistics for calculating the value of the resampled pixel, a technique applied from Remmel and Perera (2009). The minimum bounding rectangle of the block function was set to the desired grain size, which allows for each resultant block to contain the same resampled value.

2.4.6 Binary Land Cover Classes

Each insular residual patch can contain between 1 and 10 land cover classes. The collection of patches belonging to a specific land cover class is then converted to a binary map, whereby this collection of residual patches represent the foreground and the remaining residuals of the rest of the land cover classes are grouped together to represent the background. A reclassify function was used to assign new values to the remaining land cover types (the cloud and shadow class was eliminated), whereby the foreground for a specific land cover class is categorized as 2, and the background of all remaining land cover classes was categorized as 1. This reclassification was conducted for all residual patch classes in all grain sizes.

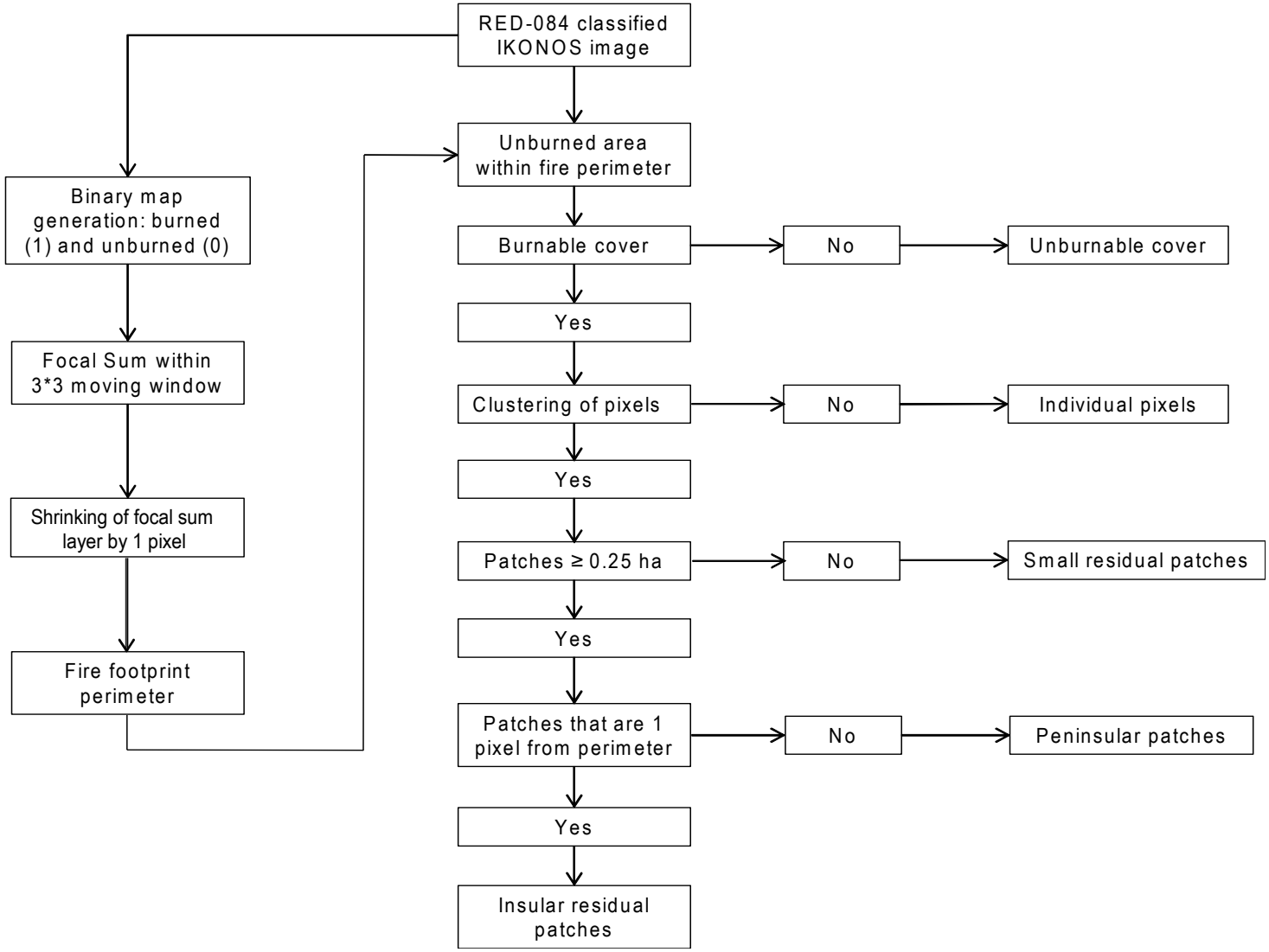

Figure 17. Decision flowchart, which delineates the fire footprint perimeter and extracts the insular residual patches.

2.6 MSPA Analysis

The *Guidos* software runs the MSPA analysis engine on binary raster layers that are expressed with a foreground-background structure (Clerici and Vogt 2013). The residual patches extracted of each land cover type and grain size are represented as binary maps; a pixel value of 2 is classified as the foreground and indicates the presence of a specific land cover class within all of the insular residual patches. A pixel value of 1 represents the presence of all other land cover types within the remainder of the insular residual patches of the study area. These areas with a pixel value of 1 are known as the *background*. For example, a binary map with a 2 pixel value can indicate open wetland residuals while a 1 pixel value would represent the remainder of the land cover class residuals. All of the 7 mutually exclusive morphological elements are measured for the foreground pixels; the background pixels are measured separately.

MSPA has been tested within a forest monitoring study conducted by Ostapowicz et al. (2008) who produced spatial pattern indicators from binary forest raster maps. They observed how MSPA pattern elements change when altering the scale of a Landsat ETM (Enhanced Thematic Mapper) image of the forests in the Carpathian Mountains (Central Europe). The spatial resolution of the binary map was aggregated 5 times from 28.5 m to 313.5 m, altering the composition and configuration of the morphological pattern elements (Ostapowicz et al. 2008). The maximum detail of the landscape elements is achieved when using the highest possible spatial resolution (smallest grain size), but the selection of the most appropriate input scale is dependent on the purpose of the study (Ostapowicz et al. 2008).

Each land cover class (10 in total) was mapped as a binary residual map, and each of these residual maps was observed at 5 grain sizes (Figure 18). Each binary map was inputted into the MSPA program and 3 main parameters (connectivity, edge width, and transitioning) were altered (Figure 18) to produce morphological maps containing the 7 morphological pattern elements and the *background* matrix. In addition to the maps, MSPA also generated ASCII outputs, which contained the frequency and relative proportions of each morphological pattern within each binary residual map. It is from these ASCII outputs that we were able to test for significant differences among morphological patterns across various land cover types, grain sizes, and parameter changes.

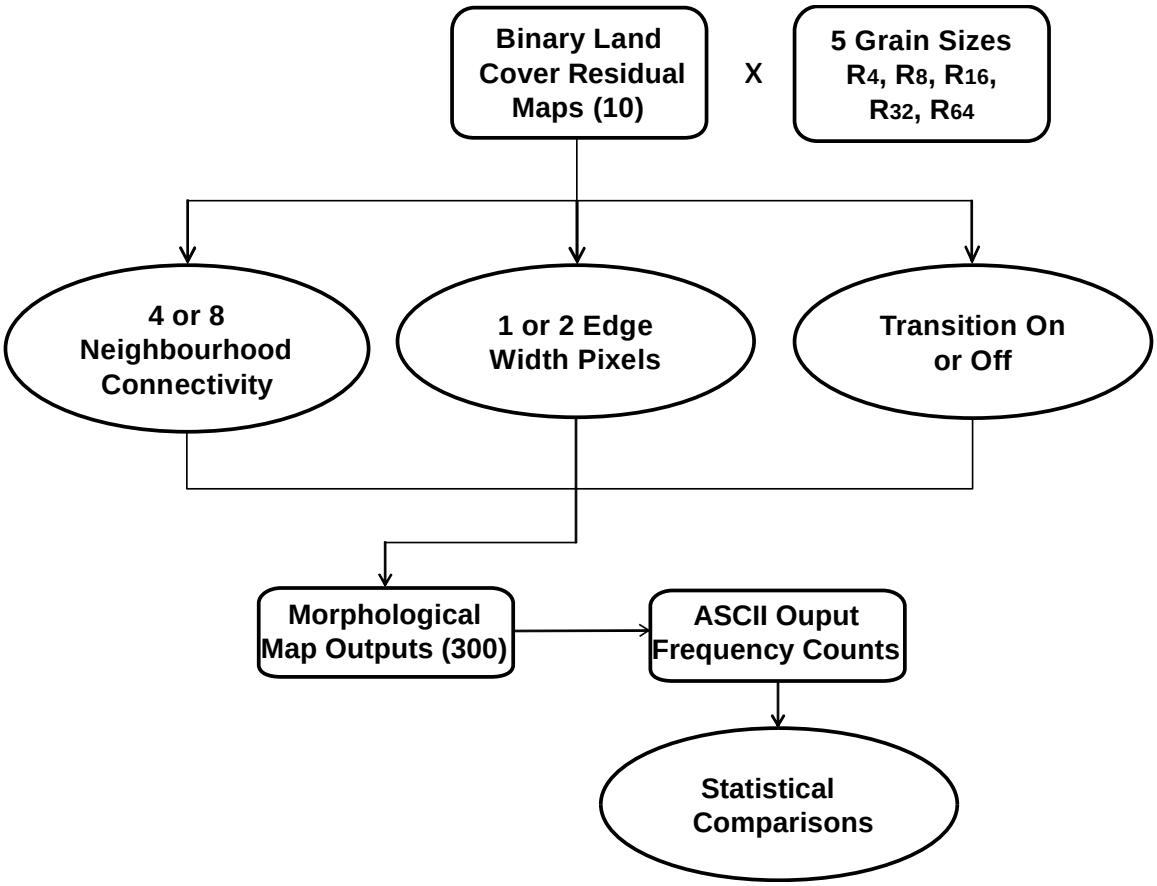

Figure 18. Connectivity, edge width and transitioning parameters are changed for each binary map input, with 1 map output created for each combination.

2.6.1 Core

A core morphological element occurs when foreground pixels exist at a distance from background pixels that is greater than the set edge width parameter (Ostapowicz et al. 2008; Soille and Vogt 2008). The core element area is separated from the background matrix via edge pixels and this allows for a clear distinction between the presence of foreground and the presence of background pixels (Figure 19). The edge width used in this study was either 1 or 2 edge width pixels.

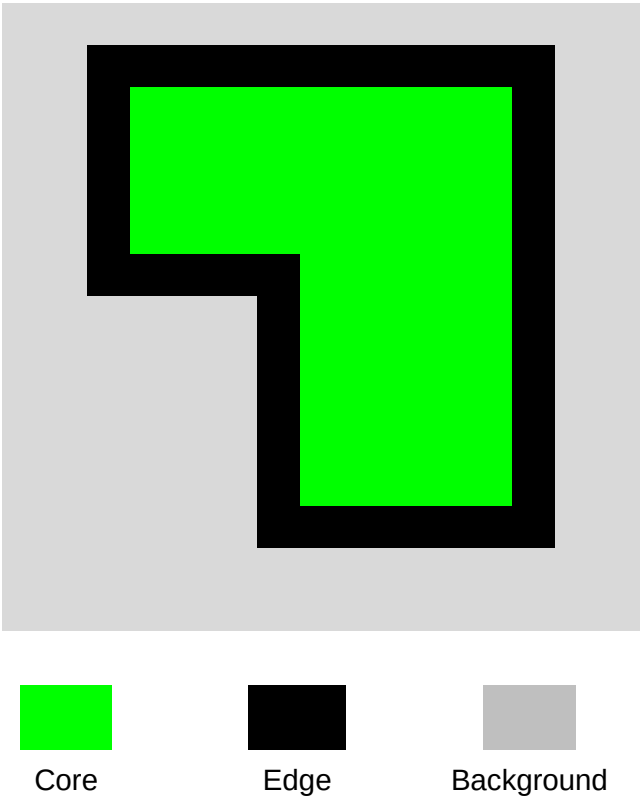

Figure 19. Core morphological elements (green) separated from the background (grey) by 1 edge width pixel (black).

2.6.2 Islet

Islet pattern elements are foreground patches that do not contain core pixels (Soille and Vogt 2008), and are fully isolated from all other morphological pattern elements (Saura et al. 2011) (Figure 20). Islets in this study will have a minimum pixel size of 1 pixel, as determined by the grain size that it is being observed at.

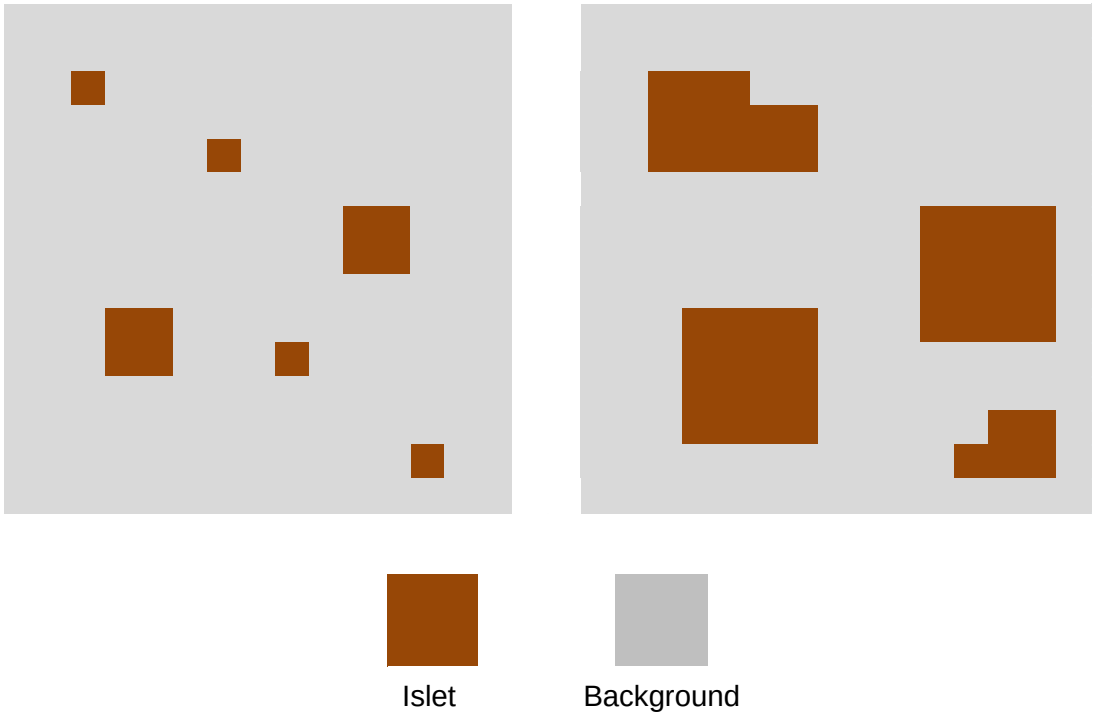

Figure 20. Islet pattern elements are ≥ 1 pixel size, depending on the distance parameter used in treating core morphology segmentation.

2.6.3 Connectors (Loop and Bridge)

Connector cells are foreground pixels which link core patches. Two types exist: A loop connector is a morphological structure that emanates from the same core, and is described as a linkage to the same component (Soille and Vogt 2008). Bridge connectors are pathways that join one core component to a different core component (Ostapowicz et al. 2008; Vogt et al. 2007) (Figure 21).

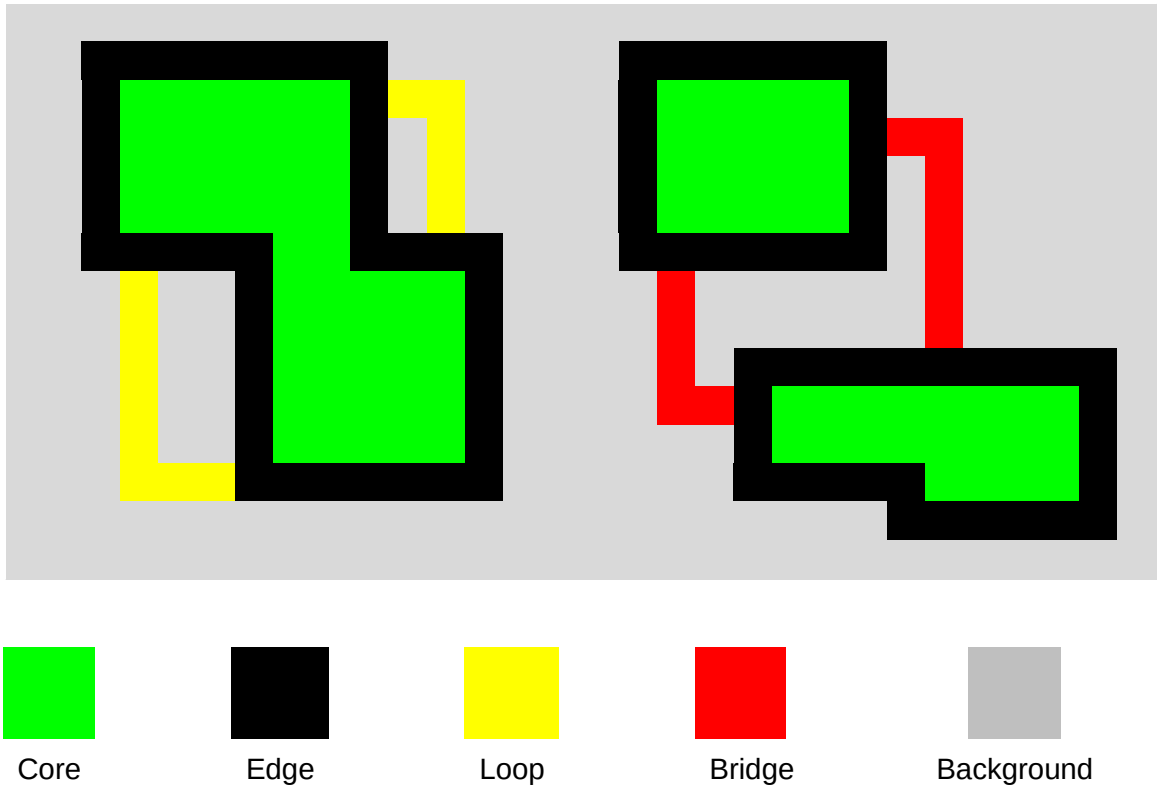

Figure 21. Core pattern elements can be connected by loops (yellow) and bridges (red). Note that the connectors do not interact with the core when the transition is turned off.

2.6.4 Boundary Patterns (Edge and Perforation)

Boundary structures are classified when foreground pixels have a distance to the core patches that is less than or equal to the distance or pixel size parameter set (Soille and Vogt 2008). Clerici and Vogt (2013) defined these morphologies as transition pixels, which provide separation of a core from the background or non-core patterns (Figure 22). There are 2 types of boundaries; outer boundaries (edges) and inner boundaries (perforations). Edge patterns are the outer boundaries of the core morphologies (Ostapowicz et al. 2008). The edge width was selected prior to running the MSPA model, and this width was set as either 1 or 2 pixels, depending on the permutation of other variables. Perforation morphology patterns are classified as the internal boundary of a core area (Saura et al. 2011), and provide a transition to background pixels that can

often be found within large patches. These background pixels that are enclosed within core morphology pattern elements are known as holes (Vogt et al. 2007).

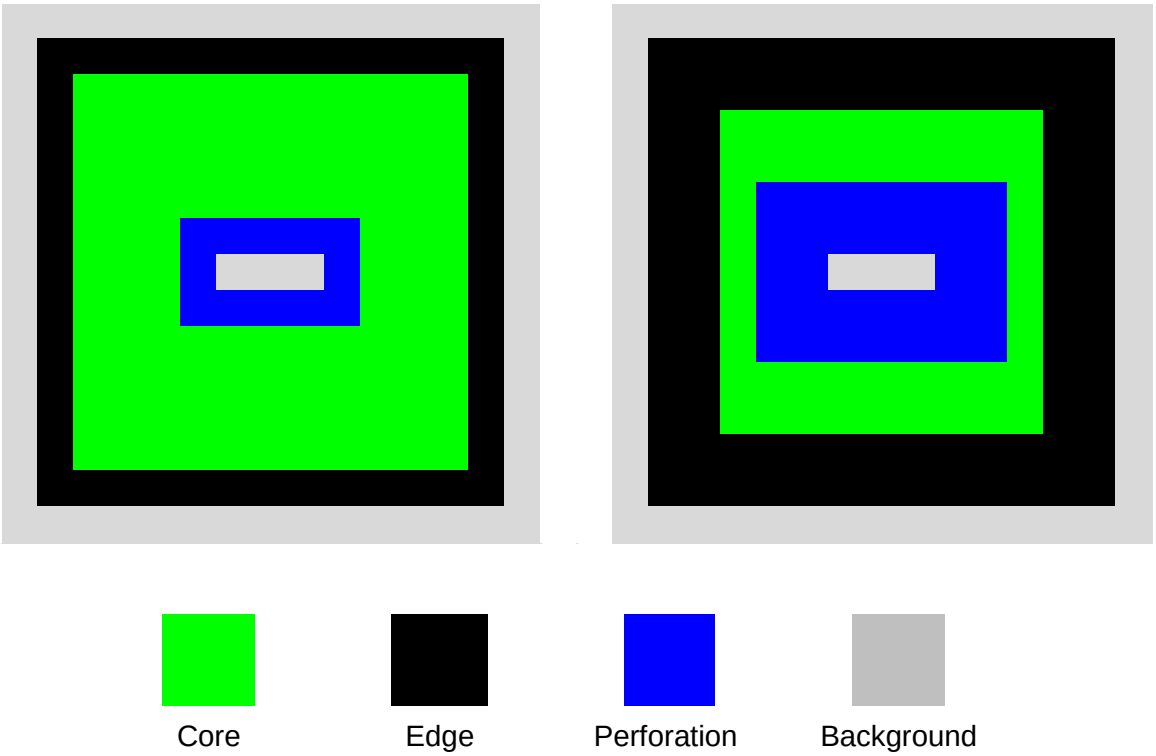

Figure 22. Edge (black) and perforation (blue) morphological pattern elements when segmented from binary maps at 1 pixel distance (left) and 2 pixel distance (right).

2.6.5 Branch

Whenever foreground pixels are linked to a core or originate from a core, these pixels form a branch pattern element (Clerici and Vogt 2013). These branch pixels do not join any other morphological pattern elements (Clerici and Vogt 2013). Soille and Vogt (2008) describe branches in terms of their geometry and positioning to other morphological pattern elements (rather than just core elements); stating that branch pixels originate from either boundary or connector morphological elements but do not connect to another pattern element (Figure 23). The reason why core is not mentioned is that the core is always surrounded by an edge pattern element, which classifies as a

boundary pattern. It is imperative to note that the non-connecting end of the branch pattern element will interact with the background matrix.

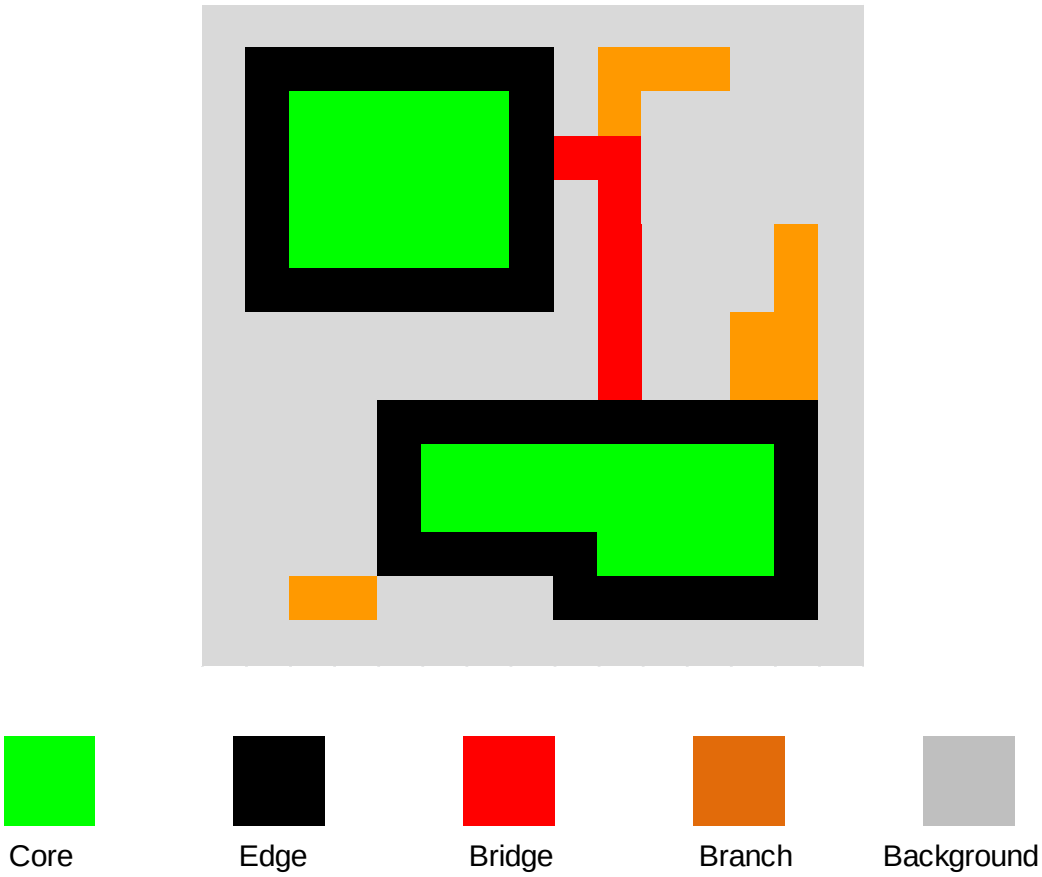

Figure 23. Branch morphological pattern elements (orange) originating from boundaries (black) and a connector (red).

2.6.6 Parameters

The results of the MSPA analysis are output as GeoTiff files, and the frequency and position of each morphological pattern element within the original binary residual layers mapped (containing each land cover type). The MSPA algorithm can be run with different parametrizations, resulting in a unique output for each binary land cover file for each grain size (Figure 18). The connectivity, edge width, and transition can be changed independently of each other. The neighbourhood connectivity was changed

from 4 to 8, whereby 4 represents the rook's case and 8 represents the queen's case (Sawada 2009). Connectivity changes the type of morphological pattern element that can emanate from or link between the edge or branch pattern elements (Figure 24). The changing of the edge width property directly affects the amount of core morphology area, for example an increase from 1 edge width pixel to 2 edge width pixels decreases the core area and increases the non-core areas. The edge width pixels are changed from 1 pixel width to 2 pixel widths (Figure 25). The transitioning parameter defines the way in which a connector pattern element is linked to the core area. Transition is turned off (0) and on (1) in this study. When the transition is turned off the connector pattern elements (bridges and loops) are separated from the core areas by closed perimeters for edges and perforations (Figure 26). Turning on the transition leads to an open perimeter allowing for the connectors to link directly with the core patterns (Figure 26). The intext parameter in the MSPA was not manipulated in this study. Intext creates a second layer of morphological pattern elements when foreground pixels are present within the hole of a perforation. The intext can either be turned on (inclusion of the second layer of classes) or off (exclusion of these classes). The intext parameter was excluded due to the very low occurrence of foreground pixels within perforations for all of the binary maps.

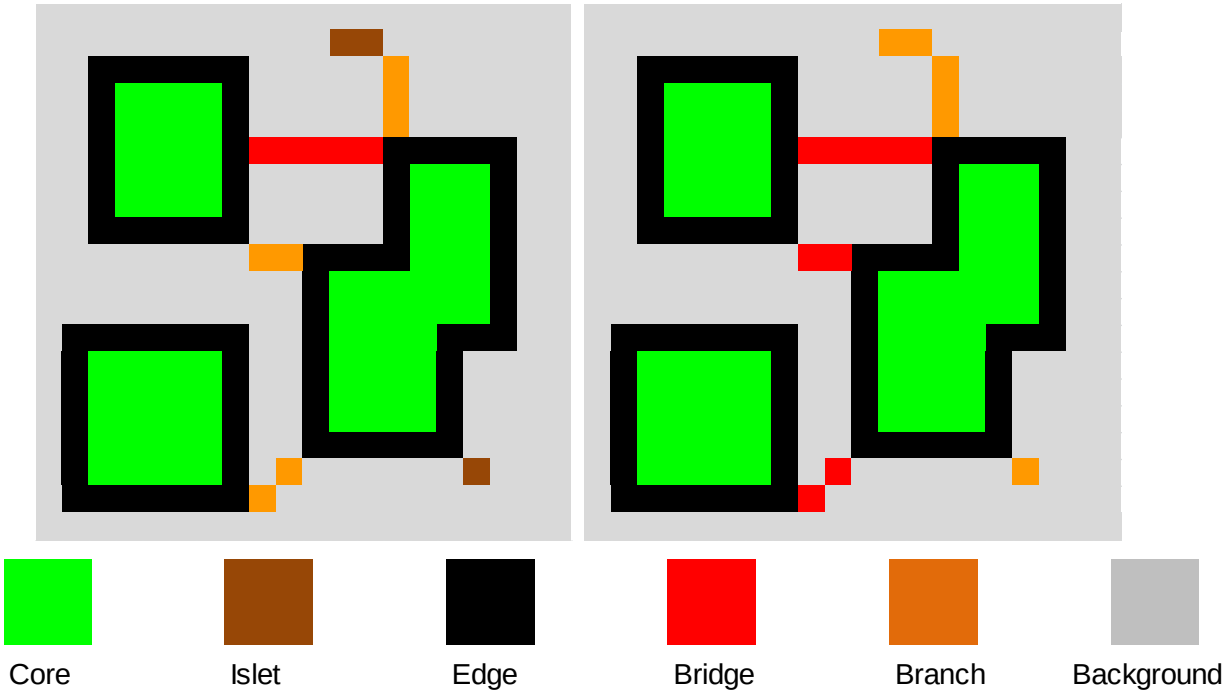

Figure 24. 4 Neighbourhood connectivity (left image) and 8 neighbourhood connectivity can change the type of morphological patterns created, especially in branches, islets and bridges.

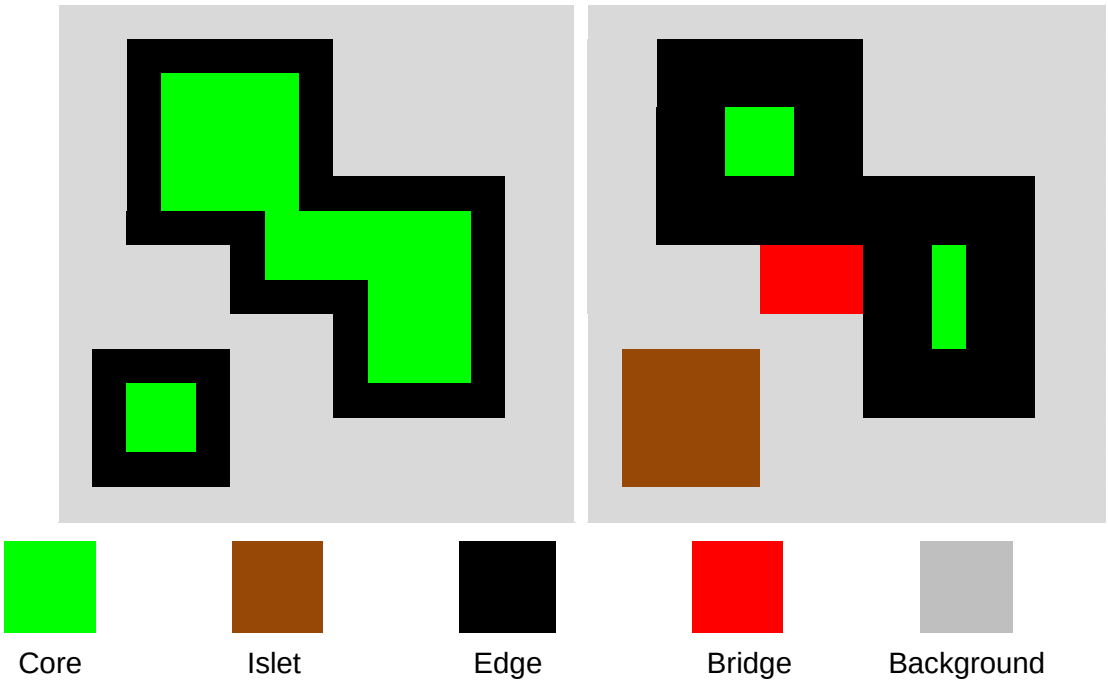

Figure 25. Edge width parameter can be changed from 1 pixel width (left) to 2 pixel width (right), altering the morphology of core areas.

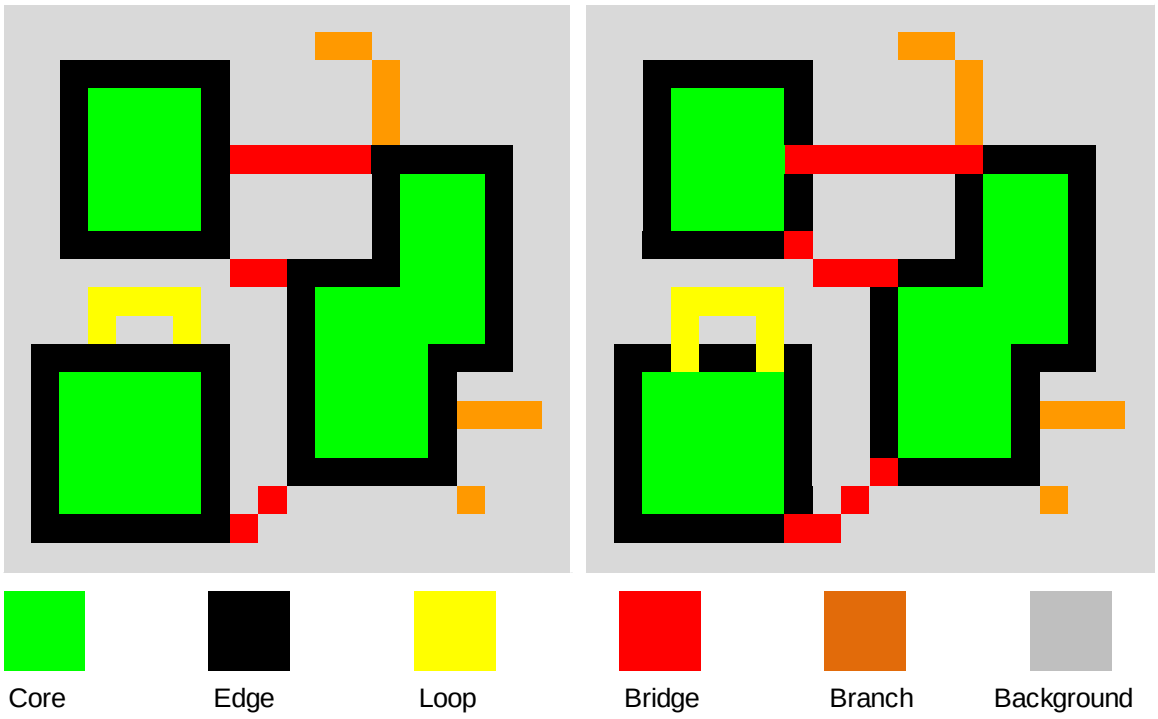

Figure 26. Turning off transition (left) results in closed edge perimeters, while turning it on (right) allows for open perimeters and links to the core morphology area.

2.7 Statistics

Each MSPA output includes a text file with frequency counts of each morphological pattern element within the treatment file along with the corresponding parameters used, and the grain size of the observation. A morphological spatial pattern treatment was therefore performed on each unique combination of grain size, land cover class, connectivity, edge width, and transition parameterization. The treatments for each morphological pattern analysis will also produce a morphological map indicating the occurrences of morphological pattern elements in each insular residual patch of that particular land cover class. These frequency counts are converted into areas (ha) and graphed in the *R Project for Statistical Computing* environment (R Core Team 2014). The boxplots produced illustrated the morphological pattern element plotted against each land cover class and each parameter iteration used, for each grain size. These boxplots provided us with important information on the how the morphology areas

change over grain size, change across land cover types, and connectivity, edge width, and transition parameters.

2.7.1 Morphological Patterns and Land Cover

The proportion of each morphological pattern element occurring within each land cover type for each grain size was calculated and graphed. Upon investigation of these graphs, ANOVA tests were conducted to test whether there was at least one land cover class that was significantly different from another class, for each grain size. If the ANOVA tests showed statistical differences at the $p < 0.05$ level, then a Tukey post-hoc test was conducted on the morphological pattern element area means. The pair-wise comparison of the morphological pattern elements will identify the land cover classes that were significantly different from other classes for each pattern element.

2.7.2 Parameter Change

The areas of each morphological pattern element for each grain size were plotted against the parameter used to highlight differences in parameter groups. The neighbourhood connectivity, edge width, and transition parameters were tested for significant differences in the usage of 4 or 8 connectivity, 1 or 2 edge width pixels, and 1 or 0 transitioning respectively. This statistical analyses testing for significant differences among parameter groups were performed by respective ANOVA tests at the $p < 0.05$ significance level, independently for each grain size.

3. Results

3.1 Core Morphology

At 4 m grain size, core morphological patterns are more frequently found in bedrock and non-vegetation, dense conifer, and sparse conifer land cover classes (Figure 27). Conversely alder-shrub, marsh, and water body classes were the least represented land cover types by core patterns (Figure 27). After conducting a one-way ANOVA of the results of Figure 26, there was a significant difference in the core areas at the $p < 0.05$ level among the land cover classes (Table 6). The greater areas of core patterns that were found in the land cover classes in Figure 27 (dense conifer, and sparse conifer) were confirmed to be consistently and statistically different from all other land cover classes (Table 7).

Dense conifer and sparse conifer classes were significantly different from all other classes at 4 m (Table 7), 8 m (Table 8), 16 m (Table 9), and 32 m (Table 10). At 32 m grain size, core morphologies were increasingly present in water bodies, and were statistically different from all other land cover classes (Table 10). At 64 m grain size, water bodies became the more dominant class in which cores were present. Table 11 illustrates that the water body class was significantly different from all other classes.

Table 6. One-way ANOVA results for core morphological elements for each land cover class at 4 m grain size.

Source of Variation	d.f.	Sum Sq	Mean Sq	F Value	P-Value
4m					
Land Cover	9	7253	805.9	30.28	<0.0000
Residuals	150	3992	26.6		
8m					
Land Cover	9	8288	920.9	26.64	<0.0000
Residuals	150	5184	34.6		
16m					
Land Cover	9	21358	2373.1	25.35	<0.0000
Residuals	150	14039	93.6		
32m					
Land Cover	9	12565	1396.1	47.95	<0.0000
Residuals	150	4367	29.1		
64m					
Land Cover	9	59902	6656.0	48.58	<0.0000
Residuals	150	20550	137.0		

Table 7. Post-Hoc Tukey results for the comparison of means of core morphological elements across all land cover classes at 4 m grain size (bold values indicate significant values at $p < 0.05$).

Land Cover	Alder	Bed	Decid	DCon	LowS	Marsh	OpenW	SCon	TreeW	Water
Alder	-									
Bed	0.0630	-								
Decid	0.9950	0.4664	-							
DCon	**0.0000**	0.7198	**0.0036**	-						
LowS	1.0000	0.2079	1.0000	**0.0006**	-					
Marsh	1.0000	0.0711	0.9965	**0.0001**	1.0000	-				
OpenW	1.0000	0.2054	1.0000	**0.0006**	1.0000	1.0000	-			
SCon	**0.0000**	**0.0000**	**0.0000**	**0.0000**	**0.0000**	**0.0000**	**0.0000**	-		
TreeW	0.9751	0.6317	1.0000	**0.0084**	0.9996	0.9808	0.9995	**0.0000**	-	
Water	1.0000	0.0598	0.9942	**0.0001**	1.0000	1.0000	1.0000	**0.0000**	0.9724	-

Table 8. Post-Hoc Tukey results for the comparison of means of core morphological elements across all land cover classes at 8 m grain size (bold values indicate significant values at $p < 0.05$).

Land Cover	Alder	Bed	Decid	DCon	LowS	Marsh	OpenW	SCon	TreeW	Water
Alder	-									
Bed	0.8739	-								
Decid	0.9997	0.9970	-							
DCon	**0.0000**	**0.0181**	**0.0008**	-						
LowS	1.0000	0.9374	1.0000	**0.0001**	-					
Marsh	1.0000	0.9087	0.9999	**0.0001**	1.0000	-				
OpenW	0.9997	0.9970	1.0000	**0.0008**	1.0000	0.9999	-			
SCon	**0.0000**	**0.0000**	**0.0000**	**0.0000**	**0.0000**	**0.0000**	**0.0000**	-		
TreeW	0.9999	0.9940	1.0000	**0.0005**	1.0000	1.0000	1.0000	**0.0000**	-	
Water	0.9982	0.9993	1.0000	**0.0014**	0.9998	0.9993	1.0000	**0.0000**	1.0000	-

Table 9. Post-Hoc Tukey results for the comparison of means of core morphological elements across all land cover classes at 16 m grain size (bold values indicate significant values at $p < 0.05$).

Land Cover	Alder	Bed	Decid	DCon	LowS	Marsh	OpenW	SCon	TreeW	Water
Alder	-									
Bed	1.0000	-								
Decid	1.0000	1.0000	-							
DCon	**0.0000**	**0.0000**	**0.0000**	-						
LowS	1.0000	1.0000	1.0000	**0.0000**	-					
Marsh	1.0000	1.0000	1.0000	**0.0000**	1.0000	-				
OpenW	1.0000	1.0000	1.0000	**0.0000**	1.0000	1.0000	-			
SCon	**0.0000**	**0.0000**	**0.0000**	**0.0008**	**0.0000**	**0.0000**	**0.0000**	-		
TreeW	1.0000	1.0000	1.0000	**0.0000**	1.0000	1.0000	1.0000	**0.0000**	-	
Water	0.4701	0.7640	0.6846	**0.0000**	0.4984	0.4842	0.7718	**0.0039**	0.5950	-

Table 10. Post-Hoc Tukey results for the comparison of means of core morphological elements across all land cover classes at 32 m grain size (bold values indicate significant values at $p < 0.05$).

Land Cover	Alder	Bed	Decid	DCon	LowS	Marsh	OpenW	SCon	TreeW	Water
Alder	-									
Bed	1.0000	-								
Decid	1.0000	1.0000	-							
DCon	**0.0004**	**0.0013**	**0.0017**	-						
LowS	1.0000	1.0000	1.0000	**0.0005**	-					
Marsh	1.0000	1.0000	1.0000	**0.0004**	1.0000	-				
OpenW	0.9984	1.0000	1.0000	**0.0082**	0.9991	0.9988	-			
SCon	**0.0000**	**0.0000**	**0.0000**	0.1313	**0.0000**	**0.0000**	**0.0000**	-		
TreeW	1.0000	1.0000	1.0000	**0.0010**	1.0000	1.0000	0.9999	**0.0000**	-	
Water	**0.0000**	**0.0000**	**0.0000**	**0.0000**	**0.0000**	**0.0000**	**0.0000**	**0.0000**	**0.0000**	-

Table 11. Post-Hoc Tukey results for the comparison of means of core morphological elements across all land cover classes at 64 m grain size (bold values indicate significant values at $p < 0.05$).

Land Cover	Alder	Bed	Decid	DCon	LowS	Marsh	OpenW	SCon	TreeW	Water
Alder	-									
Bed	1.0000	-								
Decid	1.0000	1.0000	-							
DCon	0.9604	0.9604	0.9604	-						
LowS	1.0000	1.0000	1.0000	0.9604	-					
Marsh	1.0000	1.0000	1.0000	0.9604	1.0000	-				
OpenW	1.0000	1.0000	1.0000	0.9827	1.0000	1.0000	-			
SCon	0.8762	0.8762	0.8762	1.0000	0.8762	0.8762	0.9299	-		
TreeW	1.0000	1.0000	1.0000	0.9693	1.0000	1.0000	1.0000	0.8963	-	
Water	**0.0000**	**0.0000**	**0.0000**	**0.0000**	**0.0000**	**0.0000**	**0.0000**	**0.0000**	**0.0000**	-

The dominant land cover types within core morphological patterns at 8, 16, 32, and 64 m grain sizes were both conifer classes (Figure 27). There is a gradual shift of the next dominant land cover, bedrock and non-vegetation, which decreased with increasing grain size while alternatively core patterns in water bodies increased in area (Figure 27). Core areas within the bedrock and non-vegetation classes decrease between 16 m and 64 m. An observation was made at the 32 m and 64 m grain sizes, whereby core morphological areas were at their highest frequencies in water bodies than any other land cover classes (Figure 27). The frequencies in the core morphological pattern areas matched the relative proportions of core morphologies for each land cover class (Figure 28).

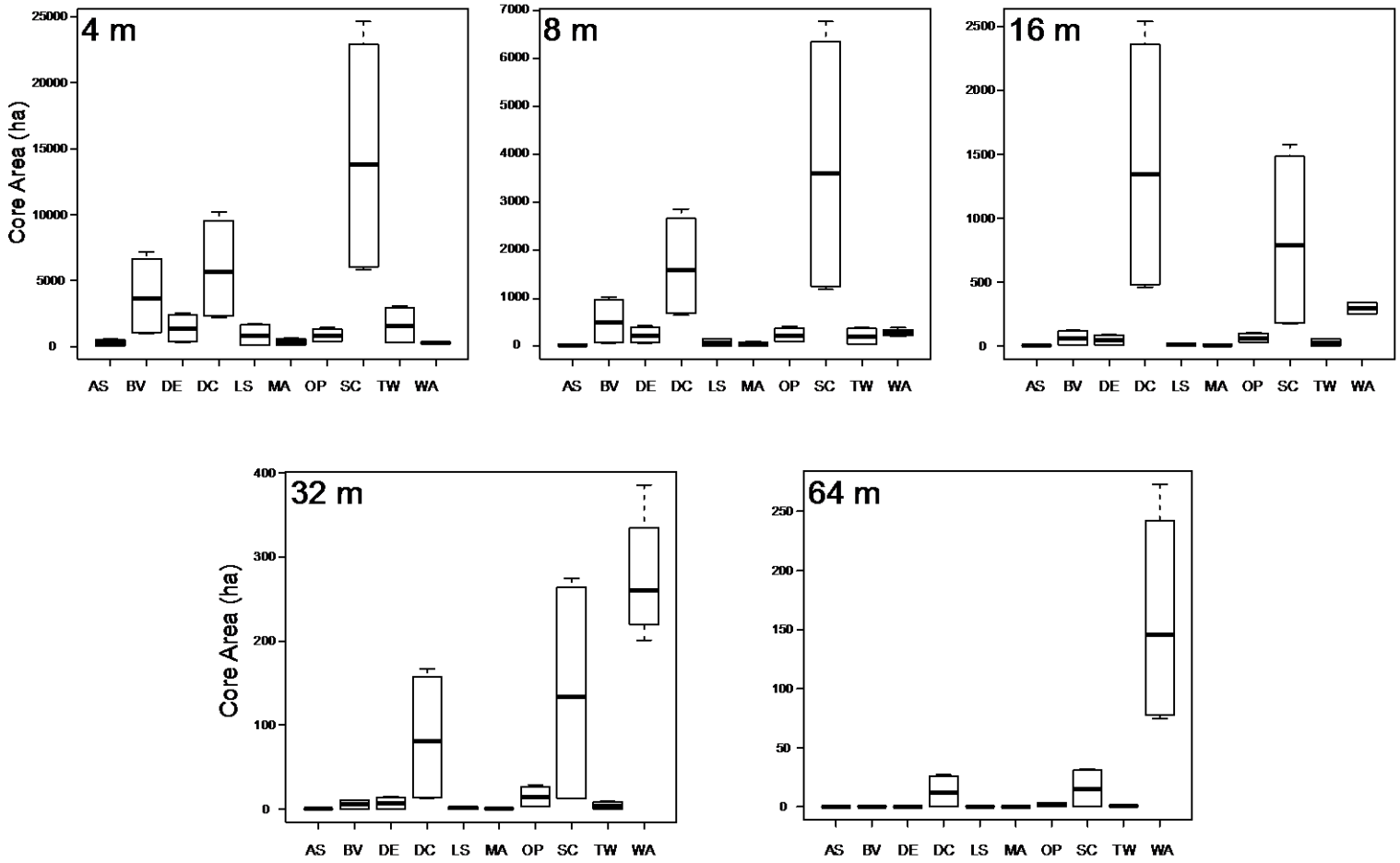

Figure 27. Core morphological element areas observed across all grain sizes within all land cover types.

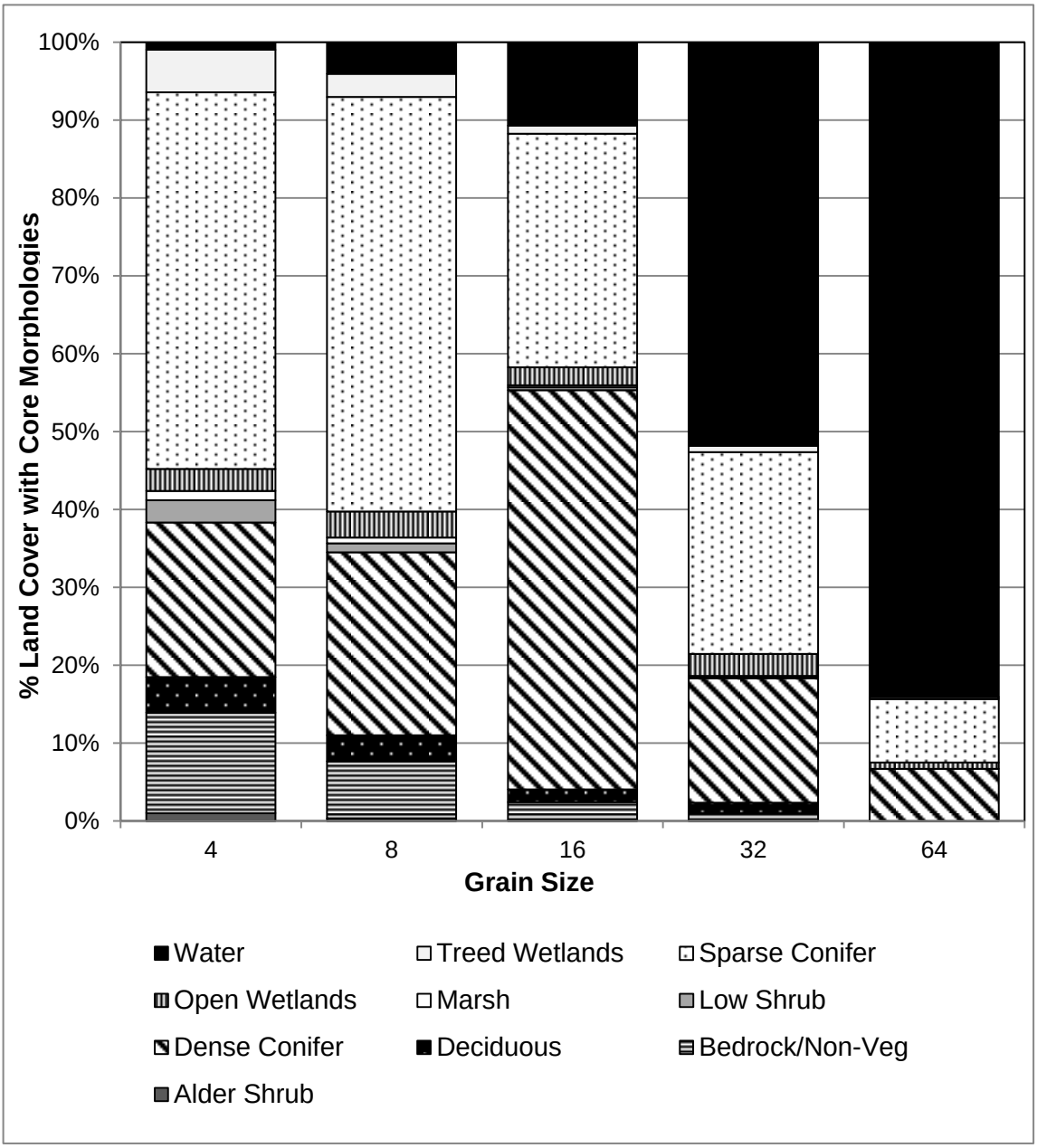

Figure 28. Land cover percentages comprising the core morphological pattern elements within insular residual patches at each of the 5 grain sizes (m).

Core morphological areas generally decrease with an increase in grain size from 4 m to 8 m (Figure 29). As the grain size increases, the outer edge boundary of the core morphology increases in size and thus constricts the available core area (Figure 29). Generally the smaller core morphological elements within residual patches are transformed into islet morphologies at large grain sizes (32 m and 64 m). Observations were also made from increasing the edge width parameter; the edge morphology would increase in size inward hence decreasing the core morphology area (Figure 29).

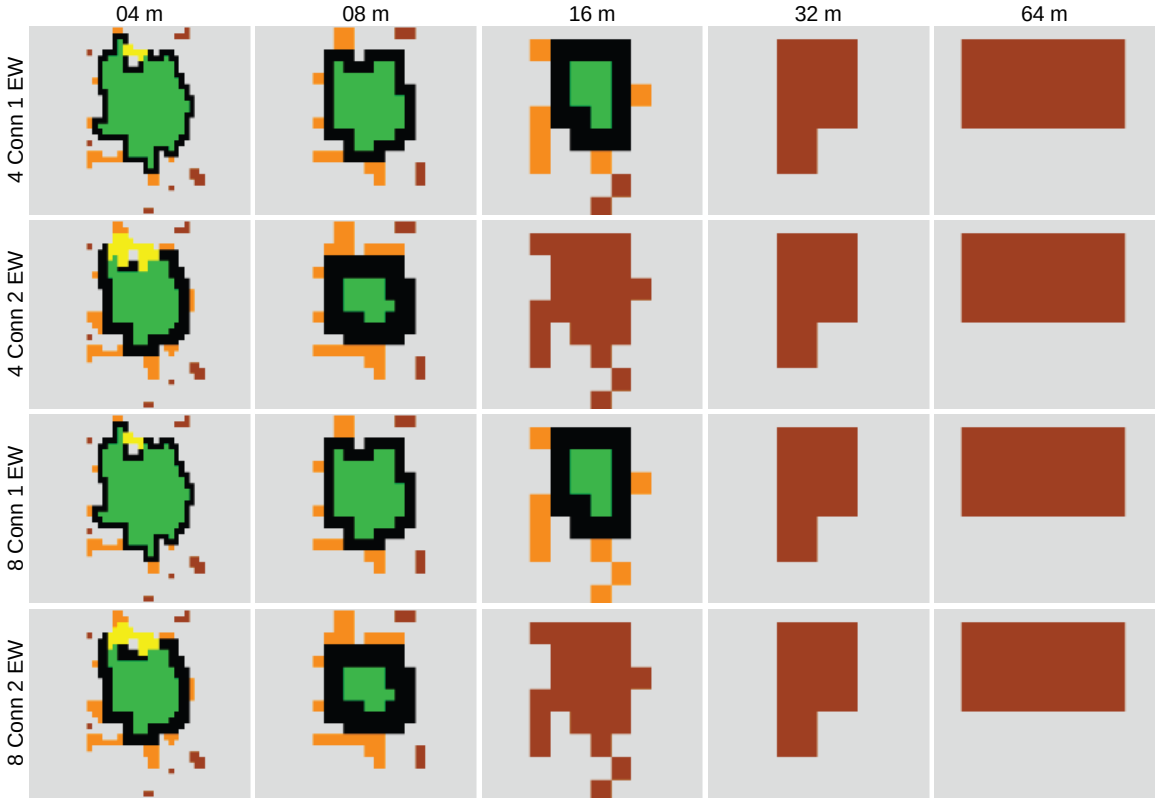

Figure 29. Core morphology observed in a section of bedrock and non-vegetation land cover across multiple grain sizes and parameter change (4 Conn – 4 Neighbourhood Connectivity, 8 Conn – 8 Neighbourhood Connectivity, 1 EW – 1 Edge Width Pixel, and 2 EW – 2 Edge Width Pixels). Note: The transitioning was turned off.

The core morphological elements were not affected when a transition was applied to the morphological maps (Figure 30). The loop morphologies in Figure 30 can be observed connecting through the edge to reach the cores but not projecting further into the cores.

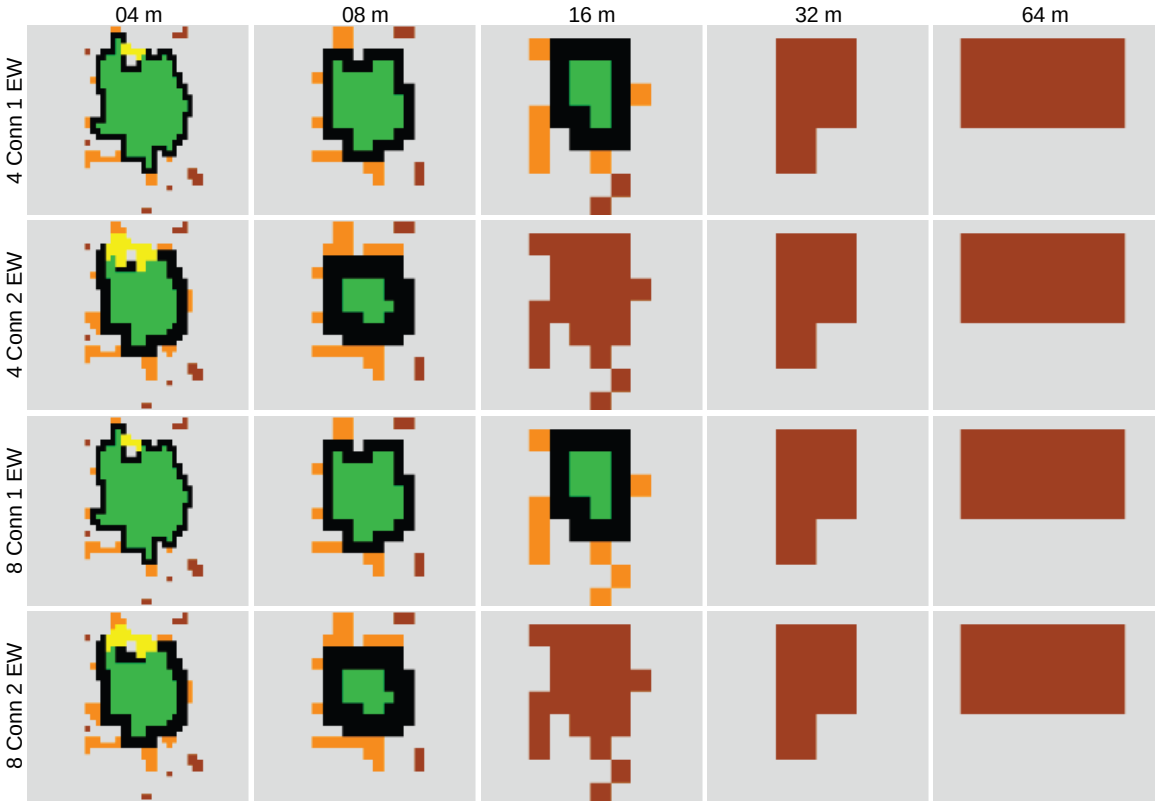

Figure 30. Core morphology observed in a section of bedrock and non-vegetation land cover across multiple grain sizes with transitioning turned on.

3.2 Islet Morphology

A one-way ANOVA test was conducted for islet morphological patterns across all land cover classes for each grain size observation (Table 12). At each grain size level, there was a significant difference in the islet areas at the $p < 0.05$ level among the land cover classes. At least one land cover class is significantly different from the other classes.

Table 12. One-way ANOVA results of islet morphological pattern elements across all grain sizes (4 m to 64 m) at the $p < 0.05$ significance level.

Source of Variation	d.f.	Sum Sq	Mean Sq	F Value	P-Value
4m					
Land Cover	9	91065	10118	308.90	<0.0000
Residuals	150	4913	33		
8m					
Land Cover	9	809733	89970	106.70	<0.0000
Residuals	150	126464	843		
16m					
Land Cover	9	1825153	202795	79.55	<0.0000
Residuals	150	382390	2549		
32m					
Land Cover	9	4162054	462450	130.00	<0.0000
Residuals	150	533658	3558		
64m					
Land Cover	9	10298518	1144280	174.90	<0.0000
Residuals	150	981360	6542		

There were significant differences in the islet morphological patterns among all land cover classes, except for treed wetland and sparse conifer classes at 4 m grain size (Table 13). At 8 m grain size, there was no significant difference in the islet morphological elements between treed wetland and dense conifer (Table 14).

Table 13. Tukey post-hoc test results for islet morphological pattern elements at 4 m grain size.

Land Cover	Alder	Bed	Decid	DCon	LowS	Marsh	OpenW	SCon	TreeW	Water
Alder	-									
Bed	**0.0000**	-								
Decid	**0.0006**	**0.0000**	-							
DCon	**0.0000**	**0.0000**	**0.0000**	-						
LowS	0.1932	**0.0000**	0.7180	**0.0000**	-					
Marsh	**0.0000**	**0.0000**	**0.0000**	**0.0000**	**0.0000**	-				
OpenW	**0.0000**	**0.0000**	**0.0000**	**0.0000**	**0.0000**	**0.0074**	-			
SCon	**0.0000**	**0.0003**	**0.0000**	**0.0060**	**0.0000**	**0.0000**	**0.0000**	-		
TreeW	**0.0000**	**0.0298**	**0.0000**	**0.0000**	**0.0000**	**0.0000**	**0.0000**	0.9561	-	
Water	**0.0000**	**0.0000**	**0.0000**	**0.0000**	**0.0000**	**0.0184**	**0.0000**	**0.0000**	**0.0000**	-

Table 14. Tukey post-hoc test results for islet morphological pattern elements at 8 m grain size.

Land Cover	Alder	Bed	Decid	DCon	LowS	Marsh	OpenW	SCon	TreeW	Water
Alder	-									
Bed	**0.0000**	-								
Decid	**0.0008**	**0.0000**	-							
DCon	**0.0000**	0.9372	**0.0000**	-						
LowS	0.8001	**0.0000**	0.1717	**0.0000**	-					
Marsh	**0.0000**	**0.0000**	**0.0000**	**0.0000**	**0.0000**	-				
OpenW	**0.0128**	**0.0000**	**0.0000**	**0.0000**	**0.0000**	0.4560	-			
SCon	**0.0000**	0.6890	**0.0000**	**0.0475**	**0.0000**	**0.0000**	**0.0000**	-		
TreeW	**0.0000**	0.6931	**0.0006**	1.0000	**0.0000**	**0.0000**	**0.0000**	**0.0098**	-	
Water	**0.0000**	**0.0000**	**0.0000**	**0.0000**	**0.0000**	0.6529	**0.0024**	**0.0000**	**0.0000**	-

All islet morphological elements within the land cover classes at 16 m were significantly different at the significance level $p < 0.05$, except for groupings low shrub - alder shrub woodland, open wetland - alder shrub, deciduous - dense conifer, low shrub, and treed wetland, treed wetland - dense conifer, water - marsh and open wetland (Table 15).

Table 15. Tukey post-hoc test results for islet morphological pattern elements at 16 m grain size.

Land Cover	Alder	Bed	Decid	DCon	LowS	Marsh	OpenW	SCon	TreeW	Water
Alder	-									
Bed	**0.0000**	-								
Decid	**0.0068**	**0.0000**	-							
DCon	**0.0000**	**0.0305**	0.0904	-						
LowS	0.9964	**0.0000**	0.1036	**0.0000**	-					
Marsh	**0.0016**	**0.0000**	**0.0000**	**0.0000**	**0.0000**	-				
OpenW	0.2139	**0.0000**	**0.0000**	**0.0000**	**0.0194**	0.8474	-			
SCon	**0.0000**	0.0639	**0.0000**	**0.0000**	**0.0000**	**0.0000**	**0.0000**	-		
TreeW	**0.0000**	**0.0356**	0.0789	1.0000	**0.0000**	**0.0000**	**0.0000**	**0.0000**	-	
Water	**0.0000**	**0.0000**	**0.0000**	**0.0000**	**0.0000**	0.9683	0.1405	**0.0000**	**0.0000**	-

The mean areas for low shrub and alder shrub, and open wetland and marsh land cover classes were not significantly different within islet morphologies at 32 m grain size ($p > 0.05$) (Table 16). The mean islet areas for the water and marsh land cover pairing were not statistically different when observed at 32 m grain size ($p > 0.05$) (Table 16).

Table 16. Tukey post-hoc test results for islet morphological pattern elements at 32 m grain size.

Land Cover	Alder	Bed	Decid	DCon	LowS	Marsh	OpenW	SCon	TreeW	Water
Alder	-									
Bed	**0.0000**	-								
Decid	**0.0021**	**0.0000**	-							
DCon	**0.0000**	0.0516	**0.0000**	-						
LowS	0.9986	**0.0000**	**0.0319**	**0.0000**	-					
Marsh	**0.0030**	**0.0000**	**0.0000**	**0.0000**	**0.0001**	-				
OpenW	0.1292	**0.0000**	**0.0000**	**0.0000**	**0.0132**	0.9685	-			
SCon	**0.0000**	**0.0000**	**0.0000**	**0.0000**	**0.0000**	**0.0000**	**0.0000**	-		
TreeW	**0.0000**	0.1022	0.1964	**0.0000**	**0.0000**	**0.0000**	**0.0000**	**0.0000**	-	
Water	**0.0005**	**0.0000**	**0.0000**	**0.0000**	**0.0000**	1.0000	0.7975	**0.0000**	**0.0000**	-

The Tukey post-hoc test on the islet morphological elements at 64 m grain size shows that there were significant differences in the land cover classes (Table 17). All comparisons of the land cover classes were significantly different from all of the pairings, with only a few exceptions. The mean islet areas for alder shrub did not significantly differ from low shrub, open wetland, and water classes ($p > 0.05$). The mean islet areas for the water and low shrub pairings were also not significantly different ($p > 0.05$) (Table 17).

Table 17. Tukey post-hoc test results for islet morphological pattern elements at 64 m grain size.

Land Cover	Alder	Bed	Decid	DCon	LowS	Marsh	OpenW	SCon	TreeW	Water
Alder	-									
Bed	**0.0000**	-								
Decid	**0.0103**	**0.0000**	-							
DCon	**0.0000**	**0.0000**	**0.0000**	-						
LowS	1.0000	**0.0000**	**0.0354**	**0.0000**	-					
Marsh	0.0957	**0.0000**	**0.0000**	**0.0000**	**0.0325**	-				
OpenW	0.9592	**0.0000**	**0.0001**	**0.0000**	0.8188	0.7913	-			
SCon	**0.0000**	**0.0000**	**0.0000**	**0.0000**	**0.0000**	**0.0000**	**0.0000**	-		
TreeW	**0.0000**	0.0537	0.1922	**0.0000**	**0.0000**	**0.0000**	**0.0000**	**0.0000**	-	
Water	1.0000	**0.0000**	**0.0162**	**0.0000**	1.0000	0.0668	0.9244	**0.0000**	**0.0000**	-

The islet morphological areas observed via the boxplots in Figure 31 were shown to be more variable than the core morphologies in their occurrences within land cover classes. The islet morphological areas measured at 4 m and 8 m grain sizes in Figure 31 revealed that open wetlands and marshes were the least represented land cover classes. The dominant land cover classes comprising islets were sparse conifer, bedrock and non-vegetation, dense conifer, treed wetland, deciduous and low shrub.

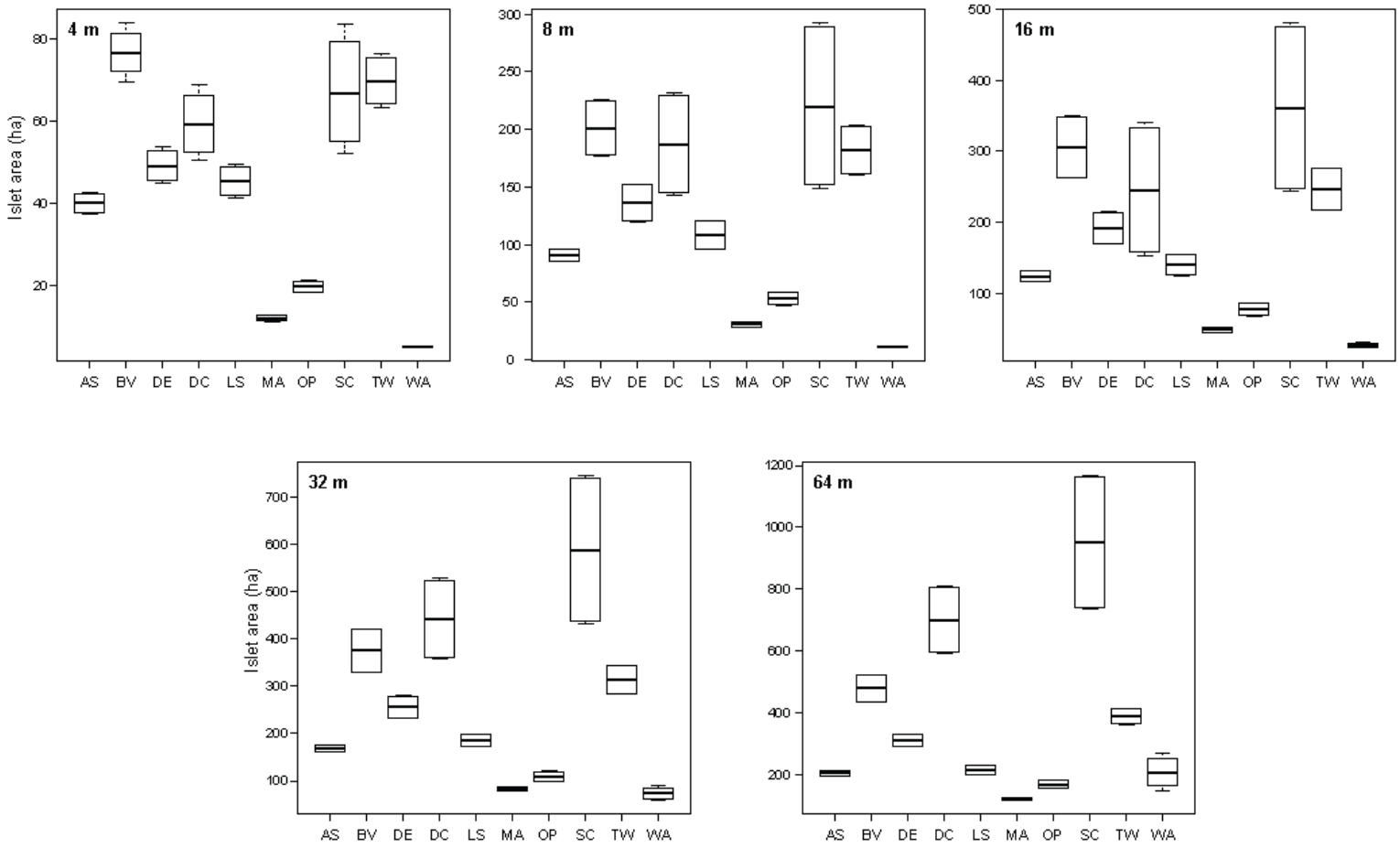

Figure 31. Islet morphological pattern areas plotted to illustrate the land cover classes in which they are most dominant.

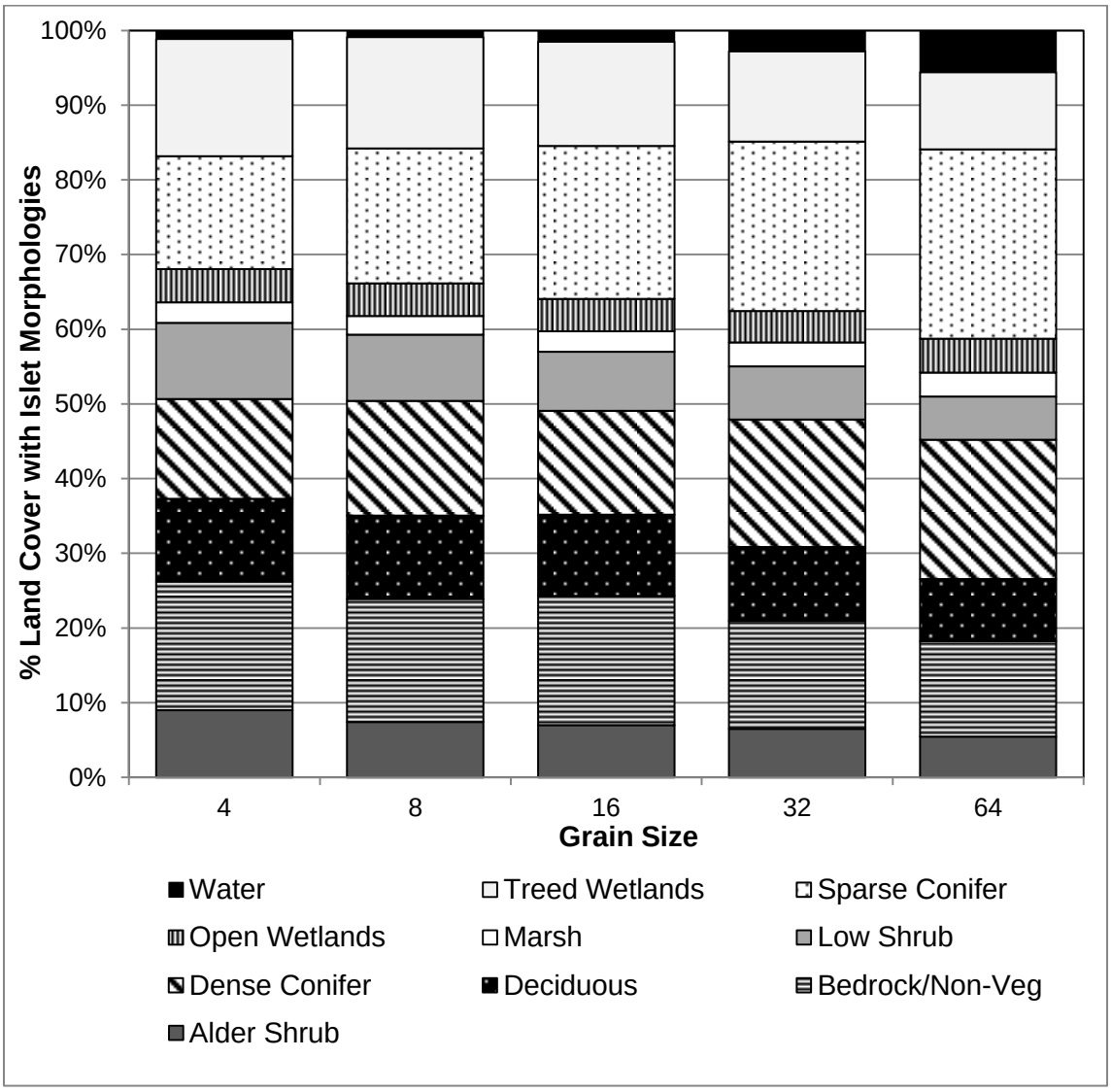

Figure 32. Land cover percentages comprising the islet morphological pattern elements within insular residual patches at each of the 5 grain sizes.

Islets are isolated morphological pattern elements but are affected by the neighbourhood connectivity, which potentially links the islets to other islets or morphological patterns. This can result in the islets being transformed into another morphology. Figure 33 shows a 4 m grain size sample site of low shrub residuals indicating the transformation of islets to loops and branches when the connectivity was set to 8 neighbouring pixels. The edge width generally has an effect on the occurrence of islets. When observing the same 4 m grain size morphological map in Figure 33 at 1 and 2 edge width pixels, it was noted that an increase in edge width pixels allowed for core and branch morphologies to be converted into islet morphologies. Generally an increase in the grain size (Figure 33) results in most morphological pattern elements to be converted into islet morphologies. Transitioning does not have an effect on the outcome of islet morphologies (Figure 34).

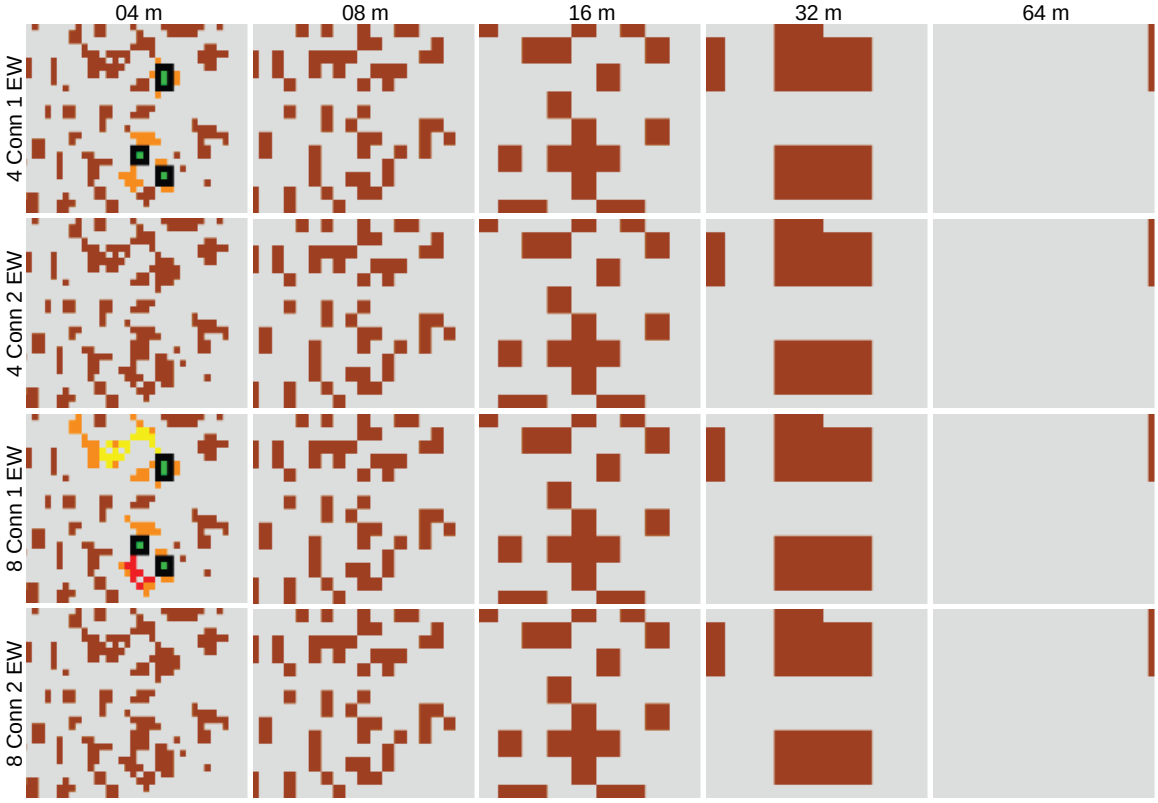

Figure 33. A sample site map of the low shrub residual morphological elements highlighting the occurrences of islets (transition turned off).

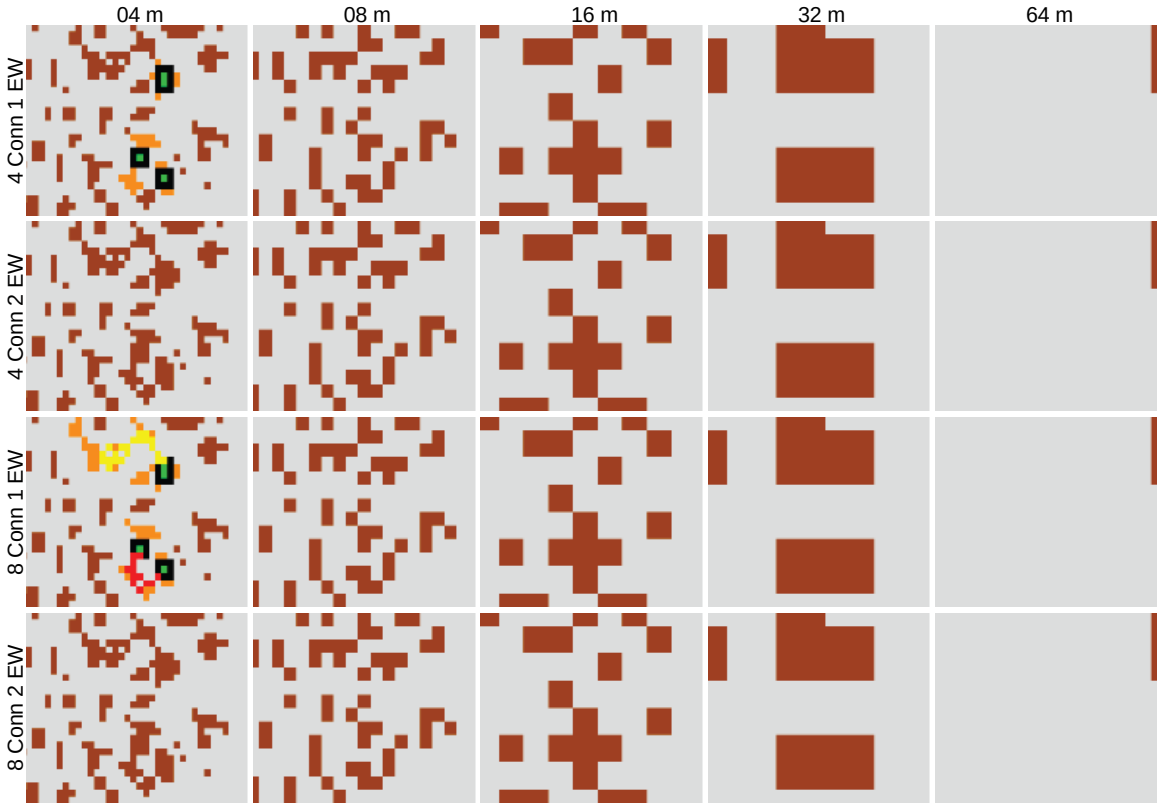

Figure 34. A sample site map of the low shrub residual morphological elements highlighting the occurrences of islets (transition turned on).

3.3 Perforation Morphology

A one-way ANOVA test among perforation morphologies was conducted to compare the effect of grain size on the occurrences of perforations within land cover classes. There was a significant difference between the means of the areas of perforation morphological elements among all of the land cover classes at each grain size ($p < 0.05$) (Table 18).

Table 18. One-way ANOVA results showing the occurrences of perforation morphological elements within each land cover class across all grain sizes.

Source of Variation	d.f.	Sum Sq	Mean Sq	F Value	P-Value
4m					
Land Cover	9	29.230	3.248	18.57	<0.0000
Residuals	150	29.230	0.175		
8m					
Land Cover	9	12.014	1.335	32.98	<0.0000
Residuals	150	6.071	0.041		
16m					
Land Cover	9	46.790	5.199	55.88	<0.0000
Residuals	150	13.960	0.093		
32m					
Land Cover	9	73.910	8.213	30.97	<0.0000
Residuals	150	39.780	0.265		
64m					
Land Cover	9	18.270	2.030	14.76	<0.0000
Residuals	150	20.640	0.138		

At 4 m grain size the following pairs of land cover classes were found to be significantly different ($p < 0.05$): dense conifer and all other classes, sparse conifer and all other classes, and water and treed wetlands (Table 19).

Table 19. Tukey post-hoc test results for perforation morphological pattern elements at 4 m grain size.

Land Cover	Alder	Bed	Decid	DCon	LowS	Marsh	OpenW	SCon	TreeW	Water
Alder	-									
Bed	1.0000	-								
Decid	1.0000	1.0000	-							
DCon	0.2765	0.5008	0.5981	-						
LowS	1.0000	1.0000	1.0000	0.2838	-					
Marsh	1.0000	1.0000	1.0000	0.2979	1.0000	-				
OpenW	1.0000	1.0000	1.0000	0.5726	1.0000	1.0000	-			
SCon	**0.0000**	**0.0000**	**0.0000**	**0.0000**	**0.0000**	**0.0000**	**0.0000**	-		
TreeW	1.0000	1.0000	1.0000	0.4840	1.0000	1.0000	1.0000	**0.0000**	-	
Water	0.9860	0.9993	0.9999	0.9187	0.9872	0.9892	0.9998	**0.0000**	0.9991	-

At 8 m grain size, the Tukey HSD results show that the mean perforation areas of the following land cover classes were significantly different from all other land cover classes when paired ($p < 0.05$): sparse conifer, dense conifer, and water (Table 20).

Table 20. Tukey post-hoc test results for perforation morphological elements at 8 m grain size.

Land Cover	Alder	Bed	Decid	DCon	LowS	Marsh	OpenW	SCon	TreeW	Water
Alder	-									
Bed	1.0000	-								
Decid	1.0000	1.0000	-							
DCon	**0.0000**	**0.0001**	**0.0001**	-						
LowS	1.0000	1.0000	1.0000	**0.0000**	-					
Marsh	1.0000	1.0000	1.0000	**0.0000**	1.0000	-				
OpenW	1.0000	1.0000	1.0000	**0.0002**	1.0000	1.0000	-			
SCon	**0.0000**	**0.0000**	**0.0000**	0.0654	**0.0000**	**0.0000**	**0.0000**	-		
TreeW	1.0000	1.0000	1.0000	**0.0001**	1.0000	1.0000	1.0000	**0.0000**	-	
Water	**0.0000**	**0.0000**	**0.0000**	**0.0000**	**0.0000**	**0.0000**	**0.0000**	0.2496	**0.0000**	-

At 16 m grain size, the Tukey HSD test determined that mean perforation areas of water and dense conifer classes when paired with all other land cover classes were statistically different ($p < 0.05$) (Table 21).

Table 21. Tukey post-hoc test results for perforation morphological elements at 16 m grain size.

Land Cover	Alder	Bed	Decid	DCon	LowS	Marsh	OpenW	SCon	TreeW	Water
Alder	-									
Bed	1.0000	-								
Decid	1.0000	1.0000	-							
DCon	**0.0000**	**0.0000**	**0.0000**	-						
LowS	1.0000	1.0000	1.0000	**0.0000**	-					
Marsh	1.0000	1.0000	1.0000	**0.0000**	1.0000	-				
OpenW	1.0000	1.0000	1.0000	**0.0000**	1.0000	1.0000	-			
SCon	1.0000	1.0000	1.0000	**0.0000**	1.0000	1.0000	1.0000	-		
TreeW	1.0000	1.0000	1.0000	**0.0000**	1.0000	1.0000	1.0000	1.0000	-	
Water	**0.0000**	**0.0000**	**0.0000**	**0.0000**	**0.0000**	**0.0000**	**0.0000**	**0.0000**	**0.0000**	-

The findings of the Tukey HSD test on mean areas of perforation patches at 32 m and 64 m only resulted in the water class being the most dominant land cover. The mean areas of perforation morphologies for the water body class were significantly different from all other land cover types at the ($p < 0.05$) (Table 22 and Table 23).

Table 22. Tukey post-hoc test results for perforation morphological elements at 32 m grain size.

Land Cover	Alder	Bed	Decid	DCon	LowS	Marsh	OpenW	SCon	TreeW	Water
Alder	-									
Bed	1.0000	-								
Decid	1.0000	1.0000	-							
DCon	1.0000	1.0000	1.0000	-						
LowS	1.0000	1.0000	1.0000	1.0000	-					
Marsh	1.0000	1.0000	1.0000	1.0000	1.0000	-				
OpenW	1.0000	1.0000	1.0000	1.0000	1.0000	1.0000	-			
SCon	1.0000	1.0000	1.0000	1.0000	1.0000	1.0000	1.0000	-		
TreeW	1.0000	1.0000	1.0000	1.0000	1.0000	1.0000	1.0000	1.0000	-	
Water	**0.0000**	**0.0000**	**0.0000**	**0.0000**	**0.0000**	**0.0000**	**0.0000**	**0.0000**	**0.0000**	-

Table 23. Tukey post-hoc test results for perforation morphological elements at 64 m grain size.

Land Cover	Alder	Bed	Decid	DCon	LowS	Marsh	OpenW	SCon	TreeW	Water
Alder	-									
Bed	1.0000	-								
Decid	1.0000	1.0000	-							
DCon	1.0000	1.0000	1.0000	-						
LowS	1.0000	1.0000	1.0000	1.0000	-					
Marsh	1.0000	1.0000	1.0000	1.0000	1.0000	-				
OpenW	1.0000	1.0000	1.0000	1.0000	1.0000	1.0000	-			
SCon	1.0000	1.0000	1.0000	1.0000	1.0000	1.0000	1.0000	-		
TreeW	1.0000	1.0000	1.0000	1.0000	1.0000	1.0000	1.0000	1.0000	-	
Water	**0.0000**	**0.0000**	**0.0000**	**0.0000**	**0.0000**	**0.0000**	**0.0000**	**0.0000**	**0.0000**	-

The perforation morphological elements observed in all residual patches were mostly found in dense conifer and sparse conifer classes in 4 m and 8 m grain sizes (Figure 35). From 32 m to 64 m, the most dominant land cover types found within perforations was water, as no perforations were found in any of the other classes (Figure 35). The dominance of perforation morphological elements in water bodies in larger grain sizes are also expressed in Figure 36. The perforation morphological elements within grain sizes from 16 m to 64 m remained intact when found in large bodies of water.

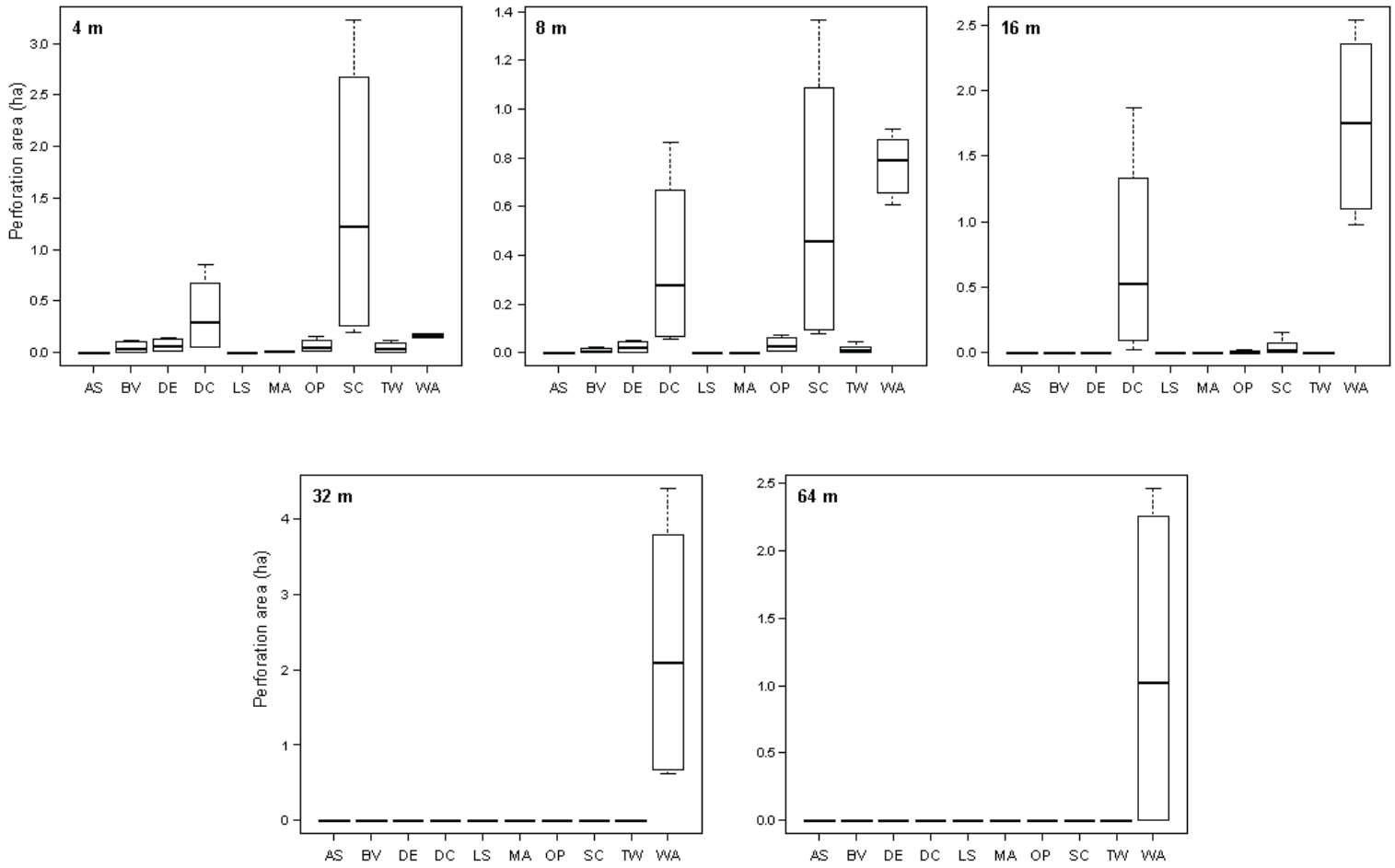

Figure 35. Perforation morphological elements were dominant in dense conifers (4 m – 16 m), sparse conifers (4 m and 8 m), and water bodies (16 m – 64 m).

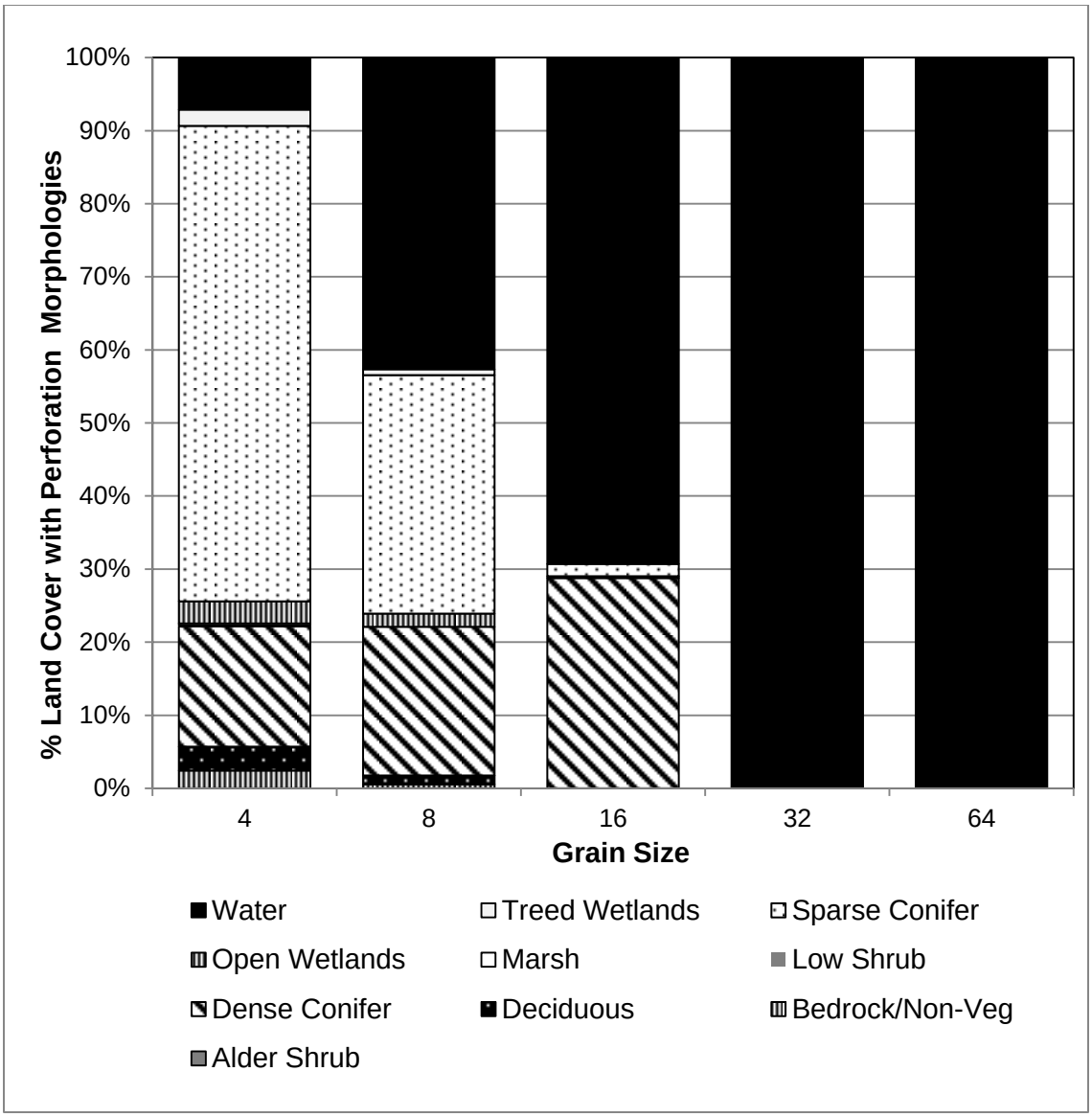

Figure 36. Land cover percentages comprising the perforation morphological pattern elements within insular residual patches at each of the 5 grain sizes.

The figure below (Figure 37) illustrates the evolution of the perforation morphology with grain size and parameter change. The neighbourhood connectivity in this scenario does not affect the outcome of the perforation but the edge width has an effect on the transformation of perforations to edges. At 4 m and 8 m grain sizes some of the perforations seem to transition into the background breaking the barrier of the core. These perforation morphological elements would then become edge

morphological elements. As the grain size increases, the perforation morphology can become edge morphology as the edges of the perforations get large enough to become an outer boundary.

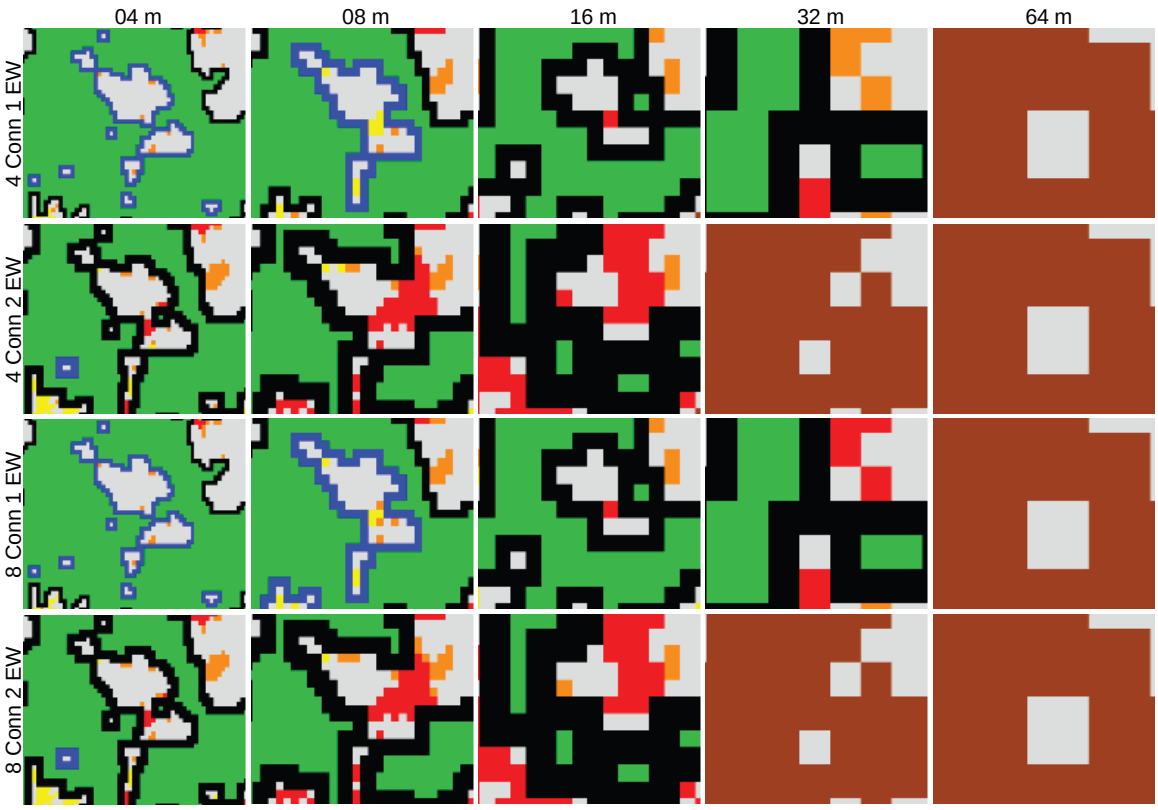

Figure 37. Perforation morphological elements changing with grain size, edge width, connectivity, and transitioning in a sample area of sparse conifer residuals (transition turned off).

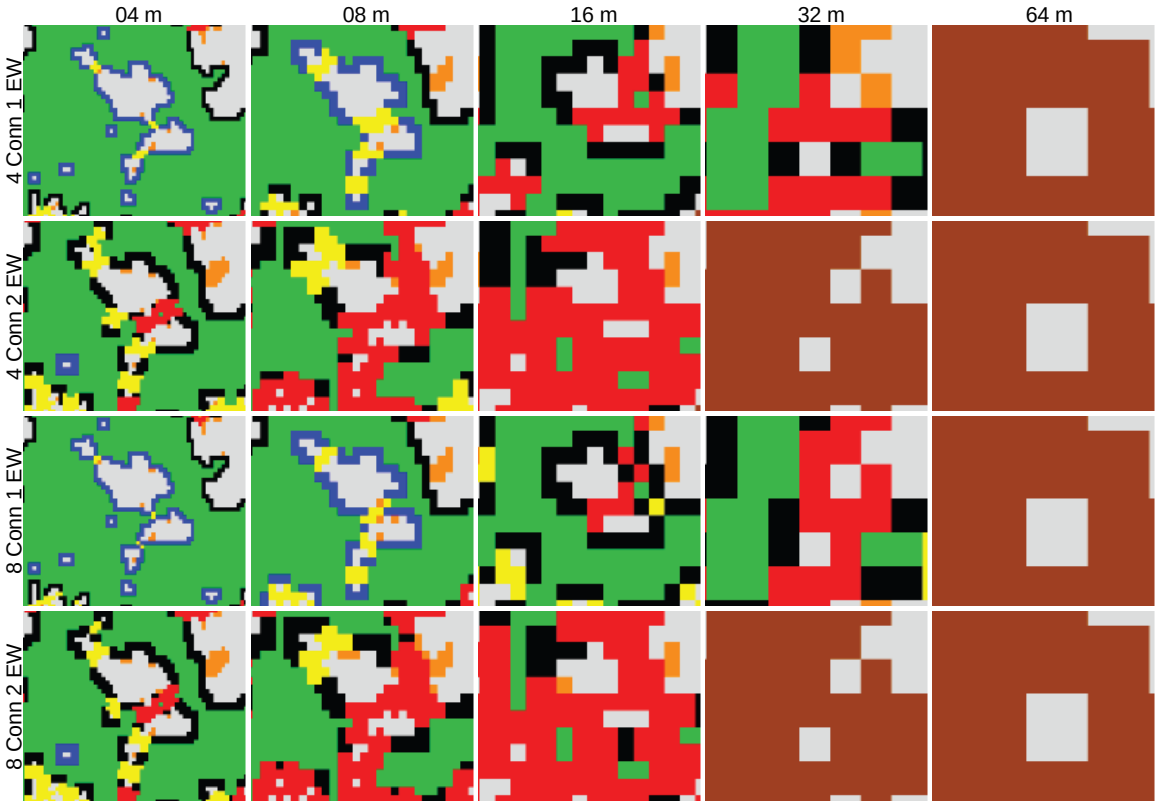

Figure 38. Perforation morphological elements changing with grain size, edge width, connectivity, and transitioning in a sample area of sparse conifer residuals (transition turned on).

3.4 Edge Morphology

A one-way ANOVA was conducted to compare the effect of grain size on the edge morphological elements within all of the land cover classes. There was a significant difference in the mean areas of edge morphologies for at least one of the land cover classes at each grain size ($p < 0.05$) (Table 24).

Table 24. One-way ANOVA results illustrating the edge morphological elements across all land cover classes for each grain size.

Source of Variation	d.f.	Sum Sq	Mean Sq	F Value	P-Value
4m					
Land Cover	9	12534	1392.6	16.17	<0.0000
Residuals	150	12918	86.1		
8m					
Land Cover	9	14804	1645.0	13.48	<0.0000
Residuals	150	18304	122.0		
16m					
Land Cover	9	36005	4001.0	15.14	<0.0000
Residuals	150	39637	264.0		
32m					
Land Cover	9	17043	1893.7	30.17	<0.0000
Residuals	150	9416	62.8		
64m					
Land Cover	9	72996	8111.0	33.27	<0.0000
Residuals	150	36571	244.0		

The Tukey post-hoc comparisons indicate that the mean edge areas of sparse conifer and dense conifer land covers differ significantly when paired with each of the other land cover classes at 4 m grain size ($p < 0.05$) (Table 25). The mean areas of bedrock and non-vegetation class were also significantly different from most land cover class pairings ($p > 0.05$). However, the mean edge areas of bedrock and non-vegetation were not significantly different when paired with deciduous and treed wetland land cover classes ($p > 0.05$) (Table 25).

Table 25. Tukey post-hoc test results for edge morphological elements at 4 m grain size.

Land Cover	Alder	Bed	Decid	DCon	LowS	Marsh	OpenW	SCon	TreeW	Water
Alder	-									
Bed	0.7537	-								
Decid	0.9998	0.9776	-							
DCon	**0.0472**	0.9041	0.2179	-						
LowS	1.0000	0.8976	1.0000	0.1026	-					
Marsh	1.0000	0.7679	0.9999	0.0505	1.0000	-				
OpenW	1.0000	0.9244	1.0000	0.1244	1.0000	1.0000	-			
SCon	**0.0000**	**0.0000**	**0.0000**	**0.0000**	**0.0000**	**0.0000**	**0.0000**	-		
TreeW	0.9993	0.9894	1.0000	0.2764	1.0000	0.9994	1.0000	**0.0000**	-	
Water	1.0000	0.7503	0.9998	**0.0465**	1.0000	1.0000	1.0000	**0.0000**	0.9992	-

The Tukey post-hoc comparisons of edge morphological areas at 8 m grain size show that dense conifer and sparse conifer were statistically different from pairings with all other land cover classes (p <0.05) (Table 26).

Table 26. Tukey post-hoc test results for edge morphological elements at 8 m grain size.

Land Cover	Alder	Bed	Decid	DCon	LowS	Marsh	OpenW	SCon	TreeW	Water
Alder	-									
Bed	0.9964	-								
Decid	1.0000	1.0000	-							
DCon	**0.0269**	0.2640	0.0906	-						
LowS	1.0000	0.9987	1.0000	**0.0375**	-					
Marsh	1.0000	0.9978	1.0000	**0.0320**	1.0000	-				
OpenW	1.0000	1.0000	1.0000	0.0968	1.0000	1.0000	-			
SCon	**0.0000**	**0.0000**	**0.0000**	**0.0001**	**0.0000**	**0.0000**	**0.0000**	-		
TreeW	1.0000	1.0000	1.0000	0.0750	1.0000	1.0000	1.0000	**0.0000**	-	
Water	1.0000	1.0000	1.0000	0.1041	1.0000	1.0000	1.0000	**0.0000**	1.0000	-

Using the post-hoc comparisons at 16 m grain size, the mean edge areas of water were significantly different from alder shrub, dense conifer, low shrub, marsh, sparse conifer, and treed wetland classes (p < 0.05) (Table 27). The mean areas of the dense conifer and sparse conifer classes were also significantly different when paired with all other land cover classes. At 32 m grain size, the mean edge areas of water were significantly different from all other land cover classes (p < 0.05) (Table 28).

Table 27. Tukey post-hoc test results for edge morphological elements at 16 m grain size.

Land Cover	Alder	Bed	Decid	DCon	LowS	Marsh	OpenW	SCon	TreeW	Water
Alder	-									
Bed	1.0000	-								
Decid	1.0000	1.0000	-							
DCon	**0.0000**	**0.0000**	**0.0000**	-						
LowS	1.0000	1.0000	1.0000	**0.0000**	-					
Marsh	1.0000	1.0000	1.0000	**0.0000**	1.0000	-				
OpenW	1.0000	1.0000	1.0000	**0.0000**	1.0000	1.0000	-			
SCon	**0.0007**	**0.0020**	**0.0015**	**0.0065**	**0.0008**	**0.0007**	**0.0021**	-		
TreeW	1.0000	1.0000	1.0000	**0.0000**	1.0000	1.0000	1.0000	**0.0011**	-	
Water	0.8874	0.9671	0.9507	**0.0000**	0.8995	0.8940	0.9679	0.1032	0.9271	-

Table 28. Tukey post-hoc test results for edge morphological elements at 32 m grain size.

Land Cover	Alder	Bed	Decid	DCon	LowS	Marsh	OpenW	SCon	TreeW	Water
Alder	-									
Bed	1.0000	-								
Decid	1.0000	1.0000	-							
DCon	**0.0330**	0.0568	0.0686	-						
LowS	1.0000	1.0000	1.0000	**0.0368**	-					
Marsh	1.0000	1.0000	1.0000	**0.0348**	1.0000	-				
OpenW	1.0000	1.0000	1.0000	0.1395	1.0000	1.0000	-			
SCon	**0.0000**	**0.0000**	**0.0000**	0.3875	**0.0000**	**0.0000**	**0.0000**	-		
TreeW	1.0000	1.0000	1.0000	0.0526	1.0000	1.0000	1.0000	**0.0000**	-	
Water	**0.0000**	**0.0000**	**0.0000**	**0.0000**	**0.0000**	**0.0000**	**0.0000**	**0.0000**	**0.0000**	-

The mean edge areas of the water body class differed statistically when paired with all other land cover classes at the 64 m grain size ($p < 0.05$) (Table 29). The large water bodies (Figure 39) represented a majority of the edge areas due to the large core areas they possessed. Although the dense conifer and sparse conifer classes comprised larger edge areas than the remaining classes at 64 m grain size (Figure 39), their mean areas were not significantly different from other classes ($p > 0.05$) (Table 29).

Table 29. Tukey post-hoc test results for edge morphological elements at 64 m grain size.

Land Cover	Alder	Bed	Decid	DCon	LowS	Marsh	OpenW	SCon	TreeW	Water
Alder	-									
Bed	1.0000	-								
Decid	1.0000	1.0000	-							
DCon	0.9933	0.9933	0.9933	-						
LowS	1.0000	1.0000	1.0000	0.9933	-					
Marsh	1.0000	1.0000	1.0000	0.9933	1.0000	-				
OpenW	1.0000	1.0000	1.0000	0.9973	1.0000	1.0000	-			
SCon	0.9719	0.9719	0.9719	1.0000	0.9719	0.9719	0.9855	-		
TreeW	1.0000	1.0000	1.0000	0.9950	1.0000	1.0000	1.0000	0.9772	-	
Water	**0.0000**	**0.0000**	**0.0000**	**0.0000**	**0.0000**	**0.0000**	**0.0000**	**0.0000**	**0.0000**	-

The boxplots below illustrate the change in edge morphological element occurrences (and area) with increasing grain size (Figure 39). Edge morphologies are observed more frequently in sparse and dense conifer at 4 m, 8 m, and 16 m. There was a subsequent decline in the edge area of both conifer types at 32 m and 64 m grain size. There was an increase in the edge morphological area in water bodies at 32 m and 64 m, as compared to its proportion from 4 m to 16 m grain size. The dense conifer class also increased in area from 4 m to 16 m for edge morphological elements (Figure 40).

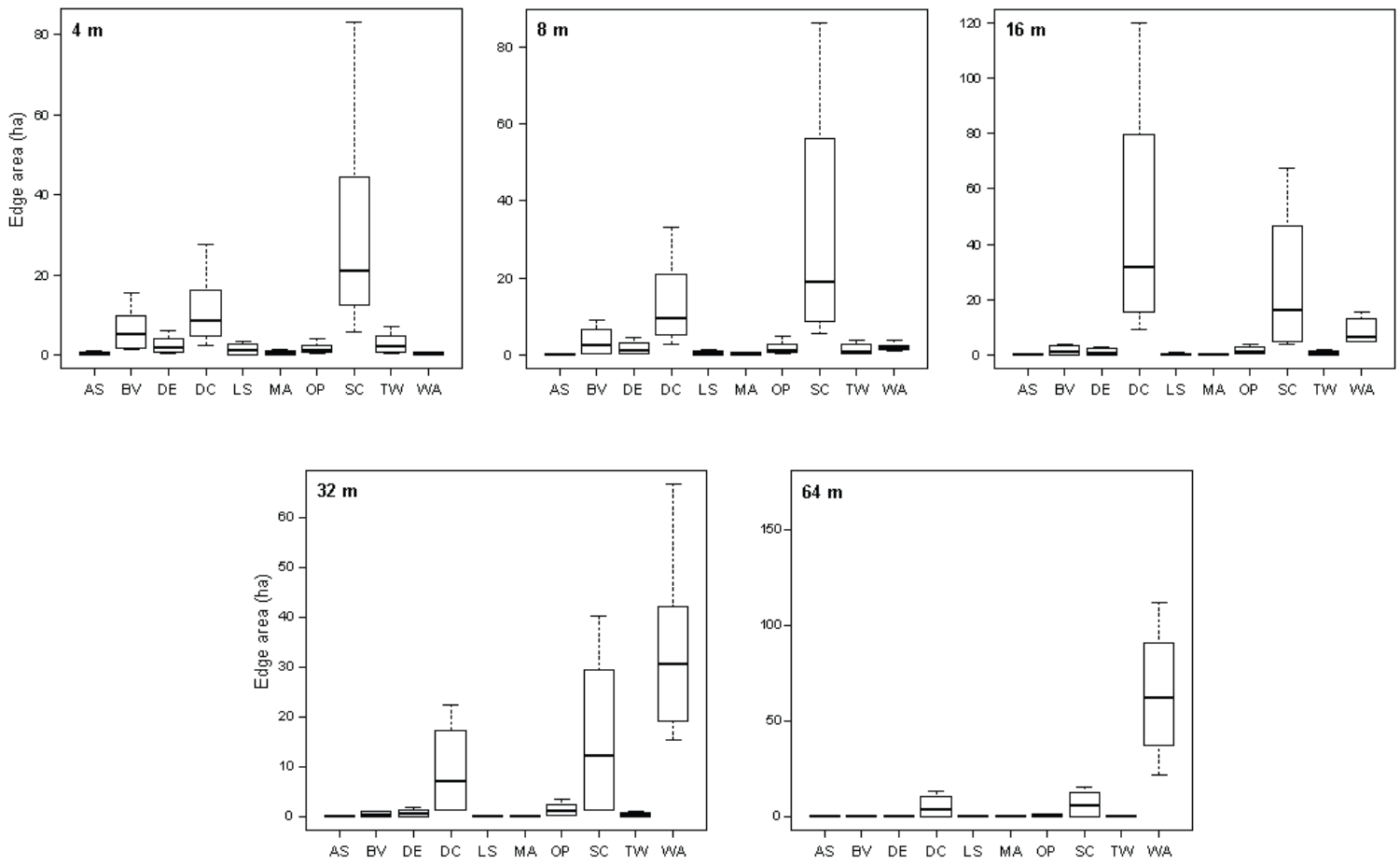

Figure 39. Edge morphologies were found to be most dominant in bedrock and non-vegetation, dense conifers, sparse conifers, and water bodies.

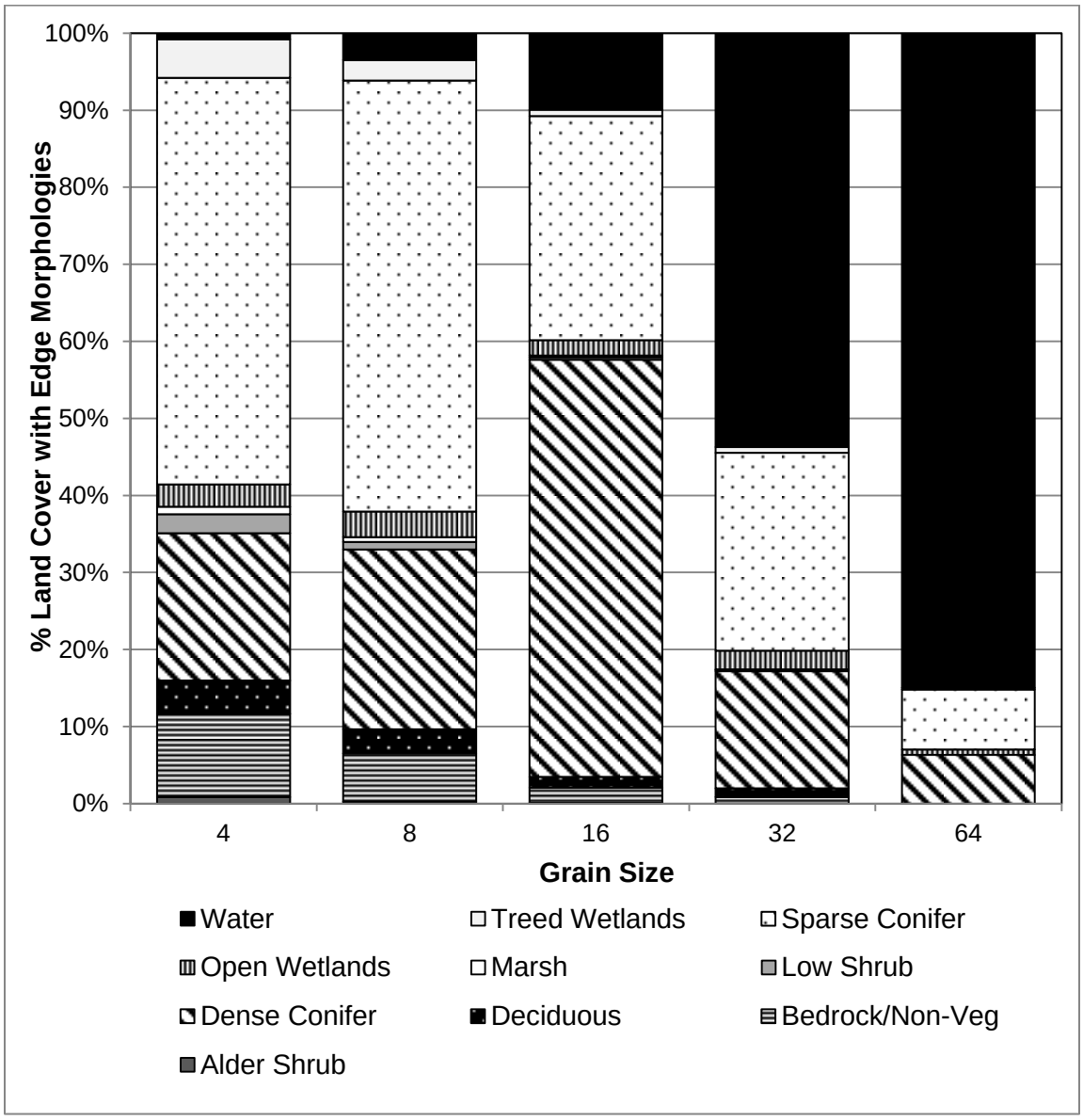

Figure 40. Land cover percentages comprising the edge morphological pattern elements within insular residual patches at each of the 5 grain sizes.

The area of edge morphological elements is dependent on the edge width parameter used and the grain size (Figure 41). As the edge width increases to 2 pixels, the edge morphological areas also increase. This pattern was also observed when increasing the grain size; the pixel size of the edge morphology increases until the core

morphology cannot be encompassed by an edge (Figure 41). This is observed in the progression from 4 m to 16 m, when the transition is turned off.

Similar trends were observed when the transitioning was turned on. There was a general increase in the edge morphological area when the grain size was also increased (Figure 42). However, with the transitioning turned on the loop and bridge morphological elements tend to infiltrate the edge patterns. These loops and bridges originate from the core patterns and thus occupy the area that was consumed by the edge pattern. Therefore the edge morphologies generally decrease when turning on the transition parameter.

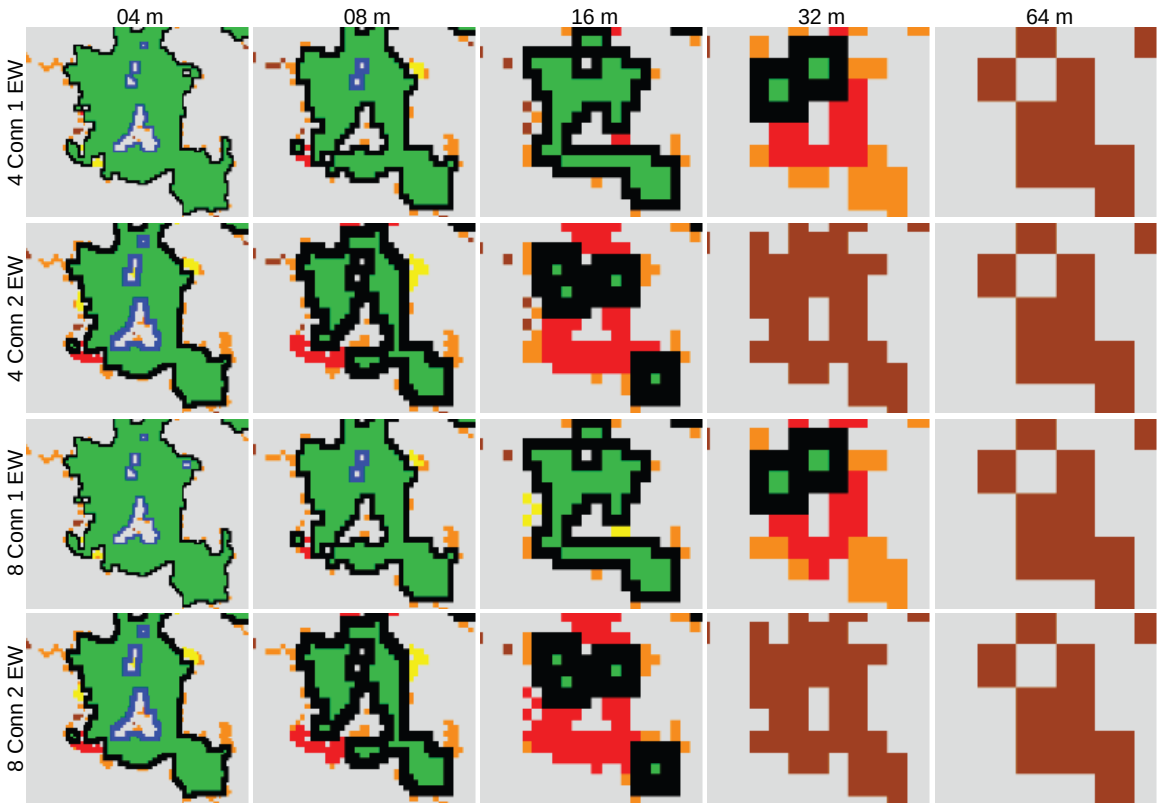

Figure 41. Morphological map showing how edge patterns change over grain size and parameter change in open wetland residuals (transition turned off).

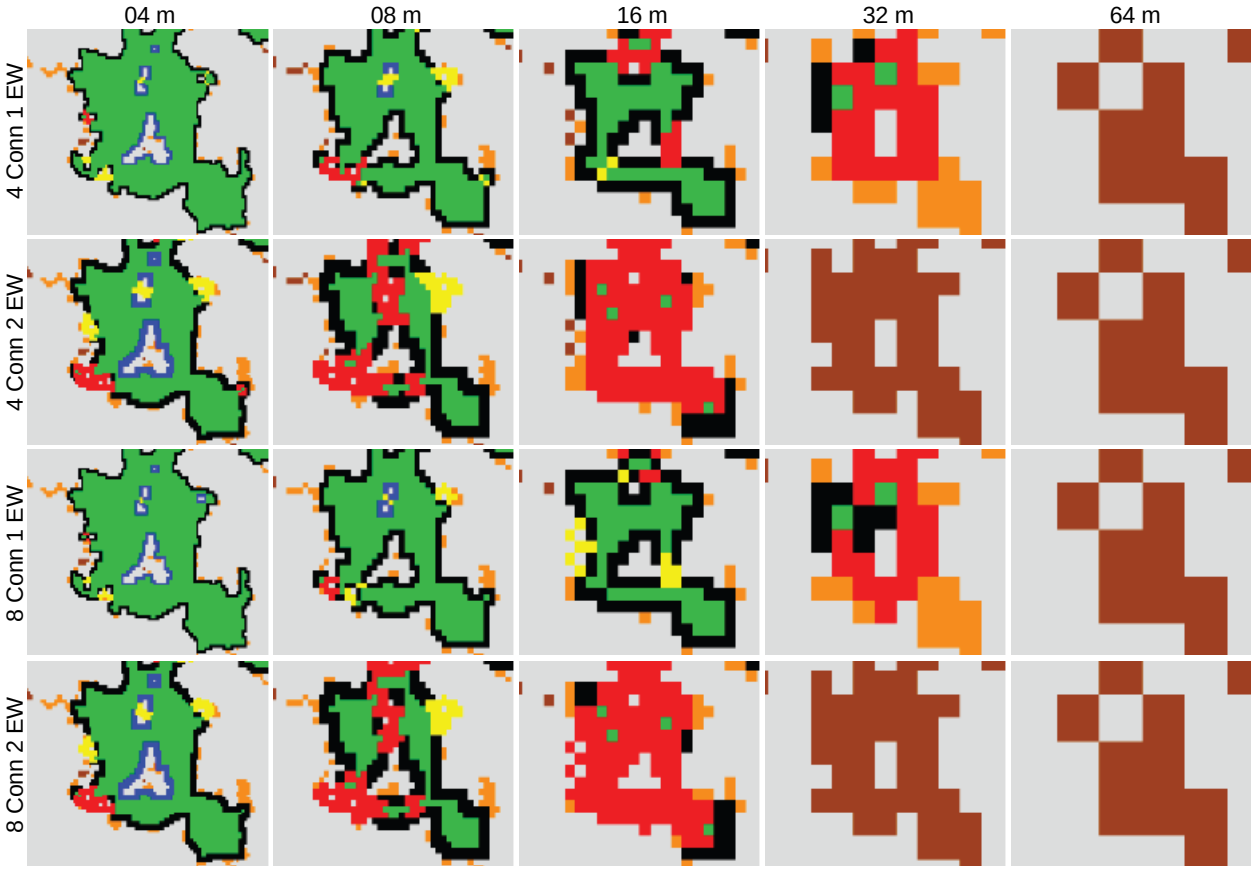

Figure 42. Morphological map showing how edge morphologies change over grain size and parameter change in open wetland residuals (transition turned on).

3.5 Loop Morphology

A one-way ANOVA test was conducted on the loop morphological areas to compare the effect of grain size on the occurrence of loops within residual patches. There was a significant effect of the grain size on the means of loop morphological areas in at least 1 land cover class at each grain size ($p < 0.05$) (Table 30).

The post hoc comparisons from the Tukey test showed that the loop morphological area means of the sparse conifer and dense conifer classes were significantly different from all other classes when paired ($p < 0.05$). This finding was observed in both 4 m and 8 m grain sizes (Tables 31 and 32).

Table 30. One-way ANOVA results illustrating that at least one land cover class was significantly different from other classes displaying loop morphology ($p < 0.05$).

Source of Variation	d.f.	Sum Sq	Mean Sq	F Value	P-Value
4m					
Land Cover	9	385.0	42.77	17.84	<0.0000
Residuals	150	359.5	2.40		
8m					
Land Cover	9	614.2	68.25	21.17	<0.0000
Residuals	150	483.6	3.22		
16m					
Land Cover	9	2234.0	248.22	28.63	<0.0000
Residuals	150	1300.0	8.67		
32m					
Land Cover	9	1167.0	129.64	18.11	<0.0000
Residuals	150	1074.0	7.16		
64m					
Land Cover	9	3694.0	410.40	14.84	<0.0000
Residuals	150	4150.0	27.70		

Table 31. Tukey post-hoc test results for loop morphological elements at 4 m grain size.

Land Cover	Alder	Bed	Decid	DCon	LowS	Marsh	OpenW	SCon	TreeW	Water
Alder	-									
Bed	0.9554	-								
Decid	1.0000	0.9989	-							
DCon	**0.0425**	0.6128	0.1624	-						
LowS	1.0000	0.9823	1.0000	0.0685	-					
Marsh	1.0000	0.9616	1.0000	**0.0465**	1.0000	-				
OpenW	0.9999	0.9990	1.0000	0.1687	1.0000	1.0000	-			
SCon	**0.0000**	**0.0000**	**0.0000**	**0.0000**	**0.0000**	**0.0000**	**0.0000**	-		
TreeW	0.9998	0.9997	1.0000	0.2084	1.0000	0.9999	1.0000	**0.0000**	-	
Water	1.0000	0.9582	1.0000	**0.0442**	1.0000	1.0000	1.0000	**0.0000**	0.9998	-

Table 32. Tukey post-hoc test results for loop morphological elements at 8 m grain size.

Land Cover	Alder	Bed	Decid	DCon	LowS	Marsh	OpenW	SCon	TreeW	Water
Alder	-									
Bed	0.9712	-								
Decid	0.9999	0.9998	-							
DCon	**0.0000**	**0.0010**	**0.0008**	-						
LowS	1.0000	0.9908	1.0000	**0.0000**	-					
Marsh	1.0000	0.9864	1.0000	**0.0000**	1.0000	-				
OpenW	0.9956	1.0000	1.0000	**0.0003**	0.9992	0.9986	-			
SCon	**0.0000**	**0.0000**	**0.0000**	**0.0007**	**0.0000**	**0.0000**	**0.0000**	-		
TreeW	0.9999	0.9997	1.0000	**0.0001**	1.0000	1.0000	1.0000	**0.0000**	-	
Water	0.9996	1.0000	1.0000	**0.0001**	1.0000	0.9999	1.0000	**0.0000**	1.0000	-

Tukey post-hoc comparison tests of loops at 16 m grain size revealed that mean loop areas of sparse conifer and dense conifer were significantly different from all other classes when those groups were compared ($p < 0.05$) (Tables 33). The mean areas for water bodies were not significantly different, except when grouped with the conifer classes ($p > 0.05$). At 32 m grain size, the mean areas for sparse conifer and water bodies were significantly different when compared with all other land cover classes ($p < 0.05$) (Table 34). The mean loop areas of dense conifers were not significantly different from other classes (except for water bodies) ($p > 0.05$).

Table 33. Tukey post-hoc test results for loop morphological elements at 16 m grain size.

Land Cover	Alder	Bed	Decid	DCon	LowS	Marsh	OpenW	SCon	TreeW	Water
Alder	-									
Bed	1.0000	-								
Decid	1.0000	1.0000	-							
DCon	**0.0000**	**0.0000**	**0.0000**	-						
LowS	1.0000	1.0000	1.0000	**0.0000**	-					
Marsh	1.0000	1.0000	1.0000	**0.0000**	1.0000	-				
OpenW	1.0000	1.0000	1.0000	**0.0000**	1.0000	1.0000	-			
SCon	**0.0000**	**0.0001**	**0.0000**	**0.0000**	**0.0000**	**0.0000**	**0.0001**	-		
TreeW	1.0000	1.0000	1.0000	**0.0000**	1.0000	1.0000	1.0000	**0.0000**	-	
Water	0.3859	0.7099	0.5868	**0.0000**	0.4339	0.3977	0.6979	0.0522	0.5502	-

Table 34. Tukey post-hoc test results for loop morphological elements at 32 m grain size.

Land Cover	Alder	Bed	Decid	DCon	LowS	Marsh	OpenW	SCon	TreeW	Water
Alder	-									
Bed	1.0000	-								
Decid	1.0000	1.0000	-							
DCon	0.3281	0.4483	0.4945	-						
LowS	1.0000	1.0000	1.0000	0.3607	-					
Marsh	1.0000	1.0000	1.0000	0.3281	1.0000	-				
OpenW	1.0000	1.0000	1.0000	0.6451	1.0000	1.0000	-			
SCon	**0.0000**	**0.0001**	**0.0001**	0.1649	**0.0000**	**0.0000**	**0.0003**	-		
TreeW	1.0000	1.0000	1.0000	0.4123	1.0000	1.0000	1.0000	**0.0001**	-	
Water	**0.0000**	**0.0000**	**0.0000**	**0.0000**	**0.0000**	**0.0000**	**0.0000**	**0.0085**	**0.0000**	-

The Tukey post-hoc test was also conducted for loop morphological mean areas at 64 m grain size. The mean areas of water bodies were statistically different from all other classes ($p < 0.05$) (Table 35).

Table 35. Tukey post-hoc test results for loop morphological elements at 64 m grain size.

Land Cover	Alder	Bed	Decid	DCon	LowS	Marsh	OpenW	SCon	TreeW	Water
Alder	-									
Bed	1.0000	-								
Decid	1.0000	1.0000	-							
DCon	0.9998	0.9998	0.9998	-						
LowS	1.0000	1.0000	1.0000	0.9998	-					
Marsh	1.0000	1.0000	1.0000	0.9998	1.0000	-				
OpenW	1.0000	1.0000	1.0000	0.9999	1.0000	1.0000	-			
SCon	0.9776	0.9776	0.9776	0.9999	0.9776	0.9776	0.9839	-		
TreeW	1.0000	1.0000	1.0000	0.9998	1.0000	1.0000	1.0000	0.9776	-	
Water	**0.0000**	**0.0000**	**0.0000**	**0.0000**	**0.0000**	**0.0000**	**0.0000**	**0.0000**	**0.0000**	-

The boxplots below highlight the change in loop morphological elements with increasing grain size (Figure 43). The higher proportion of loop morphological areas was found within dense conifer and sparse conifer residuals at 4 m, 8 m, and 16 m grain sizes (Figure 43). At 16 m and 32 m grain sizes, the loops are increasing in water bodies, and at 64 m the water body class contained the most loops. The conifer types accounted for the rest of the loop morphologies at 64 m grain size.

Loop morphological elements can change when the edge width is increased from 1 pixel width to 2 pixels (Figure 45). The morphological map below shows how the edge width can split a large core pattern into multiple core morphologies (at 4 m) resulting in some loops being converted into bridges. The loops can also change when increasing the grain size. At 8 connectivity and 1 edge width, the loops shifted to bridges at 8 m, then to a branch at 16 m, and then become non-existent at 32 m and 64 m. The neighbourhood connectivity can also affect the outcome of the loop morphologies. An example of this is illustrated at 8 m grain size (1 EW) where the connectivity of 4 neighbouring pixels resulted in a branch formation while an 8 connectivity produced a combination of a loop and several branches.

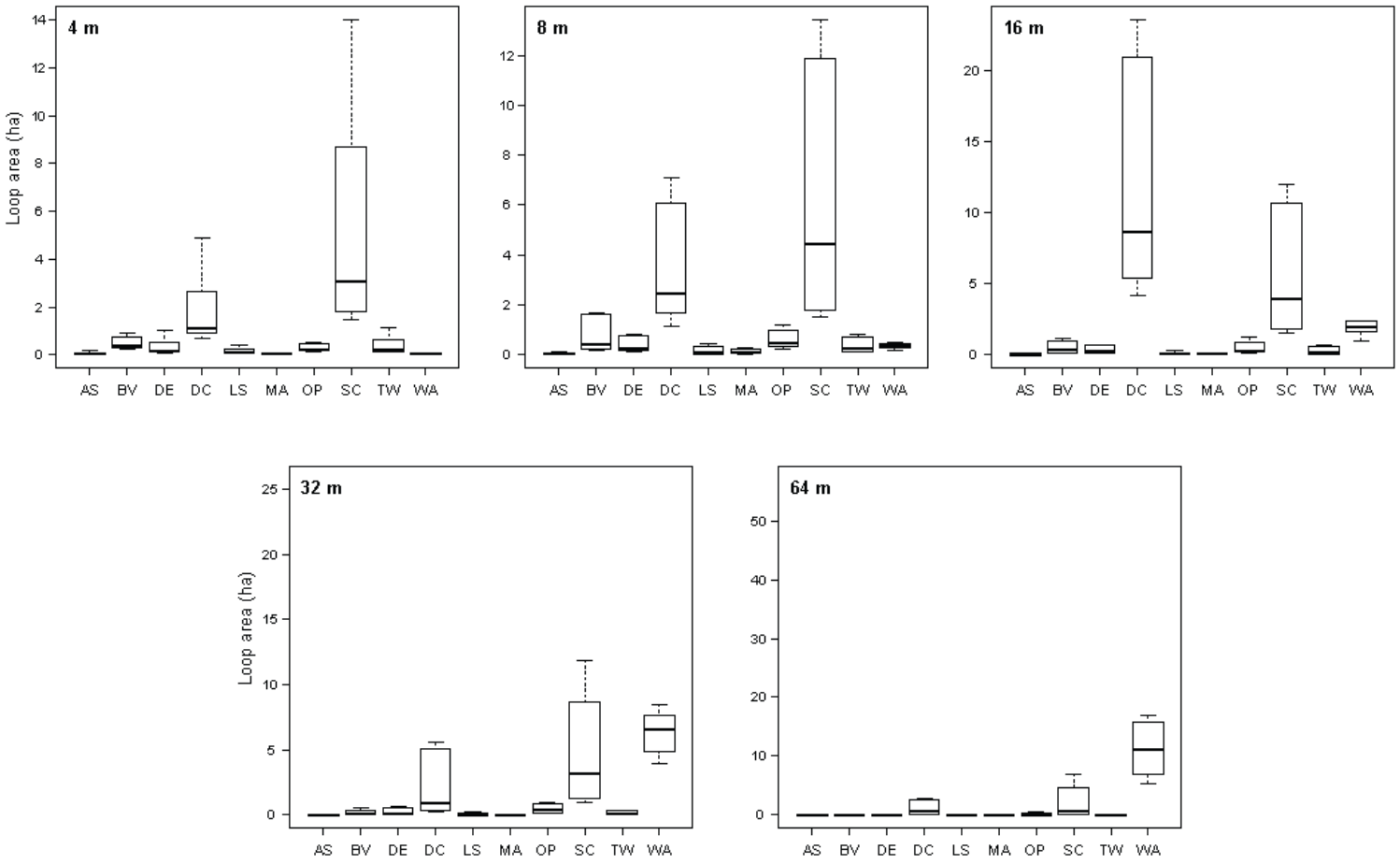

Figure 43. Boxplots illustrating the dominant land cover classes in which loop morphologies were found at each grain size.

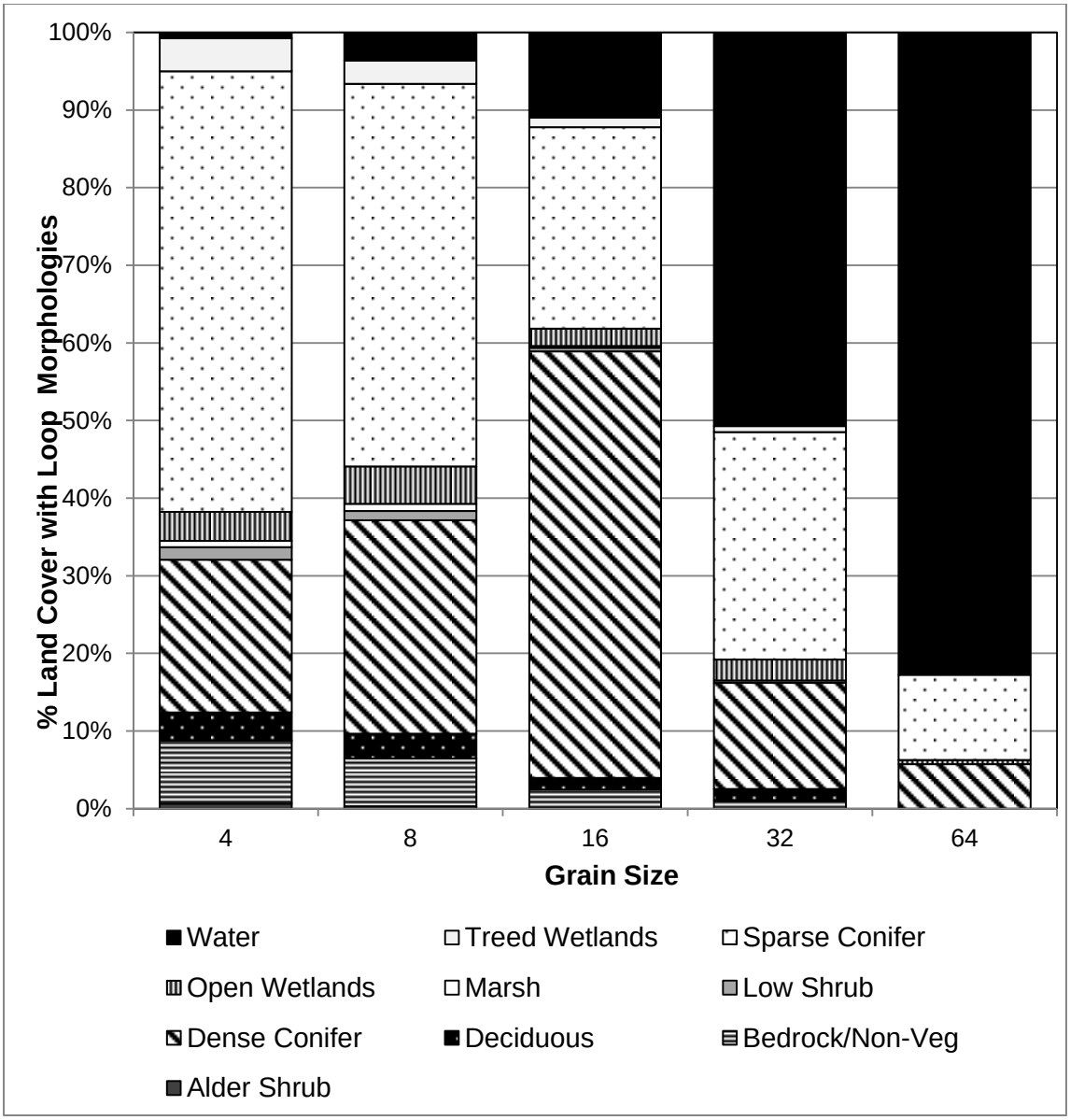

Figure 44. Land cover percentages comprising the loop morphological pattern elements within insular residual patches at each of the 5 grain sizes.

Transitioning did not change the outcome of loop morphological elements when observing both map samples (Figures 45 and 46). Instead when the transition is turned on the loops break through the edge barrier and are directly linked with the core pattern (Figure 46). The area of loops would therefore change as they generally increase when the transition is turned on.

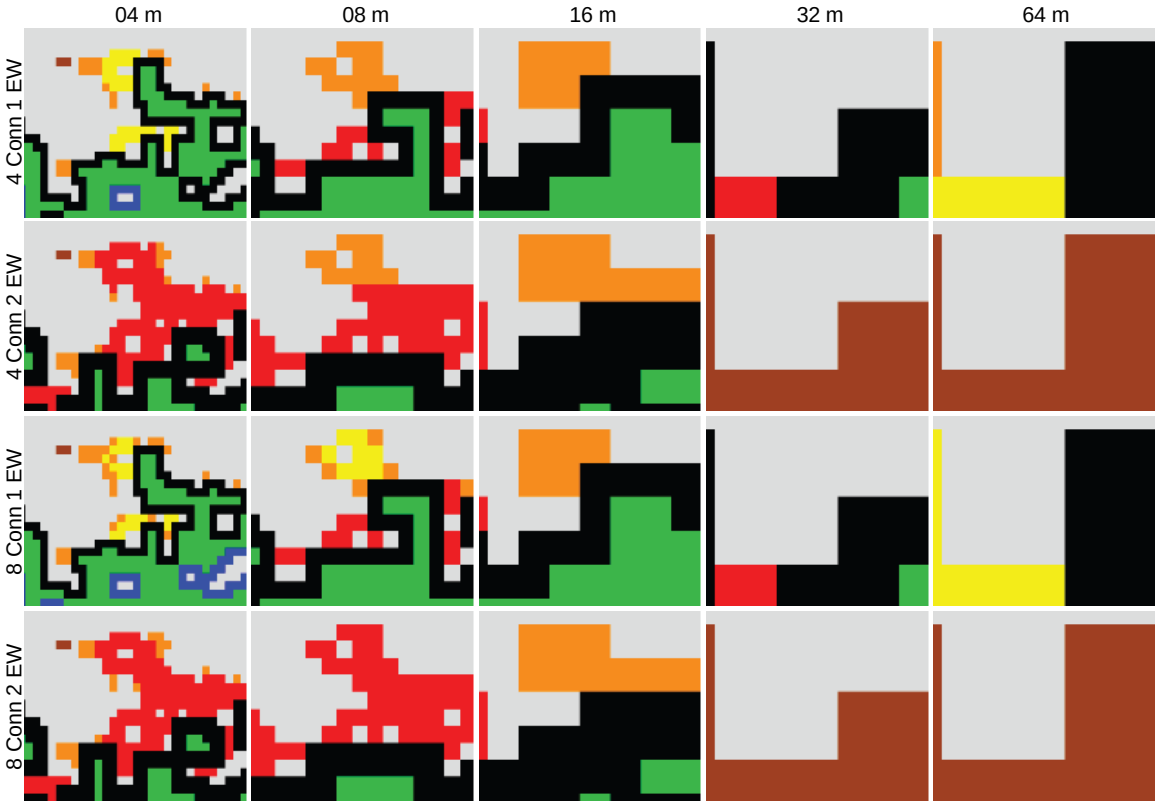

Figure 45. Loop morphologies found within sparse conifer residuals can be affected by the grain size, connectivity and edge width.

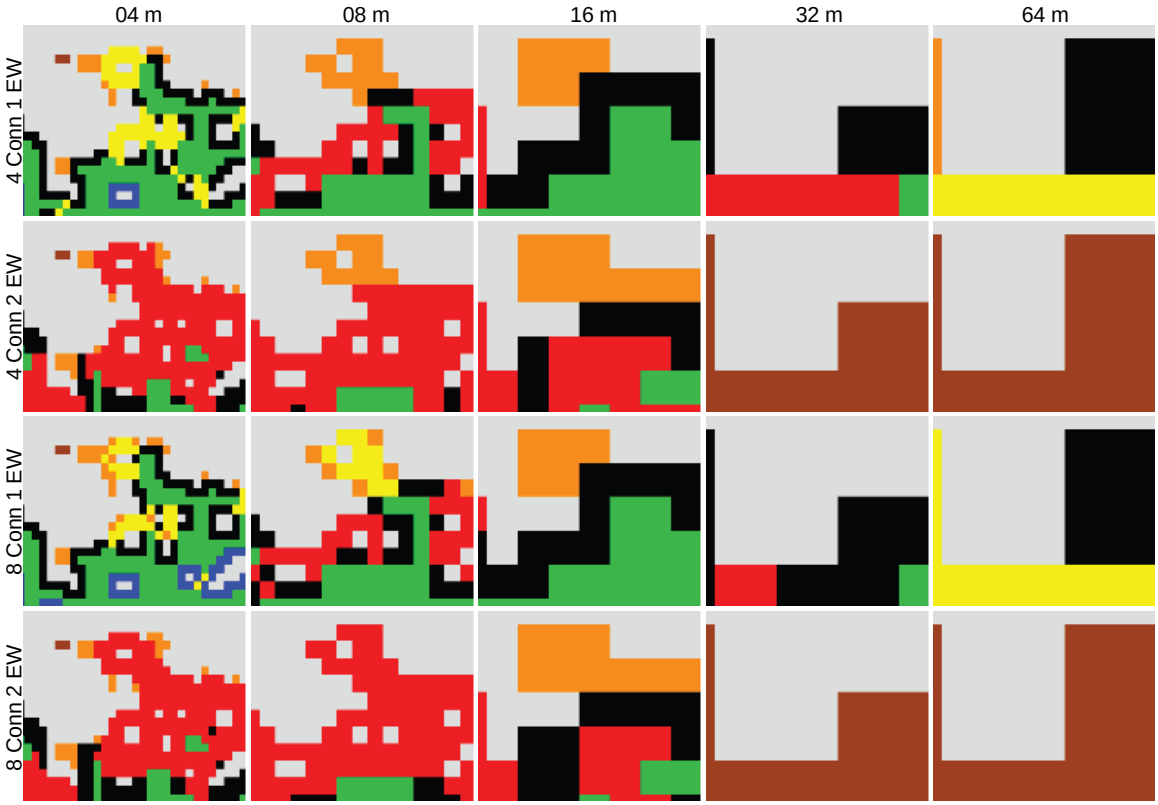

Figure 46. Morphological map showing how loop morphologies within sparse conifer can be affected by the transitioning used.

3.6 Bridge Morphology

A one-way ANOVA test was conducted on the means of bridge morphological areas to compare the effect of grain size on the occurrence of bridges within residual patches and land cover classes. There was a significant effect of the grain size on the bridge morphological areas in at least 1 land cover class at each grain size ($p < 0.05$)(Table 36).

The Tukey post-hoc tests were conducted on the bridge morphological area means to test significant differences among the land cover pairwise contrasts. At 4 m and 8 m grain sizes, the mean areas for sparse conifer and dense conifer classes were significantly different from most of the other groups ($p < 0.05$) (Table 37 and Table 38). However, the mean areas of the dense conifer and bedrock and non-vegetation pairing were not statistically different when compared together ($p > 0.05$) (Table 37 and Table 38).

Table 36. At least one land cover class was reported to be statistically different from other classes at each grain size in bridge morphologies ($p < 0.05$).

Source of Variation	d.f.	Sum Sq	Mean Sq	F Value	P-Value
4m					
Land Cover	9	3186	354.00	31.37	<0.0000
Residuals	150	1693	11.30		
8m					
Land Cover	9	2867	318.60	21.38	<0.0000
Residuals	150	2235	14.90		
16m					
Land Cover	9	6428	714.20	24.99	<0.0000
Residuals	150	4287	28.60		
32m					
Land Cover	9	2032	225.76	50.70	<0.0000
Residuals	150	668	4.45		
64m					
Land Cover	9	9107	1011.90	82.85	<0.0000
Residuals	150	1832	12.20		

Table 37. Tukey post-hoc test results for bridge morphological elements at 4 m grain size.

Land Cover	Alder	Bed	Decid	DCon	LowS	Marsh	OpenW	SCon	TreeW	Water
Alder	-									
Bed	0.8059	-								
Decid	0.9992	0.9949	-							
DCon	**0.0037**	0.3759	**0.0424**	-						
LowS	1.0000	0.9370	1.0000	**0.0113**	-					
Marsh	1.0000	0.8309	0.9995	**0.0044**	1.0000	-				
OpenW	0.9999	0.9737	1.0000	**0.0200**	1.0000	1.0000	-			
SCon	**0.0000**	**0.0000**	**0.0000**	**0.0000**	**0.0000**	**0.0000**	**0.0000**	-		
TreeW	0.9987	0.9965	1.0000	**0.0485**	1.0000	0.9992	1.0000	**0.0000**	-	
Water	1.0000	0.8064	0.9992	**0.0037**	1.0000	1.0000	1.0000	**0.0000**	0.9987	-

Table 38. Tukey post-hoc test results for bridge morphological elements at 8 m grain size.

Land Cover	Alder	Bed	Decid	DCon	LowS	Marsh	OpenW	SCon	TreeW	Water
Alder	-									
Bed	0.9939	-								
Decid	0.9999	1.0000	-							
DCon	**0.0043**	0.0876	**0.0290**	-						
LowS	1.0000	0.9977	1.0000	**0.0065**	-					
Marsh	1.0000	0.9950	0.9999	**0.0047**	1.0000	-				
OpenW	1.0000	1.0000	1.0000	**0.0217**	1.0000	1.0000	-			
SCon	**0.0000**	**0.0000**	**0.0000**	**0.0000**	**0.0000**	**0.0000**	**0.0000**	-		
TreeW	1.0000	0.9999	1.0000	**0.0173**	1.0000	1.0000	1.0000	**0.0000**	-	
Water	1.0000	0.9999	1.0000	**0.0160**	1.0000	1.0000	1.0000	**0.0000**	1.0000	-

The post-hoc comparisons using the Tukey HSD test indicated that the mean areas of bridge morphologies for sparse conifer and dense conifer land cover classes were significantly different than all of the other land cover classes ($p < 0.05$) (Table 39). These significant differences were observed at 16 m grain size.

Table 39. Tukey post-hoc test results for bridge morphological elements at 16 m grain size.

Land Cover	Alder	Bed	Decid	DCon	LowS	Marsh	OpenW	SCon	TreeW	Water
Alder	-									
Bed	1.0000	-								
Decid	1.0000	1.0000	-							
DCon	**0.0000**	**0.0000**	**0.0000**	-						
LowS	1.0000	1.0000	1.0000	**0.0000**	-					
Marsh	1.0000	1.0000	1.0000	**0.0000**	1.0000	-				
OpenW	1.0000	1.0000	1.0000	**0.0000**	1.0000	1.0000	-			
SCon	**0.0000**	**0.0000**	**0.0000**	**0.0001**	**0.0000**	**0.0000**	**0.0000**	-		
TreeW	1.0000	1.0000	1.0000	**0.0000**	1.0000	1.0000	1.0000	**0.0000**	-	
Water	0.9526	0.9861	0.9877	**0.0000**	0.9601	0.9588	0.9913	**0.0008**	0.9691	-

The post hoc comparisons at 32 m grain size illustrated that the mean areas for both conifer classes and water bodies were significantly different from all land cover classes when paired together at the ($p < 0.05$) (Table 40). The mean areas for the sparse conifer and dense conifer class comparison were not significantly different when paired together ($p > 0.05$) (Table 40). At 64 m grain size, the post hoc comparisons from the Tukey HSD test indicated that the mean bridge areas for water bodies were significantly different from all other land cover classes ($p < 0.05$) (Table 41).

Table 40. Tukey post-hoc test results for bridge morphological elements at 32 m grain size.

Land Cover	Alder	Bed	Decid	DCon	LowS	Marsh	OpenW	SCon	TreeW	Water
Alder	-									
Bed	1.0000	-								
Decid	1.0000	1.0000	-							
DCon	**0.0002**	**0.0004**	**0.0004**	-						
LowS	1.0000	1.0000	1.0000	**0.0002**	-					
Marsh	1.0000	1.0000	1.0000	**0.0002**	1.0000	-				
OpenW	1.0000	1.0000	1.0000	**0.0010**	1.0000	1.0000	-			
SCon	**0.0000**	**0.0000**	**0.0000**	0.1930	**0.0000**	**0.0000**	**0.0000**	-		
TreeW	1.0000	1.0000	1.0000	**0.0006**	1.0000	1.0000	1.0000	**0.0000**	-	
Water	**0.0000**	**0.0000**	**0.0000**	**0.0000**	**0.0000**	**0.0000**	**0.0000**	**0.0000**	**0.0000**	-

Table 41. Tukey post-hoc test results for bridge morphological elements at 64 m grain size.

Land Cover	Alder	Bed	Decid	DCon	LowS	Marsh	OpenW	SCon	TreeW	Water
Alder	-									
Bed	1.0000	-								
Decid	1.0000	1.0000	-							
DCon	0.8766	0.8766	0.8766	-						
LowS	1.0000	1.0000	1.0000	0.8766	-					
Marsh	1.0000	1.0000	1.0000	0.8766	1.0000	-				
OpenW	1.0000	1.0000	1.0000	0.8766	1.0000	1.0000	-			
SCon	0.9971	0.9971	0.9971	0.9997	0.9971	0.9971	0.9971	-		
TreeW	1.0000	1.0000	1.0000	0.8766	1.0000	1.0000	1.0000	0.9971	-	
Water	**0.0000**	**0.0000**	**0.0000**	**0.0000**	**0.0000**	**0.0000**	**0.0000**	**0.0000**	**0.0000**	-

The 4 m and 8 m boxplots of bridge morphological areas display the higher occurrences of bridges in bedrock and non-vegetation, dense conifer and sparse conifer classes, with sparse conifer being the most dominant land cover containing bridges (Figure 47). At 16 m grain size, the dense conifer class becomes the most dominant type containing bridges, and the bridge areas begin to increase in water bodies. At 32 m and 64 m grain sizes, bridges are the most dominant within water bodies, while the bridge areas in conifers decrease. Bridges were consistently dominant in the sparse conifer and dense conifer classes between 4 m and 32 m, owing to their significant differences in the Tukey post hoc tests.

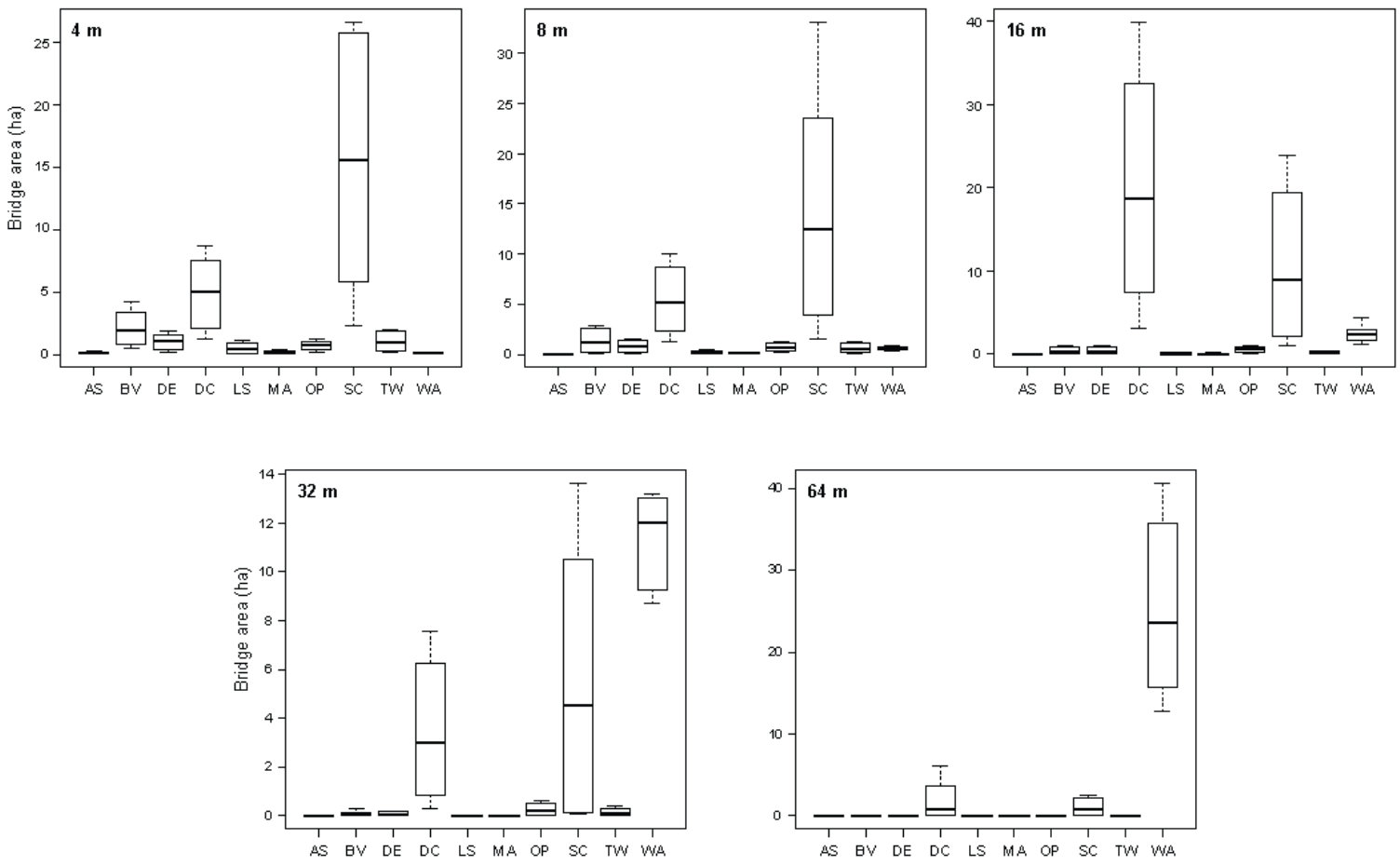

Figure 47. Boxplots of bridge morphological elements across all grain sizes illustrating the increased presence in water bodies as the grain size increased.

Bridge morphology is dependent on the transformation of the core morphologies with which they originate from. In the morphology map below, the edge width has an effect on the occurrence of bridge patterns (Figure 49). The increasing of the edge width at 8 m and 16 m grain sizes resulted in the core patterns becoming smaller in area. This created the occurrence of bridges to connect cores that once filled those residual areas at 1 edge width. The connectivity can also affect the occurrences of bridges, which can be observed in the 8 m, 16 m, and 32 m grain sizes (Figure 49). The general observation made at these grain sizes is that bridge and branch morphologies can be converted into each other depending on the orientation of the morphological spatial element in relation to the core.

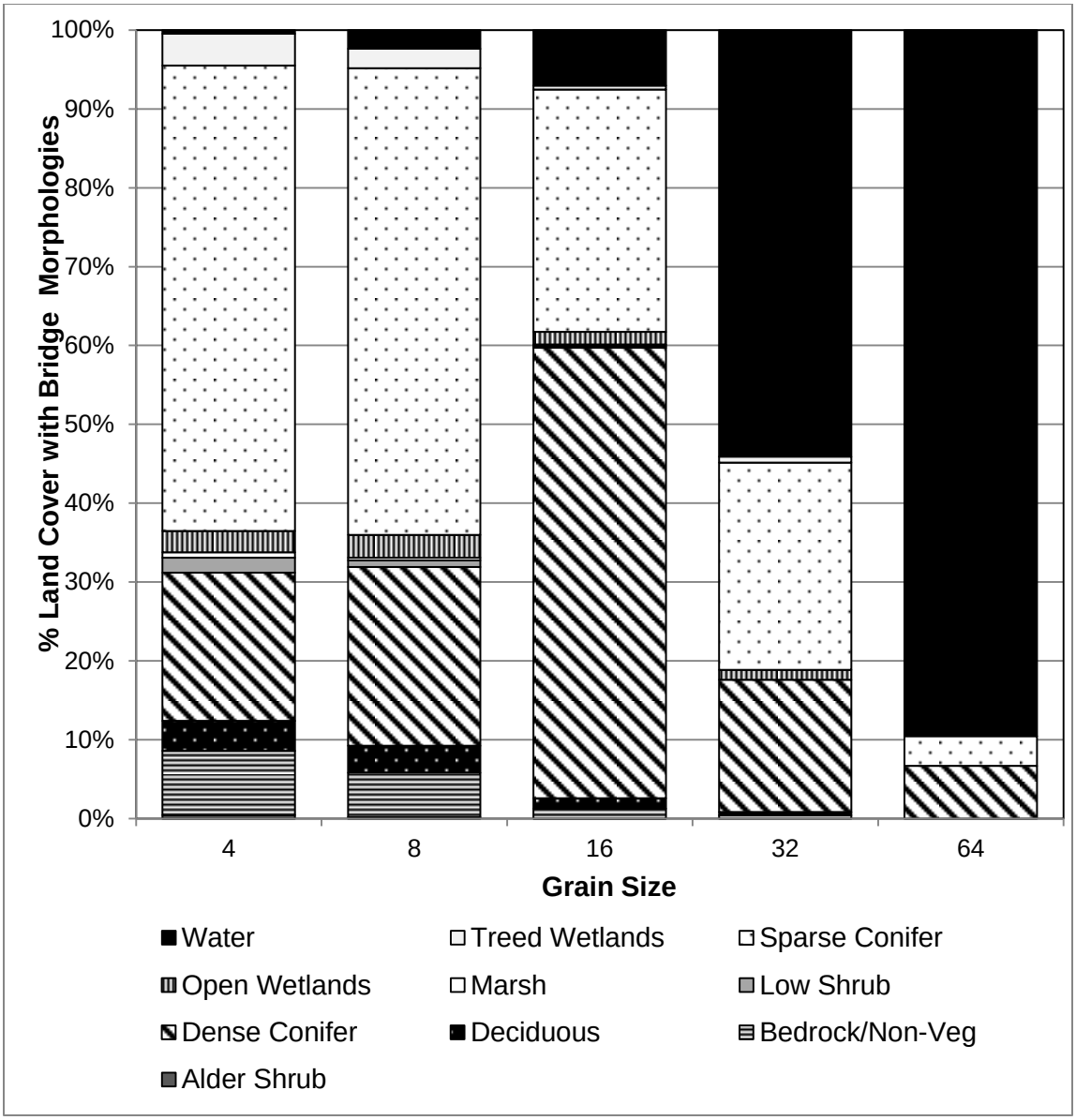

Figure 48. Land cover percentages comprising the bridge morphological pattern elements within insular residual patches at each of the 5 grain sizes.

Transitioning had an effect on the occurrences and areas of the bridge morphological elements. When the transition is turned on the bridges break through the edge boundary and are directly linked with the core pattern (Figure 50). The area of bridges therefore increase when the transition is turned on. The bridges maintained

their presence once the cores remained at the larger grain sizes. However, as 64 m, the bridge areas became non-existent, and were converted to islet morphologies.

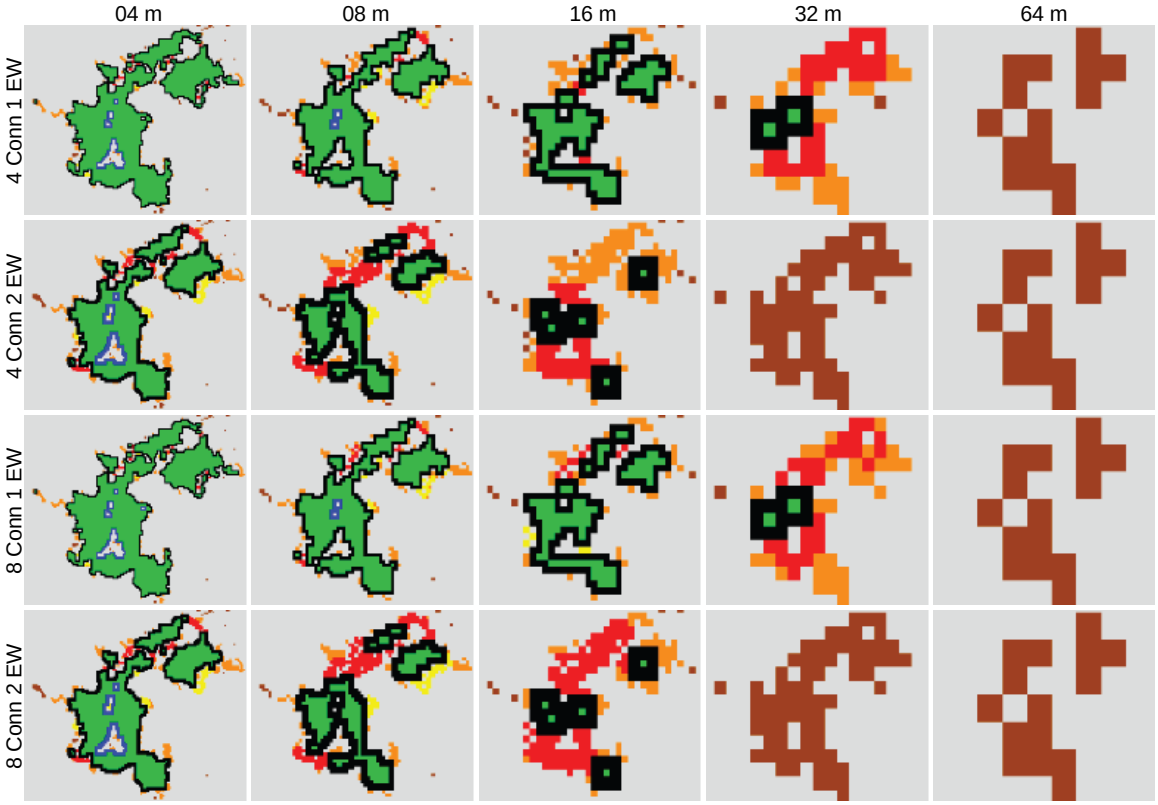

Figure 49. Morphological map illustrating the effect of grain size and MSPA parameter change on the occurrence of bridge morphological elements in open wetland residuals (transition turned off).

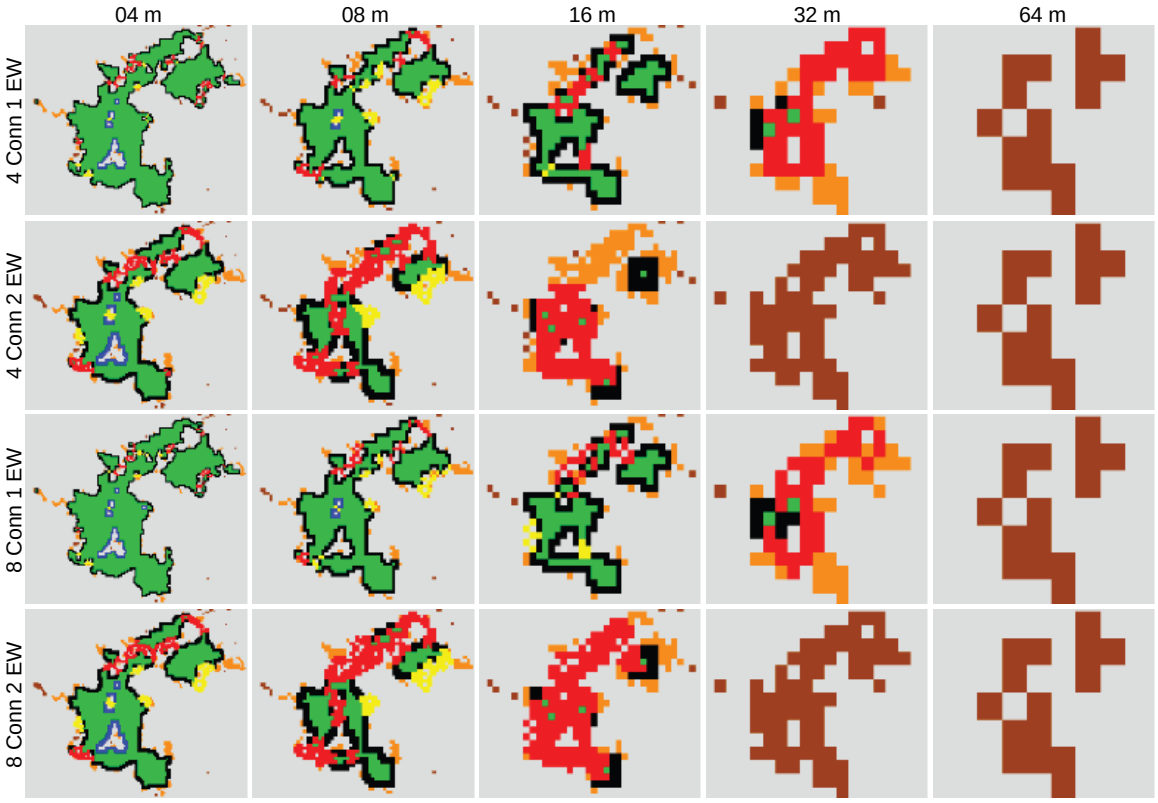

Figure 50. Morphological map illustrating the effect of turning on the transition and grain size change on the bridge morphological areas within open wetland residuals.

3.7 Branch Morphology

A one-way ANOVA test was conducted on the branch morphology areas to compare the effect of grain size on the occurrence of branches within residual patches. There was a significant effect of the grain size on the branch morphology areas in at least 1 land cover class at each grain size ($p < 0.05$) (Table 42).

The Tukey post-hoc tests were conducted on the branch morphology area means to determine which land cover classes were statistically different from other land cover classes in a pairwise comparison. At 4 m grain size, the mean branch areas of sparse conifer and dense conifer classes were found to be significantly different from all other land cover classes ($p < 0.05$) (Table 43). The mean areas for bedrock and non-vegetation were significantly different from alder shrub, marsh, and the conifer classes at 4 m ($p < 0.05$) (Table 43).

Table 42. Land cover classes were significantly different in terms of their branch morphology areas across each grain size.

Source of Variation	d.f.	Sum Sq	Mean Sq	F Value	P-Value
4m					
Land Cover	9	67598	7511	66.68	<0.0000
Residuals	150	16897	113		
8m					
Land Cover	9	160491	17832	43.56	<0.0000
Residuals	150	61407	409		
16m					
Land Cover	9	460408	51156	42.57	<0.0000
Residuals	150	180248	1202		
32m					
Land Cover	9	193275	21475	47.28	<0.0000
Residuals	150	68128	454		
64m					
Land Cover	9	601405	66823	96.22	<0.0000
Residuals	150	104168	694		

Table 43. Tukey post-hoc test results for branch morphological elements at 4 m grain size.

Land Cover	Alder	Bed	Decid	DCon	LowS	Marsh	OpenW	SCon	TreeW	Water
Alder	-									
Bed	**0.0115**	-								
Decid	0.9684	0.2944	-							
DCon	**0.0000**	**0.0084**	**0.0000**	-						
LowS	0.9995	0.0909	1.0000	**0.0000**	-					
Marsh	1.0000	**0.0137**	0.9767	**0.0000**	0.9998	-				
OpenW	0.9981	0.1256	1.0000	**0.0000**	1.0000	0.9989	-			
SCon	**0.0000**	**0.0000**	**0.0000**	**0.0000**	**0.0000**	**0.0000**	**0.0000**	-		
TreeW	0.8349	0.5563	1.0000	**0.0000**	0.9953	0.8611	0.9985	**0.0000**	-	
Water	0.9986	0.1163	1.0000	**0.0000**	1.0000	0.9992	1.0000	**0.0000**	0.9980	-

At the 8 m observation level, the post hoc comparisons indicated that the mean areas of both conifer types were significantly different from all other land cover classes ($p < 0.05$ level) (Table 44). The mean areas for the bedrock and non-vegetation class were not significantly different from other classes, as was seen in at 4 m grain size ($p < 0.05$).

Table 44. Tukey post-hoc test results for branch morphological elements at 8 m grain size.

Land Cover	Alder	Bed	Decid	DCon	LowS	Marsh	OpenW	SCon	TreeW	Water
Alder	-									
Bed	0.8508	-								
Decid	0.9993	0.9971	-							
DCon	**0.0000**	**0.0003**	**0.0000**	-						
LowS	1.0000	0.9435	1.0000	**0.0000**	-					
Marsh	1.0000	0.8930	0.9998	**0.0000**	1.0000	-				
OpenW	0.9984	0.9988	1.0000	**0.0000**	0.9999	0.9994	-			
SCon	**0.0000**	**0.0000**	**0.0000**	**0.0000**	**0.0000**	**0.0000**	**0.0000**	-		
TreeW	0.9995	0.9963	1.0000	**0.0000**	1.0000	0.9999	1.0000	**0.0000**	-	
Water	0.7943	1.0000	0.9931	**0.0004**	0.9108	0.8453	0.9966	**0.0000**	0.9915	-

At 16 m and 32 m grain sizes, the branch morphological area means were significantly different of sparse conifer and dense conifer land cover classes when paired with all other land cover classes ($p < 0.05$) (Tables 45 and 46). The post hoc comparisons from the Tukey tests illustrated that the mean areas of water bodies were significantly different from other classes at 32 m grain size ($p < 0.05$) but were not significantly different at 16 m grain size ($p > 0.05$).

Table 45. Tukey post-hoc test results for branch morphological elements at 16 m grain size.

Land Cover	Alder	Bed	Decid	DCon	LowS	Marsh	OpenW	SCon	TreeW	Water
Alder	-									
Bed	1.0000	-								
Decid	1.0000	1.0000	-							
DCon	**0.0000**	**0.0000**	**0.0000**	-						
LowS	1.0000	1.0000	1.0000	**0.0000**	-					
Marsh	1.0000	1.0000	1.0000	**0.0000**	1.0000	-				
OpenW	1.0000	1.0000	1.0000	**0.0000**	1.0000	1.0000	-			
SCon	**0.0000**	**0.0000**	**0.0000**	**0.0000**	**0.0000**	**0.0000**	**0.0000**	-		
TreeW	1.0000	1.0000	1.0000	**0.0000**	1.0000	1.0000	1.0000	**0.0000**	-	
Water	0.0792	0.2523	0.1698	**0.0000**	0.0919	0.0838	0.2456	**0.0002**	0.1291	-

Table 46. Tukey post-hoc test results for branch morphological elements at 32 m grain size.

Land Cover	Alder	Bed	Decid	DCon	LowS	Marsh	OpenW	SCon	TreeW	Water
Alder	-									
Bed	1.0000	-								
Decid	1.0000	1.0000	-							
DCon	**0.0029**	**0.0081**	**0.0070**	-						
LowS	1.0000	1.0000	1.0000	**0.0035**	-					
Marsh	1.0000	1.0000	1.0000	**0.0031**	1.0000	-				
OpenW	0.9993	1.0000	1.0000	**0.0330**	0.9996	0.9994	-			
SCon	**0.0000**	**0.0000**	**0.0000**	**0.0000**	**0.0000**	**0.0000**	**0.0000**	-		
TreeW	1.0000	1.0000	1.0000	**0.0062**	1.0000	1.0000	1.0000	**0.0000**	-	
Water	**0.0000**	**0.0000**	**0.0000**	**0.0000**	**0.0000**	**0.0000**	**0.0000**	**0.0003**	**0.0000**	-

Post hoc comparisons using the Tukey test indicated that the mean branch areas for water bodies were significantly different than the other land cover classes at 64 m grain size ($p < 0.05$) (Table 47). The higher occurrences of branch morphology in water bodies supported the statistical differences in large grain sizes (Figure 51). The branch morphologies were also found in both conifer classes, however, the mean areas of these classes were not significantly different from other classes (except for water bodies) ($p > 0.05$).

Table 47. Tukey post-hoc test results for branch morphological elements at 64 m grain size.

Land Cover	Alder	Bed	Decid	DCon	LowS	Marsh	OpenW	SCon	TreeW	Water
Alder	-									
Bed	1.0000	-								
Decid	1.0000	1.0000	-							
DCon	0.5618	0.5618	0.5618	-						
LowS	1.0000	1.0000	1.0000	0.5618	-					
Marsh	1.0000	1.0000	1.0000	0.5618	1.0000	-				
OpenW	1.0000	1.0000	1.0000	0.7117	1.0000	1.0000	-			
SCon	0.1273	0.1273	0.1273	0.9985	0.1273	0.1273	0.2097	-		
TreeW	1.0000	1.0000	1.0000	0.5848	1.0000	1.0000	1.0000	0.1378	-	
Water	**0.0000**	**0.0000**	**0.0000**	**0.0000**	**0.0000**	**0.0000**	**0.0000**	**0.0000**	**0.0000**	-

The sparse conifer land cover class is the most dominant cover type which contained branch morphologies at 4 m and 8 m grain size (Figure 51). Branch morphologies were also found in higher frequency in dense conifer, bedrock and non-vegetation, and treed wetlands at 4 m and 8 m spatial resolution. The boxplot at 16 m showed a shift in the dominance of branch morphologies, where these spatial elements occurred most frequently in dense conifer land cover class. At the larger grain sizes (32 m and 64 m), branch morphological areas in the water body class increased, and water becomes the most dominant class in 64 m.

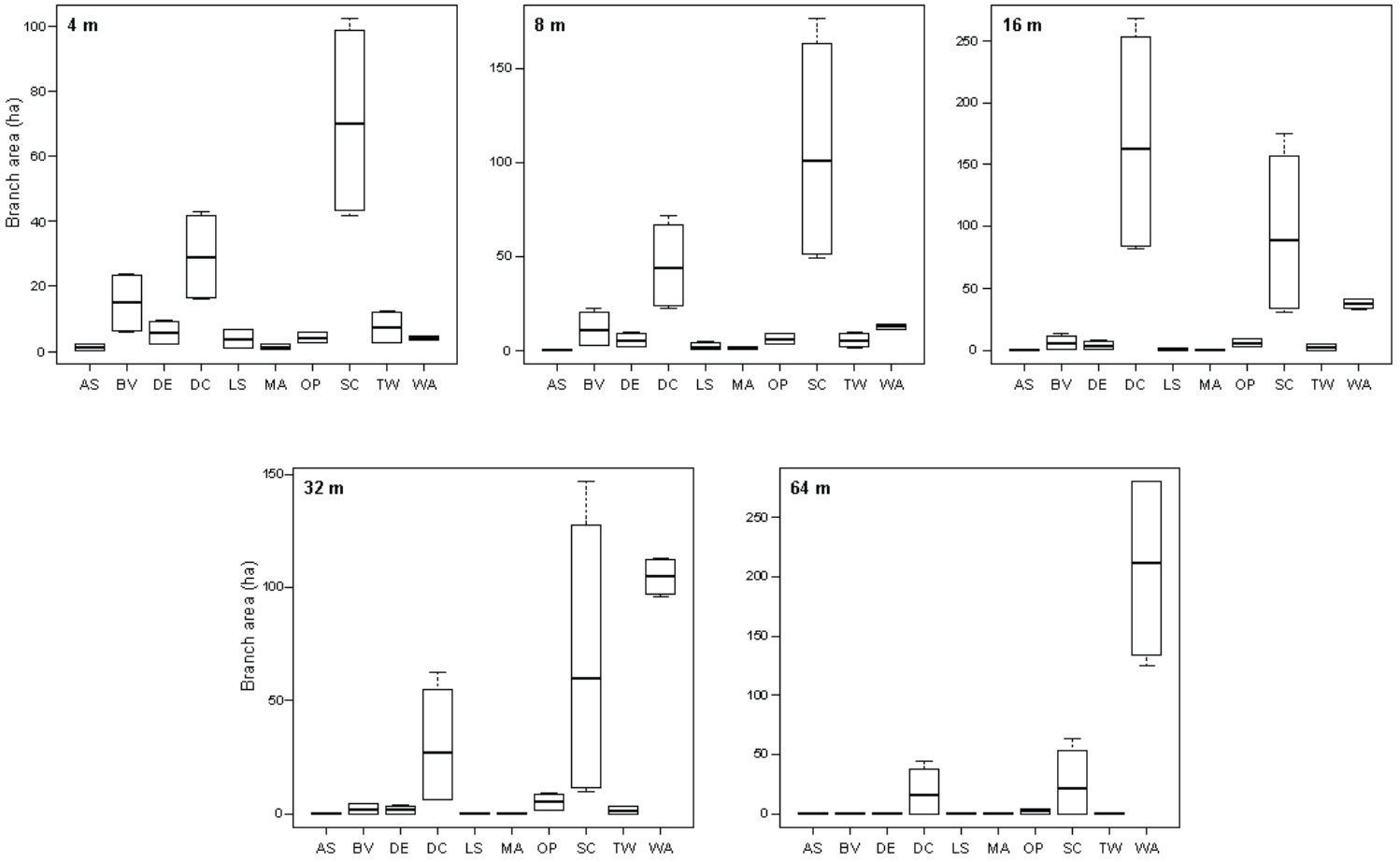

Figure 51. Branch morphological areas were significantly different in at least one land cover class in each grain size observed.

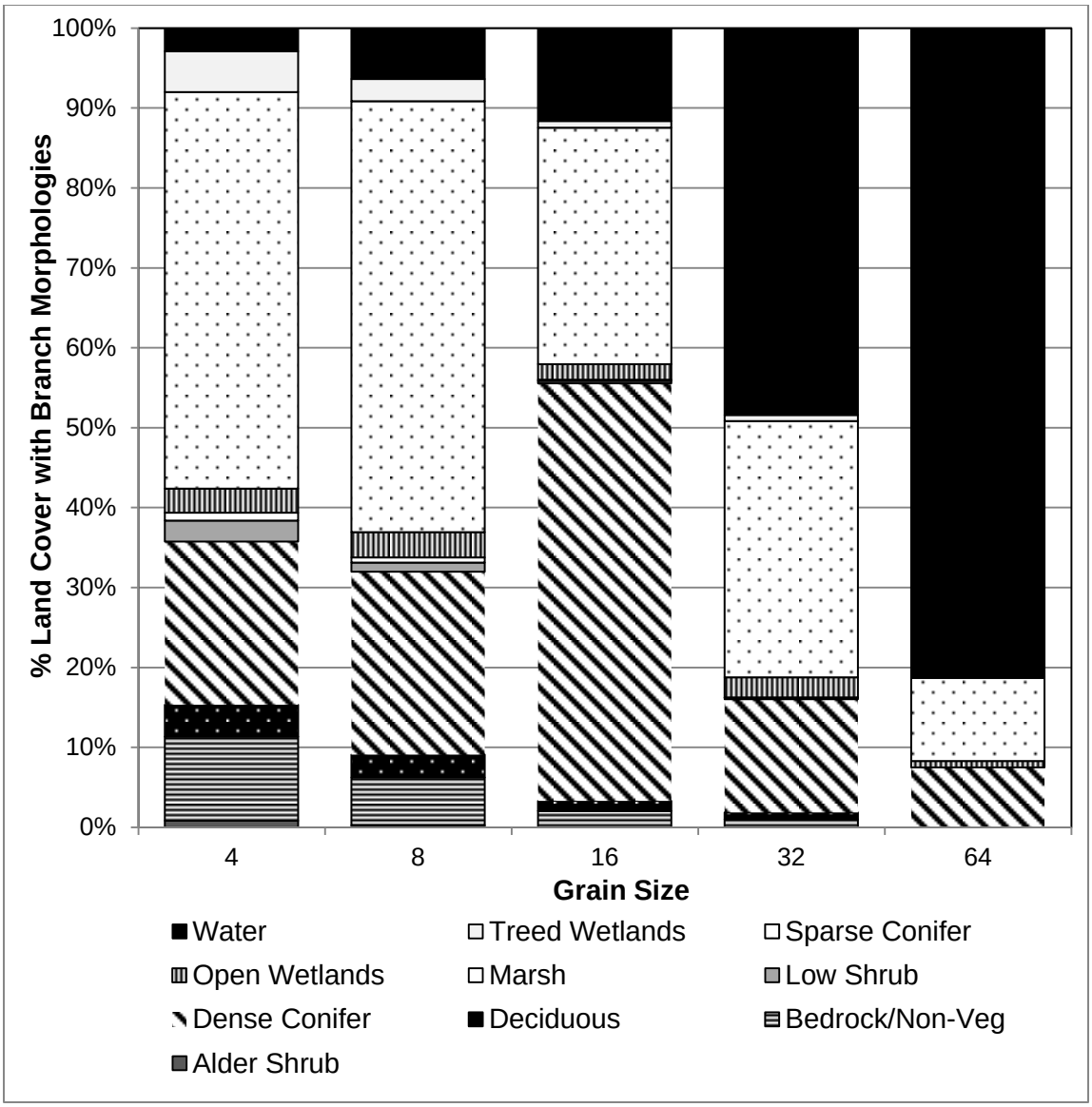

Figure 52. Land cover percentages comprising the branch morphological pattern elements within insular residual patches at each of the 5 grain sizes.

The edge width can have an effect on the occurrence of the branch morphologies, especially at the 4 m and 8 m grain sizes. The increase of the edge width to 2 pixels constricts the area of the core morphological element in both instances, as the edge area increases inwards (Figure 53). The pattern area of the branches in these examples has generally increased when the edge width increases. At 16 m grain size, the edge width's effect is even greater but with an inverse relationship with the branch

pattern areas. The edge width of 2 applied to this sample site resulted in the core morphology disappearing (unable to be defined due to edge boundary increase) and leaving behind islet morphologies (Figure 53). The absence of cores explains that the branches can no longer exist in this scenario. The transitioning parameter generally does not have an effect on the branch morphologies, as the branches can only originate from the edge boundary rather than within the cores (Figure 54).

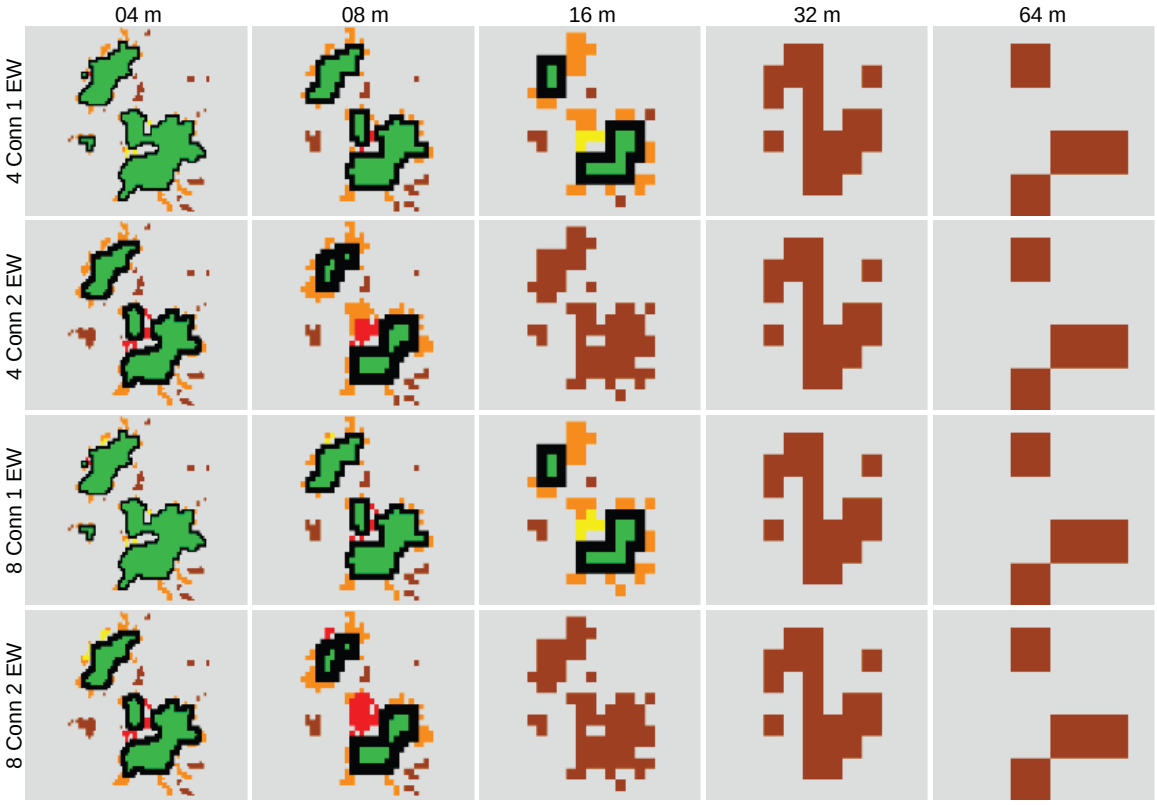

Figure 53. Branch morphological elements found within bedrock and non-vegetation residuals are affected by the grain size, connectivity, and edge width (transition off).

The table below summarizes the relative proportion of each land cover class found within each morphological pattern element at each grain size (Table 48). Table 48 illustrates the percentage land cover composition that was observed in the analysis of each morphological element in Figures 28, 32, 36, 40, 44, 48, and 52. Sparse conifer, dense conifer, and water bodies were the most frequently occurring land cover classes

in all morphological elements at each grain size except for the islet morphology (Table 48). On average, sparse conifers and water bodies accounted for 30% and 31% respectively of the total land cover comprising all morphologies across all grain sizes. Dense conifer accounted for 21% of the land cover classes.

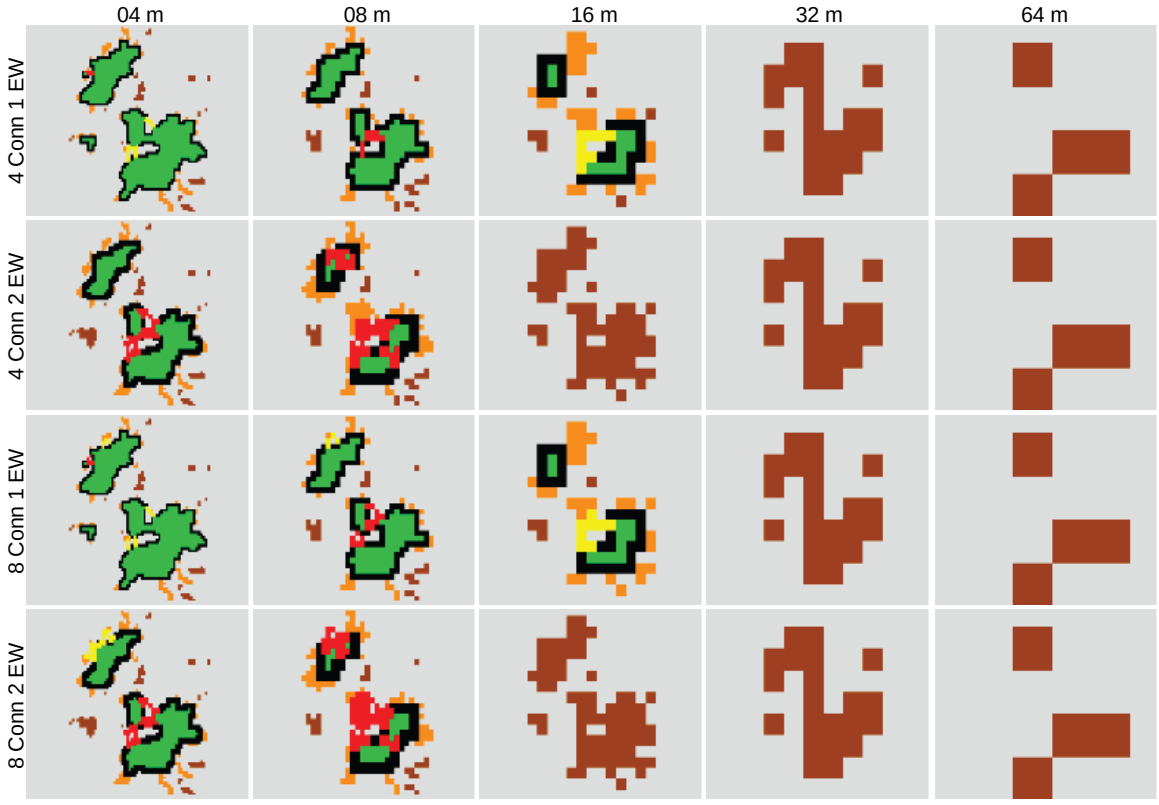

Figure 54. Turning on the transition does not seem to have an effect on the branch morphological areas within bedrock and non-vegetation land cover residuals.

At 4 m and 8 m grain sizes, sparse and dense conifers were dominant in each morphology, except for water bodies in perforations (8 m) and bedrock and non-vegetation in islets (4 m). At 16 m grain size, there is a transitioning of dominant land cover when sparse conifers decrease and dense conifers and water bodies increase in morphological area. Dense conifers increased drastically from an average of 22% of the total land cover at 8 m to an average of 46% at 16 m. Meanwhile, sparse conifers comprising all morphological elements decreased from an average of 46% at 8 m to an average of 24% at 16 m. Water bodies increased strongly in morphological area at the larger grain sizes (32 m and 64 m). At 32 m grain size, water bodies accounted for an

average of 52% of the total land cover comprising all morphological elements, while at 64 m this proportion increased to 76%.

Table 48. Summary of the percentage of each land cover class comprising all morphological elements within all residual patches across all grain sizes.

Morphology	Grain Size	AS	BV	DE	DC	LS	MA	OP	SC	TW	WA
Core	4	1	13	4	20	3	1	3	49	5	1
	8	0	7	3	23	1	1	4	53	3	4
	16	0	2	2	51	1	0	2	30	1	11
	32	0	1	1	16	0	0	3	25	1	52
	64	0	0	0	7	0	0	1	8	0	84
Islet	4	9	17	11	13	11	3	4	15	16	1
	8	7	17	11	15	9	3	4	18	15	1
	16	7	17	11	14	8	3	4	20	14	2
	32	6	15	10	17	7	3	4	23	12	3
	64	5	13	9	18	6	3	5	25	10	6
Perforation	4	0	2	4	16	0	0	4	64	3	7
	8	0	0	2	20	0	0	2	32	1	43
	16	0	0	0	29	0	0	0	2	0	69
	32	0	0	0	0	0	0	0	0	0	100
	64	0	0	0	0	0	0	0	0	0	100
Edge	4	1	11	4	19	2	1	4	52	5	1
	8	0	6	4	23	1	0	4	56	2	4
	16	0	2	2	54	0	0	2	29	1	10
	32	0	1	1	15	0	0	3	25	1	54
	64	0	0	0	6	0	0	1	8	0	85
Loop	4	1	8	3	20	2	0	4	57	4	1
	8	0	6	4	27	1	1	5	49	3	4
	16	0	2	2	55	0	0	3	26	1	11
	32	0	1	2	13	0	0	3	29	1	51
	64	0	0	0	6	0	0	0	11	0	83
Bridge	4	1	7	5	18	2	1	3	58	4	1
	8	0	6	3	23	1	0	3	59	3	2
	16	0	1	2	57	0	0	2	31	0	7
	32	0	0	1	17	0	0	1	26	1	54
	64	0	0	0	6	0	0	0	4	0	90
Branch	4	1	10	4	21	3	1	3	49	5	3
	8	0	6	3	23	1	1	3	54	2	7
	16	0	2	1	52	1	0	2	29	1	12
	32	0	1	1	14	0	0	3	32	1	48
	64	0	0	0	8	0	0	1	10	0	81

3.8 Connectivity Parameter Change

A one-way between subjects ANOVA was conducted to compare the effect of neighbourhood connectivity (4 and 8 neighbourhood pixels) on the 7 morphological pattern elements across all grain sizes. The results from the ANOVA tests showed that the connectivity change did not have a significant effect on the core element areas across all grain sizes ($p > 0.05$) (Table 48). Conversely, when observing the islet morphologies, there was a significant effect of the neighbourhood connectivity on the islet element areas at each grain size ($p < 0.05$) (Table 49). The effect of connectivity change on islet morphologies can be visualized in Figure 55, where the areas of residuals exhibiting islet morphologies noticeably decreased at the 8 neighbourhood connectivity parameter. The overall decrease in the islet areas was observed for each grain size (Figure 55).

The one-way ANOVA results displayed in Tables 50 and 51 show that perforation and edge morphological areas were not determined statistically by the connectivity. The mean perforation areas for connectivity of 4 and 8 pixels were not significantly different ($p > 0.05$) (Table 50). Similarly, the outer edge boundaries are not affected by the connectivity parameter in the MSPA analysis. The mean edge morphological areas for both connectivity parameters at each grain size were not significantly different ($p > 0.05$) (Table 51).

Table 49. One-way ANOVA results showing the effect of applying connectivity on the core morphological elements.

Source of Variation	d.f.	Sum Sq	Mean Sq	F Value	P-Value
4m					
Connectivity	1	15	14.93	0.221	0.647
Residuals	158	11230	71.08		
8m					
Connectivity	1	15	14.76	0.173	0.678
Residuals	158	13458	85.18		
16m					
Connectivity	1	44	43.64	0.195	0.659
Residuals	158	35353	223.75		
32m					
Connectivity	1	37	37.06	0.347	0.557
Residuals	158	16895	106.93		
64m					
Connectivity	1	87	87.00	0.171	0.680
Residuals	158	80366	508.60		

Table 50. One-way ANOVA results showing that connectivity has a significant effect on the islet morphological elements ($p < 0.05$).

Source of Variation	d.f.	Sum Sq	Mean Sq	F Value	P-Value
4m					
Connectivity	1	2622	2621.7	4.437	0.0367
Residuals	158	93356	590.9		
8m					
Connectivity	1	61759	61759.0	11.160	0.0010
Residuals	158	874438	5534.0		
16m					
Connectivity	1	174473	174473.0	13.560	0.0003
Residuals	158	2033069	12868.0		
32m					
Connectivity	1	227822	227822.0	8.057	0.0051
Residuals	158	4467891	28278.0		
64m					
Connectivity	1	385903	385903.0	5.597	0.0192
Residuals	158	10893975	68949.0		

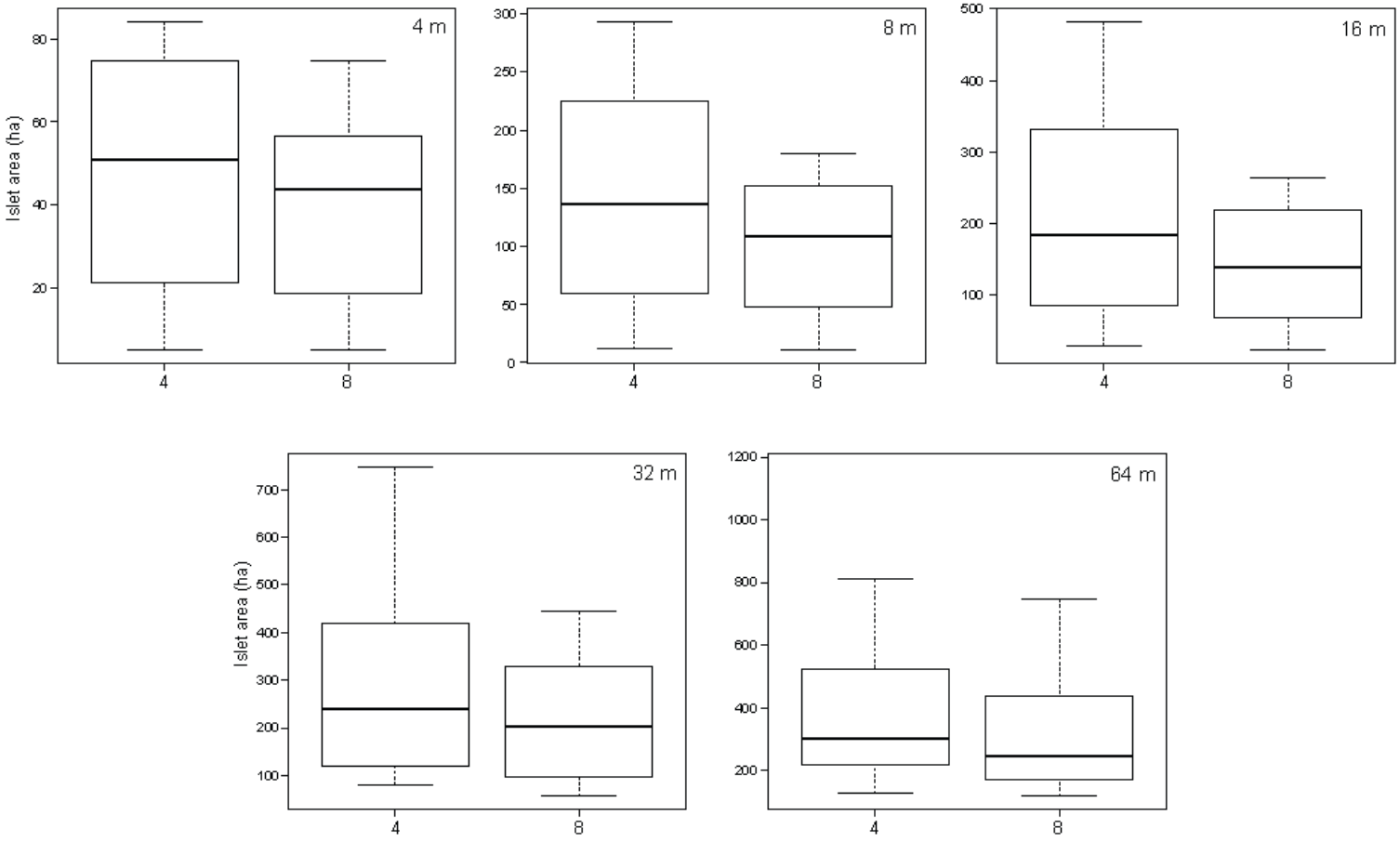

Figure 55. Boxplots illustrating the effect of applying 4 and 8 neighbouring pixels to islet morphological elements across all residual patches.

Table 51. Neighbourhood connectivity did not affect the means of the perforation morphological areas across all grain sizes.

Source of Variation	d.f.	Sum Sq	Mean Sq	F Value	P-Value
4m					
Connectivity	1	0.04	0.0350	0.100	0.752
Residuals	158	55.43	0.3508		
8m					
Connectivity	1	0.025	0.0252	0.221	0.639
Residuals	158	18.06	0.1143		
16m					
Connectivity	1	0.03	0.0332	0.086	0.769
Residuals	158	60.71	0.3842		
32m					
Connectivity	1	0.06	0.0590	0.082	0.775
Residuals	158	113.64	0.7192		
64m					
Connectivity	1	0.02	0.0168	0.068	0.794
Residuals	158	38.89	0.2461		

Table 52. One-way ANOVA results for edge boundary morphological areas across each grain size ($p > 0.05$ level) when each connectivity parameter was applied.

Source of Variation	d.f.	Sum Sq	Mean Sq	F Value	P-Value
4m					
Connectivity	1	30	29.55	0.184	0.669
Residuals	158	25423	160.90		
8m					
Connectivity	1	2	2.02	0.010	0.922
Residuals	158	33106	209.53		
16m					
Connectivity	1	3	3.30	0.007	0.933
Residuals	158	75638	478.70		
32m					
Connectivity	1	30	29.77	0.178	0.674
Residuals	158	26430	167.28		
64m					
Connectivity	1	82	82.20	0.119	0.731
Residuals	158	109485	692.90		

The one-way ANOVA results from Tables 52 and 53 illustrate that connectivity has no significant effect on the connector morphology types (loops and bridges). The mean areas of the loop and bridge morphological areas were not significantly different when connectivity was applied at 4 and 8 neighbourhood pixels ($p > 0.05$). The lack of statistical difference in the connectivity change was observed for all grain sizes. The neighbourhood connectivity did not have a significant effect on the branch morphological elements for all grain sizes ($p > 0.05$) (Table 54). The absence of connectivity effects on branch morphologies was observed for residual patches in all combined land cover classes (Table 54).

Table 53. One-way ANOVA results for the effect of connectivity on the loop connector elements at each grain size ($p > 0.05$).

Source of Variation	d.f.	Sum Sq	Mean Sq	F Value	P-Value
4m					
Connectivity	1	0.2	0.211	0.045	0.833
Residuals	158	744.3	4.711		
8m					
Connectivity	1	1.9	1.908	0.275	0.601
Residuals	158	1095.9	6.936		
16m					
Connectivity	1	4.0	4.278	0.191	0.662
Residuals	158	3530.0	22.343		
32m					
Connectivity	1	2.2	2.171	0.153	0.696
Residuals	158	2238.0	14.165		
64m					
Connectivity	1	4.0	3.530	0.071	0.790
Residuals	158	7841.0	49.620		

Table 54. ANOVA test results of the bridge morphological elements and the effect of connectivity on their area means across all grain sizes ($p > 0.05$).

Source of Variation	d.f.	Sum Sq	Mean Sq	F Value	P-Value
4m					
Connectivity	1	2	2.319	0.075	0.784
Residuals	158	4876	30.863		
8m					
Connectivity	1	0	0.350	0.011	0.917
Residuals	158	5102	32.290		
16m					
Connectivity	1	0	0.220	0.003	0.954
Residuals	158	10715	67.810		
32m					
Connectivity	1	0.1	0.067	0.004	0.950
Residuals	158	2699.7	17.087		
64m					
Connectivity	1	2	2.030	0.029	0.864
Residuals	158	10937	69.220		

Table 55. One-way ANOVA results showing the effect of connectivity on branch morphological areas across all grain sizes at the ($p > 0.05$)

Source of Variation	d.f.	Sum Sq	Mean Sq	F Value	P-Value
4m					
Connectivity	1	38	38.0	0.071	0.790
Residuals	158	84457	534.5		
8m					
Connectivity	1	267	267.1	0.190	0.663
Residuals	158	221630	1402.7		
16m					
Connectivity	1	706	706.0	0.174	0.677
Residuals	158	639950	4050.0		
32m					
Connectivity	1	375	375.0	0.227	0.634
Residuals	158	261028	1652.0		
64m					
Connectivity	1	284	284.0	0.064	0.801
Residuals	158	705289	4464.0		

3.9 Edge Width Parameter Change

A one-way ANOVA was conducted to compare the effect of changing the edge width from 1 to 2 pixels on the morphological elements across all grain sizes. There was a significant effect of an edge width increase on the mean core areas across each grain size for all residual patches ($p < 0.05$) (Table 55). Figure 56 illustrates the marked decrease in the core morphological areas when an edge width of 2 pixels was applied at each grain size. The mean islet morphological areas were not significantly different at 1 and 2 edge width pixels at each grain size ($p > 0.05$) (Table 56). The increase in edge width had no significant effect on the formation or morphology of the islets, and these islets are not bounded by edge boundaries.

Table 56. One-way ANOVA results showing the effect of edge width on core morphological elements across all grain sizes ($p < 0.05$)

Source of Variation	d.f.	Sum Sq	Mean Sq	F Value	P-Value
4m					
Edge Width	1	1461	1461.2	23.6	<0.0000
Residuals	158	9784	61.9		
8m					
Edge Width	1	1405	1405.2	18.4	<0.0000
Residuals	158	12068	76.4		
16m					
Edge Width	1	3283	3283	16.15	<0.0000
Residuals	158	32114	203		
32m					
Edge Width	1	1363	1362.7	13.83	0.0003
Residuals	158	15569	98.5		
64m					
Edge Width	1	3397	3397.00	6.966	0.0091
Residuals	158	77055	488.00		

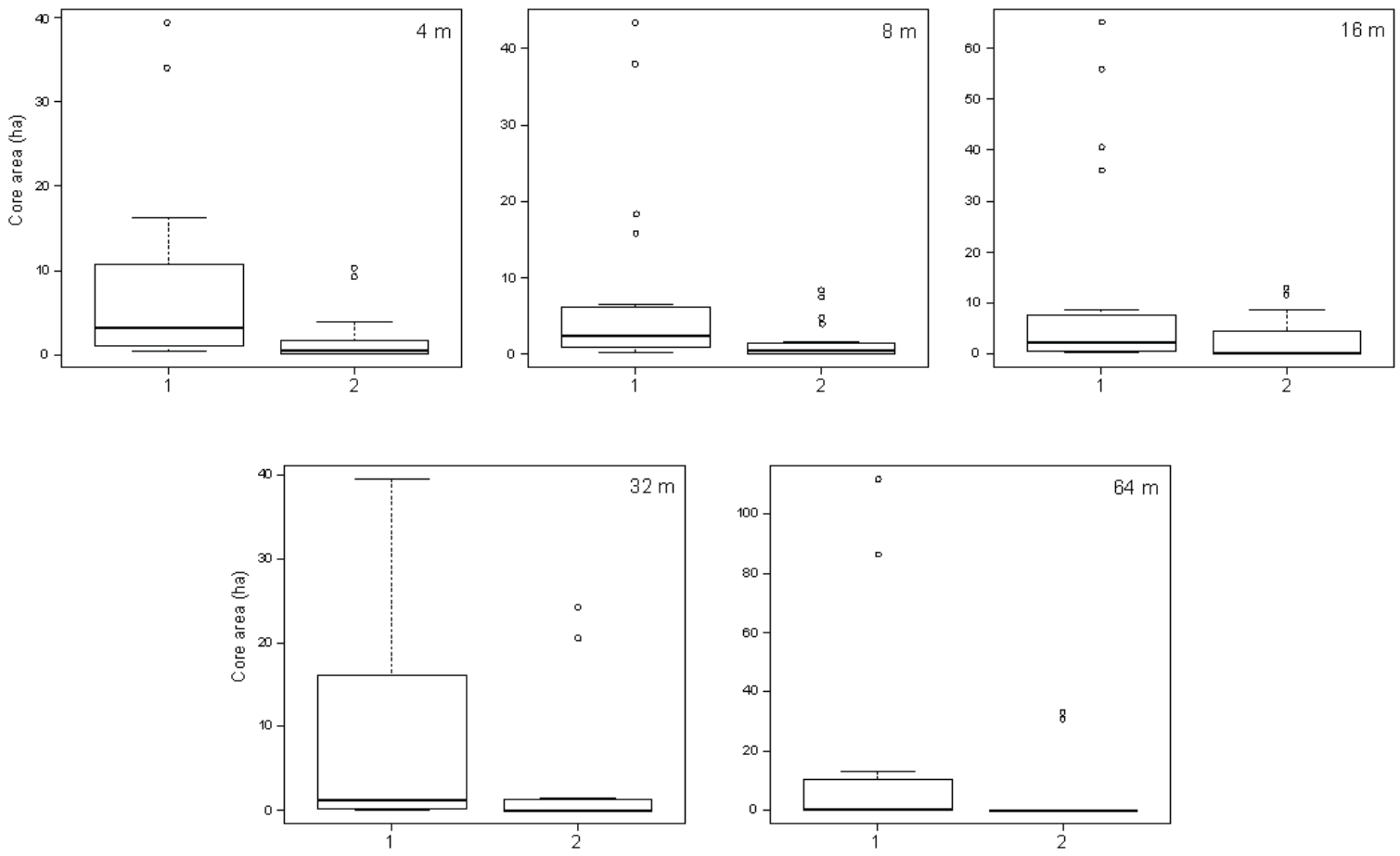

Figure 56. Core morphological element areas decrease when increasing the edge width pixels from 1 to 2 pixels.

The edge width parameter had a significant effect on the perforation and edge boundary morphological elements across each grain size (Tables 57 and 58). The one-way ANOVA results in these tables show that the means of the morphological areas differed significantly when applying an edge width of 2 pixels to the perforation or edge morphologies ($p < 0.05$). In both perforation and edge pattern morphologies, the areas have significantly decreased when the edge width was changed to 2 pixel widths (Figures 57 and 58). The trend of decreasing areas was observed in each grain size for both perforation and edge morphological pattern elements.

Table 57. One-way ANOVA results showing the effect of edge width on islet morphological elements across all grain sizes ($p > 0.05$).

Source of Variation	d.f.	Sum Sq	Mean Sq	F Value	P-Value
4m					
Edge Width	1	231	230.5	0.38	0.5380
Residuals	158	95748	606		
8m					
Edge Width	1	135	135	0.023	0.8800
Residuals	158	936062	5924		
16m					
Edge Width	1	401	401	0.029	0.8660
Residuals	158	2207142	13969		
32m					
Edge Width	1	440	440	0.015	0.9030
Residuals	158	4695272	29717		
64m					
Edge Width	1	934	934.00	0.013	0.9090
Residuals	158	11278943	71386.00		

Table 58. One-way ANOVA results showing the effect of edge width on perforation morphological elements across all grain sizes ($p < 0.05$).

Source of Variation	d.f.	Sum Sq	Mean Sq	F Value	P-Value
4m					
Edge Width	1	4.82	4.822	15.04	0.0002
Residuals	158	50.65	0.321		
8m					
Edge Width	1	1.507	1.5067	14.36	0.0002
Residuals	158	16.578	0.1049		
16m					
Edge Width	1	2.61	2.6083	7.089	0.0086
Residuals	158	58.13	0.3679		
32m					
Edge Width	1	3.84	3.838	5.52	0.0200
Residuals	158	109.86	0.695		
64m					
Edge Width	1	2.03	2.03	8.698	0.0037
Residuals	158	36.88	0.23		

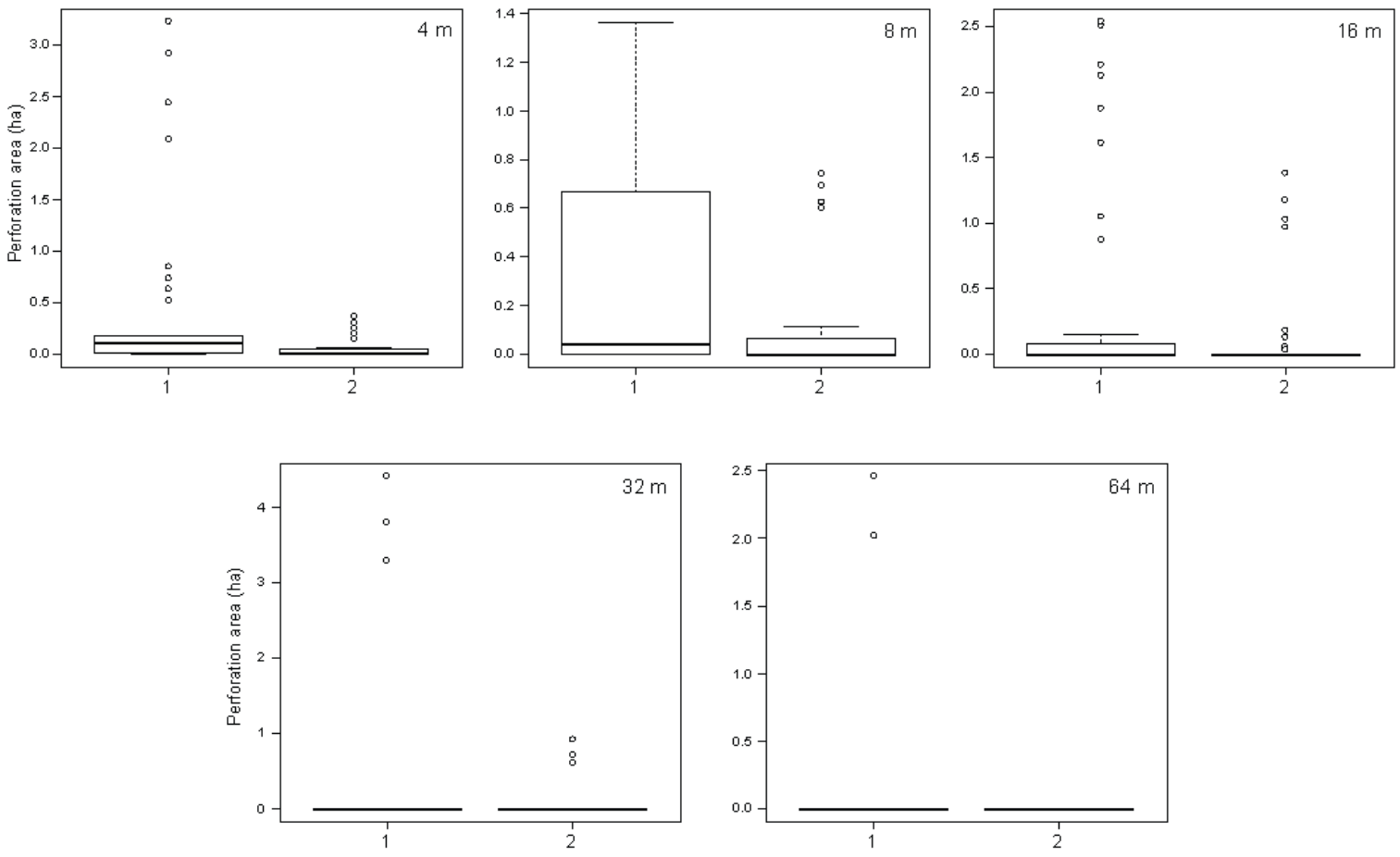

Figure 57. Boxplots showing the effect of edge width on the perforation morphological areas across 5 grain sizes.

Table 59. One-way ANOVA results showing the effect of edge width on edge morphological elements across all grain sizes ($p < 0.05$).

Source of Variation	d.f.	Sum Sq	Mean Sq	F Value	P-Value
4m					
Edge Width	1	1988	1988.2	13.39	0.0003
Residuals	158	23464	148.5		
8m					
Edge Width	1	2514	2514	12.98	0.0004
Residuals	158	30594	193.6		
16m					
Edge Width	1	5251	5251	11.79	0.0008
Residuals	158	70391	446		
32m					
Edge Width	1	1427	1426.8	9.006	0.0031
Residuals	158	25033	158.4		
64m					
Edge Width	1	3504	3504.00	5.22	0.0237
Residuals	158	106063	671.00		

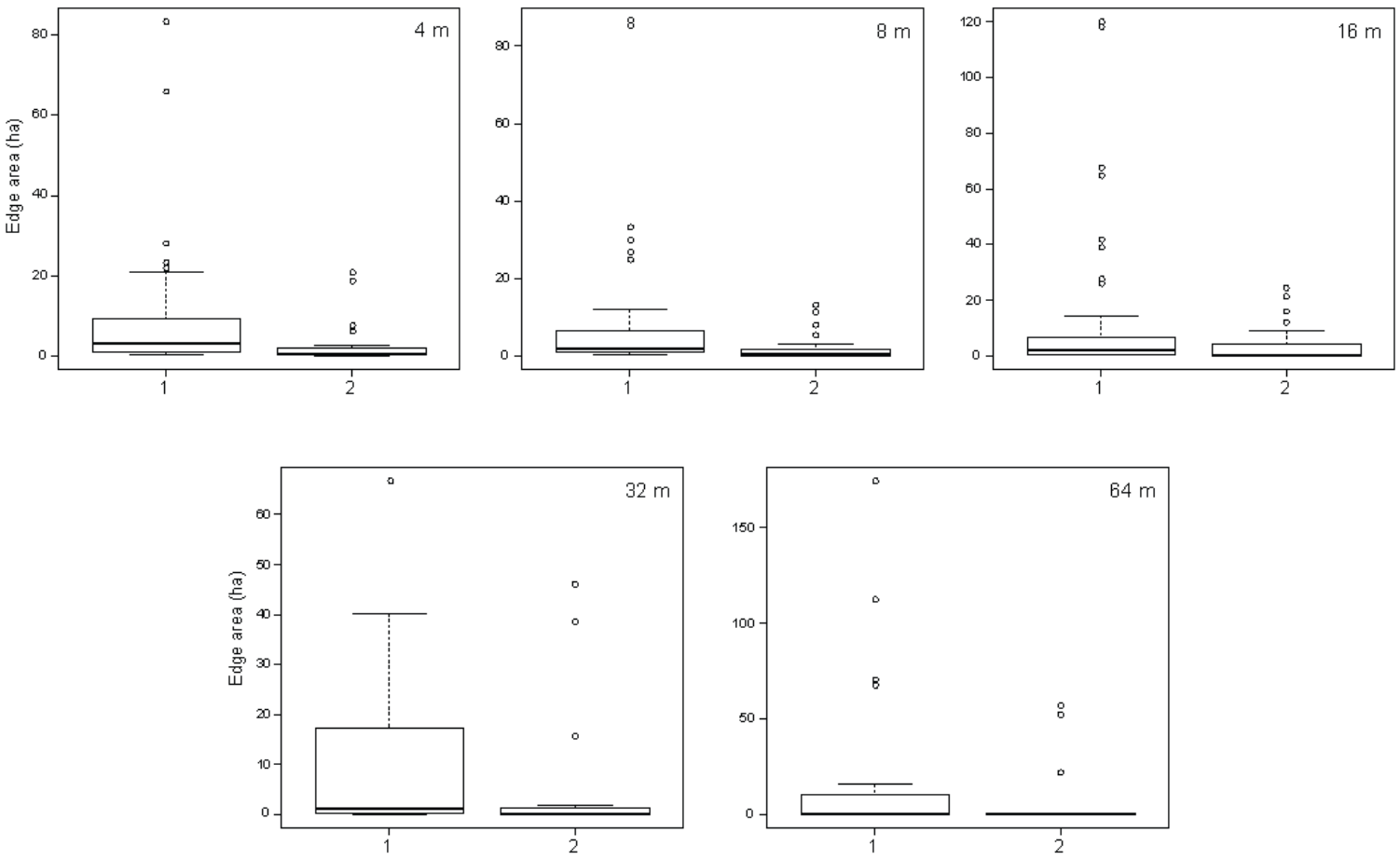

Figure 58. Boxplots showing the effect of increasing the edge width on the edge morphology across 5 grain sizes.

Connector morphological spatial elements were also affected by the edge width being applied at each grain size. Tables 59 and 60 display the one-way ANOVA results indicating that the loop and bridge connector morphological mean areas differ statistically at both edge width parameter inputs ($p < 0.05$). The significant effect of the edge width on connector morphologies was observed across all grain sizes except for the bridge morphological element at 64 m grain size (Table 60). Increasing the edge width to 2 pixels resulted in the decrease of loop and bridge morphological areas (Figures 59 and 60).

Table 60. One-way ANOVA results showing the effect of edge width on loop morphological elements across all grain sizes ($p < 0.05$).

Source of Variation	d.f.	Sum Sq	Mean Sq	F Value	P-Value
4m					
Edge Width	1	54.3	54.34	12.44	0.0006
Residuals	158	690.2	4.37		
8m					
Edge Width	1	107.6	107.56	17.16	0.0001
Residuals	158	990.2	6.27		
16m					
Edge Width	1	251	250.61	12.06	0.0007
Residuals	158	3284	20.78		
32m					
Edge Width	1	129.6	129.55	9.698	0.0022
Residuals	158	2110.7	13.36		
64m					
Edge Width	1	198	197.50	4.081	0.0451
Residuals	158	7647	48.40		

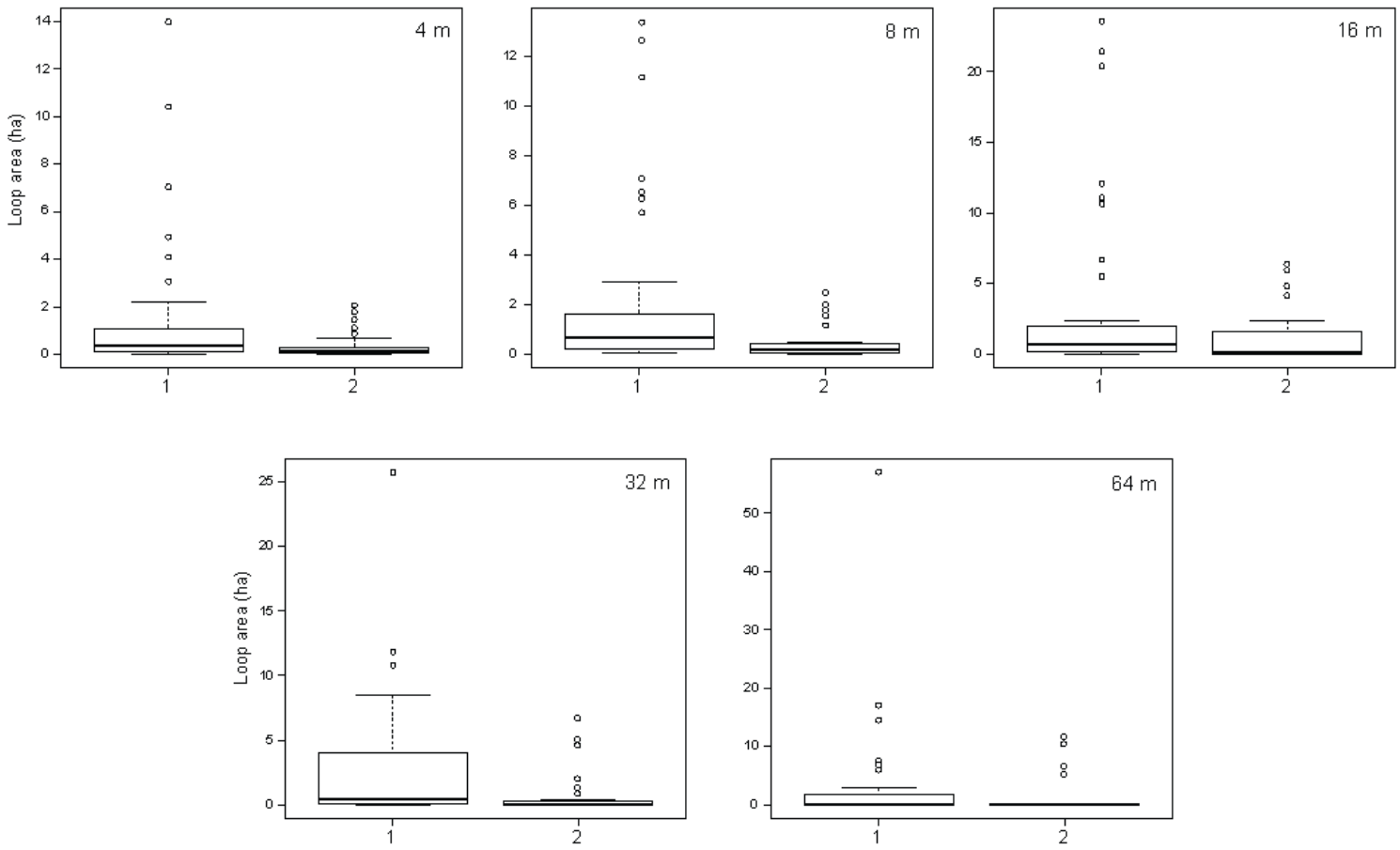

Figure 59. Loop morphological element areas decrease across grain sizes whenever an edge width pixel was increased to 2 pixel widths.

Table 61. One-way ANOVA results showing the effect of edge width on bridge morphological elements across all grain sizes ($p < 0.05$).

Source of Variation	d.f.	Sum Sq	Mean Sq	F Value	P-Value
4m					
Edge Width	1	387	386.8	13.61	0.0003
Residuals	158	4492	28.4		
8m					
Edge Width	1	398	398.5	13.38	0.0003
Residuals	158	4704	29.8		
16m					
Edge Width	1	745	744.5	11.8	0.0008
Residuals	158	9970	63.1		
32m					
Edge Width	1	110.1	110.08	6.716	0.0105
Residuals	158	2589.7	16.39		
64m					
Edge Width	1	250	249.71	3.691	0.0565
Residuals	158	10690	67.66		

The edge width parameter had a significant effect on the branch morphological areas across all grain sizes (Table 61). The branch morphological mean areas were significantly different when the edge width was increased to 2 edge width pixels ($p < 0.05$). The branch morphological areas decreased significantly when an edge width of 2 pixels was applied to the residual patches across all grain sizes (Figure 61).

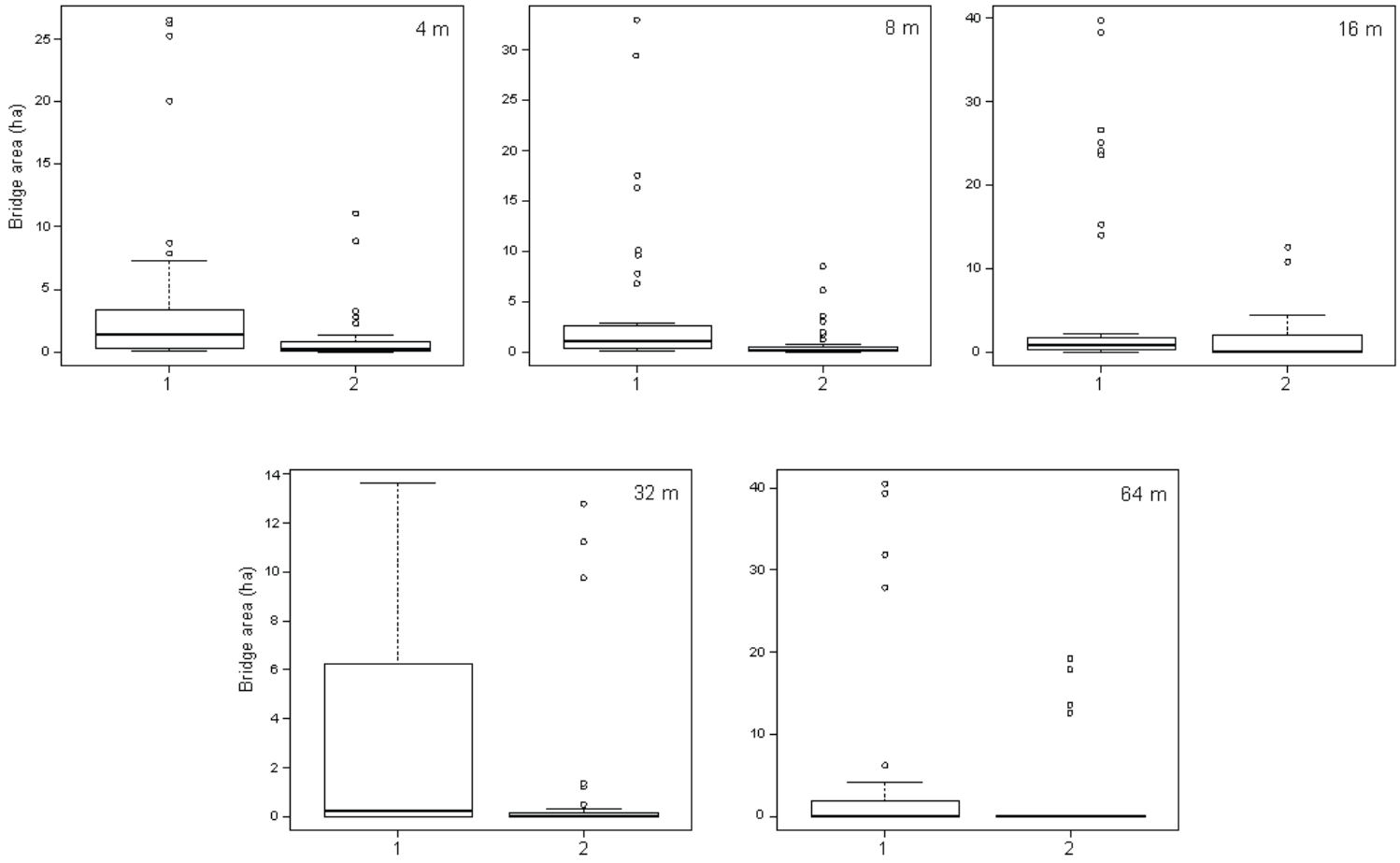

Figure 60. The edge width has a significant effect on the bridge morphological element areas across 4 m, 8 m, 16m, and 32 m grain sizes ($p < 0.05$ level).

Table 62. One-way ANOVA results showing the effect of edge width on branch morphological elements across all grain sizes ($p < 0.05$)

Source of Variation	d.f.	Sum Sq	Mean Sq	F Value	P-Value
4m					
Edge Width	1	6185	6185	12.48	0.0005
Residuals	158	78310	496		
8m					
Edge Width	1	15535	15535	11.89	0.0007
Residuals	158	206362	1306		
16m					
Edge Width	1	39747	39747	10.45	0.0015
Residuals	158	600909	3803		
32m					
Edge Width	1	15818	15818	10.18	0.0017
Residuals	158	245585	1554		
64m					
Edge Width	1	23440	23440.00	5.429	0.0211
Residuals	158	682133	4317.00		

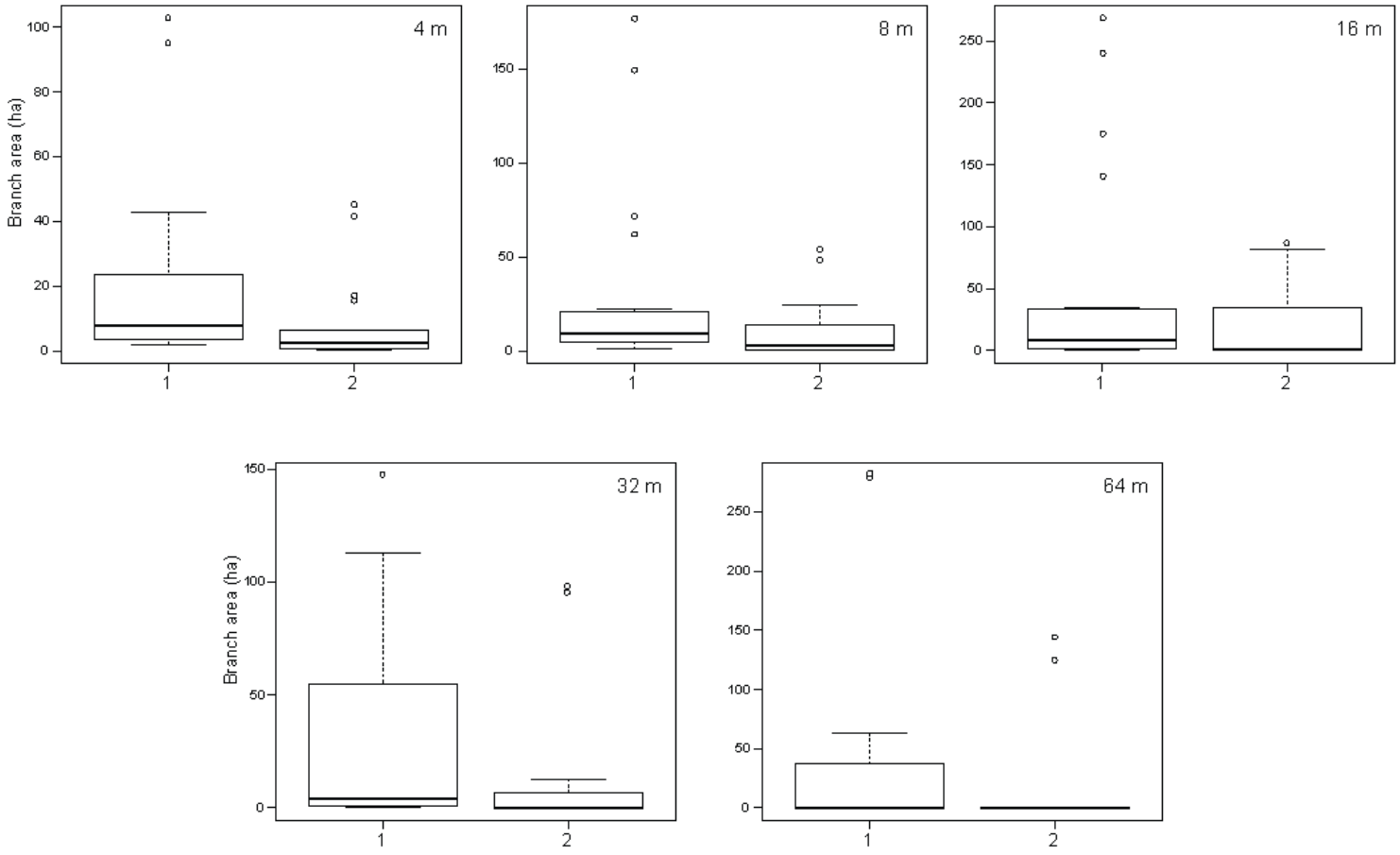

Figure 61. The pattern element areas computed from branch morphologies were significantly different when observed at 1 and 2 edge width pixels.

3.10 Transition Parameter Change

One-way ANOVA tests were conducted to compare the effect of transitioning on all of the morphological element areas in all insular residual patches for each grain size. Transition had no significant effect on the core and islet morphological elements for all observed grain sizes (Tables 62 and 63). The means of the core and islet morphological element areas were significantly different when the transitioning was turned on and off ($p > 0.05$).

Table 63. One-way ANOVA test results showing the effect of transitioning on the core morphological elements ($p > 0.05$ level).

Source of Variation	d.f.	Sum Sq	Mean Sq	F Value	P-Value
4m					
Transition	1	0	0.00	0	1
Residuals	158	11245	71.17		
8m					
Transition	1	0	0.00	0	1
Residuals	158	13473	85.27		
16m					
Transition	1	0	0.00	0	1
Residuals	158	35397	224.00		
32m					
Transition	1	0	0.00	0	1
Residuals	158	16932	107.20		
64m					
Transition	1	0	0.00	0	1
Residuals	158	80453	509.20		

Table 64. Transitioning effects on the islet pattern morphology illustrated in one-way ANOVA statistical tests ($p > 0.05$ level).

Source of Variation	d.f.	Sum Sq	Mean Sq	F Value	P-Value
4m					
Transition	1	0	0.0	0	1
Residuals	158	95978	607.5		
8m					
Transition	1	0	0.0	0	1
Residuals	158	936197	5925.0		
16m					
Transition	1	0	0.0	0	1
Residuals	158	2207543	13972.0		
32m					
Transition	1	0	0.0	0	1
Residuals	158	4695712	29720.0		
64m					
Transition	1	0	0.0	0	1
Residuals	158	11279878	71392.0		

The edge boundary morphologies had contrasting effects when the transition was applied. Perforation boundary areas were not affected by turning on the transition; their means were not statistically different from the area means when the transition was turned off ($p > 0.05$) (Table 64). The outer edge boundary mean areas were significantly different when the transitioning was turned on from 4 m to 32 m grain sizes ($p < 0.05$) (Table 65). At these observable grain sizes the edge morphological elements have increased in area whenever the transition was turned on (Figure 62). However, at 64 m grain size the transitioning did not have a significant effect on the edge morphological element areas (Table 65). The mean edge areas were not significantly different when the transition condition was altered from 0 to 1at the 64 m grain size ($p > 0.05$) (Table 65).

Table 65. One-way ANOVA results of perforation morphology across all 5 grain sizes, and the effect of transition on the element areas ($p > 0.05$).

Source of Variation	d.f.	Sum Sq	Mean Sq	F Value	P-Value
4m					
Transition	1	0.170	0.1675	0.479	0.490
Residuals	158	55.300	0.3500		
8m					
Transition	1	0.066	0.0656	0.575	0.450
Residuals	158	18.019	0.1141		
16m					
Transition	1	0.240	0.2399	0.626	0.430
Residuals	158	60.500	0.3829		
32m					
Transition	1	0.040	0.0443	0.062	0.804
Residuals	158	113.650	0.7193		
64m					
Transition	1	0.000	0.0000	0.000	1.000
Residuals	158	38.910	0.2462		

Table 66. Turning on the transition parameter results in a significant effect on the edge morphological element areas at 4 m to 32 m grain sizes ($p < 0.05$ level).

Source of Variation	d.f.	Sum Sq	Mean Sq	F Value	P-Value
4m					
Transition	1	1086	1086.0	7.042	0.00878
Residuals	158	24366	154.2		
8m					
Transition	1	1170	1170.5	5.790	0.01730
Residuals	158	31938	202.1		
16m					
Transition	1	2428	2428.2	5.240	0.02340
Residuals	158	73213	463.4		
32m					
Transition	1	692	692.2	4.245	0.04100
Residuals	158	25768	163.1		
64m					
Transition	1	1287	1287.3	1.878	0.17200
Residuals	158	108280	685.3		

The transitioning parameter did not significantly affect the connector morphological elements. The loop and bridge morphological mean areas were not significantly different when the transitioning was applied to the residual patches at each grain size ($p > 0.05$) (Tables 66 and 67). Similarly, branch morphological element areas did not display a statistical difference in their means when the transition was turned on ($p > 0.05$) (Table 68). The lack of any significant difference in the morphological area means in branches was observed across all grain sizes (Table 68).

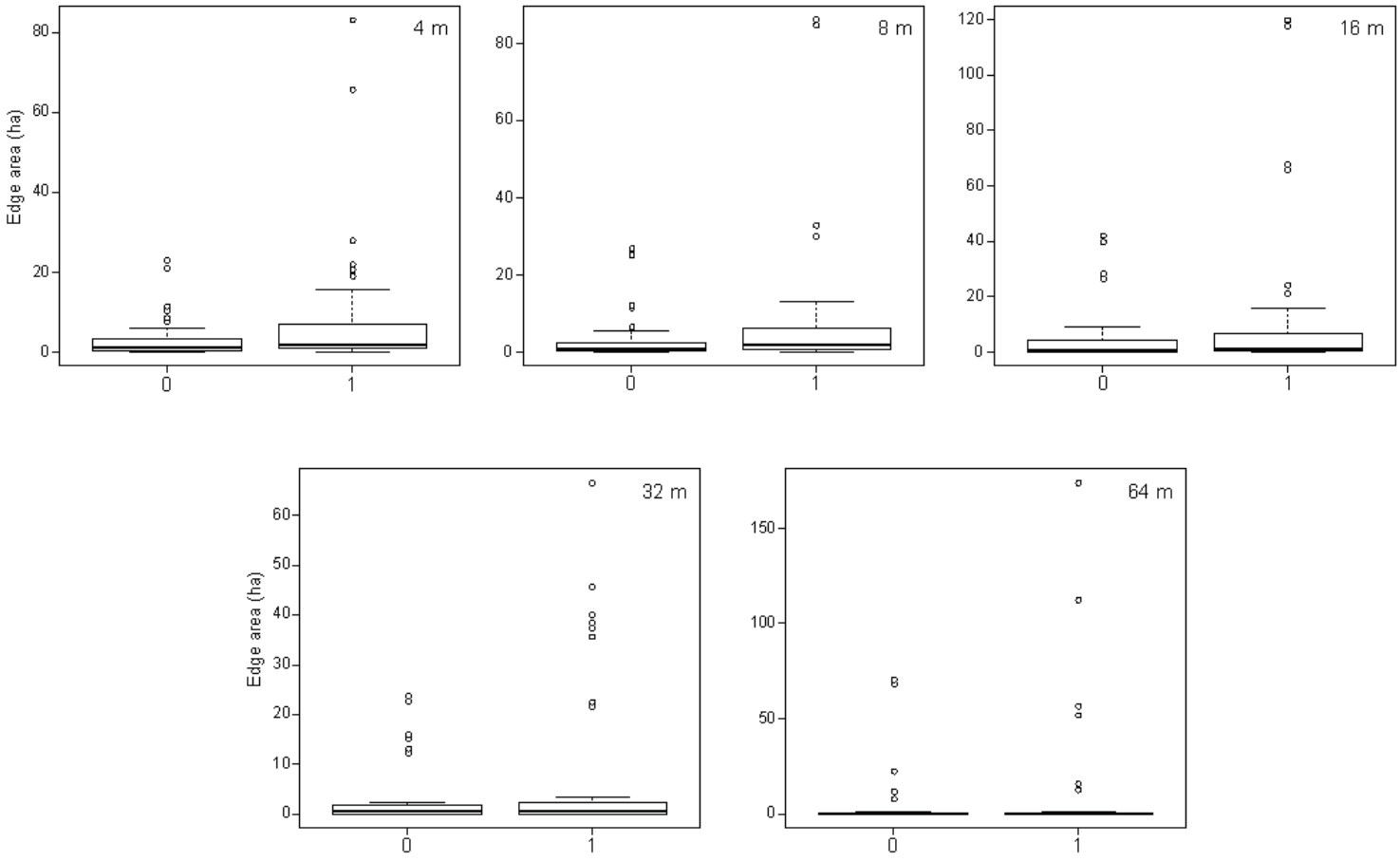

Figure 62. Boxplots showing the increase in edge morphological areas as the transition is turned on at grain size 4 m, 8 m, 16 m, and 32 m.

Table 67. Turning on the transitioning parameter did not have a significant effect on the loop morphological element areas at each grain size ($p > 0.05$ level).

Source of Variation	d.f.	Sum Sq	Mean Sq	F Value	P-Value
4m					
Transition	1	13.7	13.706	2.963	0.0871
Residuals	158	730.8	4.625		
8m					
Transition	1	5.3	5.281	0.764	0.3830
Residuals	158	1092.5	6.915		
16m					
Transition	1	14.0	14.020	0.629	0.4290
Residuals	158	3520.0	22.280		
32m					
Transition	1	19.3	19.250	1.370	0.2440
Residuals	158	2221.0	14.060		
64m					
Transition	1	68.0	67.650	1.374	0.2430
Residuals	158	7776.0	49.220		

Table 68. One-way ANOVA results of the effect of transitioning on the occurrences of bridge element areas across all grain sizes ($p > 0.05$ level).

Source of Variation	d.f.	Sum Sq	Mean Sq	F Value	P-Value
4m					
Transition	1	15	15.450	0.502	0.480
Residuals	158	4863	30.780		
8m					
Transition	1	67	67.150	2.107	0.149
Residuals	158	5035	31.870		
16m					
Transition	1	103	103.300	1.538	0.217
Residuals	158	10611	67.160		
32m					
Transition	1	0.6	0.555	0.032	0.857
Residuals	158	2699.2	17.084		
64m					
Transition	1	0	0.150	0.002	0.963
Residuals	158	10939	69.230		

Table 69. The one-way ANOVA results show that branch morphological areas were statistically different at 0 and 1 transitioning ($p > 0.05$ level).

Source of Variation	d.f.	Sum Sq	Mean Sq	F Value	P-Value
4m					
Transition	1	0	0.0	0	1
Residuals	158	84495	534.8		
8m					
Transition	1	0	0.0	0	1
Residuals	158	221898	1404.0		
16m					
Transition	1	0	0.0	0	1
Residuals	158	640656	4055.0		
32m					
Transition	1	0	0.0	0	1
Residuals	158	261403	1654.0		
64m					
Transition	1	0	0.0	0	1
Residuals	158	705573	4466.0		

4. Discussion

4.1 Residual Patch and Land Cover Classification

4.1.1 Insular Residual Patches

Area statistics were conducted on the footprint area and the residual patch area for each observable grain size. The footprint size in the RED-084 event averaged about 44000 ha, with the footprint area increasing gradually with increasing grain size (Table 70). The residual patches accounted for approximately 12 to 16% of the footprint area, depending on the grain size used to observe the study site. Within the footprint, the insular residual patches contributed an average of 6400 ha to the total footprint area (Table 70). This residual patch area corresponds to about 14.6% of the entire footprint area; averaged for all 5 grain sizes. The percentage of insular residual patches within RED-084 increased with a coarsening of the grain size.

Table 70. The relative proportion of insular residual patches found within the RED-084 footprint area at each observed grain size.

Grain Size (m)	Footprint Area (ha)	Residual Area (ha)	% Residual
4	40226.46	4994.00	12.41
8	43242.15	6330.36	14.64
16	44407.04	6481.79	14.60
32	45175.91	6969.65	15.43
64	46283.16	7448.17	16.09

4.1.2 Land Cover Classification

The land cover classification results illustrate the proportions of each of the 10 land cover classes in RED-084, and include all insular residual patches (Table 71). The land cover classes with largest proportions were sparse conifer, dense conifer, and water bodies (Table 71). The relatively large proportions of dense conifer and sparse conifer coincide with the statistical differences observed in the ANOVA and Tukey post-hoc results from testing whether certain land cover classes were significantly different in particular morphologies across various grain sizes. Water bodies were also very abundant within the RED-084 footprint, contributing to an average of 5280 ha of land

cover across all grain sizes (Table 71). In the larger grain sizes (32 m and 64 m), water bodies retained their structure due to the lakes and rivers covering large, continuous, and unimpaired tracts of cover throughout the footprint.

Bedrock and non-vegetation also had a relatively large composition within the RED-084 footprint, occupying on average 710 ha of the landscape at each grain size. The proportion of bedrock and non-vegetation land cover resulted in some significant differences in the morphologies, especially at the smaller grain sizes (4 m and 8 m). The lowest land cover proportions were the wetland classes (treed, open, and marsh), low shrub (often associated with wetland areas), and deciduous forest class (Table 71). With the exception of treed wetland at 32 m and 64 m grain sizes, each of these land cover classes contributed to less than 500 ha of the total footprint area. In the statistical tests (ANOVA and Tukey post-hoc) these land cover classes were not significantly different from each other, owing to their relatively small land cover composition.

Table 71. The areal proportions of each land cover class found within RED-084 fire footprint at each observed grain size.

	Area (ha)					
Land Cover	**4 m**	**8 m**	**16 m**	**32 m**	**64 m**	**Total**
AS	132	151	176	216	250	925
BV	664	723	734	715	719	3555
DE	336	405	417	457	451	2066
DC	1131	1640	4783	1838	2034	11426
LS	220	253	261	291	287	1312
MA	76	88	96	127	151	538
OP	211	253	261	285	307	1317
SC	2487	3074	3089	3248	3409	15307
TW	401	464	482	505	554	2406
WA	3262	4885	5444	5944	6858	26393
Total	8920	11936	15743	13626	15020	

4.2 Morphological Pattern Elements, Land Cover Classes, and Grain Sizes

4.2.1 Core Morphology

Core morphologies are mostly represented in sparse conifer and dense conifer land cover classes from 4 m to 32 m grain sizes. Water bodies account for a significant portion of the core morphologies at 32 m and 64 m grain sizes. The higher proportions of the aforementioned land cover classes are the main reasons why the ANOVA results showed a significant difference in at least one of the land cover classes at any given grain size. The core element areas decreased across most land cover classes; bedrock and non-vegetation, deciduous, low shrub, open wetland, and treed wetland as the observed grain size increased. This trend was noted in these land cover classes because of their overall low proportion of residual patches (as compared to the conifer classes and water bodies). Furthermore, these land cover classes have relatively small core morphological elements within their patches, hence the probability of these cores becoming islets increases. At 4 m and 8 m grain sizes the bedrock and non-vegetation class was statistically different as their core areas were larger than other land cover classes (except for the conifers).

The Tukey post-hoc tests revealed that dense conifer, sparse conifer, and water bodies were consistently different than other land cover groups when observed for their core morphologies, especially at 16 m and 32 m grain sizes. These land cover classes generally contain larger patch sizes and larger core elements, with larger areas of homogeneous conifers, lakes, and rivers within RED-084. Therefore, at the larger grain sizes (16 m to 64 m) there was a marked decrease in the core pattern elements in dense and sparse conifers, while the core areas in water bodies increased. Water bodies occur in more contiguous and larger configuration patterns, especially due to high occurrences of lakes in RED-084.

4.2.2 Islet Morphology

Islet morphologies were unpredictable in relation to their presence within the various land cover classes. The randomness was observed in the Tukey post-hoc results at the 4 m and 8 m grain sizes, whereby each land cover class was significantly different from every other class (with the exception of sparse conifer and treed wetland,

and dense conifer and treed wetland pairings). At these grain sizes islet morphological pattern elements are widespread throughout each land cover class. This implies that islets occur in almost the same proportions across each land cover class, and that the RED-084 event is thoroughly covered with residual patch islets. The connectivity among residual patches is decreased with an increased presence of islets.

Low shrub and alder shrub, and water and marsh land cover pairings were significantly different, while all other land cover classes were not statistically different at the 16 m and 32 m grain sizes. Alder shrub was also significantly different when paired with low shrub, open wetland, and water at 64 m grain size. As the grain size increases, the islets become more prevalent in all land cover classes.

The dominant classes were highly variable in the islet morphologies as compared to the other morphological pattern elements. Bedrock and non-vegetation, dense conifer, sparse conifer, and treed wetlands were the most dominant classes in islet formations but not one was consistently higher than other classes. When the grain size increases, other morphological pattern elements tend to morph or change into islets. The edges or boundaries of cores and perforations will dissipate at a threshold pixel size as the observable grain size continues to increase. Once the grain size reaches at least 16 m or 32 m, most of the other morphological patterns elements would have changed to islets (Figure 63). At 64 m grain size, islets would become the most dominant morphological pattern element.

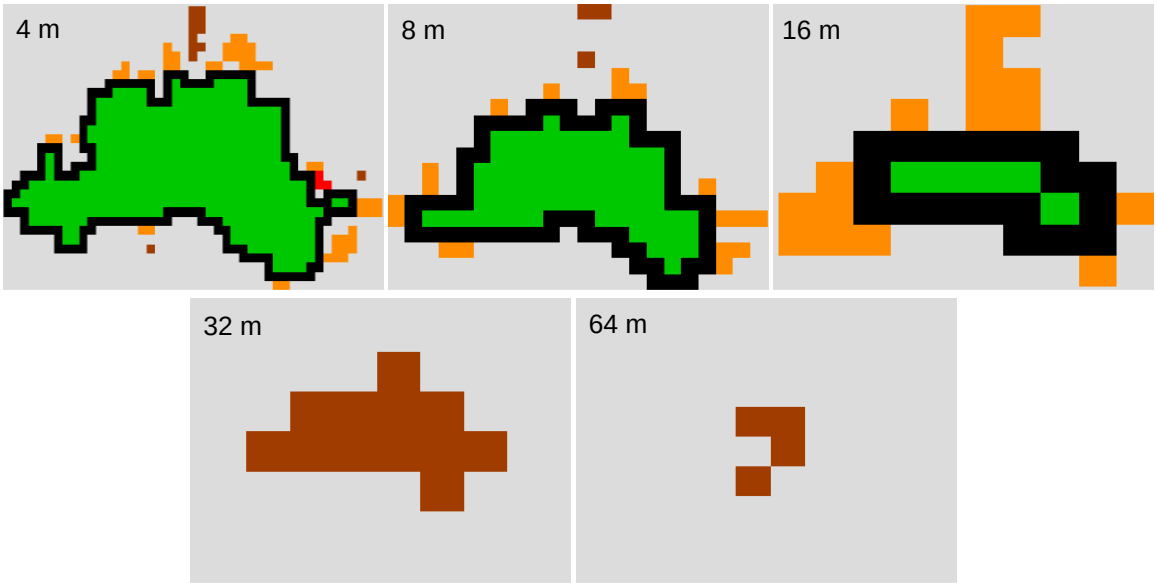

Figure 63. The increase in pixel size facilitates the increased occurrences of larger islet pattern elements as core pattern elements and other elements cannot be observed in their original form at larger grain sizes (Bedrock and non-vegetation land cover class at 4 connectivity, 1 edge width and transition off).

4.2.3 Perforation Morphology

Perforation morphological elements were found to be most present in dense conifer and sparse conifer classes at 4 m and 8 m grain sizes, in dense conifer and water classes at 16 m grain size, and in water at 32 m and 64 m grain sizes. The Tukey post-hoc test results revealed that these land cover classes when paired with all other classes, were statistically different. Perforation morphologies represented the least areas among all of the morphological pattern elements. As the perforations are scarce, the land cover classes that are the least dominant (aldershrub, deciduous, low shrub, marsh, open wetland, and treed wetland) do not contain perforations, especially at the larger grain sizes. Perforation formation also depends on a relatively low probability of a *background* hole being found within a core pattern.

The increase in grain size also allows for the perforations to be converted to edges or bridges (Figure 37). The perforations that occur in close proximity to the *background* matrix outside of the cores will be lost when the grain size reaches a threshold value (will vary depending on the land cover class). The edge boundaries of

the core are breached resulting in the creation of 2 adjacent core pattern elements, this causes the perforation to be dissolved into an edge or bridge. The perforation cannot be connected directly to the outside *background* matrix. The corner of the perforation can interact with the corner of an edge element, only if the connectivity is set to 8 neighbouring pixels.

4.2.4 Edge Morphology

The dominant classes; dense conifer, sparse conifer, and water, were statistically different from other classes at 4 m, at 8 m (conifers and bedrock), at 16 m (conifers and most pairing with water), at 32 m (conifers and water), and at 64 m (water). The edge patterns increased in area from 4 m to 16 m but decreased at 32 m and 64 m. This change marks a point where edges are being converted into another morphological pattern element (s). Depending on the land cover type, the edges can become islets especially given that core pattern elements (which are surrounded by edge boundaries) can dissipate in larger grain sizes. The open wetland morphological maps show that at 32 m, edges were constricted to a smaller area, and most of the other edges were now bridges, branches, and islets (Figure 64).

Edge pattern elements are always dependent on the existence of core elements and to a lesser extent, perforation pattern elements. The steady increase in edge pattern element areas in water bodies was unexpected, as these edges should be lost at larger grain sizes. However, the large and contiguous lakes, ponds, and rivers allow most of the edges to remain intact, completely engulfing the large core surfaces. Another reason for the increase in edge pattern areas with grain size is the conversion of perforation boundary elements to edge boundary elements. At larger grain sizes perforations can be lost to the shrinking of the core elements, this creates gaps in the cores that can only be separated from the *background* matrix as edge boundaries. In addition, perforation boundaries that occur in close proximity to the edge boundaries can become assimilated into edges if the grain size increases. An increase in the grain size or change in connectivity to 8 neighbourhood pixels would frequently result in the exposure of these perforations to the exterior (with respect to the core element) *background* matrix. This results in the conversion of the perforation boundaries to edge boundaries, leading to an increase in edge areas in the water body class.

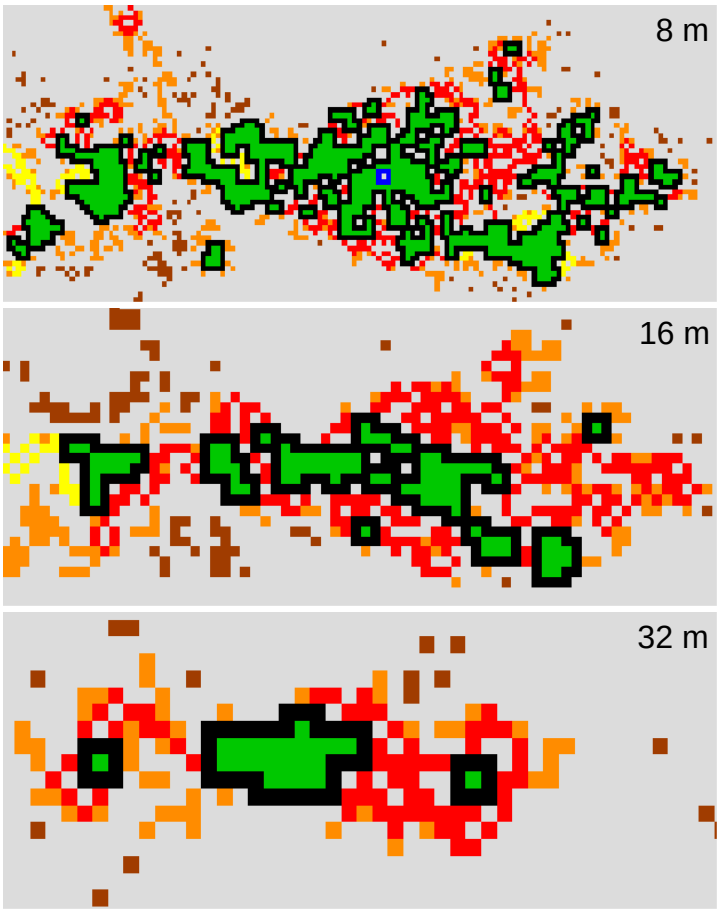

Figure 64. Edge boundary elements in these open wetland patches decrease as the grain size increases; edges become enveloped and converted to bridges and branches as the cores dissipate.

4.2.5 Loop Morphology

Loop morphological pattern elements were found in lower proportions across all land cover classes as compared to other morphological elements. Loop patterns were found mostly in sparse and dense conifer classes from 4 m to 32 m grain sizes, as shown by their relative proportion of areas and the results of Tukey post-hoc tests. The loop pattern areas in both conifer types increased between 4 m and 16 m but subsequently decreased at 32 m and 64 m grain sizes. Conifer types were abundant in the RED-084 footprint and loops may be formed as a result of the edges of cores being broken when grain size increases. In order to link the core, loops would have to form in

the place of edges. Loops were predominantly found in water bodies at 32 m and 64 m, at these larger grain sizes water bodies can still maintain their shape and area. The water bodies in RED-084 were mainly in the form of lakes, which cover relatively large, contiguous areas. Water bodies' core areas would have to be relatively large as well, hence any loops connecting the same core would tend to increase over a larger grain size.

4.2.6 Bridge Morphology

At 4 m bridge pattern elements were significantly different in the most abundant land cover classes in which they were found; bedrock and non-vegetation, dense conifer, and sparse conifer. At 16 m grain size, bridges were most abundant and their mean areas significantly different in conifers when compared to other land cover classes. There is also a gradual increase in bridge pattern elements in dense conifer when the grain size increases from 4 m to 16 m. This relationship can be a result of larger core areas becoming segmented as the grain size increases; the minimum mapped unit would be too large to sustain a core morphological element (Figure 65). At 32 m however, there is a significant decrease in the bridge element areas of these land cover classes. Numerous cores would be transformed into islets and/or branches. Cores become smaller and constricted to the grain size, therefore any patches emanating from cores may not join with other cores. These would lead to the lowering of branch areas in all of the land cover classes except water bodies.

Bridge pattern elements within water body residuals increased in area when the grain size increased to 32 m and 64 m. Bridges are dependent on the adjacency between core morphologies. At larger grain sizes, water bodies contain numerous core elements, which can have irregular configurations (Figure 65). Relatively thin and narrow sections in the core elements can morph into bridges so where there was one core with a narrow section now changes into 2 cores with a connecting bridge in a larger observable grain size.

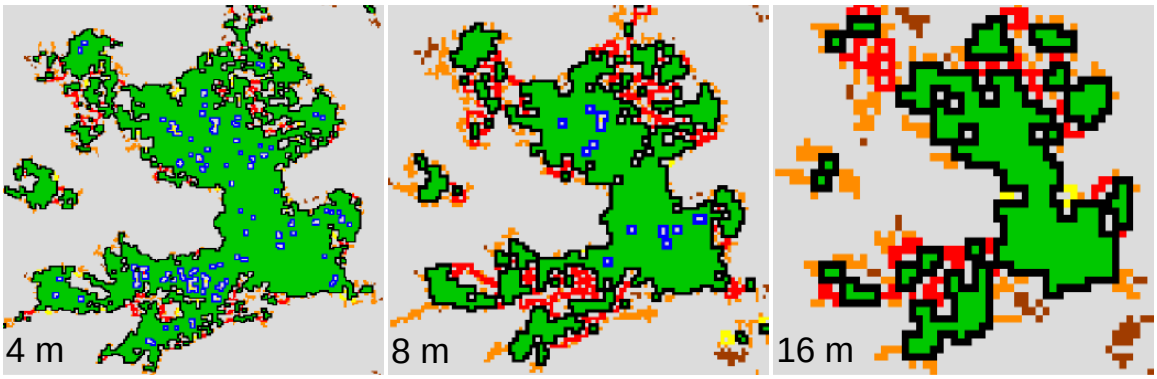

Figure 65. Bridge morphological elements in larger sparse conifer cores can become larger themselves as the core begins to disintegrate with a higher grain size (observed at 4 connectivity, 1 edge width, and transition turned off).

4.2.7 Branch Morphology

Branch morphological pattern elements followed similar trends to branches at 4 m and 8 m grain sizes; the more abundant conifer types and bedrock and non-vegetation were significantly different from other land cover types when paired with them. Upon further observations of the morphological maps, smaller core patterns from which branches originate often become islets at larger grain sizes. The branches attached to these smaller cores would also be converted to islets, leading to the decrease in branch element areas.

At 16 m, the larger and irregularly shaped core pattern elements can shrink along their narrower and elongated segments. This promoted the formation of more branch elements as was observed in their increase from 4 m to 16 m, especially in the sparse conifer and dense conifer classes. The branch pattern elements decreased in all land cover classes from 16 m to 64 m, except for the water bodies. Given the large size of lakes and the elongated shapes of the rivers, the frequency of branches increased with grain size. The edges and cores would become constricted in larger patches, and notably in narrower patches (rivers and streams); resulting in the formation of branches (and bridges).

4.3 Connectivity Effects on Morphological Pattern Elements

4.3.1 Core Morphology

The p-values were not significant when tested for core pattern area means undergoing a connectivity change from 4 to 8 neighbouring pixels. The neighbourhood connectivity affects the patterns which emanate from or connect to core patterns via their surrounding edges. Therefore, a change in connectivity would not affect the areas or formations of core morphological patterns elements. There are instances of 2 or more core patterns connected to each other by their edges, however the connectivity does not alter the configuration of the adjacent cores.

4.3.2 Islet Morphology

Islet morphological pattern elements significantly decreased in areas as the neighbourhood connectivity was changed from 4 to 8 pixels. At 4 neighbourhood connectivity islet elements can form at the corner of core and/or branch morphological elements. These same islet elements are converted into another morphological element when the connectivity changes to 8 neighbouring pixels. The Queen's case allows for the corner islets to become mostly branches, and sometimes loops (depending on the surrounding pixels). There are more islets converted to branch elements under this parameter change, hence the islet areas would decrease for any given grain size.

4.3.3 Perforation Morphology

Perforations behave in a similar way to core features when a connectivity change is applied. They do not emanate or connect core elements but instead are inner boundaries. The 8 neighbourhood connectivity did not significantly affect the means of the perforation element areas. The rare occasions of perforations occurring near the corner edges of cores can result in these perforations changing into edge elements. There were insufficient instances of this morphological shift occurring to cause a significant change in the ANOVA results.

4.3.4 Edge Morphology

Edge morphological pattern elements are not affected by connectivity change as their boundary areas are not breached by other morphologies unless the transition was changed. The morphologies often originate from the edge elements (when the transition is turned off) and if they originate from the corners they would more than likely be affected by the connectivity parameter. As stated in the previous section, edges can be formed when a connectivity of 8 is applied to a perforation element which interacts with a core element's edge boundary.

4.3.5 Loop Morphology

According to the ANOVA results on loop morphological areas, the means were not statistically different when the neighbourhood connectivity was changed. However, when we observed the morphological maps, loop elements seemed to have been affected by the connectivity, most notably when islets or branches were the connecting elements. Loops can be formed from the islets that occur in a continuous configuration near the edges of cores (Figure 66). The connectivity changes the way in which the loops interact with the core element. Branches can also be changed to loops if the branches are extensive and complex. There are numerous examples of the change in loop pattern areas, mainly an increase in area (islets to loops and/or branches to loops), however the ANOVA test results did not suggest these changes were significant. Upon further observations of morphological maps, loop elements can also transform into branches and bridges (Figure 66). There may have been enough examples of this transformation to counteract the increase in loop morphological elements.

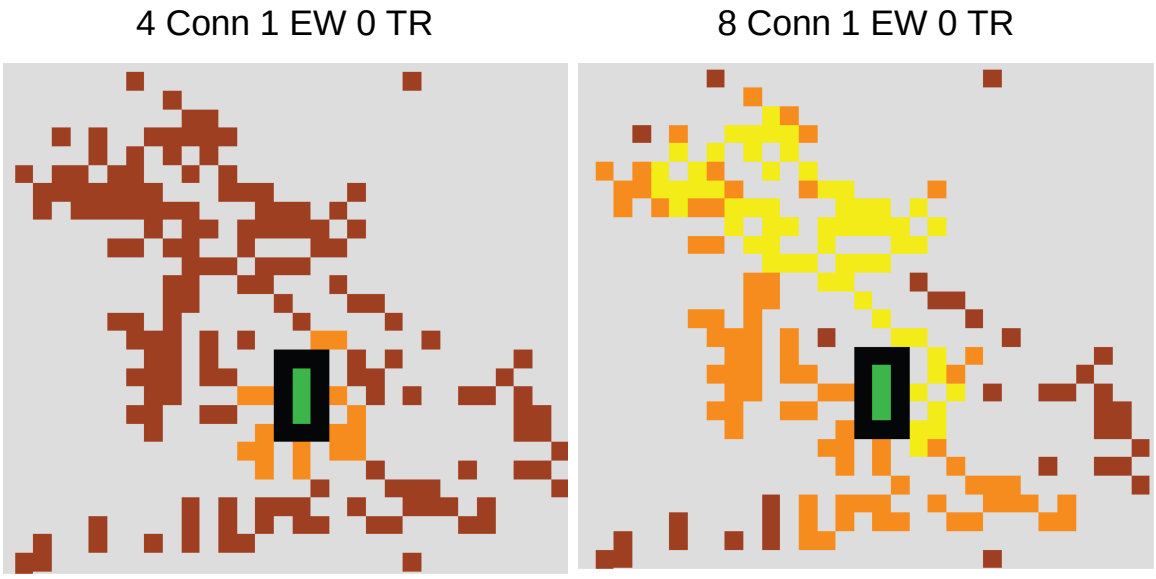

Figure 66. Low shrub residual patches at 16 m grain size; an 8 neighbourhood connectivity allows connecting islet elements to be converted to 1 larger loop element.

4.3.6 Bridge Morphology

According to the results of the ANOVA one-way tests, bridge morphological pattern elements were not significantly affected by the change in neighbourhood connectivity. There were instances where the bridge elements can form or dissipate between 4 and 8 neighbouring pixels. At 4 neighbourhood connectivity, cores that are only 1 pixel thick are separated from each other and are hence defined as different cores (rather one core). When an 8 neighbourhood connectivity is applied these cores now become 1 core as by definition they are diagonally connected. The bridge would then transform into a loop linking one part of the core to another part of the same core.

2 separate cores cannot be completely linked with bridges if a 4 neighbouring pixel connectivity is applied. Figure 67 illustrates that a branch can occupy the space between 2 cores if a connectivity of 4 pixels is set. However, as the connectivity changes to 8 pixels, the same branch can be defined as a bridge (Figure 67). The connectivity now accounts for the neighbouring diagonal pixels originating from the edges of cores. According to the definition of connectivity, the branch pixels can connect to another core element but then are transformed into bridge pixels if the connectivity increases. The main reason for the ANOVA results being insignificant was

the similar losses and gains in bridge elements; with losses including the conversion to loops and gains including conversion from branches.

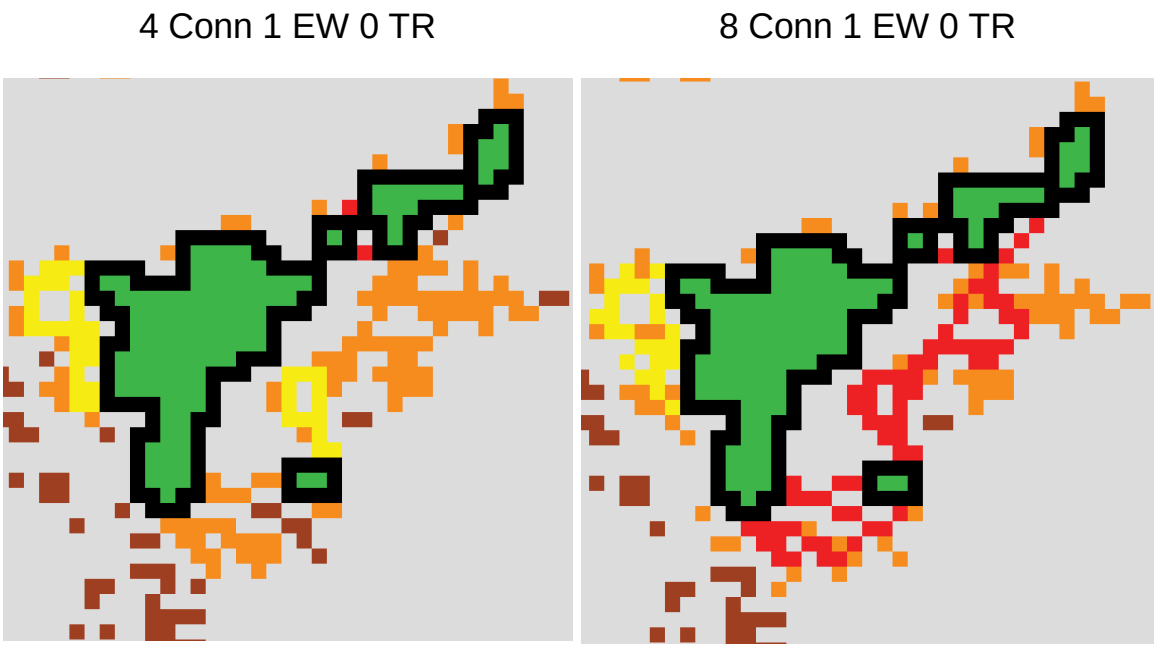

Figure 67. Bridge morphological elements can be formed at the 8 connectivity parameter setting by allowing the former branches to link core morphologies.

4.3.7 Branch Morphology

The results of the ANOVA tests carried out on branch morphologies revealed that neighbourhood connectivity did not have a significant effect on the branch element areas. Branch morphologies however, can change depending on the connectivity parameter set. Figure 68 illustrates 2 branch elements emanating from the 2 most southerly cores, and these branches appear connected and seamless between the cores. However, they are not connected as the neighbourhood connectivity was set to 4 pixels at the rook's case orientation. The corner edge where the 2 branches interact does not offer a connection point, by definition of the neighbourhood connectivity. The branches change to one continuous bridge element when the neighbourhood connectivity was changed to 8 pixels (Figure 68). The corner edge interaction was now considered as a continuous connection point allowing for the formation of the bridge.

The instances of these phenomena occurring may have been relatively low to cause a significant change in the branch element means.

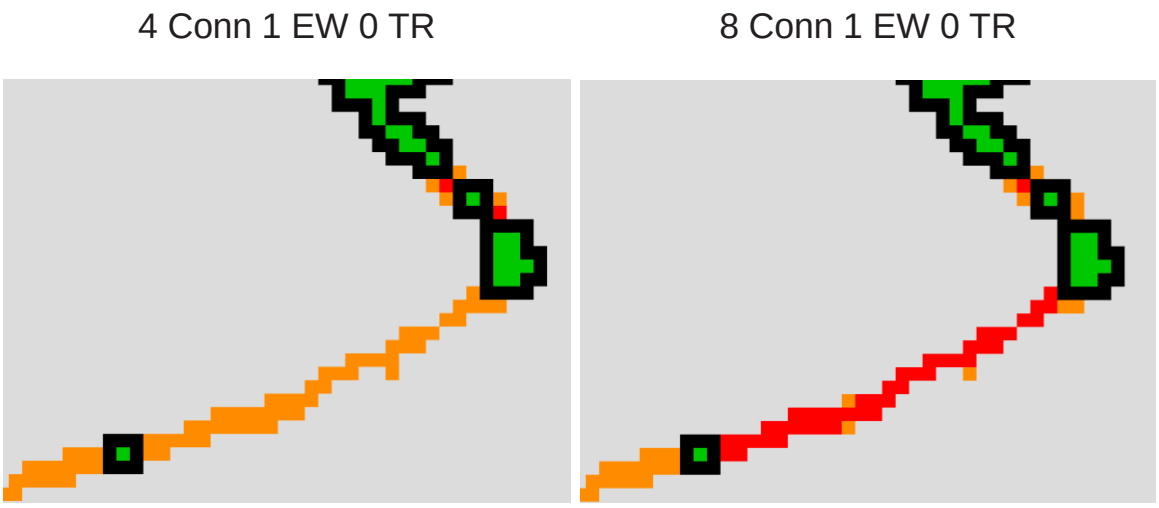

Figure 68. A connectivity change can result in the conversion of an originating branch (from the core) to a bridge connecting 2 cores (water body class at 16 m grain size).

4.4 Edge Width Effects on Morphological Pattern Elements

4.4.1 Core Morphology

Changing the edge width parameter from 1 to 2 pixels significantly altered the areas of the core morphological elements. The boxplots displaying the results of the core morphology with edge width used, show a common trend of a decrease in core pattern areas at 2 edge width pixels across all grain sizes. When the edge width is increased, the morphological area occupied by the edge increases inwards (in relation to the core). This allows for the reduction of the core morphology at most scenarios, especially when the core elements are thicker than 2 pixels.

The smaller core elements can be diffused and dissipated entirely resulting in the formation of different morphologies. This can be observed in Figure 69, where the adjoining core elements on the right side of the figure have enclosed entirely by the increase in the edge area. These core elements have now been converted to branch elements as they have become an extension of the core in the lower right of the figure. The core pattern element at the bottom of the image (Figure 69) was separated from the

core to its right via 2 adjacent edge elements. Once the edge width parameter was increased, the core dissipated giving way to a bridge pattern element which links the cores (Figure 69).

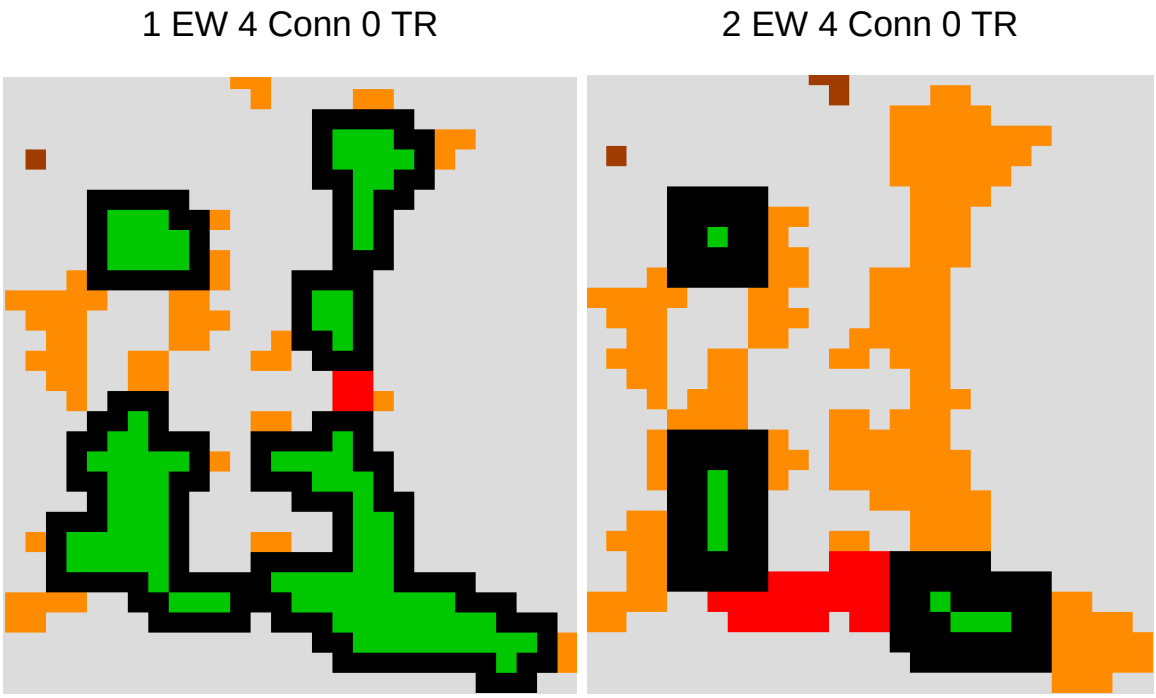

Figure 69. Core pattern elements in marsh residual patches at 4 m grain size were observed to decrease in area as the edge width increased; constricting smaller cores to a certain degree until they transformed into branches.

4.4.2 Islet Morphology

Islet morphological elements were not affected by a change in edge width; there was no significant difference in the means of the islet areas at each grain size. The islet morphology represents isolated pixels which are not surrounded by edge boundaries. Therefore, a change in edge width would not reflect a significant change in the formation or loss of islet pattern elements.

4.4.3 Perforation Morphology

Perforation area means were significantly lower at 2 edge width pixels than at 1 edge pixel according to the boxplots and ANOVA results. These results may be illogical

considering that perforations are inner edge boundaries occurring within core pattern elements, and are therefore a type of edge morphology. An increase in edge width should equate to an increase in the perforation morphological area. When observing some of the morphological maps, we can clearly see that this increase of the perforation is occurring with the parameter change. However, this observation is made mostly in residual patches that contain relatively large core elements. The reason is that an increase in the edge width in a perforation can only occur outwards into the core, as the perforation cannot expand into the *background* or areas devoid of residual patches. The bigger the core the more available residual patch space there is to facilitate the gain in perforation edge width.

The decrease in the overall perforation element areas across all grain sizes and collectively for all land cover classes can be explained by the size of the perforation, the size of the core morphology, and the proximity of the perforations to the edge boundaries of cores. In Figure 70, the perforations closer to the edge break the boundary if the edge width is increased; this results in the perforation boundary interacting with the edge boundary. These 2 boundary types interact with each other as the edge increases inwards of the core and the perforation increases outwards of the core. This will force the MSPA to create a different morphology to occupy the space of the interaction. The morphological map example in Figure 70 shows a loop taking the place of edge and perforation boundaries, hence eliminating the perforation.

Smaller core areas also account for the dissipation of the perforation areas at 2 edge width pixels. The smaller patch size reduces the area that supports the expansion of the perforation boundaries, hence the increase in edge width may not accommodate all perforation increase in smaller patches. The smaller patch sizes and smaller core morphologies would also determine the proximity of perforations to the outer edge boundaries. This interaction would therefore result in perforations being converted to mostly edge morphological elements, and to a lesser extent the formation of loops and bridges (Figure 71).

1 EW 4 Conn 0 TR

2 EW 4 Conn 0 TR

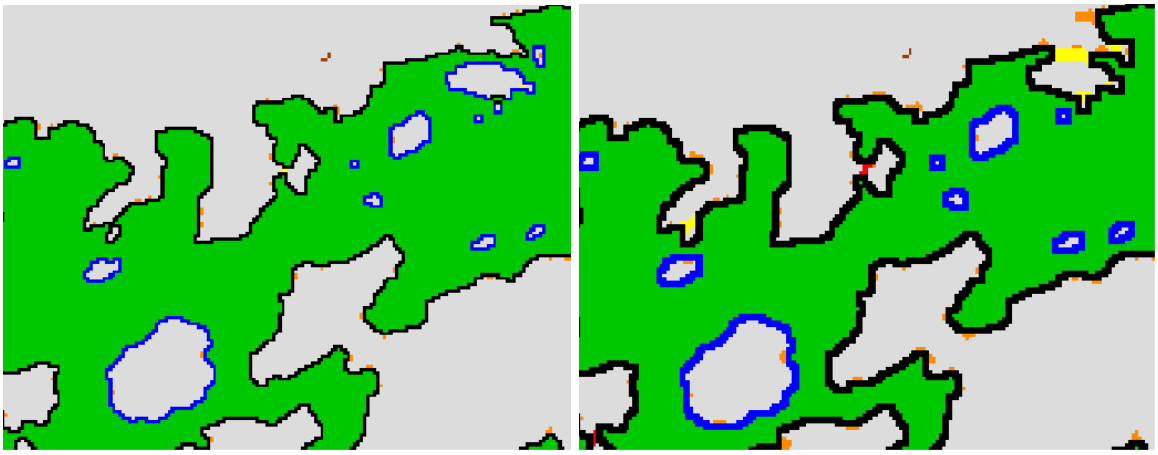

Figure 70. At 16 m grain size the perforations can increase their boundary width as the edge width increases outward (into the core, as observed in this large water residual patch).

1 EW 4 Conn 0 TR

2 EW 4 Conn 0 TR

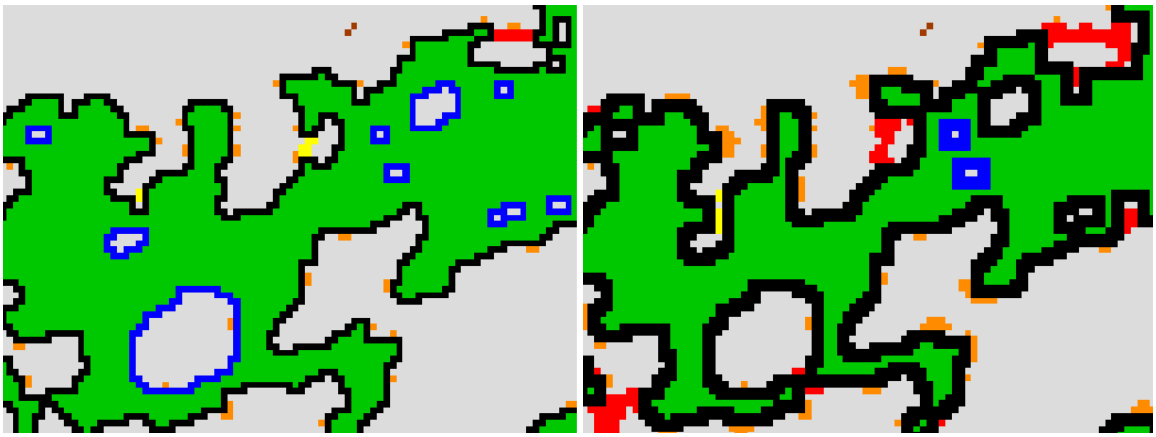

Figure 71. At 32 m grain size some of the smaller perforations and perforations closer to the outer edge boundary tend to be disconnected or dissipated from the core.

4.4.4 Edge Morphology

The edge boundary morphology was significantly affected by the change in edge width parameter across all grain sizes for all land cover classes. The increasing of the edge width pixels should increase the area of the edge boundary but this is not the case when observing the boxplots across all grain sizes (Figure 72). In a similar situation to

perforations, the edge elements precisely decreased in area as the edge width increased to 2 pixels. The area occupied by edges increases inwards with respect to the cores causing the cores to become smaller.

To entirely explain the decrease in the overall edge element areas, we first have to observe the smaller core elements. If these core morphologies are only 1 or 2 pixel wide, then applying an edge width of 2 would cause the dissipation in the core and edge morphology. An edge boundary cannot exist alone and therefore has to encompass a core element so without the cores the edges would also dissipate. Figure 72 illustrates this phenomenon of core and edge conversion to islets and bridges. At larger grain sizes (32 m and 64 m) many core morphologies often become islets, therefore removing the edge boundaries in the process. This supports the one-way ANOVA test results and the resulting boxplots indicating a marked decrease in edge pattern areas at 2 edge width pixels.

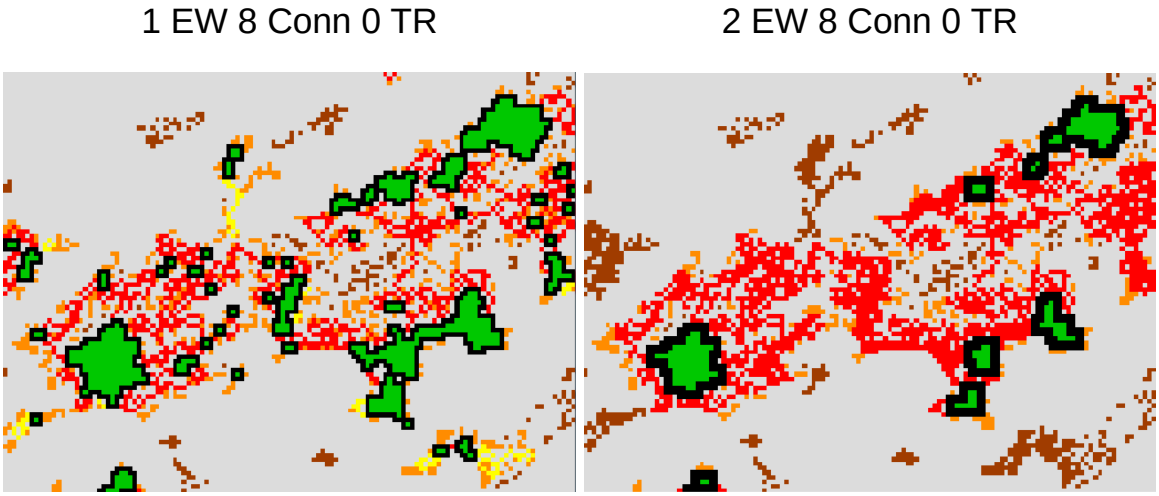

Figure 72. Edge width increase can lead to the dissipation of core morphological elements, and potential linkages of bridge elements connecting the remaining larger cores.

4.4.5 Loop Morphology

Applying an edge width increase had a significant effect on the loop morphologies; there has been a slight decrease in the morphological areas at 2 edge width pixels. The loop elements are not directly influenced by the edge width parameter

but are dependent on the outcome of the core elements from which they originate from. Similar to perforations and edges, loop elements are often affected by the size of the core elements. Smaller core elements tend to dissipate when the edge width is increased; hence this results in the conversion of loop elements to mainly islet elements.

There are instances where the edge width can cause an increase in the loop morphological areas. This increase is often dependent on the shape of the core morphological elements, especially in the case of narrow or elongated cores. The increase in the edge boundary reduces the core area completely in the top right corner of the figure, however the larger central core reduces in size but still remains relatively intact. The elongated part of the core is then converted to a loop element. The left side of the figure also shows the total dissipation of the core element at 2 edge width pixels, resulting in the increase in branch and loop morphologies. Irregular core elements, especially with smaller parts of the core extending out into the *background* are often subjected to loop conversions as the edge width is increased.

4.4.6 Bridge Morphology

Bridge morphological areas decrease with an increase in the edge width parameter for grain sizes 4 m to 32 m. The bridge morphology morphs to other elements depending on a couple of factors: the size of core patch and the distance between core patches. The edge width cannot directly affect the width of the bridge element, however it affects the size of the core element. An edge width of 2 pixels decreases the core morphological areas significantly enough to alter some cores to islets, branches or loops. This results in the loss of bridge elements, which was evident from the one-way ANOVA results and boxplots indicating the decrease in bridge morphological areas at 2 edge width pixels.

Larger core pattern elements remain intact after the edge width was increased. This has the opposite effect on the bridge element areas (as compared to the observations made in smaller core elements); there was a notable increase in these areas. The further clustering of these large core pattern elements interspersed with smaller core elements can result in a higher probability of bridge elements created in order to link the larger cores. However, the occurrences of cores being linked like in this

scenario may not be enough to counteract the loss of bridges in the smaller patches (at 2 edge width pixels).

4.4.7 Branch Morphology

The branch pattern elements were significantly affected by the edge width parameter change across all grain sizes and collective land cover classes. The edge width does not directly affect the size of the branch elements, but can alter the core elements (and associated loops and bridges) to cause a significant change in the branch elements. The shape and size of the core morphology can have an important impact on the formation of new branch elements when the edge width is changed. The increase in edge width can constrict the amount of patch area in which the edge boundaries can occupy especially in the narrow or constricted sections of the core morphology. These sections cannot support the increased edge width, and as a result the edge pixels are lumped together and thus have to be redefined as branch elements. This formation of new branch pattern elements however does not explain the reduction in the overall branch element areas at 2 edge width pixels in our study site. The smaller core elements are usually responsible for the decline in branch element areas when increasing the edge width parameter.

4.5 Transition Effects on Morphological Pattern Elements

4.5.1 Core Morphology

According to the one-way ANOVA results for all land cover classes at all grain sizes, the transitioning does not affect the outcome of core morphological elements. The transitioning affects the pattern elements which emanate from or connect the core elements. Turning on the transition results in those pattern elements having the capability to penetrate the edge boundary and come in contact with the core element. The core pattern element would neither increase nor decrease in area.

4.5.2 Islet Morphology

Islet pattern element areas were not significantly affected by the transitioning parameter change. The islet elements do not directly interact with the core morphology and can only interact with the edge pattern element. Islet elements are isolated and occur away from the core patterns. They can only interact with the core and edge boundary if the connectivity is set at 8 neighbouring pixels. Turning on the transition does not result in the islet penetrating the edge boundary and interacting with the core element. This effect does not support an increase in the islet element area.

4.5.3 Perforation Morphology

Perforation pattern elements were not significantly affected by the transitioning change for all land covers across all grain sizes. However, we have observed that perforations behave like edge boundaries, and can therefore be impacted by the transition. When the transition is turned on loops and bridges found within the *background* of the perforation holes can penetrate the perforation boundaries and interact with the core morphological elements. The figures below illustrate the loss of perforation morphological element areas as the loop and bridge elements penetrate the boundaries when the transition parameter was switched on. The reason for the one-way ANOVA results of the perforation element areas not being significant was that the number of loop and bridge elements occurring within these perforation holes were not sufficient to cause a statistical change.

4.5.4 Edge Morphology

The change in transition had a significant effect on the edge morphological element areas for all land cover classes from 4 m to 32 m grain sizes. When the transition was activated the loop and bridge pattern elements were able to penetrate through the edge boundaries and interact directly with the core pattern elements. The loops and bridges will originate from the cores rather than the edge boundaries when the transition is turned on. However, upon observing the box plots indicating the one-way ANOVA results, we see a slight increase in the edge element area means at transition 1

from transition 0. This observation goes against the notion that edge elements are dissipated to accommodate the loop and bridge elements, thus losing their areas.

There are a given set of scenarios where the significant changes in edge pattern elements occur. The transitioning was set at 1 or 0, at either 1 or 2 edge width pixels.

4.5.5 Loop and Bridge Morphologies

Loop and bridge morphological connector elements are similar in configuration and are the only pattern elements which penetrate the edge boundaries when transitioning is turned on. However, the one-way ANOVA results showed that loop and bridge pattern elements were not significantly affected by the transition parameter change. This observation opposed the notion that loop and bridge element areas tend to increase when the transition is turned on and the edge boundary becomes breached by the loop patterns. This increase was observed throughout all land cover class morphological maps, however, the settings for the other parameters may determine the overall effects of transitioning in loops and bridges. It is important to note that the same loop and bridge pattern elements decreased when the edge width increased and the transition turned off.

4.5.6 Branch Morphology

The transition parameter did not have a significant impact on the branch pattern element areas across all grain sizes for all combined land cover classes. These results were expected as transitioning does not allow the branch elements to penetrate past the edge boundary elements. The branch pattern elements originate from edge boundaries but under all circumstances (via definition of their structure and morphological maps) do not originate directly from core elements. Branch elements also emanate from loop and bridge connector elements, which directly link with the core elements when the transition is turned on. The figures illustrate that branch elements neither increase or decrease in area at each parameter set.

5. Conclusions

The morphological elements found within residual patches of most land cover classes decreased with increasing grain size, and this trend was stable across all grain sizes. Morphologies found within dense conifer residual patches behaved differently from most other land cover classes. The percentage of dense conifer land cover comprising core, perforation, edge, loop, bridge, and branch elements increased as grain sizes increased from 4 m to 16 m, when all other land cover classes (except for water bodies) decreased in representation of the same morphologies. Subsequently, at 32 m grain size the morphologies within dense conifer classes decreased.

A similar boreal site to the RED-084 study site in the AOU that has been selected for harvesting can benefit from the general residual patch composition observed in this research. A managed footprint area of 40000 ha to 46000 ha (observed from 4 m to 64 m) can be potentially harvested to leave behind insular residual patches of varying land cover class combinations ranging from 5000 ha to 7500 ha. The proportion of total residual patch area within the disturbed footprint observed at 4 m, 8 m, and 16 m, can be 12.41%, 14.64%, and 14.6% respectively.

The percentages of land cover classes within various morphologies all behaved in similar ways when observed at different grain sizes. The patterns observed from the percentage cover graphs and the sample morphological maps at 4 m, 8 m, and 16 m indicate that the more abundant land cover classes were bedrock and non-vegetation, sparse conifer, and dense conifer. At 32 m and 64 m throughout all morphologies, the water body class remained intact and was the most frequently observed land cover class as water does not burn and will remain after fire events. It was noted that at 16 m and 32 m grain sizes the morphological elements started dissipating severely to the degree that the pixel could not support the a majority of the element. Islets were the most representative morphology across most of the land cover classes at the larger grain sizes. Islets are the simplest morphology and are not bounded by edge boundaries and do not need to be in contact with other morphologies to sustain their configuration and structure. The conversion of some morphological elements into different morphological elements (especially islet elements) at the 32 m and 64 m grain sizes can provide

planners and managers with the notion that these grain sizes may not be suitable to conduct studies of potential management of forest perimeters similar to the size of RED-084.

The dominant land cover classes that can potentially remain in residual patches after harvesting are sparse conifer and dense conifer. The conifer classes can make up on average at least 51% of the total land cover classes comprising morphological elements across all grain sizes. Core, perforation, edge, loop, bridge and branch morphological elements increase in area in dense conifer from 4 m to 8 m grain size; an increase from an average of 19% to 23% across these morphological elements. However, at 16 m the change in composition of dense conifer occurs drastically; dense conifer land cover found within the aforementioned morphological elements accounted for 50% of the total land cover classes in the residual patches. Conversely, sparse conifer, although contributing to a very large area of the residual patches, decreased in proportion from an average of 54% at 4 m to 51% at 8 m across the core, perforation, edge, loop, bridge, and branch morphological elements. Subsequently, there was an immense drop in proportion at 16 m, with sparse conifer accounting for 24.5% of the land cover classes comprising those morphological elements.

The emulation of natural disturbances can be improved with the MSPA results; the composition and configuration of the morphologies within residual patches can potentially be mimicked in an anthropogenic setting. The AOU is predominantly in the boreal zone of northern Ontario, and RED-084 is reflective of the land cover composition within the AOU. The residual patches were dominated by sparse conifer, dense conifer, bedrock and non-vegetation, and water bodies. At smaller grain sizes (4 m and 8 m), sparse and dense conifers should comprise about 40% of the land cover that is being left behind after harvesting a site similar to RED-084. The conifer composition can be lowered by 3 to 4% when the grain size of observation increases to 32 m and 64 m. The coniferous forest is harvested in this region, hence leaving behind the different morphologies of sparse conifer and dense conifer can closely match the disturbed boreal landscape. Bedrock and non-vegetation land cover classes can account for 6 to 7.5% of the total residual patches left behind at 4 m and 8 m grain sizes, and about 4 to 5% of the land cover classes at 32 m and 64 m grain sizes.

Changing the neighbourhood connectivity did not significantly affect the morphological element areas, except for islet morphologies. When the neighbourhood connectivity was changed from 4 to 8 neighbouring pixels the islet areas decreased, and this trend was observed for all grain sizes. An 8 neighbourhood rule should therefore be used to minimize the occurrences of the islet pattern elements. The edge width change from 1 pixel to 2 pixels had a significant effect on the areas of every morphological pattern elements at each grain size, with the exception of islet morphologies (all grain sizes) and bridge morphologies at 64 m grain size. When the edge width parameter was increased, core, loop, branch, and bridge areas decreased at 4 – 32 m grain sizes. Applying the transition parameter (turning it on) in the MSPA analysis resulted in a significant effect on the edge morphological areas across all grain sizes. The mean edge areas across all land cover classes were statistically different when the transition was set to 1 across all grain sizes ($p < 0.05$). When the transition was turned on, the edge areas increased across each grain size.

Perforations, loops, and bridges were not as abundant as core, islets, edges, and branches across the land cover types. Perforations may not occur in abundant instances in the naturally disturbed environment, hence the forest managers can overlook the harvesting of forested patches within core patches. Islet morphologies did not contribute to a large area within the footprint but they were abundant especially at larger grain sizes when most morphological elements were converted to islets. Loops, bridges, and branches are also relatively small in comparison to cores, and they present more edges per unit area than cores. Preserving the interior cores can give forest managers useful insight on the conservation of both vegetation and wildlife species.

The formation of the morphological elements within the binary maps of residual patches is indicative of the types of processes existing in the post-fire boreal landscapes. The larger core areas can potentially represent contiguous residual vegetation which enables secondary succession. The cores can also represent the refuges for wildlife, and can possess wetlands, which often remain after a wildfire. Wetlands successfully store water to assist with regeneration of trees and shrubs, and preserve nutrients that would have otherwise been depleted during the wildfire.

Bridge and branch morphologies link directly to ecological processes as they create corridors in which wildlife can migrate in search for more suitable habitats. These

habitats can be in the form of core elements or larger islet elements. Ecological corridors can counteract the problems of habitat fragmentation as they facilitate dispersion and improve habitat expansion. Bridge elements in particular can represent rivers, streams or wetlands that join large lakes or rivers. In describing the bridge morphological elements, forest managers can gain insight to the hydrological and drainage flows and cycles existing in post-disturbed boreal forests.

Edge and perforation boundaries surrounding cores and matrix holes respectively, are important in the understanding of habitat fragmentation. Smaller and irregularly shaped cores would create more edges per core area. Therefore, the edge effect increases while the interior habitat decreases, leading to less biodiversity, species richness, species interactions, and food web disruptions. The larger and more intact core residual patches if left behind after harvesting would counteract the problem of habitat fragmentation. In addition, more complexly shaped core residuals would result in more edges being created. The resulting edge effects would need to be minimized to limit habitat fragmentation.

References

Akther, M.S., & Hassan, Q. K. (2011). Remote sensing-based assessment of fire danger conditions over boreal forest. *IEEE Journal of Selected Topics in Applied Earth Observations and Remote Sensing*, 4(4), 992-999.

Alexander, M. E., Cole, F. V. (2001). Rating fire danger in Alaska ecosystems: CFFDRS provides an invaluable guide to systematically evaluating burning conditions. *Fireline*, 12, 2-3.

Amiro, B. D., Stocks, B. J., Alexander, M. E., Flannigan, M. D., & Wotton, B. M. (2001). Fire, climate change, carbon and fuel management in the Canadian boreal forest. *International Journal of Wildland Fire*, 10, 405-413.

Baker, W. L. (2001). *The r.le programs: A set of GRASS programs for the quantitative analysis of landscape structure, Version 5.0*. University of Wyoming, Laramie, Wyoming.

Baldwin, D. J. B., Weaver, K., Schnekenburger, F., & Perera, A. H. (2004). Sensitive of landscape pattern indices to input data characteristics on real landscapes: implications for their use in natural disturbance emulation. Landscape Ecology, 19, 255-271.

Bogdanski, B. E. C. (2008). *Canada's Boreal Forest Economy: Economic and socio-economic issues and research opportunities*. Natural Resources Canada, Canadian Forest Service, Pacific Forestry Centre. Victoria, B. C. Information Report BC-X-414.

Bourgeau-Chavez, L. L., Kasischke, E. S., & French, N. H. F. (1994). Using ERS-1 SAR Imagery to Monitor Variations in Burn Severity in an Alaskan fire-Disturbed Boreal Forest Ecosystem. *Geoscience and Remote Sensing Symposium, 8-12 Aug, 1994, Pasadena, CA*. Ann Arbor, MI. (Editor unknown).

Brandt, J. P. (2009). The extent of the North American boreal zone. *Environmental Reviews*, 17 (1), 101-161.

Brandt, J. P., Flannigan, M. D., Maynard, D. G., Thompson, I. D., & Volney, W. J. A. (2013). An introduction to Canada's boreal zone: ecosystem processes, health, sustainability, and environmental issues. *Environmental Review*, 21, 207-226.

Burke, R. A., Zepp, R. G., Tarr, M. A., Miller, W. L., & Stocks, B. J. (1997). Effect of fire on soil-atmosphere exchange of methane and carbon dioxide in Canadian boreal forest sites. *Journal of Geophysical Research*, 102, 29289-29300.

Burton, P. J., Parisien, M-A., Hicke, J. A., Hall, R. J., & Freeburn, J. T. (2008). Large fires as agents of ecological diversity in the North American boreal forest. *International Journal of Wildland Fire,* 17, 754-767.

Canadian Interagency Forest Fire Centre 2003. *The 2003 Glossary of Forest Fire Management Terms*. Winnipeg, Manitoba: The Glossary Team.

Chu, T., & Guo, X. (2014). Remote Sensing Techniques in Monitoring Post-Fire Effects and Patterns of Forest Recovery in Boreal Forest Regions: A Review. *Remote Sensing*, 6, 470-520.

Chuvieco, E., & Congalton, R . G. (1989). Application of remote sensing and geographic information systems to forest fire hazard mapping. Remote Sensing of Environment, 29, 147-159.

Chuvieco, E., Englefield, P., Trishchenko, A. P., & Luo, Y. (2008). Generation of long time series of burn area maps of the boreal forest from NOAA-AVHRR composite data. *Remote Sensing of the Environment*, 112, 2381-2396.

Clerici, N., & Vogt, P. (2013). Ranking European regions as providers of structural riparian corridors for conservation and management purposes. *International Journal of Applied Earth Observation and Geoinformation*, 21, 477-483.

Corona, P., Lamonaca, A., & Chirici, G. (2008). Remote sensing support for post fire forest management. *iForest – Biogeosciences and Forestry* 1, 6-12.

Cullinan, V. I., & Thomas, J. M. (1992). A comparison of quantitative methods for examining landscape pattern and scale. Landscape Ecology, 7 (3), 211-227.

Cushman, S. A., McGarigal, K., & Neel, M. C. (2008). Parsimony in landscape metrics: Strength, universality, and consistency. *Ecological Indicators*, 8 (5), 691-703.

De Blij, H. J., Muller, P. O., Williams Jr., R. S., Conrad, C. T., & Long, P. (2009). *Physical Geography: The Global Environment*. 2nr Edition. Don Mills, Ontario: Oxford University Press. 776 p.

de Groot, W., Bothwell, P., Carlsson, D., Logan, K., Wein, R., & Li, C. (2002). Forest fire management adaptation to climate change in the Prairie Provinces; Canadian Forestry Service, University of Alberta and Prairie Adaptation Research Collaborative, 97 p.

Delcourt, H. R., & Delcourt, P. A. (1988). Quaternary landscape ecology: Relevant scales in space and time. *Landscape Ecology*, 2 (1), 23 – 44.

DeLong, S. C., & Tanner, D. (1996). Managing the pattern of forest harvest: lessons from wildfire. *Biodiversity and Conservation*, 5, 1191-1205.

Dungan, J. L., Perry, J. N., Dale, M. R. T., Legendre, P., Citron-Pousty, S., Fortin, M.-J., Jakomulska, A., Miriti, M., & Rosenberg, M. S. (2002). *Ecography*, 25, 626-640.

Du-ning, X., & Xiu-zhen, L. (1999). Core concepts of landscape ecology. *Journal of Environmental Sciences*, 11 (2), 131 – 135.

Eberhart, K. E., & Woodard, P. M. (1987). Distribution of residual vegetation associated with large fires in Alberta. *Canadian Journal of Forest Research*, 17, 1207-1212.

EUFOFINET: European Forest Fire Networks (2012). European Glossary for wildfires and forest fires (1st ed.). Northumberland, UK: Stacey, R.

Fahrig, L. (2003). Effects of habitat fragmentation on biodiversity. *Annual review of Ecology, Evolution, and Systematics*, 34(1), 487 – 515.

Fauria, M. M., & Johnson, E. A. (2008). Climate and wildfires in the Northern American boreal forest. *Philosophical Transactions of the Royal Society*, 363, 2317-2329.

Forman, R. T. T. (1995). Land Mosaics: The ecology of landscapes and regions. Cambridge, NY: Cambridge University Press. 632 p.

Forman, R. T. T., & Godron, M. (1986). Landscape Ecology. Toronto, Ontario: John Wiley and Sons Inc.

Fortin, M.-J., Boots, B., Csillag, F., & Remmel, T. K. (2003). On the role of spatial stochastic models in understanding landscape indices in ecology. *Oikos*, 102, 203-212.

Foster, D. R. (1983). The history and pattern of fire in the boreal forest of southeastern Labrador. *Canadian Journal of Botany*, 61, 2459-2471.

Fraser, R., Li, Z., & Cihlar, J. (2000). Hotspot and NDVI differencing synergy (HANDS): A new technique for burned area mapping over boreal forest. *Remote Sensing of the Environment*, 74, 362-376.

French, N. H. F., Kasischke, E. S., & Bourgeau-Chavez, L. L. (1994). Multi-sensor analysis of the effects of fire in the Alaskan boreal forest. *Proceedings of the IEEE National*, 2, 1085-1089.

Frolking, S., Palace, M. W., Clark, D. B., Chambers, J. Q., Shugart, H. H., & Hurtt, G. C. (2009). Forest Disturbance and recovery: A general review in the context of spaceborne remote sensing of impacts on aboveground biomass and canopy structure. *Journal of Geophysical Research*, 114, G00E02.

Gairola, S., Procheş, S., & Rocchini, D. (2013). High-resolution satellite remote sensing: a new frontier for biodiversity exploration in Indian Himalayan forests. International Journal of Remote Sensing, 34 (6), 2006-2022.

Gerard, F., Plummer, S., Wadsworth, R., Ferreruela, S., Iliffe, L., Balzter, H., & Wyatt, B. (2003). Forest Fire scar detection in the boreal forest with multitemporal SPOT-Vegetation data. IEEE Transactions on Geoscience and Remote Sensing, 41(11), 2575-2585.

Gitas, I., Mitri, G., Veraverbeke, S., & Polychronaki, A. (2012). Advances in remote sensing of post-fire vegetation recovery monitoring – a review. *In*: Fatoyinbo, L. (Editor). Remote Sensing of Biomass - Principles and Applications. Rijeka, Croatia: Intech. 143-176 p.

Gustafson, E. J. (1998). Quantifying landscape spatial pattern: What is the state of the art? *Ecosystems*, 1, 143-156.

Haines-Young, R., & Chopping, M. (1996). Quantifying landscape structure: a review of landscape indices and their application to forested landscapes. *Progress in Physical Geography*, 20 (4), 418-445.

Hengl, T. (2006). Finding the right pixel size. *Computers and Geosciences*, 32, 1283-1298.

Hunter Jr., M. L. (1993). Natural fire regimes as spatial models managing boreal forests. *Biological Conservation*, 65, 115-120.

Hurteau, M. D., Hungate, B. A., & Koch, G. W. (2009). Accounting for risk in valuing forest carbon offsets. *Carbon balance and Management*, 4 (1).

James, R. D. (1984). Habitat Management Guidelines for Ontario's Forests: Nesting Accipiters, Buteos and Eagles. Wildlife Branch, Ontario Ministry of Natural Resources, Queen's Printer for Ontario, Peterborough. 23 p.

Kachmar, M., & Sánchez-Azofeifa, G. A. (2006). Detection of post-fire residuals using high- and medium-resolution satellite imagery. *The Forestry Chronicle*, 82 (2), 177-186.

Kashian, D. M., Tinker, D. B., Turner, M. G., & Scarpace, F. L. (2004). Spatial heterogeneity of lodgepole pine sapling densities following the 1988 fires in Yellowstone National Park, Wyoming, USA. *Canadian Journal of Forest Research*, 34, 2263-2276.

Kasischke, E. S., French, N. F. H., Bourgeau-Chavez, L. L., Ustin, S. L., & Christensen Jr., N. L. (1994). Estimating release of carbon from forest fires in Alaska using satellite remote sensing data. Paper presented at the Geoscience and Remote Sensing Symposium, Pasadena, California.

Kasischke, E. S., Christensen Jr, N. L., & Stocks, B. J. (1995). Fire, Global Warming, and the Carbon Balance of Boreal Forests. *Ecological Applications*, 5(2), 437-451.

Kasischle, E. S., Hoy, E. E., French, N. H. F., & Turetsky, M. R. (2007). Post-Fire Evaluation of the Effects of Fire on the Environment using Remotely-Sensed Data. *In*: Gitas, I., & Carmona, C. (Editors). Towards an Operational Use of Remote Sensing in Forest Fire Management. Luxembourg, Office for Official Publications of the European Communities. 34-52 p.

Kazanis, D., & Arianoutsou, M. (2004). Long-term post-fire vegetation dynamics in *Pinus halepensis* forests of Central Greece: A functional group approach. *Plant Ecology*, 171, 101-121.

Keeley, J. E. (1987). Role of fire in seed germination of woody taxa in California chaparral. Ecology, 68(2), 434-443.

Kellomäki, S., Karjalainen, T., & Väisänen (1997). More timber from boreal forests under changing climate? *Forest Ecology and Management*, 94, 195-208.

Kimmins, J. P. (2004). Emulating Natural Forest Disturbance: What does this mean? . *In*: Perera, A. H., Buse, L . J., & and Weber, M . G. (Editors). Emulating Natural Forest Landscape Disturbances: Concepts and Applications. New York City, NY: Columbia University Press. 8-28 p.

Kurz, W. A., Shaw, C. H., Boisvenue, C., Stinson, G., Metsaranta, J., Leckie, D., Dyk, A., Smyth, C., & Neilson, E. T. (2013). Carbon in Canada's boreal forest – A synthesis. *Environmental Reviews*, 21 (4), 260-292.

Lasaponara, R., & Lanorte, A. (2007). Remotely sensed characterization of forest fuel types by using satellite ASTER data. *International Journal of Applied Earth Observation and Geoinformation*, 9, 225-234.

Lathrop Jr., R. G. (1994). Impacts of the 1988 wildfires on the water quality of Yellowstone and Lewis Lakes, Wyoming. *International Journal of Wildland Fire*, 4, 169-175.

Leckie, D. G. (1990). Advances in remote sensing technologies for forest surveys and management. Canadian Journal of Forest Research, 20, 464-483.

Leitão, A. B., Miller, J., Ahern, J., & McGarigal, K. (2006). *Measuring Landscapes:A Planner's Handbook*. Washington D.C., United States of America: Island Press. 245 p.

Li, H. & Wu, J. (2004). Use and misuse of landscape indices. *Landscape Ecology*, 19, 389-399.

McGarigal, K., & Marks, B. J. (1995). FRAGSTATS: Spatial pattern analysis program for quantifying landscape structure (Version 2.0). Portland, OR: USDA Forest Service, Pacific Northwest Research Station.

McGarigal (2013). Landscape Pattern Metrics. *In*: El-Shaarawi, A. H., & Piegorsch, W. W. (Editors). Encyclopedia of Environmetrics Second Edition. Chichester, England: John Wiley and Sons Inc. 1441-1451 p.

McNicol, J. G., & Baker, J. A. (2004). Emulating Natural Forest Disturbance: From Policy to Practical Guidance in Ontario. *In*: Perera, A. H., Buse, L . J., & and Weber, M . G. (Editors). Emulating Natural Forest Landscape Disturbances: Concepts and Applications. New York City, NY: Columbia University Press. 251-262 p.

Mitasova, H., Mitas, L., Brown, W. M., Gerdes, D. P., Kosinovsky, I., & Baker, T. (1995). Modelling spatially and temporally distributed phenomena: new methods and tools for GRASS GIS. *International Journal of Geographical Information Systems*, 9 (4), 433-446.

O'Neill, R. V., DeAngelis, D. L., Waide, J. B., & Allen, T. F. H. (1986). *A Hierarchical Concept of the Ecosystem*. Princeton University Press, Princeton, New Jersey.

O'Neill, R. V., Hunsaker, C. T., Timmins, S. P., Jackson, B. L., Jones, K. B., Riitters, K. H., & Wickham, J. D. (1996). Scale problems in reporting landscape pattern at the regional scale. *Landscape Ecology*, 11 (3), 169 – 180.

OMNR (2001). Forest management guide for natural disturbance pattern emulation (Version 3.1). Ontario Ministry of Natural Resources, Queen's Printer for Ontario, Toronto. 40 p.

OMNR (2010). Forest Management Guide for Conserving Biodiversity at the Stand and Site Scales – Background and Rationale for Direction. Toronto: Queen's Printer for Ontario. 575 pp.

OMNR (2014). Forest Management Guide for Boreal Landscapes. Toronto: Queen's Printer for Ontario. 104 pp.

Ontario Forest Research Institute (2008). *Boreal forest succession in Ontario: an analysis of the knowledge space*. Ontario Ministry of Natural Resources, Forest research report no. 171, Sault Ste. Marie, Ontario: Queen's Printer for Ontario.

Ostapowicz, K., Vogt, P., Riiters, K. H., Kozak, J., & Estreguil, C. (2008). Impact of scale on morphological spatial pattern of forest. Landscape Ecology, 23, 1107-1117.

Pasch, B., & Koprowski, J. L. (2011). Impacts of fire suppression on space use by Mexican fox squirrels. *Journal of Mammalogy*, 92 (1), 227-234.

Patriquin, M. N., Parkins, J. R., & Stedman, C. (2007). Socio-economic status of boreal communities in Canada. *Forestry*, 80, 279-291.

PCI Geomatics (2003). *Geomatica OrthoEngine: User Guide*. PCI Geomatics Enterprises Inc., Geomatica Version 9.0. Richmond Hill, ON. 168 p.

Perera, A. H., Buse, L. J., & Weber, M. G. (2004). *Emulating Natural Forest Landscape Disturbances: Concepts and Applications*. New York City, NY: Columbia University Press. 315 p.

Perera, A. H., & Buse, L. J. (2004). Emulating Natural Disturbance in Forest Management: An Overview. *In*: Perera, A. H., Buse, L . J., & and Weber, M . G. (Editors). Emulating Natural Forest Landscape Disturbances: Concepts and Applications. New York City, NY: Columbia University Press. 3-7 p.

Perera, A. H., & Buse, L. J. (2014). *Ecoloygy of Wildfire Residuals in Boreal Forests*. West Sussex, UK: Wiley-Blackwell, 272 p.

Qi, Y., & Wu, J. (1996). Effects of changing spatial resolution on the results of landscape pattern analysis using spatial autocorrelation indices. *Landscape Ecology*, 11 (1), 39-49.

R Core Team (2014). R: A language and environment for statistical computing. R Foundation for Statistical Computing, Vienna, Austria. http://www.R-project.org/

Racey, G., Harris, A., Gerrish, L., Armstrong, E., McNicol, J., & Baker, J. (1999). Forest management guidelines for the conservation of woodland caribou: a landscape approach. MS draft. Ontario Ministry of Natural Resources, Thunder Bay, Ontario. 69 pp.

Remmel, T. K., & Perera, A. H. (2001). Fire mapping in a northern boreal forest: assessing AVHRR/NDVI methods of change detection. *Forest Ecology and Management*, 152, 119-129.

Remmel, T. K., & Csillag, F. (2003). When are two landscape pattern indices significantly different? Journal of Geographical Systems, 5, 331-351.

Remmel, T. K., & Perera, A. H. (2009). Mapping natural phenomena: Boreal forest fires with non-discrete boundaries. Cartographica, 44(4), 274-288.

Remmel, T. K., & Fortin, M-J (2013). Categorical, class-focused map patterns: characterization and comparison. *Landscape Ecology*, 28, 1587-1599.

Riitters, K. H., O'Neill, R. V., Hunsaker, C. T., Wickham, J. D., Yankee, D. H., Timmins, K. B. J., & Jackson, B . L. (1995). A factor analysis of landscape pattern and structure metrics. *Landscape Ecology*, 10, 23-39.

Rogan, J., & Miller, J. (2006). Integrating GIS and Remotely Snesed Data for Mapping Forest Disturbance and Change. *In:* Wulder, M. E., & Franklin, S. E. (Editors). Understanding Forest Disturbance and Spatial Pattern: Remote Sensing and GIS Approaches. Boca Raton, FL: CRC Press. 133-170 p.

Rowe, J. S., & Scotter, G. W. (1973). Fire in the Boreal Forest. *Quaternary Research*, 3, 444-464.

Rykiel Jr., E. J. (1985). Towards a definition of ecological disturbance. *Australian Journal of Ecology*, 10, 361-365.

Saura, S. (2004). Effects of remote sensor spatial resolution and data aggregation on selected fragmentation indices. *Landscape Ecology*, 19, 197 – 209.

Saura, S., Vogt, P., Velazquez, J., Hernando, A., & Tejera, R. (2011). Key structural forest connectors can be identified by combining landscape spatial pattern and network analyses. Forest Ecology and Management, 262, 150-160.

Sawada, M. (2009). Global spatial autocorrelation indices - Moran's I, Geary's C and the general cross-product statistic. http://www.lpc.uottawa.ca/publications/moransi/moran.htm.

Šímová, P., & Gdulová, K. (2012). Landscape indices behavior: A review of scale effects. *Applied Geography*, 34, 385-394.

Soille, P., & Vogt, P. (2008). Morphological segmentation of binary patterns. *Pattern Recognition Letters*, 30 (4), 456-459.

Stocks, B. J., Fosberg, M. A., Lynham, T. J., Mearns, L., Wotton, B. M., Yang, Q., Jin, J-Z, Lawrence, K., Hartley, G. R., Mason, J. A., & McKenney, D. W. (1998). Climate change and forest fire potential in Russian and Canadian boreal forests. *Climate Change*, 38, 1-13.

Sunar, F., & Özkan, C. (2001). Forest fire analysis with remote sensing data. *International Journal of Remote Sensing*, 22(12), 2265-2277.

Turner, M. G. (1989). Landscape Ecology: The effect of pattern on process. *Annual Review of Ecology and Systematics*, 20, 171-197.

Turner, M. G. (1990). Spatial and temporal analysis of landscape patterns. Landscape Ecology, 4 (1), 21-30.

Uuemaa, E., Antrop, M., Roosaare, J., Marja, R., & Mander, U. (2009). Landscape metrics and indices: An overview of their use in landscape research. Living Reviews in Landscape Research, 3, 1.

Van Wagner, C. E. (1977). Conditions for the start and spread of crown fire. *Canadian Journal of Forest Research*, 7, 23-34.

Vogt, P., Riitters, K. H., Iwanowski, M., Estreguil, C., Kozak, J., & Soille, P. (2007). Mapping landscape corridors. Ecological Indicators, 7, 481-488.

Vogt, P., Riitters, K. H., Estreguil, C., Kozak, J., Wade, T. G., & Wickham, J. D. (2007). Mapping spatial patterns with morphological image processing. Landscape Ecology, 22, 171-177.

Vogt, P., Ferrari, J. R., Lookingbill, T. R., Gardner, R. H., Riiters, K. H., & Ostapowicz, K. (2009). Mapping functionality connectivity. *Ecological Indicators*, 9, 64-71.

Volney, W. J. A., & Hirsch, K. G. (2005). Disturbing forest disturbances. *The Forestry Chronicle*, 81, 662-668.

Wang, X., Hamann, A., & Cumming, S. G. (2012). Measuring boreal forest fragmentation after fire: Which configuration metrics are best? *Ecological Indicators* 13, 189-195.

Watkins, L. (2011). *The Forest Resources of Ontario*. Ontario Ministry of Natural Resources, Sault Ste. Marie, Ontario, Forest Evaluation and Standards Section, Forests Branch 307 pp.

Weber, M. G., & Stocks, B. J. (1998). Forest Fires and Sustainability in the Boreal Forests of Canada. *Royal Swedish Academy of Sciences*, 27, 545-550.

Westervelt, J. (2004, September). GRASS Roots. Paper presented at the proceedings of the FOSS/GRASS Users Conference, Bangkok, Thailand.

Wickham, J. D., & Riitters, K. H. (1995). Sensitivity of landscape metrics to pixel size. *International Journal of Remote Sensing*, 16 (18), 3585-3594.

Wu, J. (1999). Hierarchy and scaling: Extrapolating information along a scaling ladder. *Canadian Journal of Remote Sensing*, 25, 367-380.

Wu, J., Jelinski, D. E., Luck, M., & Tueller, P. T. (2000). Multiscale analysis of landscape heterogeneity: Scale variance and pattern metrics. *Geographic Information Sciences*, 6 (1), 6 – 19.

Wu, J., Shen, W., Sun, W., & Tueller, P. T. (2002). Empirical patterns of the effects of changing scale on landscape metrics. *Landscape Ecology*, 17, 761-782.